Faculty of Science and Engineering

Department of Chemical Engineering

Enhanced Photocatalytic Degradation of Biorefractory Pollutants in Petroleum Refinery Wastewater

Abdul Basit Mohamad S Abeish

This thesis is presented for the Degree of

Doctor of Philosophy

of

Curtin University

June 2015

DECLARATION

To the best of my knowledge and belief this thesis contains no material previously published by any other person except where due acknowledgment has been made.

This thesis contains no material which has been accepted for the award of any other degree or diploma in any university.

Signature: 

Date: 01/06/2015

ACKNOWLEDGEMENT

All praises and glories to Almighty Allah (SWT) who has bestowed me courage and patience upholding this work.

There have been many people who have supported to this thesis. First and foremost, I would like to thank my research project supervisors, Dr Hussein Znad and Prof. Ming Ang for their enduring guidance and patience during my study.

I gratefully acknowledge the valuable support provided by staff in Chemical Engineering, Curtin University, and Technical staff, Ms Karen Haynes, Mr Jason Wright, Mr Xia Hua and Mr Araya for the laboratory support during my work. I would also like to thank my friend Mr Feisal Ali Mohammed who assisted me tirelessly throughout the writing of this research.

Finally, I would like to thank other people not mentioned here, but in my sincerest mind and heart.

DEDICATIONS

This work is dedicated to my mother and father for their loving support.

This work is also dedicated to my wife Ibtisam and my super kids, Nura and Mohamad in appreciation of their loving support, understanding and encouragement during my study in Australia.

PUBLICATIONS

Peer-reviewed Journal Publications

Abeish, Abdulbasit M., Ha Ming Ang, and Hussein Znad, 2015. "Solar photocatalytic degradation of 4-chlorophenol: mechanism and kinetic modelling." *Desalination and Water Treatment* no. 35 (11): 2915-2923.

Abeish, Abdulbasit M, Ha Ming Ang, and Hussein Znad, 2015. "Solar photocatalytic degradation of chlorophenols mixture (4-CP and 2, 4-DCP): Mechanism and kinetic modelling." *Journal of Environmental Science and Health, Part* A no. 50 (2):125-134.

Abeish, Abdulbasit M, Ha Ming Ang, and Hussein Znad, 2014. "Enhanced solar-photocatalytic degradation of combined chlorophenols using ferric ions and hydrogen peroxide." *Industrial & Engineering Chemistry Research* no. 53 (26):10583-10589.

Abeish, Abdulbasit M., Ha Ming Ang, and Hussein Znad, 2015 "Role of ferric and ferrous ions in the enhancement of the heterogeneous solar photocatalytic degradation of chlorophenols combined mixture" accepted for publication in *Water Science and Technology*.

Abeish, Abdulbasit M., Ha Ming Ang, and Hussein Znad, 2015 "Photocatalytic degradation of pollutants from petroleum refinery effluent". To be submitted to *Chemical Engineering Science.*

Peer-reviewed International Conference Proceedings

Abeish, Abdulbasit M, Ha Ming Ang, and Hussein Znad "Solar Photocatalytic Degradation of 4-Chlorophenol: Optimization and Kinetic Analysis" WCCE9 & APCCHE 2013 9th World Congress of Chemical Engineering August 18-23, 2013/ Coex, Seoul, Korea.

Abeish, Abdulbasit M, Ha Ming Ang, and Hussein Znad "Solar advanced oxidation treatment of synthesis petroleum refinery effluent: Mechanism and kinetic modelling" *Chemica* 28 Sept-01 Oct/ 2014 Perth, Australia *http://search.informit.com.au/fullText;dn=701131259109415;res=IELENG*

TABLE OF CONTENTS

LIST OF TABLES

LIST OF FIGURES

ACRONYMS

Ag_2O	Silver oxide
AOPs	Advanced oxidation processes
API	American petroleum institute
ASUs	Activated sludge units
BOD	Biochemical oxygen demand
BP	British petroleum
BQ	Benzoquinone
C_0	Initial concentration
CB	Carbon band
C_e	Concentration at equilibrium
CFFP	Cascade falling films photoreactors
C_i	Concentration of component *i*
cm	Centimetre
COD	Chemical oxygen demand
CPC	Compound parabolic collector
CPI	Corrugated plate interceptor
C_t	Concentration at any time
DAF	Dissolved air floatation
DOC	Dissolved organic carbon
E_b	Energy band-gap
EPA	Environmental protection agency

EU	European Union
Fe^{2+}	Ferrous iron
Fe^{3+}	Ferric iron
FFR	Falling film reactor
g	Gram
g_{cat}	Gram of the catalyst
h	Hour
H_2O_2	Hydrogen peroxide
HHQ	Hydroxyhydroquinone
HPLC	High-performance liquid chromatography
HQ	Hydroquinone
kg	Kilogram
K_i	Adsorption constant
k_i	Reaction rate constant
L	Litre
ƛ	Wavelength
L-H	Langmuir Hinshelwood
LPG	Liquefied petroleum gas
m	Metre
M_{cat}	Mass of the catalyst
mg	Milligram
min	Minute
mW	Milliwatt

PAH	Polycyclic aromatic hydrocarbon
Ph	Phenol
PPI	Parallel plate interceptor
PTFE	Polytetrafluoroethylene
Q_e	Adsorption capacity
Q_{max}	Adsorption capacity
$Q_{overall}$	Overall quantum yield
r_i	Reaction rate
t	Time
TDS	Total dissolved salts
TiO_2	Titanium dioxide
TOC	Total organic carbon
TPH	Total petroleum hydrocarbon
USEPA	United states environmental protection agency
UV	Ultra violet
V	Volume
VB	Valance band
VOC	volatile organic compound
WO_3	Tungsten trioxide
ZnO	Zinc oxide
^0C	Degree Celsius
2,4-DCP	2,4-dichlorophenol
4cCat	4-chlorocatechol

4-CP	4-chlorophenol
4-NP	4-nitrophenol
η	Degradation efficiency
μ	Micro

ABSTRACT

The removal of organic pollutants from petroleum refinery effluent is a matter of great interest in the field of wastewater treatment. The effluents generated from many petroleum refineries around the world contain various highly toxic organic pollutants that significantly affect water sources and the aquatic life. Generally, different techniques are used for the removal of organic pollutants from wastewater. Advanced Oxidation Processes (AOPs) are chemical treatment methods that can be used to completely mineralise biorefractory pollutants in wastewater. Among these chemical methods is photocatalysis.

This research firstly focuses on the effectiveness of solar photocatalytic degradation to degrade one organic pollutant, 4-chlorophenol (4-CP), in water. Different doses of titanium dioxide (TiO_2) associated with solar light were used in the experiments. The results showed that up to 76 % of 4-CP elimination was obtained after 180 min of treatment at the following conditions: TiO_2 = 0.5 g/L, light intensity = 1000 mW/cm^2. The major organic intermediates formed during the degradation of 4-CP were hydroquinone (HQ), 4-chlorocatechol (4cCat) and phenol (Ph). Among these intermediates, HQ was the most abundant and Ph the least. Based on these results a reaction kinetic model was developed to predict the rate of reaction of 4-CP and its main aromatic intermediates. The proposed model provides very good fit to the experimental data and works very well for a wide range of 4-CP initial concentrations (50-100 mg/L).

Due to real wastewater which usually contains more than one pollutant, the study was upgraded to investigate the solar photocatalytic degradation of two synthetic organic pollutants. 4-CP and 2,4-dichlorophenol (2,4-DCP) were employed as model pollutants. The solar-photocatalytic degradation of a mixture containing 4-CP and 2,4-DCP (50 mg/L of each) led to lower degradation efficiency of both compounds compared to the individual degradation. The maximum degradation efficiencies of 4-CP and 2,4-DCP were 91 % and 82 % respectively at optimum conditions: pH = 3, TiO_2 = 0.5 g/L, light intensity = 1000 mW/cm^2, irradiation time = 240 min. Three major intermediates named HQ, Ph, and 4cCat were observed during 240 min solar-photocatalytic degradation of 4-CP, whereas only two main intermediates named 4-

CP and Ph were detected during the degradation of 2,4-DCP at the same conditions. According to the suggested pathway, a modified Langmuir Hinshelwood (L-H) kinetic model including the interaction between the main pollutants and all the detected intermediates was developed.

The enhancement of solar photocatalytic degradation employed in this research was performed using iron ions and hydrogen peroxide (H_2O_2). The results obtained in this study showed that these chemical enhancers associated with TiO_2 can effectively increase the degradation efficiency of organic pollutants under solar irradiation. Four different advanced oxidation processes were conducted including Solar/TiO_2/Fe^{2+}, Solar/TiO_2/Fe^{3+}, Solar/Fe^{3+}/H_2O_2 and Solar/TiO_2/Fe^{3+}/H_2O_2. Among these degradation methods Solar/TiO_2/Fe^{3+}/H_2O_2 has shown the highest degradation efficiency for the main pollutants and their intermediates. The relative efficiencies of these processes are in the following order: Solar/TiO_2/Fe^{3+} < Solar/TiO_2/Fe^{2+} < Solar/Fe^{3+}/H_2O_2 < Solar/TiO_2/Fe^{3+}/H_2O_2. The results of the present study indicated that there is no significant difference between using ferrous (Fe^{2+}) and ferric (Fe^{3+}) ions in the solar photocatalytic degradation of chlorophenols mixture. According to the presented results, two kinetic reaction pathways for this combined mixture were proposed. This reaction mechanism involved all possible intermediates detected during the degradation.

Finally, the enhanced solar photocatalytic degradation was also carried out to remove organic pollutants from real petroleum refinery effluent. Raw samples were collected from BP Kwinana refinery (Western Australia). These effluent samples were collected from a location between Dissolved Air Flotation (DAF) and Activated Sludge Unit (ASU). Before the treatment several physical and chemical investigations such as pH, total organic compounds (TOC), chemical oxygen demand (COD) and turbidity were conducted. The pH values of the samples were between 9 to 9.2 which is slightly high due to the high concentration of amino and alkaline organic compounds in the wastewater. The initial concentrations of TOC and COD in the samples were 120 mg/L and 840 mg/L respectively. The influence of several key parameters such as TiO_2 loading, pH, Fe^{2+} ions, and Fe^{3+} ions on the solar photocatalytic degradation of raw samples was investigated. The maximum COD degradation efficiency (77 %) was achieved at the following optimum conditions: pH = 5, TiO_2 = 7 mg/L, Fe^{2+} = 15 mg/L, light intensity = 1000 mW/cm^2,

and solar irradiation time = 240 min. A kinetic model using L-H equation which considers the adsorption of chemicals on the photocatalyst surface was developed. This model was effective to predict the COD degradation of the real samples during solar irradiation time. A good agreement between experimental and theoretical data was achieved.

CHAPTER 1

INTRODUCTION

1.1 General overview

Water pollution has become one of the main threats that face humanity today. Increasingly, everyday people activities lead to contamination of water sources including oceans, rivers, lakes and ground water. This contamination contributes to generating large amounts of polluted water that people cannot use in their daily life. Contaminated water is generated from many different sources involving petroleum refineries, dyes, drugs, paper, textile dye, detergents, surfactants, pesticides, herbicides, insecticides and pharmaceutical manufacturers (Chong et al. 2010). These chemical contaminants can be organic pollutants such as alkanes, aliphatic, alcohols and aromatic compounds or inorganic like heavy metals, including lead, mercury, nickel, silver and cadmium. In addition, water can be contaminated by pathogens such as bacteria, viruses and fungi (Gogate and Pandit 2004).

One of the main sources of chemical toxic pollutants in water is petroleum refineries and oil industries. Oil refineries usually need large amounts of water to perform several processes like crude distillation and catalytic cracking units. The amount of water used for refinery processes is 0.4-1.6 times the amount of oil processed (Coelho et al. 2006). The use of water in these processes leads to polluted water by many highly toxic compounds such as aliphatic and aromatic petroleum hydrocarbons. Aromatic hydrocarbons such as chlorophenols are well known toxic compounds due to their high polycyclic aromatics content leading to more environmental problems (Sun et al. 2008). Petroleum refinery effluents depend on the process configuration and operating procedures. Table 1.1 shows the general physical-chemical characteristics of refinery wastewaters (Mota et al. 2009). All of these pollutants can exist in groundwater and surface waters which can cause environmental problems for both aquatic life and human health.

Table 1.1 Physical-Chemical characteristics of oil refinery wastewater (Mota et al. 2009)

Parameter	Minimum	Maximum
Temperature (^{0}C)	22	41
pH	6.2	10.6
BOD (mg/L)	17	280
COD (mg/L)	140	3340
Sulfides (mg/L)	0	38
Hardness as $CaCO_3$ (mg/L)	139	510
Oil (mg/L)	23	200
Phosphorus (mg/L)	0	97
NH_3 (mg/L, as N)	0	120
Chlorides (mg/L)	19	1080
Sulfates (mg/L)	0	182
Benzene (mg/L)	1	100
Phenols (mg/L)	20	200

Most of the petroleum refinery pollutants are extremely toxic and can lead to serious diseases to humans even at very low concentrations. For instance, the presence of chlorophenolic compounds, which are one of the main contaminants in refinery effluents, in drinking water can negatively affect the human central nervous system and might cause some carcinogenic diseases at higher doses (Bandara et al. 2001a). Among these organic pollutants, 4-chlorophenol (4-CP) has been recognised as a real threat to human health by both European Union (EU) and United States Environmental Protection Agency (USEPA) (Yang et al. 2009, Wang et al. 2005, Bandara et al. 2001b, Melián et al. 2013). Another chlorinated phenolic compound, which is 2,4 –dichlorophenol (2,4-DCP), has been listed as a very toxic pollutant by USEPA since 1976 (Melián et al. 2013). Another negative effect of refinery effluents on the environment is the destruction of aquatic life such as algae, invertebrates and fish (Wake 2005).

To overcome these environmental problems, polluted water has to be treated and reused efficiently. Generally, wastewater treatment can be divided into four categories: mechanical, biological, physical and chemical processes (Mahamuni and Adewuyi 2010). Usually, the first step of petroleum refinery wastewater treatment is filtration and elimination of the suspended solids, followed by biological treatment. Other physical treatments such as activated carbon and air stripping can be used to treat non-biodegradable compounds. However, these methods have some limitations and disadvantages. For instance, activated carbon adsorption can only change the phase of contaminants without destroying them and leading to another pollution problem (Kusvuran et al. 2005). In biological treatment processes, there are also several drawbacks including the slow reaction rates, the control of temperature and disposal of activated sludge (Kusvuran and Erbatur 2004). Therefore, more effective treatment processes, which can completely degrade and mineralise all organic and inorganic pollutants, are required.

Advanced Oxidation Processes (AOPs) are one of the most effective and widely used methods for wastewater treatment. These methods offer several advantages including the complete mineralisation of the organic contaminants, using solar light as a viable alternative source of UV and cheaper than the granular-activated carbon and UV/O_3 processes (Salaices et al. 2004). The main power of this chemical treatment comes from producing hydroxyl radicals ($^{\bullet}OH$) which can effectively destroy all organic contaminants and mineralise them into CO_2 and H_2O. The AOPs can be classified into two main types, homogeneous and heterogeneous processes which can be conducted with or without light irradiation. The common homogeneous process called photo-Fenton which is the reaction between iron ions and hydrogen peroxide (H_2O_2) in the presence of light (Czaplicka 2006a). Among all heterogeneous methods, the photocatalytic degradation process has been stated as appropriate technique to destroy and mineralise refractory organic pollutants (Adán et al. 2009b, Saien and Nejati 2007). The efficiency of this method usually comes by using a suitable photocatalyst such as titanium dioxide (TiO_2) and UV or solar source. In addition, it has some features such as ambient operating conditions, complete destruction of pollutants and their intermediates, and relatively low operating cost (Ahmed et al. 2010). However, some challenges such as separation of

TiO_2 photocatalyst after water treatment and theories of the kinetic modelling during the photocatalytic degradation (Gaya and Abdullah 2008) will need to be addressed.

Most research studies on photocatalytic degradation use Langmuir-Hinshelwood (L-H) equation to address the kinetic models. In addition, most of the kinetic models developed in the literature consider a single model pollutant. However, during the photocatalytic degradation of pollutants many intermediate compounds are formed before converting into CO_2 and H_2O. These intermediates could be more toxic and non-biodegradable than the original pollutant (Vinu and Madras 2011a). Furthermore, dealing with a single model contaminant does not give realistic approach to real samples which usually contain a lot of compounds. Therefore, there is a need to enhance and develop the photocatalytic degradation of organic pollutants in petroleum refinery wastewater. Some chlorophenols such as 4-CP and 2,4-DCP were chosen as representative compounds in petroleum refinery wastewater. Also, real wastewater samples from BP refinery (Kwinana, Western Australia) are investigated. In this PhD dissertation the enhancement involves the use of solar light instead of UV to reduce the operating cost. In addition, the photocatalytic degradation efficiency may be increased by using some metals and oxidants with TiO_2 photocatalyst. Furthermore, the identification and quantification of the intermediates are investigated. Finally, kinetic models to calculate the rate constants and concentration profiles of the model pollutants and their intermediates were developed.

1.2 Research objectives

The main objective of the current PhD dissertation is to enhance the photocatalytic degradation of some organic pollutants that are present in petroleum refinery wastewater by using solar light, metals and oxidants together with TiO_2. Therefore, the specific objectives of this research are outlined below:

- Investigate the potential of advanced oxidation processes (AOPs) for treating biorefractory pollutants in petroleum refinery effluent such as 4-Chlorophenol and 2,4-Dichlorophenol under different conditions.
- Identify and quantify the intermediate compounds formed during the photocatalytic degradation under different conditions.

- Explore the photocatalytic degradation mechanism for the organic pollutants, considering the role of OH radical and the intermediates formed.
- Develop a kinetic model for the photocatalytic degradation of the organic pollutants, considering all intermediates formed during the degradation.
- Enhance the solar photocatalytic degradation using iron ions and hydrogen peroxide.
- Apply and investigate the enhancement technique using actual refinery effluent samples obtained from Kwinana Refinery (Perth-Australia)

1.3 Organisation of the Thesis

The thesis consists of eight chapters systematically linked with each other toward achieving the targeted objectives. Below is a brief description of these chapters and Figure 1.1 shows the thesis structure.

Chapter 1 Provides a general overview of this research project which includes the background and progress in this area, the main objectives, and the organisation of the thesis.

Chapter 2 Covers the literature review and current state of the developments relevant to the area of the research including heterogeneous photocatalysis processes and its fundamentals.

Chapter 3 Describes the experimental methods, materials, and analytical equipment used in this study.

Chapter 4 Reports the results and discussions of the oxidation of one organic compound (4-CP). The photocatalytic degradation models and mechanisms are also reported.

***Chapter* 5** Presents the experimental and kinetic modelling results of the photocatalytic degradation of combined chlorophenols mixture (4-CP and 2,4-DCP). This chapter also establishes the results of the combined mixture adsorption and their intermediates.

Chapter 6 Includes the enhancement of solar photocatalytic degradation of chlorophenols mixture using iron ions and hydrogen peroxide. The optimisation among some advanced oxidation processes is also reported.

Chapter 7 Reports the solar-photocatalytic degradation results of real petroleum refinery effluent samples. Measurements of total organic carbons (TOC) and chemical oxygen demand (COD) and some other investigations are presented.

Chapter 8 An overview of the major conclusions of this work is presented along with some suggestions and recommendations for further work.

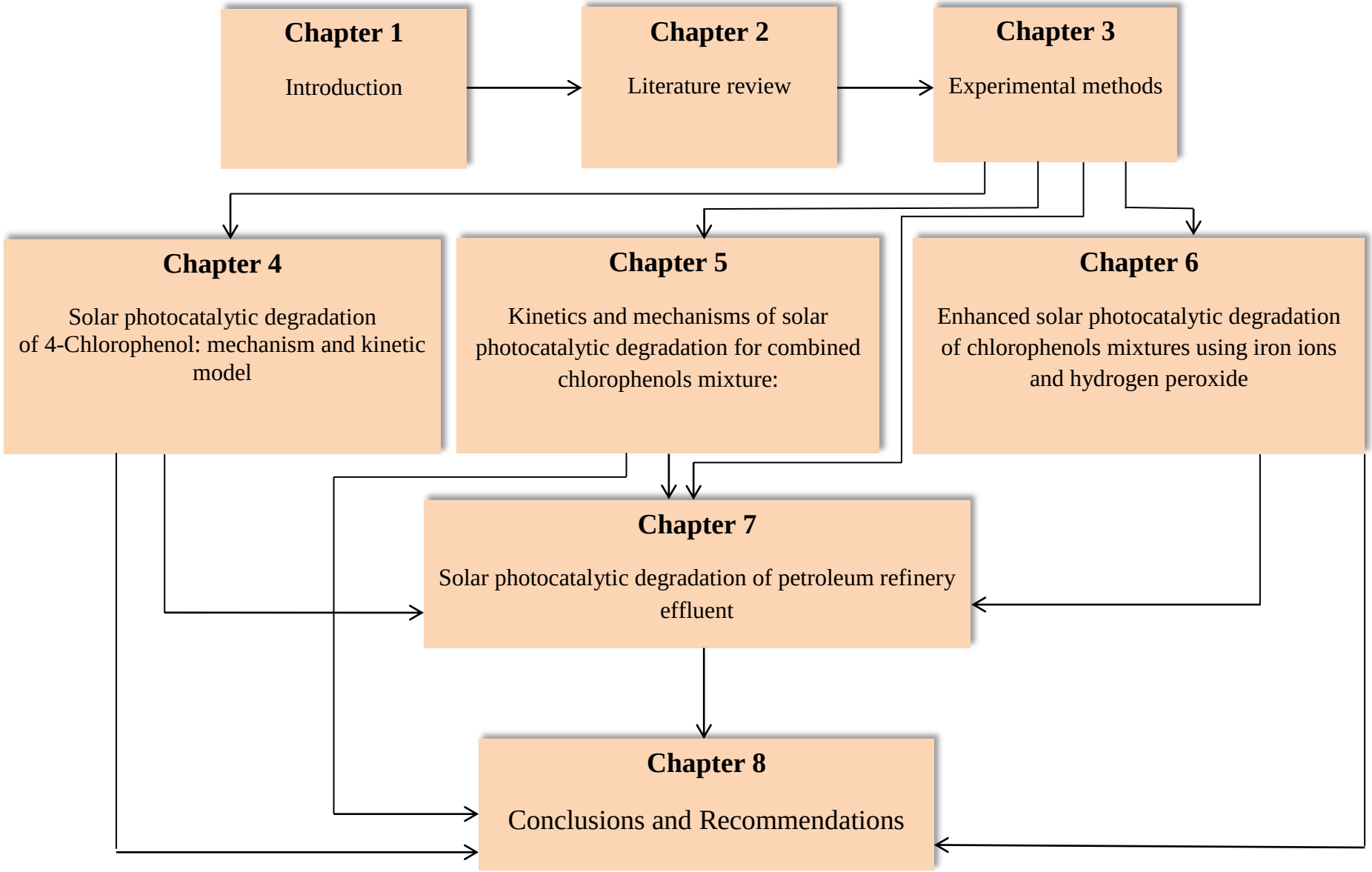

Figure 1.1 Thesis mapping

CHAPTER 2

LITERATURE REVIEW

Summary

This chapter provides a review of present knowledge on petroleum refinery effluent characteristics along with a review on its current treatment methods. Additionally, a critical literature survey on heterogeneous degradation processes and the technical literature specifically related to the objectives of this PhD thesis is covered in detail. Moreover, a review on the principle mechanism of photocatalysis, photocatalysts, and major operating parameters are reported. The kinetic model and reaction pathways of photocatalytic degradation of organic compounds in wastewater are also discussed. In addition, the enhanced solar photocatalytic degradation using chemical enhancer is reported in detail. The practical applications of photocatalytic degradation to treat biorefractory pollutants are addressed as well.

2.1 Introduction

Petroleum refinery effluents are mainly generated from oil and petrochemical industries. These effluents constitute the major source of aquatic environmental pollution (Wake 2005). The amount of wastewater produced from petroleum refineries is relatively proportional to the quantity of oil refined. For instance, 11.7 billion barrels of petroleum refinery effluents are produced in US annually (Li et al. 2006). In general, a barrel of crude oil consumes 65-90 gallon (246-341L) of water to produce the final products (Alva-Argáez al. 2007). Despite the great efforts devoted to replace fossil fuels by renewable energy sources such as wind and solar energies, crude oil is still the main source of energy. The world oil demand may reach to 107 mbpd in the next two decades, therefore; the effluents from petroleum industries will continually increase leading to more contamination of the world's water bodies (Yan et al. 2010).

These massive amounts of contaminated water can negatively affect the aquatic environment such as algae, which is a very significant link in the food chain (Pardeshi and Patil 2008). Petroleum refinery effluents contain many organic and inorganic toxic compounds which are harmful and dangerous to human, animal and plant life. Among these pollutants, phenolic compounds which are categorised by United States Environmental Protection Agency (USEPA) as priority contaminants due to their negative effects to human nervous system (Peng et al. 2012).

Several methods for treating petroleum refinery effluent have been applied, including coagulation (Tansel and Regula 2000), biological treatments (Ma et al. 2009), adsorption (El-Naas et al. 2010), electrochemical oxidation (Abdelwahab et al. 2009), catalytic wet hydrogen peroxide oxidation (Pariente et al. 2010), microwave-assisted catalytic wet air oxidation (Sun et al. 2008). However, all of these methods have limitations and drawbacks such as low efficiencies, limited pH, and large amounts of oxidants required (Diya'uddeen et al. 2011). One of the most effective chemical methods which have been reported in the literature is the advanced oxidation processes (AOPs) (Kamble et al. 2004, Jr. et al. 2013). The AOPs can be classified into homogeneous and heterogeneous processes that can be conducted with or without light irradiation. One of the common homogeneous process is the photo-Fenton reaction which is a reaction between iron ions and hydrogen peroxide (H_2O_2) in the presence of light (Czaplicka 2006a). Among all heterogeneous methods, the photocatalytic degradation process such as ZnO/UV and TiO_2/solar has been stated as appropriate technique to destroy and mineralise refractory organic pollutants(Adán et al. 2009b, Parilti 2010, Stepnowski et al. 2002, Shahrezaei et al. 2012).

2.2 Petroleum refinery effluent

2.2.1 Refinery structure

Refinery configurations are classified based on the required final products such as gasoline, kerosene, and petrochemical feed stocks. In general, petroleum refineries are categorised to hydro-skimming, including distillation, reforming and desulfurisation or complex which involves a catalytic cracking unit(Al Zarooni and Elshorbagy 2006). All of these operation units use large amounts of water resulting in generating petroleum refinery effluents. In addition there are some other units such as sanitary and laboratories which increase the total amount of effluent discharge. For instance Al Zarooni and Elshorbagy (2006) reported the volume percent of wastewater produced in Al Ruwais refinery (Fig. 2.1). These various sources include sour water, draining, pump flushes, laboratory, and flare system. The polluted water from these processes is sent to corrugated plate interceptor (CPI) to separate oil from wastewater, and then it is transferred to mixing pit where the effluent is diluted.

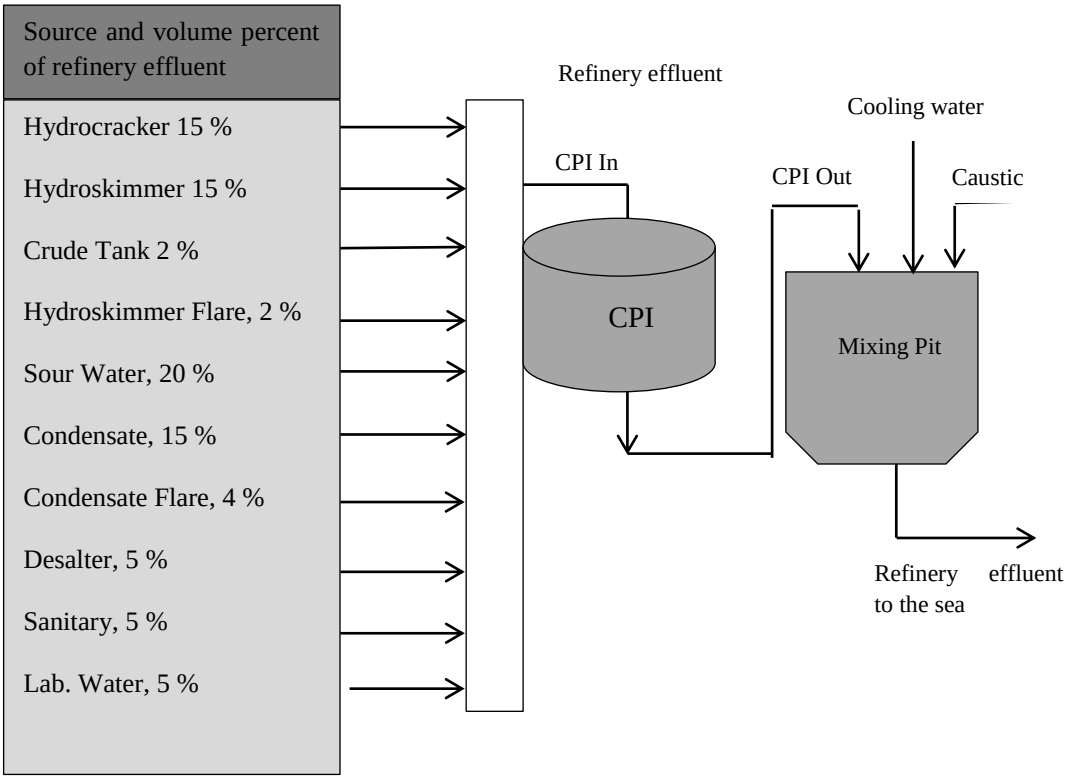

Figure 2.1 Petroleum refinery effluent of Al Ruwais refinery (Al Zarooni and Elshorbagy 2006)

2.2.2 Characteristics of petroleum refinery effluent

Compositions of petroleum refinery effluent vary considerably depending on crude oil specifications and the processing units of the refinery. However, all of these waters contain a high number of biorefractory toxic compounds (compounds that cannot be biologically treated) including hydrocarbons, phenols, ammonia, sulphur, and sulphide (Abdelwahab et al. 2009). Crude oil which contacts with water and produce petroleum refinery effluent consists of five different compounds including parafins, cycloalkanes, alkenes, aromatics, and non-hydrocarbons (Aruldoss and Viraraghavan 1998). Usually, refinery effluents have low hydrocarbon and high polycyclic aromatics compounds that increase the effluent toxicity. (Tatem et al. 1978). Table 2.1 presents qualitative evaluations of petroleum refinery effluent flow and characteristics relevant to each refinery process (Wong and Hung 2004). It is clear from this table that the major effluent sources come from desalting, distillation,

Table 2.1 Qualitative evaluation of effluent flow and characteristics related to each refinery process (Wong and Hung 2004).

Production process	Flow	BOD	COD	Phenols	Sulfide	Oil	Emulsified Oil	pH	Temperature	Ammonia	Chloride	Acidity	Alkalinity	Suspended solids
Crude oil	XX	X	XXX	X		XXX	XX	0	0	0		0		XX
Crude desalting	XX	XX	XX	X	XXX	X	XXX	X	XXX	XX	XXX	0	X	XXX
Crude distillation	XXX	X	X	XX	XXX	XX	XXX	X	XX	XXX	X	0	X	X
Thermal cracking	X	X	X	X	X			XX	XX	X	X	0	XX	X
Catalytic cracking	XXX	XX	XX	XXX	XXX	X	X	XXX	XX	XXX	X	0	XXX	X
Hydrocracking	X			XX	XX				XX	XX				
Polymerisation	X	X	X	0	XX	X	0	XX	X	X	X	X	0	X
Alkylation	XX	X	X	0	XX	X	0	XX	X	X	XX	XX	0	XX
Isomerisation	X													
Reforming	X	0	0	X	X	X	0	0	X	X	0	0	0	0
Solvent refining	X		X	X	0		X	X	0			0	X	
Asphalt blowing	XXX	XXX	XXX	X		XXX								
Dewaxing	X	XXX	XXX	X	0	X	0							
Hydrotreating	X	X	X		XX	0	0	XX		XX	0	0	X	0
Drying and sweetening	XXX	XXX	X	XX	0	0	X	XX	0	X	0	X	X	XX

XXX=major contribution; XX = moderate contribution; X = minor contribution; 0 = insignificant; Blank = no data.
BOD = biological oxygen demand; COD = chemical oxygen demand.

and catalytic cracking. In addition, phenols exist in most refinery processes leading to generation of large amounts of phenolic compounds, which are priority toxic contaminants. In addition to the number of the conventional pollutant constituents, USEPA categorised 126 toxic contaminants as priority pollutants such as phenols, benzene, toluene, and carbon tetrachloride (Snider and Manning 1982). American Petroleum Institute (API) and Environmental protection Agency (EPA) conducted a survey of priority pollutants across 17 refineries in the USA and found that more than 34 phenolic and organic compounds discharged in all refinery streams (Table 2.2) (Snider and Manning 1982). Wong and Hung (2004) reported that the effluent limitations established by USEPA included that the total organic carbon concentration in the refinery wastewater must be less than 5 mg/L. Table 2.3 reports the effluent standards for five subcategories of the petroleum refining point source category made by (EPA) (Jou and Huang 2003). These standard limitations should be followed in order to reduce the adverse impacts on the environment.

2.2.3 Impacts of petroleum refinery effluent on the environment

Petroleum refineries and petrochemical industries generate massive amounts of effluent which contain a high number of toxic biorefractory pollutants such as phenolic compounds, aldehydes, polyaromatics and aliphatic compounds. These pollutants have many negative effects on human beings, plants, and the aquatic environment. Generally, petroleum refinery effluents consist of different petroleum hydrocarbons which have limited solubility in water at environmental conditions. In addition, some fuel additives such as t-butyl methyl ether are used to enhance the octane number of gasoline. These additives have been listed as priority toxic compounds due to their carcinogenic effects (Tansel and Regula 2000). Among these contaminants, phenolic compounds can cause serious health problems such as carcinogenic diseases if they reach drinking water (Bandara et al. 2001b). For instance, 4-CP has been recognised as a threat to human health by both European Union (EU) and USEPA (Yang et al. 2009, Wang et al. 2005, Bandara et al. 2001b, Melián et al. 2013). Another chlorinated phenolic compound, which is 2,4-DCP, has been listed as a very toxic pollutant by USEPA since 1976 (Melián et al. 2013).

Table 2.2 Concentration ranges of priority contaminants reported in API and EPA priority pollutants survey (Snider and Manning 1982)

	Refinery category [a]				
Compound (µg/L)	A	B	C	E	D
Phenol	13	50-16000	3000-8000	40-1300	10-4900
2-Chlorophenol	1	10-3000	1	71-100	80
2,4-Dimethylphenol	1		1	50	
2,4-Dichlorophenol	2	10-500	1	80-200	100
2-Nitrophenol				50	0.1
4-Nitrophenol				50	
Pentaachlorophenol		10-850		50	
p-Chloro-m-cresol		50		50	0.6
4,6-Dinitro-o-cresol				50	1
N-Nitrosodiphenyl amine		10			1
1,4-Dichlorobenzene				1	0.3
1,2-Dichlorobenezene	1.5	5	1		2
Dimethyl phthalate		10	2	1	
Diethyl phthalate	12	5.5-60			10-16
Di-n-butyl phthalate	1.3	1-2.8	1	1	
Butyl benzyl phthalate			1	0.1-10	
Bis(2-ethyl hexyl) phthalate		1-600		1	0.1-1100
Naphthalate	68	1-1100	106	27-302	10-1100
Acenaphthylene	4	0.1-1		1-87	
Acenaphthene	37	0.1-3000	149	1-522	
Fluorene		2.9-304	106	1	21
Phenathrene		2.7-32	0.5	0.01-28	
Anthracene		0.01-0.03	2	0.1-0.2	
Fluoranthene		0.1-30	1-8	1-7.5	3.9-40
Pyrene		1-20	3	0.7-16	5.4
Chrysene		0.1-1.4		1	
Benzo(a)anthracene		1-1.5	1	1	
Chrysene/Benz(a)anthracene		0.3-550			1.8-40
Benzo(b)/(k)fluoranthene		1		1	
Benzo(k)fluoranthene				0.3-5	
Benzo(a)pyrene		0.1-9.5		1	
Indeno(1,2,3-c,d)pyrene		1		1	
Dibenzo(a,h)anthacene		0.3		1	
Benzo(g,h,i)perylene		0.2-3		1	

[a] The seventeen refineries considered in this study were distributed as follows: Class A = 1; Class B = 7; Class C = 3; Class E = 1; Class D = 5. Concentrations ranges, when given, are the minimum and maximum data in µg/L.

Table 2.3 Effluent standards for five subcategories of the petroleum refining point source category (Jou and Huang 2003)

Effluent limitation (daily average for 30 consecutive days, in Ibs/ 1000bbl of feedstock					
Parameters	Topping	Cracking	Petroleum	Lube	Integrated
BOD_5	4.25	5.5	6.5	9.1	10.2
TSS	3.6	4.4	5.25	8.0	8.4
COD	31.3	38.4	38.4	66.0	70.0
O&G	1.3	1.6	2.1	3.0	3.2
Phenolic compounds	0.027	0.036	0.0425	0.065	0.068
Ammonia as N	0.45	3.0	3.8	3.8	3.8
Sulfide	0.024	0.029	0.035	0.053	0.056
Total chromium	0.071	0.088	0.107	0.160	0.17
Hexavalent chromium	0.0044	0.0056	0.0072	0.160	0.011

BOD, biological oxygen demand; TSS, total suspended solids; COD, chemical oxygen demand; O&G, oil and grease, pH (within the range of 6.0 to 9.0).

The C-Cl bond in chlorophenols is highly stable and has been reported as a main reason of their toxicity (Ba-Abbad et al. 2012). Wake (2005) reported that refinery effluent is toxic at various levels to algae, invertebrates and fish. He also stated that the increase of wastewater temperature can significantly increase the chemical toxicity in marine life. In addition, some other inorganic pollutants such as ammonia and sulphides have adverse impacts on organisms that live close to outfalls. The minimum concentration of dissolved oxygen required in an aquatic environment is 2 mg/L (Attiogbe et al. 2007). This amount can be consumed by microorganisms if the refinery effluent contains high concentrations of organic compounds, which have a negative impact on the aquatic life. Therefore, all of inorganic and organic contaminants need to be effectively treated before discharging to the water bodies.

2.3 Treatment technologies

Mechanical and physicochemical methods such as oil-water separation and coagulation are the main pre-treatment steps for refinery effluent treatments (see Fig. 2.2). the raw refinery effluents contain solid particles, suspended solids, immiscible liquids, oils, and grease (Ishak et al. 2012). These contaminants need mechanical treatment using American Petroleum Institute (API) and Parallel Plate Interceptor (PPI) separators or separation tanks which depend on specific gravity differences between oil and wastewater (Santo et al. 2012). Physicochemical treatment such as coagulation/flocculation or coagulation-dissolved air flotation processes is necessary in the second stage of wastewater pre-treatment (Santo et al. 2012). Several coagulants such as iron salts, alum, and lime can be effectively used to increase the agglomeration of particles leading to promote the precipitation (Karthik et al. 2008). This treatment offers several features including high efficiency, fast treatment, small space requirement, and low cost (Chavadej et al. 2004).

Biological treatment is the process that follows the pre-treatment stages in order to remove Dissolved Organic Carbons (DOC). This traditional method utilises microorganisms including naturally-occurring, commercial, specific groups, and acclimatised activated sludge to mineralise organic pollutants into CO_2 and H_2O_2 (Fratila-Apachitei et al. 2001). Biological treatments are categorised as suspended-growth (microorganisms in the suspension), immobilised growth (microorganisms on inert materials), and a combination of suspended and immobilised -growth (Chan 2011). Even though the biological treatment is capable to

oxidise some pollutants, it cannot completely degrade recalcitrant components (biorefractory compounds) present in petroleum refinery effluent. In addition, there are several drawbacks including the slow biodegradation, the control of temperature and disposal of activated sludge (Kusvuran and Erbatur 2004). Therefore, an effective advanced treatment is required to destroy and mineralise these non-biodegradable compounds.

The advanced oxidation processes (AOPs) are effective methods to treat refinery effluent pollutants including electrochemical (Yavuz et al. 2010), catalytic oxidation (Santo et al. 2012), solar photo-Fenton (da Rocha et al. 2013), catalytic wet oxidation (Pariente et al. 2010), microwave catalytic wet air oxidation (Sun et al. 2008) and photocatalytic degradation (Saien and Nejati 2007). The AOPs offer several advantages including the complete mineralisation of the organic contaminants, using solar light as a viable alternative source of UV and cheaper than the granular-activated carbon and UV/O_3 processes (Salaices et al. 2004). Among the AOPs, the photocatalytic degradation using TiO_2 and UV light has been applied for mineralising most of organic contaminants presented in wastewater without significant drawbacks except the cost of energy (Jia et al. 2012). However, using solar light instead of UV light can effectively reduce the operating cost and making this method economically feasible. Figure 2.2 shows the overall steps for treating petroleum refinery effluent. In addition, Table 2.4 summaries different AOPs that have been used for treating petroleum refinery effluent including the treatment technique and target pollutant.

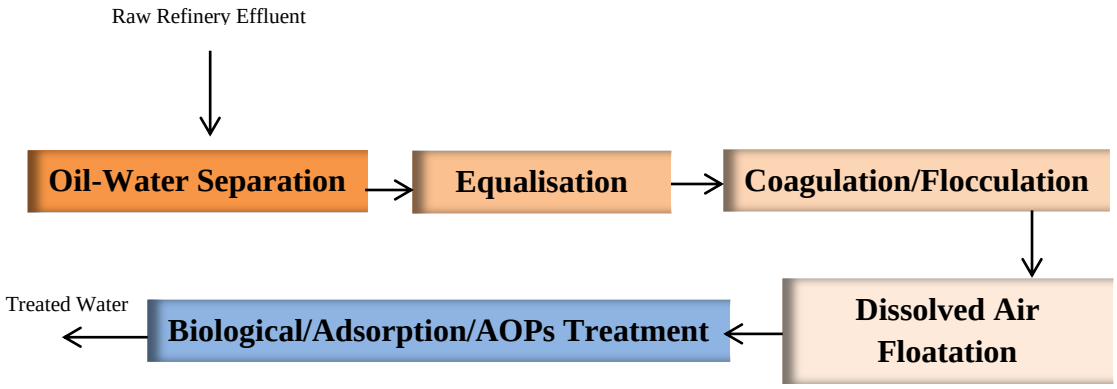

Figure 2.2 Steps of petroleum refinery effluent treatment

Table 2.4 Different AOPs used for treating petroleum refinery effluent.

Treatment technique	Target pollutant	Degradation rate %	Ref.
Photocatalytic degradation	COD	73	(Saien and Nejati 2007)
Photocatalytic degradation	Phenol and Phenolic derivatives	83	(Shahrezaei et al. 2012)
Photocatalytic degradation	COD	72	(Saien and Shahrezaei 2012)
Photocatalytic degradation	Phenols, DOC	Phenols 93, DOC 63	(Santos et al., 2006)
Solar-photocatalytic degradation	TOC	75	(Alhakimi et al., 2003)
Fe(III)/H_2O_2/Solar	TOC	49	(Parilti 2010)
Fenton process	COD	44.81	(Zhang and Yang 2011)
Fenton-like process	COD, TOC	COD 70, TOC 98.1	(Hasan et al., 2012)
Fenton-like process	COD	92	(Cao et al., 2013)
Photo-Fenton process	COD	70	(Tony et al. 2009)
Solar photo-Fenton process	PAH, aromaticity	PAH 92.7, aromaticity 96.2	(da Rocha et al. 2013)
Photo-Fenton process	COD	81	(GUNES 2008)
Photo-Fenton process	COD	87	(Coelho et al., 2006)
Photo-Fenton process	COD	75	(Tony et al., 2012)
Fenton/TiO2 /UV/Air	COD	84	(Tony et al. 2009)
Electrochemical process	Phenol, COD	Phenol 98.74, COD 75.71	(Yavuz et al., 2010)
Electrochemical process	COD	89.1	(Yan et al. 2014)
Electrochemical process	Phenol	94.5	(Abdelwahab et al., 2009)
Electrochemical process	COD, Phenol, Hydrocarbon, Turbidity	COD 85, Phenol 56, Hydrocarbon 67; Turbidity 83	(Dimoglo et al. 2004)
Electro-oxidation process	Phenol	99	(Oller et al., 2011)
Photoelectrocatalytic degradation	COD	47.4	(Li et al. 2006)
Microwave catalytic wet air oxidation	COD	90	(Sun et al., 2008)
UV/H_2O_2 process	COD	50	(Juang et al., 1997)
UV/H_2O_2	TPH	69	(Stepnowski et al. 2002)
Catalytic oxidation	Sulphide	90	(Santo et al. 2012)
Catalytic wet hydrogen peroxide oxidation	TOC	43	(Pariente et al. 2010)
O_3/UV	TOC	79	(Souza et al. 2011)

COD, chemical oxygen demand; DOC, dissolved organic carbon; TOC, total organic carbon; TPH, total petroleum hydrocarbon; PAH, polycyclic aromatic hydrocarbon.

2.4 Photocatalytic degradation

Heterogeneous photocatalytic degradation is one of the most effective methods among AOPs used for wastewater remediation due to its ability to destroy lots of organic and inorganic contaminants at ambient temperature and pressure (Herney et al. 2010, Fujishima et al. 2008). The idea of photocatalytic reaction is the interaction of photons which have suitable wavelength with a semiconductor particle (Gaya and Abdullah 2008). Additionally, the photocatalytic degradation process under optimum conditions (catalyst loading, pH, oxidants concentration and light intensity) can mineralise organic pollutants to CO_2 and H_2O (Diebold 2003). The principle mechanism of photocatalysis is shown in Figure 2.3. When the energy of photons (*hv*) is equal to or greater than the band gap energy, E_b, of the photocatalyst, electrons are excited and transfer from the valance band (VB) to the conduction band (CB). This step creates holes in the valance band (h^+) and free electrons (e^-) in the conduction band. This mechanism is represented by the following equations (Ireland et al. 1995, Konstantinou and Albanis 2003, Pelizzetti and Minero 1993):

Photoexcitation: $TiO_2 + h_v \rightarrow e^- + h^+$ (2.1)

Charge-carrier trapping of e^- : $e^-_{CB} \rightarrow e^-_{TR}$ (2.2)

Charge-carrier trapping of h^+: $h^+_{VB} \rightarrow h^+_{TR}$ (2.3)

Electron-hole recombination: $e^-_{TR} + h^+_{VB} \rightarrow heat$ (2.4)

Photoexcited e^- scavenging: $(O_2)_{ads} + e^- \rightarrow O^{\bullet -}_2$ (2.5)

Oxidation of hydroxyls: $OH^- + h^+ \rightarrow {}^{\bullet}OH$ (2.6)

Photodegradation by $^{\bullet}OH$: $R\text{-}H + {}^{\bullet}OH \rightarrow R^{\bullet} + H_2O$ (2.7)

The e^-_{TR} and h^+_{VB} in equation 2.4 are the surface trapped valence electron and conduction band hole respectively. In the absence of electron acceptors, the e^-_{TR}/ h^+_{VB} recombination is highly expected, therefore; the presence of electron scavengers are very important to avoid this undesired reaction (Malato et al. 2002). The heterogeneous photocatalytic process is effectively used to completely degrade organic pollutants such as phenol, chlorophenols, and oxalic acid presented in effluent. This organic photocatalytic degradation involves the form of some intermediates such as aldehydes and carboxylic acids prior to produce the final products CO_2 and H_2O (Eq. 2.8) (Ahmed Rasul et al. 2011).

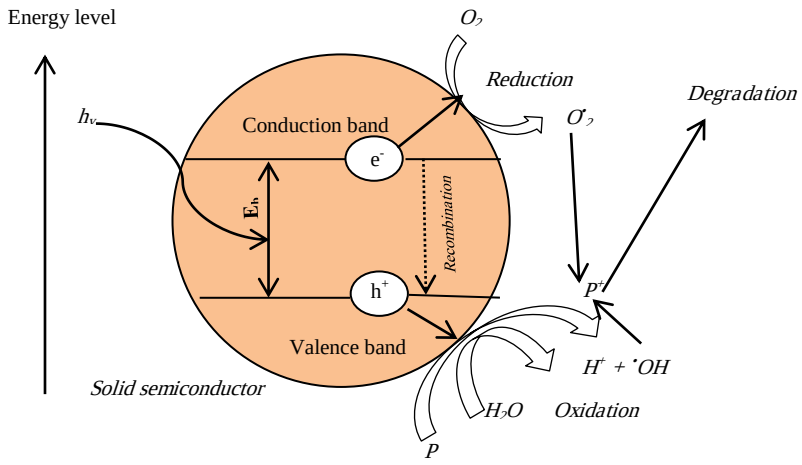

Figure 2.3 Principle mechanisms of photocatalysis

$$\text{Organic pollutants} \xrightarrow{\text{Photocatalyst/ } h_v} \text{Intermediates} \rightarrow CO_2 + H_2O \qquad (2.8)$$

Figure 2.4 shows the overall complete photocatalytic reaction involving five steps as follows (Herrmann 1999):

1. Mass transfer of the organic pollutant (A) in the bulk phase to the semiconductor surface.
2. Adsorption of the organic pollutant onto the photon activated semiconductor surface.
3. Photocatalysis reaction for the adsorbed phase on the semiconductor surface.
4. Desorption of the products from the semiconductor surface.

5. Mass transfer of the products from the interface region to the bulk fluid (B).

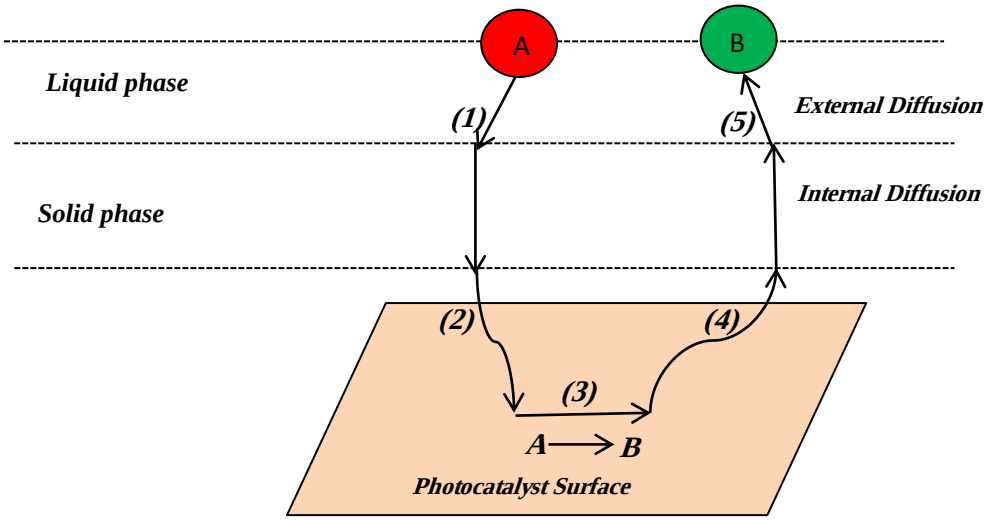

Figure 2.4 Steps of heterogeneous catalytic reaction (Ahmed et al. 2011)

Steps 1 and 5 represent the mass transfer and reaction rates which are physical steps for transferring a pollutant between the bulk to the particle surface. If these steps occur slowly, the mass transfer processes are limiting and will decrease the overall rate of photocatalytic reaction and versa vice (Chong et al. 2010).

2.4.1 Semiconductors used in heterogeneous photocatalytic degradation

Several metal oxides and chalcogenides such as TiO_2, ZnO, MgO_3, CeO_2, ZrO_2, SnO_2, WO_3, α-FeO_3, ZnS, CdS, CdSe, WS_2, and MgS_2 are used as photocatalysts (Mills and Le Hunte 1997, Fujishima et al. 2000, Vinu and Madras 2011a). For semiconductors to be effective, the redox potential of photogenerated VB holes must be positive to generate hydroxyl radicals and for CB electrons must be negative to generate superoxide radicals (Vinu and Madras 2011a). The energy required for the electron excitation varies according to the specific characteristics of the semiconductor and the minimum wavelength needed for the photo-excitation depends on the band-gap of the photocatalyst. Table 2.5 summaries the band-gap energies for some common semiconductors (Bhatkhande et al. 2002). Among these semiconductors TiO_2 has been reported as a suitable photocatalyst used to degrade organic pollutants in aqueous solutions. TiO_2 has several features including safety,

resistance to photo corrosion, catalytic efficiency and low cost, as well as the ability to absorb radiation at wavelengths below 400 nm, meaning the potential to utilise sunlight as light source (Diebold 2003, Czaplicka 2006b). Additionally, anatase TiO_2 has been reported to be photocatalytically more active than the rutile due to the higher electron transfer rate of anatase (Bhatkhande et al. 2002). However, this activity contributes to increasing the e^-/h^+ recombination rate in anatase which could lead to the deactivation of photocatalytic surface.

Table 2.5 Band-gap energy and wavelength (λ) of different photocatalysts (Bhatkhande et al. 2002).

Photocatalyst	**Band-gap (eV)**	**Wavelength (λ nm)**
Si	1.1	1127
WSe_2	1.2	1033
Fe_2O_3	2.2	564
CdS	2.4	517
WO_3	2.7	459
SnO_2	3.5	354
α-FeO_3	3.1	400
ZnS	3.7	335
ZnO	3.2	388
$SrTiO_3$	3.4	365
TiO_2(rutile)	3.0	413
TiO_2(Anatase)	3.2	388

Thus, the presence of rutile TiO_2 is important to reduce the e^-/h^+ recombination due to the various recombination lifetimes and interfacial electron transfer rate constants (Hoffmann et al. 1995). Degussa P25 TiO_2 has a typical ratio of anatase and rutile (70:30) which has been recognised as an effective photocatalyst for photocatalytic degradation of organic pollutants (Lazar et al. 2012).

2.4.2 Parameters affecting photocatalytic degradation

There are several operational parameters affecting typical organic pollutants found in petroleum refinery effluent. The effects of these parameters on the photocatalytic degradation rate vary from being minor to significant.

2.4.2.1 Temperature

The effect of temperature on photocatalytic degradation is not significant due to the low photonic activation temperature which is in the range of 20-80^{0}C (Herrmann 1999). However, an increase in photocatalytic reaction temperature (>80^{0}C) leads to promoting the e^-/h^+ recombination and decreasing the dissolved oxygen (DO) levels in water which result in low photocatalytic reaction rate. Additionally, higher temperatures promote desorption of organic pollutants from the photocatalyst surface before starting the reaction, again leading to low photocatalytic reaction rate (Naeem et al. 2010, Rincon and Pulgarin 2003). Naeem et al., (2010) investigated TiO_2 photocatalysed degradation of phenol, 4-Chlrophenol and 4-nitrophenol under different temperatures and concluded that increasing the reaction temperature does not significantly increase the photocatalytic degradation rate. On the contrary, some researchers noticed that there is enhancement in the photocatalytic degradation rate by increasing the reaction temperature. For instance, Sain and Shahrezaei (2012) photocatalytically degraded organic pollutants from petroleum refinery effluent and found that the rise of temperature from 20^{0}C to 45^{0}C can effectively reduce the reaction time of 60% COD removal from 100 min to 60 min. They also stated that this result is due to TiO_2 electron transfers in valance band to higher energy levels leading to increase of e^-/h^+ production, however; increasing the temperature above 45^{0}C can cause vaporisation of wastewater and change the effluent characteristics. Similar results were observed for removing phenol and phenolic compounds from petroleum refinery effluent by Shahrezaei et al. (2012).

2.4.2.2 pH

This parameter plays a significant role in the photocatalytic degradation of organic pollutants. This is due to the dependence of the adsorption and photocatalytic reaction of organic compounds onto the photocatalyst surface on the surface charge of TiO_2 by protonation or deprotonation as follows (Gaya and Abdullah 2008):

Acidic medium:

$$Ti\text{-}OH + H^+ \rightarrow Ti\text{-}OH^+_2 \quad (2.9)$$

Basic medium:

$$Ti\text{-}OH + OH^- \rightarrow TiO^- + H_2O \quad (2.10)$$

Generally, the photocatalytic efficiency of organic and phenolic compounds increases in acidic medium between 4 and 6 pH (Pino and Encinas 2012). This is due to the positively TiO_2 surface charged with iso-electric point pH_{pzc}=6.25 and the phenolate ion is negatively charged leading to more electrostatic attractions which help to increase the adsorption and degradation rates (Ding et al. 2000, Akbal and Onar 2003). Shahrezaei et al., (2012) pointed out that most of the organic pollutants in petroleum refinery effluent are phenol and phenolic compounds, which are negatively charged due to the OH groups, therefore; the photocatalytic degradation of these pollutants is favourable in acidic medium. Table 2.6 shows the influence of pH on the photocatalytic degradation of various phenols. Ahmed et al., (2010) reported that the photocatalytic degradation of 4-chlorophenol in the acidic pH can significantly enhance the degradation rate. Saien et al., (2012) stated that the maximum photocatalytic degradation efficiency for the removal of phenolic compounds in petroleum refinery effluent occurs at pH=3, however; the minimum removal efficiency is at pH=10. Some studies showed that the photocatalytic degradation of organic compound can be favoured by different pH values. For instance, Aceituno et al., (2002) noticed that the photocatalytic oxidation of metol (*N*-methyl-*p*-aminophenol) and its intermediates is favourable at pH values between 6 and 9. However, complete mineralisation was also obtained at acid pH values.

2.4.2.3 Photocatalyst loading

The concentration of photocatalyst is one of the main parameters which significantly affect the overall photocatalytic degradation rate of organic compounds. In general, the degradation rate increases with an increase in photocatalyst concentration due to the availability of active photocatalyst sites at higher doses resulting in the generation of more hydroxyl radicals (Ahmed et al. 2010). However, further increase of photocatalyst concentration beyond a certain limit leads to increase in turbidity and decrease the degradation rate due to light scattering (Ahmed et al. 2011).

Table 2.6 Influence of pH on the photocatalytic degradation of phenol and phenolic compounds presented in petroleum refinery effluent

Pollutant	Photocatalyst	Light source	pH range	Optimum pH	Ref.
Phenol	ZnO	Solar	3.0-11.0	5.0	(Pardeshi and Patil 2008)
Phenol	TiO_2	UV	3.0-9.0	5.0	(Kashif and OUYANG 2009)
Phenol	TiO_2	UV	2.0-10.0	3.2	(Ortiz-Gomez et al. 2007a)
Phenol	TiO_2	Solar	3.0-9.0	7.0	(Chowdhury et al. 2012)
Phenol+*m*-nitrophenol	TiO_2	UV	4.1-12.7	7.4	(Chiou et al., 2008b)
4-Chlorophenol	TiO_2	Solar/UV	2.0-10.0	5.0	(Alhakimi et al., 2003)
4-Chlorophenol	ZnO	UV	4.0-10.0	6.0	(Gaya et al. 2009)
4-Chlorophenol	NiO/H_2O_2	UV	4.0-10.0	7.0	(Alimoradzadeh et al. 2012)
4-Chlorophenol	TiO_2	UV	2.0-12.0	7.0	(Theurich et al., 1996)
4-Chlorophenol+2,6 -Dichlorophenol	TiO_2	UV	6.0-3.0	3.8	(Pino and Encinas 2012)
2,4-Dichlorophenol	ZnO	UV	5.0-10.0	6.0	(Gaya et al. 2010a)
2,4-Dichlorophenol	Fe/TiO_2	UV	2.0-10.0	4.0	(Liu et al. 2012b)
2-Chlorophenol and 2,4-Dichlorophenol	ZnO	Solar	4.0-10.0	6.0	(Ba-Abbad et al. 2013)
2,6-Dichlorophenol	TiO_2	UV	3.0-11.0	4.0	(Kansal and Chopra 2012)
Metol(*N*-methyl-*p*-aminophenol)	TiO_2/H_2O_2	UV	2.0-12.0	6.0-9.0	(Aceituno et al. 2002)
Hydroxylphenol+4-Nitrophenol+2,4-Dichlorophenol+2,4,6-Trinitrophenol	TiO_2	UV	2.0-10.0	3.0	(Ksibi et al., 2003b)
2-Chlorophenol+2-Nitrophenol	TiO_2	UV	2.0-11.0	3.0	(Wang et al. 1999)
Real petroleum refinery wastewater	TiO_2	UV	2.0-10.0	3.0	(Shahrezaei et al. 2012)
Real petroleum refinery wastewater	TiO_2	UV	2.0-10.0	3.2	(Saien and Shahrezaei 2012)
Real petroleum refinery wastewater	TiO_2	UV	2.0-10.0	4.0	(Shahrezaei et al. 2012)

Table 2.7 summarises the influence of different photocatalyst loading on the photocatalytic degradation of various phenol and phenolic pollutants. Marci et al., (2001) investigated the effect of ZnO loading in the range of 0.2 to 2.0 g/L on the photocatalytic oxidation of 4-nitrophenol under solar light. They found that the degradation rate above 2.0 g/L was stable and no significant change, however; at low concentrations the degradation efficiency increases up to 0.6 g/L. Bayarri et al., (2007) studied the influence of TiO_2 loading (0-2.0 g/L) on the photocatalytic degradation of 2,4-dichlorophenol using UV light. The maximum 2,4-dichlorophenol removal (80%) was achieved at 0.5 g/L of TiO_2 and further photocatalyst loading did not show significant degradation.

2.4.2.4 Initial pollutant concentration

Initial pollutant concentration is an important parameter in photocatalytic investigations. It is well known that the degradation efficiency decreases with increasing the initial concentration. This result can be clarified by the fact that, at high initial 4-CP concentration, the amount of 4-CP adsorbed on the photocatalyst surface increases leading to decrease active sites and •OH radical formation (Romero et al. 1999). Chiou et al., (2008) investigated the influence of phenol and m-nitrophenol initial concentrations on the photocatalytic degradation rate using UV/TiO_2. During 60 min irradiation, more than 90% of phenol is removed at 15.3 mg/L initial concentration, whereas only 42% of phenol is degraded during 60 min irradiation time when the initial concentration was 83.5 mg/L. This is due to the limited number of active sites on TiO_2 and more pollutant molecules need to be adsorbed on the photocatalyst surface. Ahmed et al., (2010) stated that high initial pollutant concentrations can lead to the formation of more intermediates which can be competitive substances for the main pollutant. The mathematical relationship between initial concentration and the reaction rate can be described by Langmuir-Hinshelwood (L-H) kinetic model (Mills and Morris 1993).

Table 2.7 Influence of photocatalyst loading on the photocatalytic degradation of phenol and phenolic pollutants

Pollutant	Light source	Photocatalyst	Optimum dose (g/L)	Ref.
4-Chlorophenol	UV	TiO_2	2.0	(Venkatachalam et al., 2007)
4-Chlorophenol	UV	ZnO	2.0	(Gaya et al. 2009)
4-Chlorophenol	UV	NiO	0.05	(Alimoradzadeh et al. 2012)
Phenol	UV	ZnO	2.0	(Chiou et al., 2008b)
Phenol	UV	TiO_2	2.0	(Hong et al. 2001)
Phenol	UV	TiO_2	0.2	(Kashif and OUYANG 2009)
Phenol	UV	Pr-TiO_2	1.0	(Chiou and Juang 2007)
2-Chlrophenol	UV	Co-TiO_2	0.01	(Barakat et al. 2005)
4-Nitrophenol	Solar	ZnO	0.6	(Marci et al. 2001)
2,4-Dichlorophenol	UV	TiO_2	0.5	(Bayarri et al. 2007)
2,4-Dichlorophenol	UV	ZnO	1.5	(Gaya et al. 2010a)
2,6-Dichlorophenol	UV	TiO_2	1.25	(Kansal and Chopra 2012)

2.4.2.5 TOC and COD Loadings

Concentrations of total organic carbon (TOC) and chemical oxygen demand (COD) are water quality parameters that give a general picture for the pollution of petroleum refinery effluent. TOC is defined as any compound containing carbon atoms except CO_2 and related substances such as carbonate, bicarbonate and the like. It includes all organic pollutants dissolved in water like hydrocarbons, benzene, and phenols. However, petroleum refinery effluent contains many different inorganic contaminants which cannot be measured using TOC. Chemical oxygen demand (COD) is the standard method for indirect measurement of the amount of pollutants that can be oxidized chemically. It is based on the chemical decomposition of organic and inorganic contaminants, dissolved or suspended in water. COD test indicates the amount of water-dissolved oxygen (mg/L) consumed by the

contaminants. The highly concentrated petroleum refinery effluent characterised by, low pH, brown colour, and high COD in the range of 80,000-1000,000 mg/L(Vineetha et al. 2013). COD has detrimental environmental impacts due to high oxygen demand and toxicity of the individual components such as phenols, cresols, sulfides, ammonia and cyanides. TOC and COD are useful for the design and the assessment of the treatment stages. However, these parameters cannot give the specific characterisation of the petroleum refinery effluent that is essential for choosing treatment methods.

2.4.2.6 Wavelength and Light intensity

Light is a source of energy for the photocatalysis process to initiate the degradation of contaminant and there is a relationship between the wavelength (λ) and the energy band-gap (E_b), which is the energy difference between the conduction band and valence band of a catalyst. This relation can be represented by Equation 2.11 (Gaya and Abdullah 2008).

$$\lambda = \frac{1.24 \times 10^3}{E_b} \tag{2.11}$$

Where E_b is the energy band gap (eV) and λ is the wavelength of light (nm).

Based on Equation 2.11, the photons of light must be equal to or greater than the energy ban-gap of the semiconductor photocatalyst. For instance, the energy band-gap of anatase TiO_2 is +3.2 eV. The wavelength to activate the oxidation can be calculated which is equal to about 400 nm. This wavelength is the ultraviolet (UV-A) range and as solar light contains 3-5% UV, it can be utilised in photocatalysis processes (Vinu and Madras 2011a).

The light intensity (Φ) depends on the photon energy flux, which is the energy of photons per second per unit area radiated on the suspension, and quantum yield of the photoprocess ($Q_{overall}$) . The overall quantum yield ($Q_{overall}$) of light absorbed by any photocatalyst is given in Equation 2.12 (Herrmann 2005):

$$Q_{overall} = \frac{\text{rate of reaction}}{\text{rate of absorption of radiation}} \tag{2.12}$$

The effects of light intensity on the photocatalytic degradation rate of organic pollutants are classified into three categories as follows (Vinu and Madras 2011a):

- At low Φ, the degradation rate is linearly proportional to Φ.
- At intermediate Φ, the degradation rate is proportional to $\Phi^{0.5}$.
- At high Φ, the degradation rate is independent of Φ, due to the saturation of photocatalyst surface, resulting mass transfer limitation.

Some attempts have been made in order to investigate the influence of light intensity on the photocatalytic of organic contaminants. For instance, Bayarri et al., (2005) experimentally estimated the radiation reached the photoreactor and the absorbed by TiO_2 for degradation of 2,4-dichlorophenol using an actinometric method. They stated that the increase of TiO_2 can lead to more radiation absorption by TiO_2 resulting in decrease the radiation absorption by the solution. Generally, the influence of light intensity on the photocatalytic degradation rate cannot be straightforward due to the effects of other parameters related to the process such as the photoreactor configuration and the photocatalyst loading.

2.4.2.7 Presence of anions and metal ions

Petroleum refinery effluent contains large amounts of anions such as carbonate (CO_3^{2-}), bicarbonate (HCO_3^{2-}), chloride (Cl^-) and sulphate ($SO_4^{\bullet-}$) which inhibit the photocatalytic degradation rate of organic pollutants. These anions adsorb onto the active sites of the photocatalyst leading to reduction in the generation of $^{\bullet}OH$ radicals and scavenge them by the anions as represented in the following Equations, (2.13-17) (Abdullah et al. 1990).

$$CO_3^{2-} + {}^{\bullet}OH \rightarrow CO_3^{\bullet-} + {}^{\bullet-}OH \quad (2.13)$$

$$HCO_3^- + {}^{\bullet}OH \rightarrow CO_3^{\bullet} + H_2O \quad (2.14)$$

$$Cl^- + {}^{\bullet}OH \rightarrow Cl^{\bullet} + OH^- \quad (2.15)$$

$$SO_4^{2-} + {}^{\bullet}OH \rightarrow SO_4^{\bullet-} + OH^- \quad (2.16)$$

$$SO_4^{\bullet-} + H_2O \rightarrow SO_4^{2-} + {}^{\bullet}OH + H^+ \quad (2.17)$$

The influence of these anions on the photocatalytic degradation of phenol and phenolic compounds is investigated by several researchers. Kashif and Ouyang (2009) studied the effect of chloride, carbonate, nitrate, and sulphate on the photocatalytic oxidation of phenol. They concluded that all of these inorganic anions inhibit the photocatalysis process, with order of $Cl^- > SO_4^{2-} > NO_3^- > CO_3^{2-}$. This negative impact due to their acting as scavengers for h_{VB}^+ and $^{\bullet}OH$ according to following equations.

$$Cl^- + {}^{\bullet}OH \rightarrow Cl^{\bullet} + OH^- \quad (2.18)$$

$$Cl^- + h_{VB}^+ \rightarrow Cl^{\bullet} \quad (2.19)$$

$$SO_4^{2-} + h_{VB}^+ \rightarrow SO_4^{\bullet-} \quad (2.20)$$

$$SO_4^{2-} + {}^{\bullet}OH \rightarrow SO_4^{\bullet-} + OH^- \quad (2.21)$$

Therefore, the adsorbed anions can significantly compete with organic pollutants for the adsorption on the photocatalyst surface leading to lower photocatalytic degradation efficiency.

The presence of metal ions such as Mg^{2+}, Cu^{2+}, Ca^{2+}, Fe^{2+}, and Fe^{3+} in petroleum refinery effluent also play different roles in the photocatalytic oxidation process. All of these transition metal ions enhance the photocatalytic degradation of organic contaminants except Cu^{2+} due to the increase of charge separation by accepting the conduction band electrons (Selvam et al. 2007). For instance, addition of Fe^{3+} ions effectively enhances the degradation of phenol and phenolic compounds due to electron scavenger effect that prevent the e^-/h^+ recombination and generate more $^{\bullet}OH$ radicals (Ahmed et al. 2010). Selvam et al., (2007) studied the influence of metal ions on the photocatalytic degradation of 4-flurophenol and found that the degradation efficiency in the following order: $Mg^{2+} > Fe^{2+} > Fe^{3+} > Cu^{2+}$.

2.4.2.8 Oxidants/electron acceptors

The main drawback of heterogeneous photocatalytic degradation processes using TiO_2 as photocatalyst is the e^-/h^+ recombination. This step can significantly leads to decrease the generation of •OH radicals, energy wasting and low efficiency. Therefore, there is a need to prevent this phenomenon in order to enhance the efficiency and reduce operating cost. Generally, molecular oxygen is used as an electron acceptor in heterogeneous photocatalytic reactions. In addition, proper electron acceptors such as $S_2O_8^{2-}$, BrO_3^-, and H_2O_2 are also used to enhance the oxidation efficiency of organic pollutants. These oxidants offer several advantages including the reduction of recombination, generating more $^{\bullet}OH$ radicals, and creating other oxidising species which improve the degradation efficiency of intermediate pollutants (Bahnemann et al. 2007). This enhancement to generate more $^{\bullet}OH$ radicals either by direct photolysis of H_2O_2 or by reacting with dissolved oxygen can be represented by Equations (2.22, 23).

$$H_2O_2 + h_v \rightarrow 2\,{}^{\bullet}OH \qquad (2.22)$$

$$H_2O_2 + O_2^{\bullet -} \rightarrow {}^{\bullet}OH + O_2 + OH^- \qquad (2.23)$$

Kashif and Ouyang (2009) studied the effect of H_2O_2, $S_2O_8^{2-}$, and BrO_3^- on the photocatalytic degradation of phenol. All of these oxidants enhanced the degradation efficiency in order of $BrO3^- > H_2O_2 > S_2O_8^{2-}$. Ahmed et al., (2010) reported that the photocatalytic degradation efficiency of organic pollutants in UV/TiO_2/oxidant processes is higher in an acidic medium than of a basic medium due to increase the ion reduction.

2.4.2.9 Effect of substituent group of phenolic compounds

The photocatalytic degradation rate of phenolic compounds is significantly affected by the type, number, and position of substituted groups on the aromatic ring. This effect can be investigated by comparing the initial degradation rates of each phenolic pollutant. Table 2.8 summarises the influence of phenolic substituted groups on the photocatalytic degradation rate of different phenolic pollutants. Ksibi et al., (2003) investigated the photocatalytic degradation of six phenolic substituted including hydroquinone (HQ), resorcinol (RS), phenol (Ph), 4-nitrophenol (4-NP),

Table 2.8 Influence of substituted groups on the photocatalytic degradation rate of different phenolic pollutants.

Pollutant	Light and Photocatalyst	The photocatalytic degradation order	Ref.
Hydroquinone (HQ), Resorcinol (RS), Phenol (Ph), 4-nitrophenol (4-NP), 2,4-dinitrophenol (2,4-DNP), 2,4,6-trinitrophenol (2,4,6-TNP)	UV/TiO_2	RS >Ph >4-NP >2,4-DNP >HQ >2,4,6-TNP	(Ksibi et al., 2003b)
4-chlorophenol (4-CP), 2-chlorophenol (2-CP), 2,4-dichlorophenol (2,4-DCP)	Solar/TiO_2	4-CP > 2-CP, > 2,4-DCP	(Karunakaran and Dhanalakshmi 2008)
Catechol (Cat), hydroquinone (HQ), Resorcinol (RS)	UV/TiO_2	Cat > HQ > RS	(Parra et al. 2003)
Phenol (Ph), Guaiacol (Gua), 2-chlorophenol (2-CP), Catechol (Cat)	UV/TiO_2	Cat > Ph ≈ 2-CP > Gua	(Ahmed et al. 2010)
p-fluorophenol (*p*-FP), *p*-chlorophenol (*p*-CP), Phenol (Ph), *p*-bromophenol (*p*-BP), *p*-iodophenol (*p*-IP).	UV/TiO_2	*p*-FP ≈ *p*-CP ≈ Ph > *p*-BP > *p*-IP	(Lapertot et al. 2006)
Pentachlorophenol (*p*-PCP), *o*-chlorophenol (*o*-CP), Trichlorophenol (TCP), Dichlorophenol (DCP), *p*-chlorophenol (*p*-CP), *m*-methylphenol (*m*-MP), *o*-methylphenol (*o*-MP), Phenol (Ph)	UV/TiO_2	*p*-PCP > TCP > DCP > *p*-CP ≈ *o*-CP > ≈ *m*-MP ≈ *o*-MP > Ph	(Sivalingam et al., 2004)
4-chlorophenol (4-CP), 3-methylphenol (3-MP), 2-chlorophenol (2-CP), 4-methylphenol (4-MP), 2-nitrophenol (2-NP), 3-nitrophenol (3-NP)	UV/TiO_2	4-CP > 2-CP > 3-MP > 4-MP > 2-NP > 3-NP	(Priya and Madras 2006b)
m-cresol, *o*-cresol, Phenol, *p*-cresol	Solar/TiO_2/H_2O_2	*m*-cresol > *o*-cresol > Phenol > *p*-cresol	(Adishkumar and Kanmani 2010)

2,4-dinitrophenol (2,4-DNP), 2,4,6-trinitrophenol (2,4,6-TNP).The degradation rate was found to decrease in the order as follows: RS >Ph >4-NP >2,4-DNP >HQ >2,4,6-TNP. This is due to the changed photoreactivity by electron withdrawing or electron donor depending on the position of the substituted group in the aromatic ring. Karunakaran and Dhanalakshmi (2008) studied the photocatalytic degradation of 4-chlorophenol (4-CP), 2-chlorophenol (2-CP), 2,4-dichlorophenol (2,4-DCP) using solar/TiO_2. They found that the degradation rate order as follows: 4-CP > 2-CP, > 2,4-DCP and stated that more chlorine atoms in the aromatic ring inhibits the degradation efficiency. Additionally, Cl^- might be adsorbed onto the photocatalyst surface during the degradation process reacting with electrons and holes leading to reduction of •OH radical. Priya and Madras (2006) studied the influence of substitution groups of six phenols; 4-chlorophenol (4-CP), 3-methylphenol (3-MP), 2-chlorophenol (2-CP), 4-methylphenol (4-MP), 2-nitrophenol (2-NP), and 3-nitrophenol (3-NP) on the photocatalytic degradation efficiency using UV/TiO_2. The degradation rate followed the order: 4-CP > 2-CP > 3-MP > 4-MP > 2-NP > 3-NP. They found that the degradation of chloromethylphenols is faster than chloronitrophenols due to the nature of substituent groups which plays more significant role than the position in phenolic structure.

2.4.3 Intermediates and mechanism

The photocatalytic degradation of organic pollutants produces some chemical intermediates before completing the mineralisation to CO_2 and H_2O. These intermediates can be more toxic and persistent than the original contaminants(Li et al. 1999). Five major types of intermediates can be formed during photocatalytic degradation of organic pollutants as follows (Malato et al. 2009):

- Hydroxylated and halogenated intermediates.
- Oxidation products.
- Intermediates yielded from opening aromatic rings.
- Intermediates of decarboxylation.
- Intermediates of isomerisation and cyclation.

Most of research studies collectively consider the total mineralisation of phenolic compounds as chemical oxygen demand (COD) or total organic carbon (TOC). This approach does not give good understanding for the degradation pathway and kinetic

models. However, some investigations regarding intermediates and reaction pathways have been implemented(Li et al. 1999, Li et al. 1999, Gaya et al. 2009, Gaya et al. 2010a, Gaya et al. 2010, Pardeshi and Patil 2008, Ba-Abbad et al. 2013, Aceituno et al. 2002, Svetlichnyi et al. 2001). Svetlichnyi et al., (2001) investigated the photolysis of phenol and para-chlorophenol and found that the introduction of a chlorine atom into the phenol molecule increases the efficiency of photolysis of *para*-chlorophenol by excitation in the long-wavelength absorption band. In addition, the first step in 4-CP degradation is the C-Cl bond cleavage and the main intermediate is hydroquinone (HQ). However, other researchers (Lipczynska-Kochany and Bolton 1991, Czaplicka 2006b) stated that the 4-CP degradation in aqueous solutions yield 1,4-benzoquinone (1,4-BQ) as shown in Figure 2.5. Several researchers stated that the pathway of chlorophenols degradation can be adsorption, dechlorination, hydroxylation and cleavage the aromatic rings to form inorganic products (Liu et al. 2012a, Araña et al. 2007b). Therefore, the qualitative and quantitative evaluation of the intermediates generated during the photocatalytic degradation of organic pollutants is a very hot topic and needs more attention.

2.4.4 Kinetic models for the photocatalytic degradation of organic pollutants

Generally, an approach to the kinetic study by assuming that the photocatalytic reaction follows a pseudo-first-order kinetics has been used (Rayne et al. 2009). Moreover, the previous studies have used two main kinds of kinetic models including the linear model according to first order kinetics and the Langmuir-Hinshelwood (L-H) non-linear model associated with adsorption processes of the photocatalytic pollutant on the catalyst surface (Ortiz-Gomez et al. 2008, Gomez et al. 2010). The form of L-H kinetic equation is given in Equation 2.24 (Rayne et al. 2009).

$$-r_i = -\frac{dC_i}{dt} = \frac{k_i K_i C_i}{1 + K_i C_i} \tag{2.24}$$

Where, $-r_i$ is the reaction rate of the component i being degraded, C_i is the concentration of component i, k_i is the reaction rate constant, K_i is the adsorption constant.

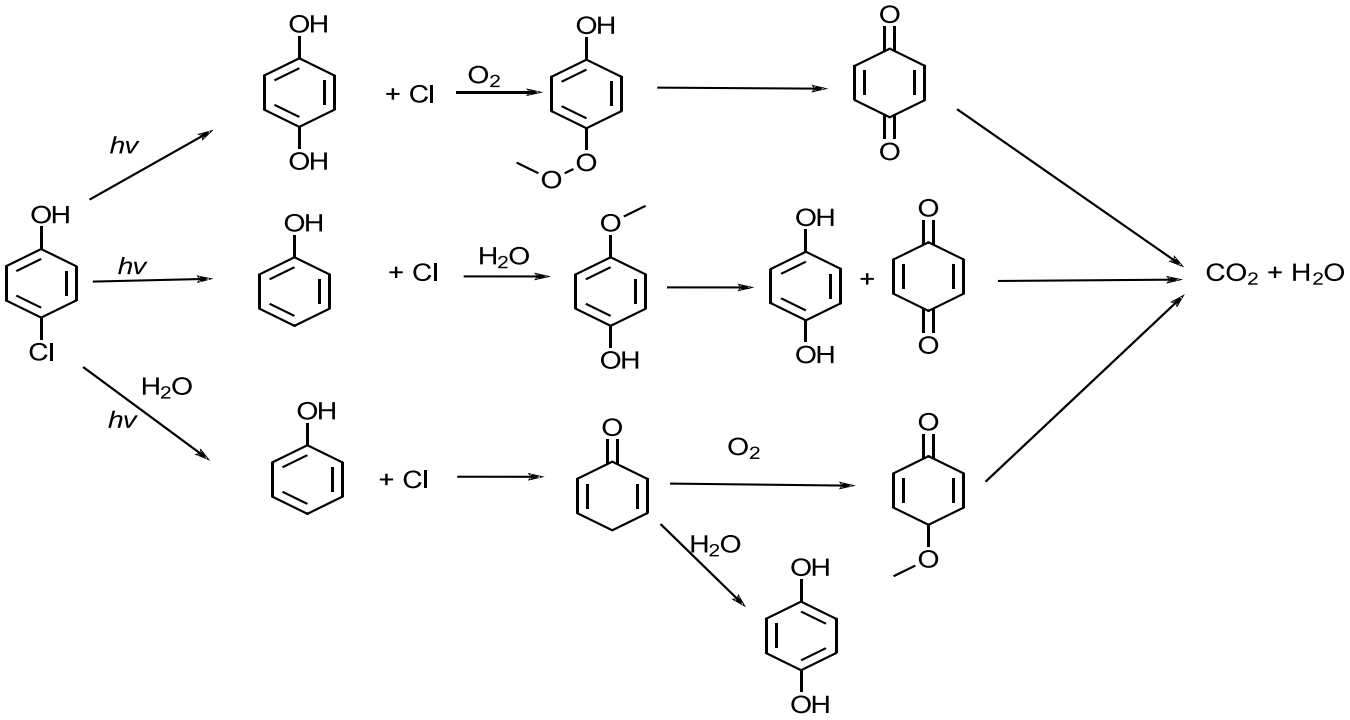

Figure 2.5 Possible degradation pathways of 4-CP (Svetlichnyi et al., 2001)

To estimate the parameters, Eq. (2.24) can be rewritten in reciprocal form and then plotted at various initial concentrations Eq. (2.25).

$$\frac{1}{-r_i} = \frac{1}{k_i} + \frac{1}{k_i K_i}\left(\frac{1}{C_i}\right) \tag{2.25}$$

Most of the kinetic reaction models reported in the literature deal with a single reactant chemical species. These proposed kinetic models for the photocatalytic degradation of organic compounds have been mainly obtained based on the initial rates method. This method does not consider the chemical intermediates species formed during the photoconversion process. Furthermore, when values of the initial rates are small, only a few experimental points will be considered as well as neglecting the intermediate species (Moreira et al. 2012). Nonetheless, some researchers have tried to propose several kinetic models including multi chemical species and suggesting the degradation mechanisms of these models (Li Puma et al. 2007, Gora et al. 2006). They used the L-H equation to estimate the values of the kinetic reaction constants for each of the chemical intermediate species as shown in Equation 2.26.

$$\frac{dC_i}{dt} = \frac{k_i C_i}{1 + \sum_{j=1}^{n} K_j^A C_j} \tag{2.26}$$

Therefore, the kinetic reaction models for the photocatalytic degradation of multi organic pollutants involving all observed intermediates are required in order to clearly understand the degradation mechanism as well as for scale-up purposes.

2.4.5 Enhanced photocatalytic degradation

The main drawback of the photocatalytic processes is the recombination of e^-/h^+ pairs leading to lower degradation efficiency (Salaices et al. 2004). To overcome this issue, many techniques have been applied mainly using TiO_2 (anatase, rutile or brookite) as the photocatalyst in order to enhance the photocatalytic degradation efficiency. Different AOPs have been applied such as $H_2O_2/TiO_2/UV$ (Stepnowski et al. 2002), Solar/TiO_2/photo-Fenton (Nogueira et al., 2004), $Ag^+/TiO_2/UV$ (Sclafani et al., 1991), Mg^{2+}/ZnO/UV (Selvam et al. 2007), $BrO^-_3/TiO_2/UV$ (Burns et

al. 1999), WO_3/UV (Sayama et al. 2010), and doping of photocatalysts with metals (Biyoghe et al. 2014, Znad and Kawase 2009, Selvam et al. 2007). Doping might not be economically feasible for large-scale applications due to the expensive chemicals used and the high calcination temperatures applied (Arana et al. 2001). The use of metals like iron ions (Fe^{2+}/Fe^{3+}) as additives in the photocatalytic process could reduce the operating cost as well as the experimental procedures. Different techniques have been developed and applied to enhance the photocatalytic degradation efficiency as follows:

2.4.5.1 Modified TiO_2

To increase the photoactivity of TiO_2, activated carbon have been used for the degradation of organic contaminants such as phenol (Matos et al. 2007, Matos et al., 1998) and 4-chlorophenol (Matos et al., 2001). The results showed that there was significant enhancement of the degradation efficiency due to the increase of TiO_2 surface area and absorbance of pollutants and their intermediates onto activated carbon surface, reducing the deactivation of TiO_2. Using activated carbon with TiO_2 can be implemented through two types including TiO_2 loaded on activated carbon and carbon-coated TiO_2. For instance, Zhong et al., (2009) used carbon-deposited TiO_2 to degrade 2,4-dichlorophenol and found the visible light degradation efficiency was remarkably increased due to enhanced absorptivity of TiO_2. Generally, the efficiency of loading TiO_2 on activated carbon is higher than that of carbon-coated TiO_2 (Di Paola et al. 2012).

2.4.5.2 N-doped TiO_2

One of the main disadvantages of TiO_2 is the wide band-gap which needs short wavelength of UV light (<388) leading to the limitation of employing the solar light. To reduce the band gap, a dopping of TiO_2 with N allows to extend the adsorption light from UV to the visible region by narrowing the band-gap of TiO_2 (Zhang et al. 2010). This type of doping can be conducted by various methods such as high-temperature exposure of TiO_2 to NH_3 and hydrolysis of titanium compounds with aqueous ammonia (Di Paola et al. 2012). In spite of the improvement still the photoactivity of TiO_2 under visible light is lower than that of UV light (Ma et al. 2010).

2.4.5.3 ZnO

Zinc oxide is one of the important binary oxides that can effectively decompose most organic pollutants. Several studies reported that ZnO was active under solar light for the photocatalytic degradation of organic compounds (Gaya et al. 2010b, Ba-Abbad et al. 2013, Shinde et al. 2011). Ba-Abbad et al., (2013) investigated the photocatalytic degradation of 2,4-dichlorophenol using commercial ZnO catalyst radiated under direct sunlight. They found that the complete degradation of the pollutant and its intermediates using 2 g/L ZnO was achieved at 120 min. Dhir et al., (2012) studied the influence of TiO_2 and ZnO on the degradation of 4-chlorocatechol and concluded that ZnO was more active than TiO_2. The optimum values of both photocatalysts were 1.5 g/L and 2.5 g/L respectively. Despite the high photoactivity of ZnO there are two crucial drawbacks including the occurrence of high photocorrosion and low susceptibility (Modirshahla et al. 2011). These issues have significantly limited its application in photocatalysis processes.

2.4.5.4 WO_3

WO_3 is one of the photocataysts that has been used to degrade many organic pollutants present in water. This photocatalyst can absorb light up to 459 nm which is higher than that of TiO_2 (388 nm) (Sayama et al. 2010). Gondal et al., (2007) investigated the influence of four semiconductors WO_3, TiO_2, NiO, and Fe_2O_3 on the degradation of phenol using pulsed laser irradiation. They concluded that the maximum removal of phenol from water was achieved with WO_3 due to its band-gap suitability and higher activity under laser irradiation. However, several studies reported that WO_3 has a low photoactivity under UV light to degrade organic pollutants due to the high recombination rate and low activity of electron transfer to O_2 (Sclafani et al. 1998, Di Paola et al. 2012).

2.4.5.5 Ag oxides

Silver oxides such as α-$AgGaO_2$ and β-$AgGaO_2$ are usually used as photocatalysts or additives due to their ability to destroy organic pollutants under UV or visible light. Singh and Uma (2009) investigated the photocatalytic degradation of 4-chlorophenol and methyl blue using $AgSbO_3$ under UV and visible light irradiation. The obtained results showed great degradation efficiencies for the organic pollutants under UV and visible light due to the electronic structure of the Sb^{5+} ion with Ag^{+}. However,

most of Ag-based oxides are very sensitive to the electronic structure making them quite expensive and not feasible.

2.4.5.6 H_2O_2 oxidant agent

The presence of oxidising agents such as H_2O_2 in wastewater has a positive effect on the degradation rate of the organic pollutants due to the more generations of hydroxyl radicals Eqs. (2.22-23). This activity of H_2O_2 can be increased in the presence of other metal ions such as ferrous and ferric ions. Adan et al., (2009a) studied the influences of two oxidants oxygen and hydrogen peroxide with TiO_2 on the photodegradation of phenol. They concluded that the TOC removal efficiency of the H_2O_2 oxidant was higher than that of O_2 oxidant agent and the photocatalytic reactions were favourable at pH 3. Aceituno et al., (2002) investigated the applicability of H_2O_2 to increase the efficiency of TiO_2 in order to degrade metol (*N*-methyl-*p*-aminophenol) under UV light. The results showed that 0.4 M H_2O_2 with 5 mg/L TiO_2 at pH 9 can significantly increase the degradation efficiency of metol and its intermediates. In addition, the high degradation was achieved at basic pH values avoiding the necessity of adjusting this key parameter for treatment. Chu and Wong (2004) reported that a low H_2O_2 dosage in photocatalysis using UV 300 nm can effectively enhance the degradation rate of dicamba by 2.4 times. Additionally, a neutral initial pH value was found to favour for using H_2O_2 in the photocatalysis at UV 300 nm. However, they stated that the use of H_2O_2 in the photocatalysis process is not recommended at 350 nm due to the low molar absorptivity of H_2O_2. Wei et al., (1990) studied the photocatalytic oxidation of phenol in the presence of hydrogen peroxide and titanium dioxide powders. Their results indicated that when the H_2O_2 to phenol molar ratio is above 12, a 1000 mg/L phenol solution can be completely degraded within 1 hr and TOC removal reaches 80%. The presence of iron oxides (Fe^{2+} or Fe^{3+}) with H_2O_2 in the suspension solution of photocatalytic degradation processes can effectively enhance the degradation rate due to more generation of $^{\bullet}OH$ radicals Eqs. (2.27-28).

$$H_2O_2 + Fe^{2+} \rightarrow Fe^{3+} + {}^{\bullet}OH + OH^- \quad (2.27)$$

$$H_2O_2 + TiO_2\,(e^-) \rightarrow TiO_2 + {}^{\bullet}OH + OH^- \quad (2.28)$$

However, excessive amounts of H_2O_2 significantly reduce the degradation efficiency of organic pollutants which is attributed to the consumption of $^{\bullet}OH$ radicals via H_2O_2 Eqs. (2.29-30). In addition, the high dose of H_2O_2 might absorb the incident UV light available for the photocatalysis process. (Vinu and Madras 2012):

$$H_2O_2 + {}^{\bullet}OH \rightarrow H_2O + {}^{\bullet}OOH \quad (2.29)$$

$$^{\bullet}OOH + {}^{\bullet}OH \rightarrow H_2O + O_2 \quad (2.30)$$

Therefore, appropriate concentrations of H_2O_2 in photocatalysis processes should be used for achieving the maximum photocatalytic degradation rates.

2.4.5.7 Iron oxides

Iron oxides are effectively used in different AOPs such as photo-Fenton and photocatalytic degradation processes due to their ability to oxidise and destroy organic pollutants. It is well known that iron doping can negatively affect the photoactivity of doped TiO_2 by increasing the thermal instability. In addition, the implementation of doping processes needs expensive facilities (Ahmed et al. 2011). Therefore, the use of these oxides (Fe^{2+}/Fe^{3+}) as additive in the photocatalytic oxidation of organic compounds has been reported in many studies (Kashif and Ouyang 2009, Rodríguez et al. 2009, Doong et al. 2000, Ortiz-Gomez et al. 2008). Such additivities have a potential alternative role to enhance the performance of photocatalytic degradation by inhibiting the e^{-}_{cb}/h^{+}_{vb} recombination rates and reducing the operating cost, thus; increase the oxidation efficiency. Additionally, using iron oxides such as ferrioxalate $[Fe(C_2O_4)_3]^3$, which is one of the iron sources, the higher portion of the solar spectrum can be used compared to TiO_2 due to its higher absorption which is 450 nm (Selvam et al. 2005). Selvam et al., (2005) investigated the influence of ferrrioxalate as a source of Fe^{3+} on the degradation of reactive Orange-4 using TiO_2 and solar light and found that the ferrioxalate in solar light can effectively work with small amounts of photocatalysts. Kim et al., (2005) studied the effect of ferric ion addition on photodegradation of alachlor in the presence of TiO_2 and UV radiation. They found that the rate constant of photodegradation of alachlor was enhanced by 80% at 7.5 mg/L Fe^{3+}. This result was due to the small band-gap of Fe_2O_3 (2.1eV) formed and covered TiO_2 (3.0 eV) during the irradiation time. Selvam et al., (2001) investigated the influence of metal

ions including Mg^{2+}, Fe^{3+}, Fe^{2+}, and Cu^{2+} on the photocatalytic degradation of 4-fluorophenol under UV light using TiO_2 or ZnO. Their results showed that there was a significant enhancement of the degradation efficiency by using metal oxides and TiO_2 and the order of activity was Mg^{2+}>Fe^{3+}> Fe^{2+}> Cu^{2+}. Bandara et al., (2001a) studied the photocatalytic oxidation of different chlorophenols on aqueous suspensions of α-Fe_2O_3 and α-FeOOH under visible light using TiO_2. α-Fe_2O_3 was more active for the degradation of chlorophenols than α-FeOOH due to the weak adsorption of chlorophenols on α-FeOOH hindering the activity of the electron-hole pair generated under light irradiation. The role of Fe^{2+}/Fe^{3+} ions in solar photocatalytic degradation processes strongly depend on several key parameters such as oxidation state, pH, and type of metallic salt used as a source of iron as well as the presence of other oxidants like H_2O_2 and O_2.(Kavitha and Palanivelu 2004). For instance, Nogueira et al.,(2005) investigated the influence of two different iron sources, $Fe(NO_3)_3$ and complexed ferrioxalate (FeO_x) on the solar photocatalytic degradation of organic compounds. They found that the efficiency of $Fe(NO_3)_3$ is less than that of FeO_x due to the presence of nitrogen leading to low quantum yield of Fe^{2+} generation. Generally, the presence of iron ions (Fe^{2+} or Fe^{3+}) can effectively enhance the photocatalytic degradation efficiency of organic compounds. However, there is a need to determine the residual iron at the end of degradation processes because the excess concentrations might negatively affect the aquatic life. Thus, minimum amounts of iron should be used in this kind of degradation or alternatively the residual amounts might be recovered and used again in the treatment system. Muthuvel and Swaminathan (2007) stated that there are no negative impacts on the catalytic activity when using recovered iron in the degradation processes. There has been strong debate about the role of iron ions in photocatalytic degradation processes and which one of them gives better degradation efficiency. As a result there is a need for further investigations and clarifications to conclude if there is a significant difference between Fe^{2+} and Fe^{3+} in the oxidation processes. Generally, the most effective chemical enhancers for the photocatalytic degradation of organic contaminants are iron oxides and hydrogen peroxide due to their strong abilities to mineralise and destroy most organic compounds present in petroleum refinery effluent. Table 2.9 summarises various enhancements of photocatalytic oxidations of organic pollutants using iron oxides and H_2O_2 agent.

Table 2.9 Various photocatalytic enhancements of organic pollutants using iron oxides and H_2O_2

Pollutant	Light and Photocatalyst	Oxidising agent	Optimum dose	Ref.
Phenol	UV/TiO_2	H_2O_2	0.3 M	(Wei et al., 1990)
Monochlorobenzene	UV/TiO_2	H_2O_2	22.5 mg/L	(Harbour et al., 1985)
Metol (*N*-methyl-*p*-aminophenol)	UV/TiO_2	H_2O_2	0.4 M	(Aceituno et al. 2002)
Phenol	UV/TiO_2/O_2	H_2O_2	28 mM	(Adán et al. 2009a)
Dicamba (2,5-Dichloro-6-methoxybenzoic acid)	UV/TiO_2	H_2O_2	4.94 mmol/L	(Chu and Wong 2004)
Citric acid	UV/TiO_2	H_2O_2	0.024 M	(Quici et al. 2007)
Microcystin-LR	UV/TiO_2	H_2O_2	0.02 M	(Cornish et al., 2000)
Oil-water emulsion	UV/TiO_2	$FeCl_2.4H_2O$ (Fe^{2+})	40 mg/L	(Tony et al. 2009)
Monuron (3-(4-chlorophenyl)-1,1-dimethylurea)	UV/TiO_2	$(Fe(ClO_4)_3.9H_2O$ (Fe^{3+})	0.0003 mol/L	(Měšťánková et al. 2005)
2-Chlorophenol	UV/TiO_2	$Fe_2SO_4.7H_2O$ (Fe^{2+})	100 mg/L	(Doong et al., 2000)
4-Fluorophenol	UV/TiO_2	$FeCl_2.4H_2O$ (Fe^{2+})	10 mg/L	(Selvam et al. 2007)
Bisphenol	Visible/TiO_2	α-Fe_2O_3 (Fe^{3+})	.005 M	(Rodríguez et al. 2010)
Alachlor(2-Chloro-N-(2,6-diethylphenyl)-N-(methoxymethyl)acetamide	UV/TiO_2	$FeCl_3$ (Fe^{3+})	7.5 mg/L	(Kim et al., 2005)
4-Chlorophenol	Solar/TiO_2	$Fe(NO_3)_3.9H_2O$ (Fe^{3+})	1.00 M	(Nogueira et al., 2004)
Phenol	UV/TiO_2	$Fe_2(SO_4)_3$ (Fe^{3+})	0.0005 M	(Sclafani et al., 1991)
Emergent contaminants (testosterone, bisphenol, acetaminophen)	UV/TiO_2/O_2	$FeCl_3$ (Fe^{3+})	0.004 M	(Rodriguez et al. 2012)
Phenol	UV/TiO_2	$Fe_2(SO_4)_3$ (Fe^{3+})	5 mg/L	(Ortiz-Gomez et al., 2008)

Table 2.9 *(Continued)*

Bisphenol	UV/TiO_2/Oxlic acid	Fe_2O_3 (Fe^{3+})	2 mg/L	(Rodríguez et al. 2011)

2.4.6 Pilot scale photo-catalytic reactors

Generally, photo-catalytic reactors can be classified into: slurry photoreactors such as compound parabolic collector (CPC) offering high contacting between pollutants and photocatalyst leading to high reaction rates. However, the photocatalyst cannot be recovered by using this kind of photoreactors, thus; increasing in operating costs. The other type of photo-catalytic reactors is an immobilised photoreactor such as cascade falling films photoreactors (CFFP) where the photocatalyst is supported on a fiber glass and it can be recovered and reused. For both types of reactors, it is better to use natural solar light instead of UV light as a irradiation source to make this process economically feasible. Herrmann (1999) studied the influence of both types of pilot-scale photorectors using natural solar light on the photocatalytic degradation of 4-chlorophenol Fig. (2.6). The surface of sun collector in both photoreactors was the same as well as the TiO_2 loading and initial concentration of 4-chlorophenol. Similar results in the total degradation of 4-chlorophenol as indicated by the TOC removal was obtained Fig. (2.6). He also stated that one of the drawbacks of solar photocatalysis of pilot plants is the fouling of supported glasses which is due to dust and atmospheric particles and to overcome this issue, an invisible thin layer of titania is used to coat the glass. Vargas and Núñez (2010) investigated the photocatalytic degradation of oil industry hydrocarbons models at laboratory and pilot-plant scale. They used three different photoreactors: batch bench reactor, tubular bench reactor, and tubular pilot-plant Fig. (2.7). They concluded that the tubular pilot-plant reactor was the most efficient of the three reactors tested and the total mineralisation achieved was 90% in 60 min at any pH used. The solar CPC system offers significant advantages including cost-effective, simplicity and easy to use and the high efficiency of collecting UV from sunlight (Malato et al. 2002). Saggioro et al., (2014) studied the solar CPC pilot-plant photocatalytic degradation of bisphenol A in wastewater using suspended and supported-TiO_2. The results showed that the suspension of 0.1 g/L of TiO_2 was efficient to remove 58% of TOC from real wastewater, however; supported-TiO_2 has the advantage of avoiding the photocatalyst removal step leading to reduce the treatment cost. CPCs are mostly used at pilot-scale applications due to their effective ability to collect sunlight and simplicity of design.

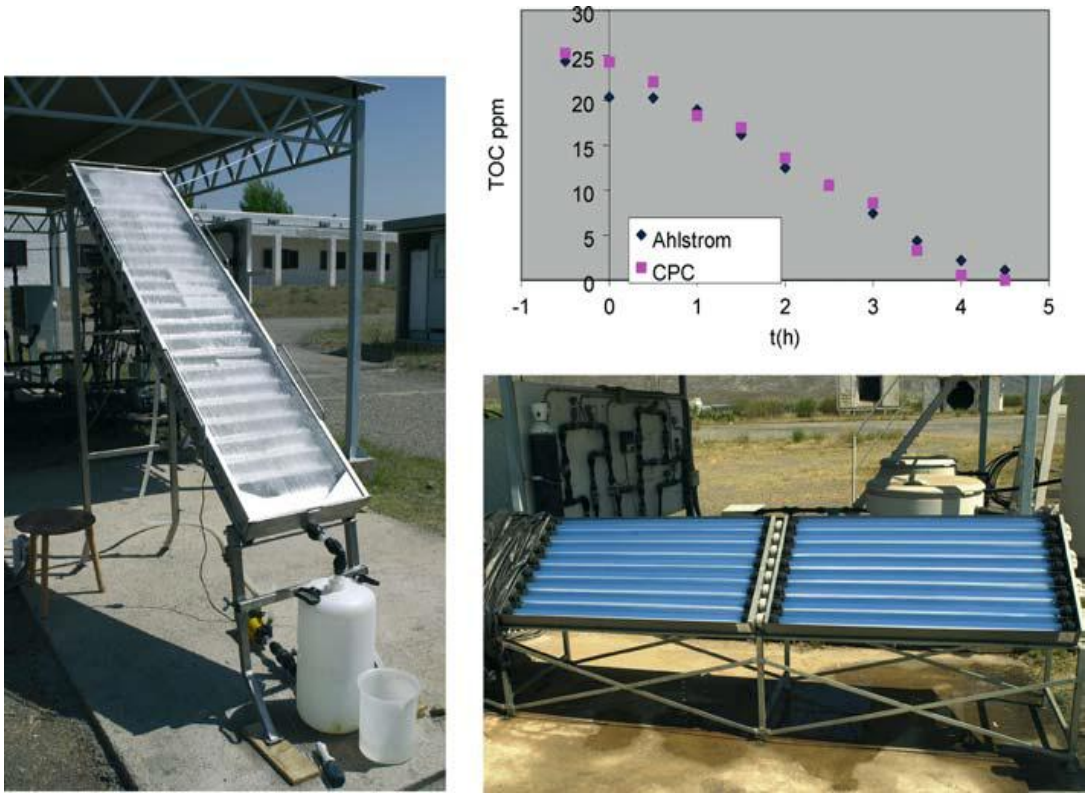

Figure 2.6 Comparison of the activities of titania photocatalysts used (i) in a compound parabolic collector (CPC) slurry photoreactor (picture bottom right) and (ii) in a cascade falling films photoreactors (CFFP) using a titania fixed bed deposited on an Ahlstrom paper (picture bottom left). The photocatalytic activity is based on the rate of TOC removal from a solution containing 50 mg/L of 4-CP chosen as a model pollutant (Herrmann 1999).

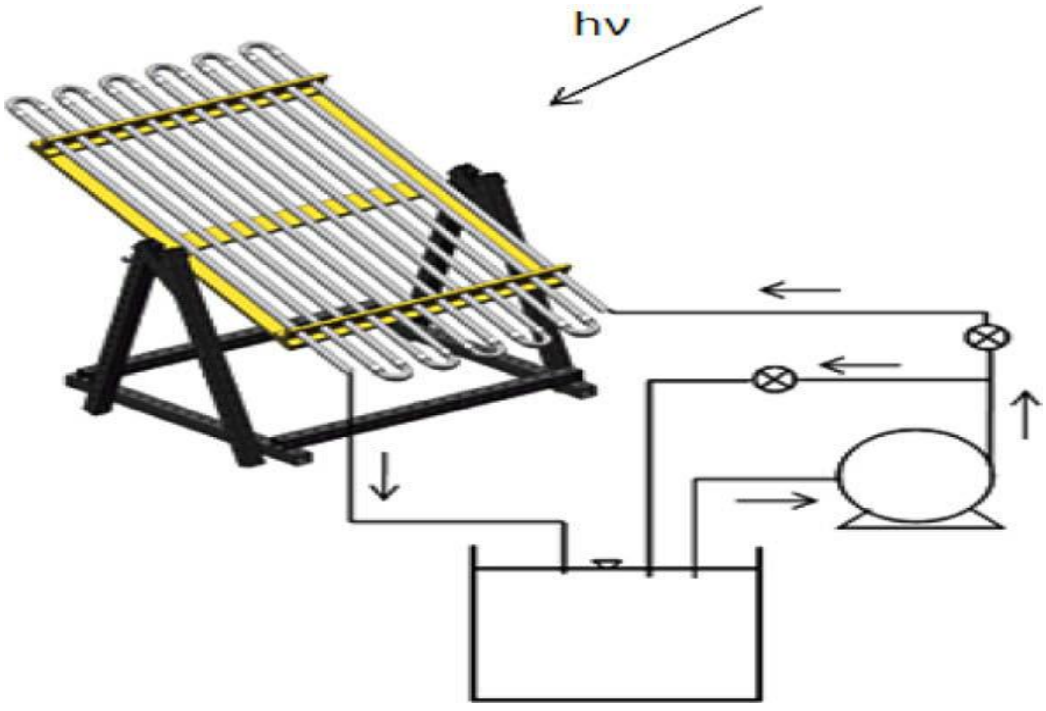

Figure 2.7 Tubular pilot-plant design (Vargas and Núñez 2010)

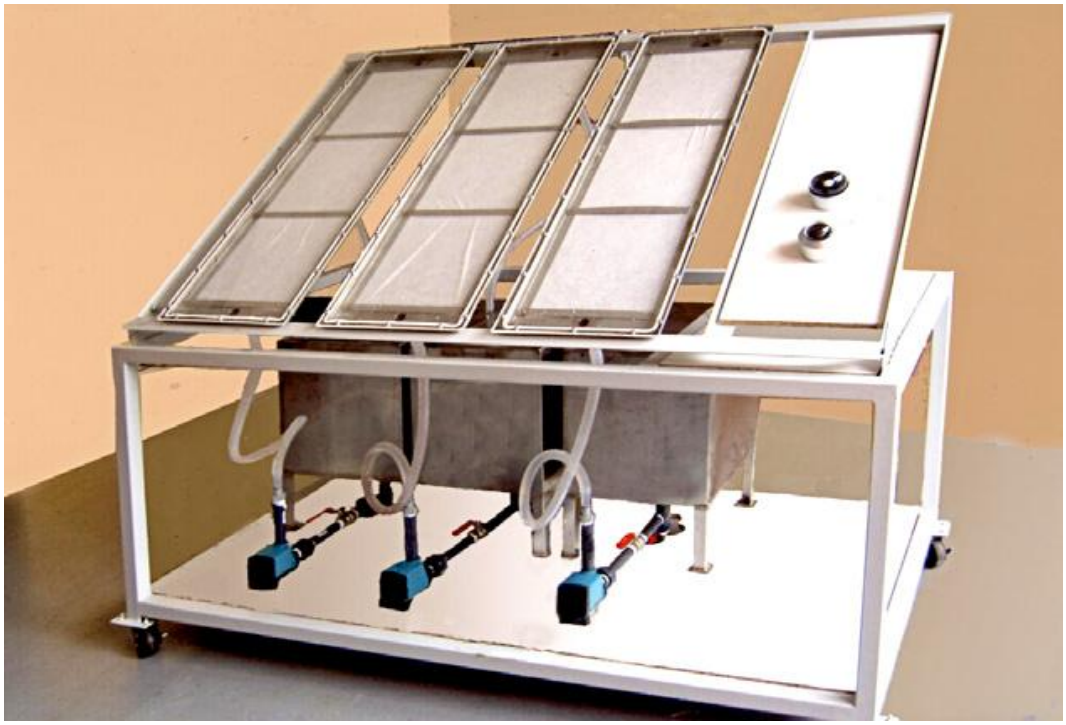

Figure 2.8 Solar photocatalytic reactor (Janin, et al., 2013)

Janin et al., (2013) investigated the solar photocatalytic mineralisation of 2,4-dichlorophenol at a pilot-plant scale using immobilised TiO_2 (Fig. 2.8). This photoreactor was able to remove 70% of TOC from the wastewater in 12 h. They reported that the capacity of the reactor for treating large amounts of extremelly polluted wastewater can be performed at low operating cost. Bayarri et al., (2013) compared the laboratory and pilot-plant performance of 2,4-dichlorophenol solar photocatalytic degradation using UV lamp and solar CPC respectively Fig. (2.9). They concluded that the TOC degradation was much faster at the pilot-plant which might be due to the high radiation flux density used in laboratory set-up leading to higher the e^-/h^+ recombination. Several attempts have been implemented to combine two of AOPs such as photo-Fenton process and photocatalytic oxidation for treating polluted water.

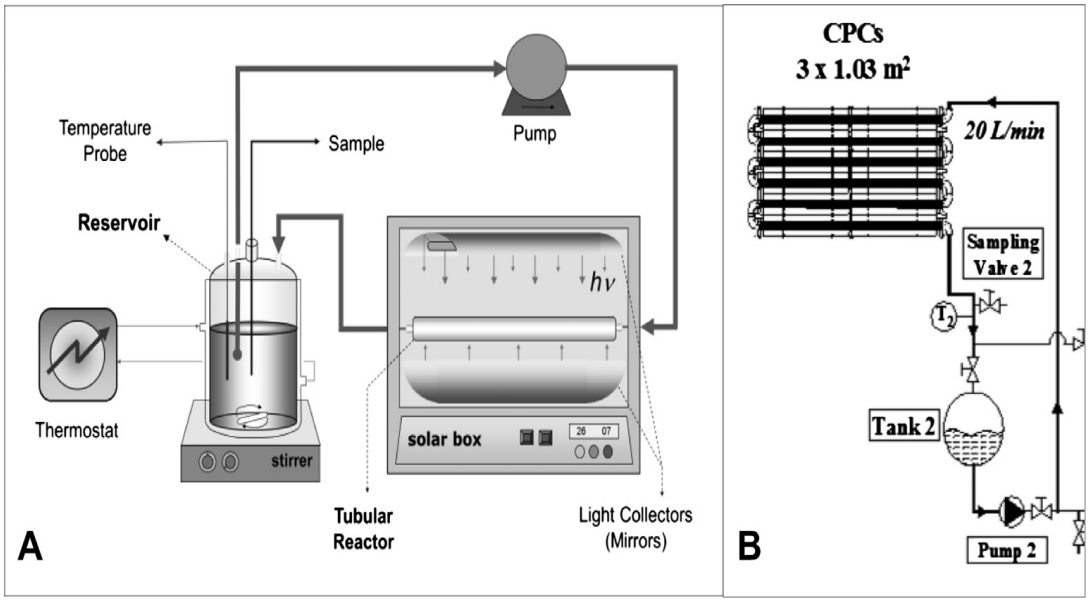

Figure 2.9 Laboratory set-up (A) and pilot set-up (B) (Bayarri, et al., 2013)

Pineda Arellano et al., (2013) used a two step treatment of photo-Fenton process followed by susppended TiO_2 photocatalysis to degrade Atrazine (herbicide) Fig. (2.10). The total volumes of photo-Fenton and photocatalysis reactors were 100 L and 60 L respectively and the initial TOC for both was 19 mg/L. The results showed that photo-Fenton process followed by TiO_2 photocatalysis produced 72% of mineralisation of TOC in 6 h irradiation time.

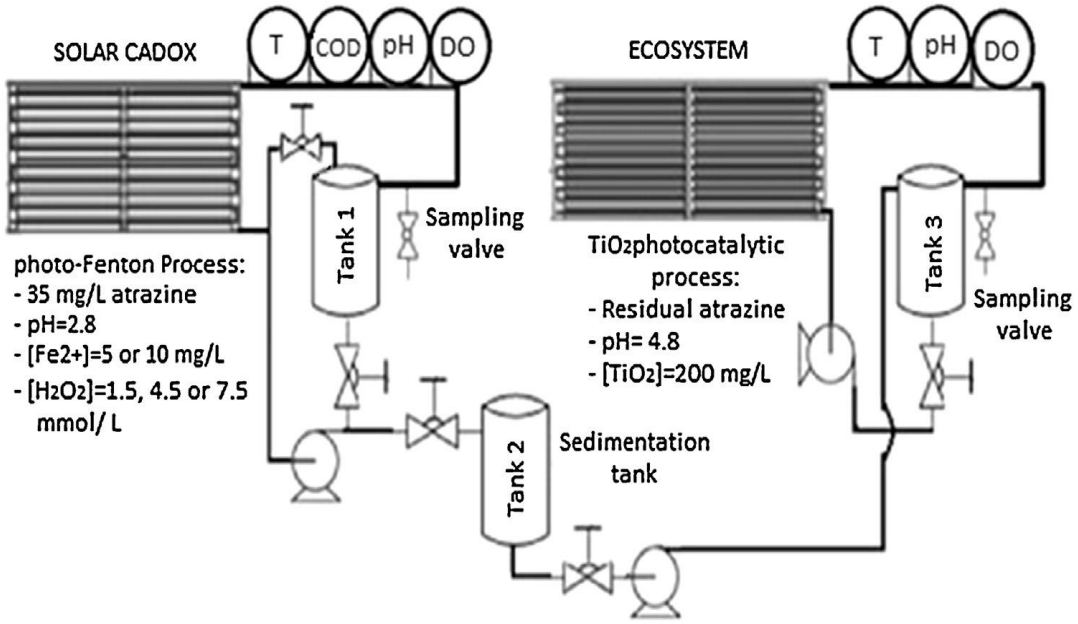

Figure 2.10 Schematic diagrams of the couple solar reactors systems (Pineda et al., 2013)

Gernjak et al., (2004) also investigated the pilot-plant treatment of olive mill wastewater by solar TiO_2 photocatalysis and solar photo-Fenton using two pilot-plant reactors: CPC and an open non-concentrating Falling Film Reactor (FFR) Fig. (2.11). The comparison of two AOPs showed that photo-Fenton method successfully removed 85% COD and 100% of phenol index of olive mill wastewater with different initial concentrations and from different sources. Moreover, the degradation efficiency of CPC was slightly higher than that of FFR due to the unstable homogeneity of the falling film during strong wind. According to the literature review, it seems that CPCs are more efficient and most commonly used pilot-plant reactors.

Figure 2.11 Falling Film Reactor (FFR) (Gernjak et al., 2004)

Table 2.10 summarises the performance summary of CPCs utilizing solar irradiation for wastewater treatment. According to the literature mentioned above, CPCs technology are currently most suited for operation at pilot scale due to the significant knowledge and experience in the design of these reactors. Additionally, the reflector geometry of CPCs can effectively allow indirect light to be reflected onto the absorber tube surface which can be useful to work on cloudy days. However, other pilot-scale reactors such as CFFP and FFR demonstrated to be effective designs but

are still for small operations. Generally, scale-up of the photocatalytic degradation technology is hindered by several significant technical issues that need to be further investigated. For instance, the ability of the photocatalytic degradation to be a stand-alone treatment or it has to be a pre-treatment step to enhance biological wastewater treatment. Another interesting issue is the limited volume capacity of the photoreactors which makes the treatment unfeasible. To promote this kind of wastewater treatment to be feasible in the future, several technical obstacles have to be overcome including (i) development of photocatalysts that can gain a high photo-efficiency to utilise natural solar light; (ii) immobilisation of photocatalysts to reduce the cost of catalyst separation (iii) using effective chemical enhancers to increase the degradation efficiency (iv) effective design of photocatalytic reactors for high collection of solar energy to reduce electricity costs. Pilot-plant investigations with various photoreactor configurations are required to promote this technology to be feasible. Finally, the photocatalytic degradation process using natural solar light and low site area requirements promises to be an effective and feasible wastewater treatment technology.

Table 2.10 Performance summary of CPC photoreactors using solar irradiation for wastewater treatment

Pollutant			Photocatalyst					
Type	Initial Conc	Volume (L)	Type	Conc (g/L)	Statue	Final Conc	Time (h)	Ref.
4-Chlorophenol	20 mg/L	247	TiO_2 (P-25)	0.2	Supported	11 mg/L	1	(Fernandez-Ibañez et al., 1999)
Oxalic acid	10 mM	10	TiO_2 (P-25)	0.5	Suspended	1.5 mM	2	(Bandala et al. 2004)
2,4-Dichlorophenol	50 mg/L	247	TiO_2 (P-25)	0.2	Suspended	2.5 mg/L	3.7	(Malato et al. 1997)
Lincomycin (antibiotic)	75 µM	39	TiO_2 (P-25)	0.2	Suspended	0.0 µM	2	(Augugliaro et al. 2005)
Municipal wastewater	200 mg/L	35	TiO_2 (P-25)	0.2	Suspended	80 mg/L	5	(Kositzi et al. 2004)
Formetanate (pesticide)	50 mg/L	35	TiO_2 (PC-500)	3	Suspended	0 mg/L	2	(Thu et al. 2005)
Dichloroacetic acid	57.8 mg/L	159	TiO_2 (P-25)	5	Suspended	30.4 mg/L	4	(Dillert et al. 1999)
Real wastewater	50 mg/L	40	TiO_2 (P-25)	3	Suspended	5 mg/L	3	(Gernjak et al. 2004)
Atrazine (herbicide)	19 mg/L	60	TiO_2 (P-25)	0.2	Suspended	5.32 mg/L	6	(Pineda et al. 2013)
2,4-Dichlorophenol	125 mg/L	35	TiO_2 (P-25)	0.5	Suspended	30 mg/L	10	(Bayarri et al. 2013)
2,4-Dichlorophenol	25 mg/L	50	TiO_2 (P-25)	0.1	Suspended	6 mg/L	7.5	(Janin et al. 2013)
Bisphenol A	20 mg/L	32	TiO_2 (P-25)	0.6	Supported	3 mg/L	4	(Saggioro et al. 2014)

2.5 Conclusions

The following are the conclusions of this chapter:

- Phenol and phenolic compounds such as 4-chlorophenol and 2,4-dichlorophenol are some of the major toxic pollutants present in petroleum refinery effluent. These contaminants negatively affect human, animal, and the aquatic environment.

- Photocatalytic degradation is a potential treatment for complete mineralisation of organic pollutants present in water. Using solar light and TiO_2 photocatalyst can effectively reduce operating cost. To further enhance this technology, some oxidants such as H_2O_2 and metal ions like Fe^{+3} are recommended.

- More work on the photocatalytic degradation of multi organic compounds system is needed. Therefore, the solar photocatalytic degradation of chlorophenols has been experimentally analysed in this study. This would give more realistic approach to treat real petroleum refinery effluent.

- The qualitative and quantitative evaluation of the intermediates generated during the photocatalytic degradation of organic pollutants is very hot topic and need more attention.

- Most of kinetic studies in the literature deal with simple approaches and single pollutant. However, the photocatalytic degradation of organic contaminants should cover all chemical species including more than one pollutant and all the intermediates formed.

- The possible application of the photocatalytic technology for the industry is still under investigation at pilot-plant scale.

- Solar-driven, photoreactor configurations, and low site area requirements are the key parameters to promote the photocatalytic degradation technology for large scale operation.

CHAPTER 3

EXPERIMENTAL METHODS

3.1 Introduction

This chapter describes the experimental procedure and equipment used in this PhD research project. Moreover, the chemicals and the analytical methods for the identification and quantification of the pollutants and their intermediates are also reported.

3.2 Materials

The following chemicals were used as received without any further treatment: 4-Chlorophenol (4-CP, 99%), 2,4-Dichlorophenol (2,4-DCP 98%), Hydroquinone (HQ, 98%), 4-Chlorocatechol (4cCat, 99%), Phenol (Ph, 99%), Benzoquinone (BQ, 98%), Hydrogen peroxide (H_2O_2, 30w/w%), Hydrochloric acid (HCl, 32%), Ferrous sulphate hydrate ($FeSO_4$. $7H_2O$, 99%), chloride hexahydrate ($FeCl_3 \cdot 6H_2O$, 97%) and Titanium (IV) oxide (TiO_2-P25, 99.7% anatase). All these chemicals were purchased from Sigma-Aldrich. Table 3.1 shows the names, abbreviations and chemical structures for the organic compounds used in this study.

3.3 Solar-photocatalytic degradation experiments

All experiments of synthetic samples were conducted using a 1 L Pyrex glass beaker as a reactor, equipped with a magnetic stirrer. Solar Simulator (Sun 2000 210 × 210 mm, Abet Technologies Model 11044) was employed as a source of light as shown in Figure 3.1. The light intensity of Solar Simulator was 1000 mW/cm^2. The pH values of the solutions were monitored using a pH meter (SP-701LI 120).

Table 3.1 Names, abbreviations and chemical structures for the organic compounds used in this study

Name	Abbreviation	Chemical Structure
4-Chlorophenol	4-CP	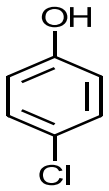
2,4-Dichlorophenol	2,4-DCP	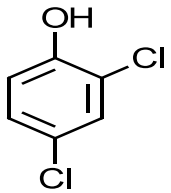
Hydroquinone	HQ	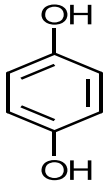
4-Chlorocatechol	4-cCat	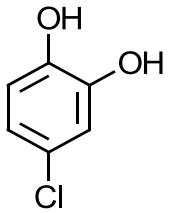
Phenol	Ph	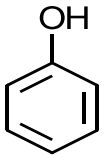
Benzoquinone	BQ	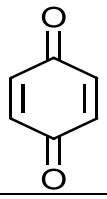

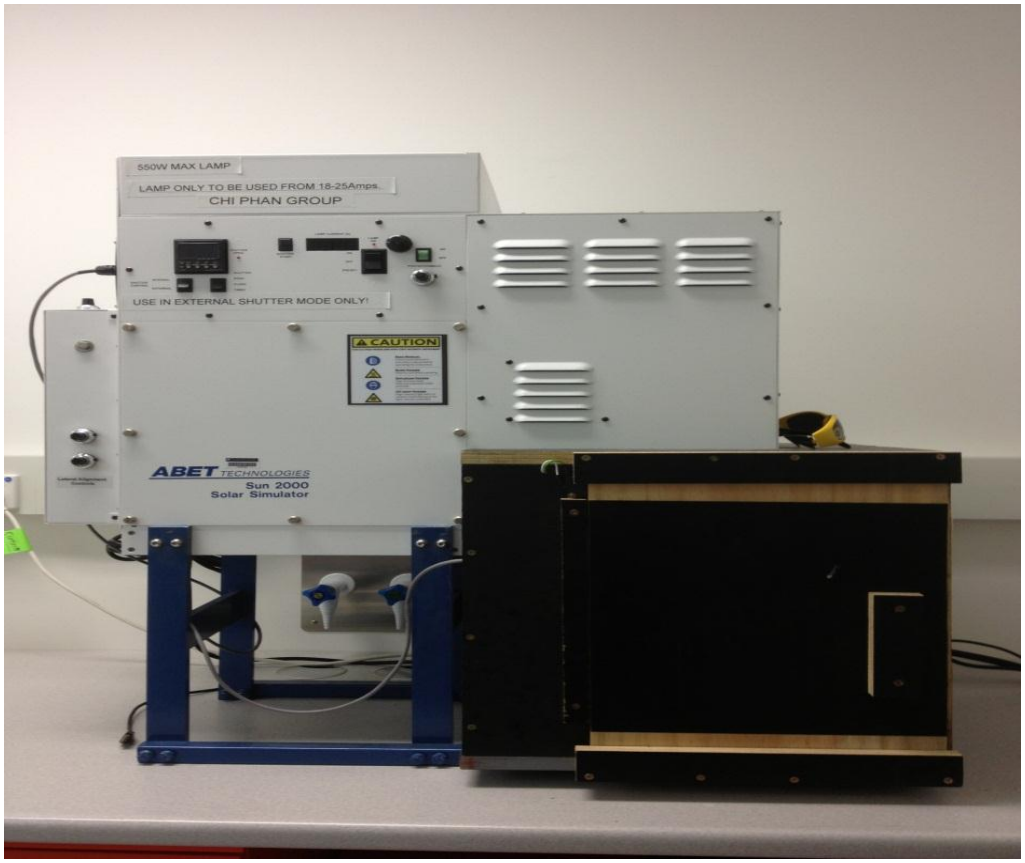

Figure 3.1 Solar simulator (1000mW/cm^2) used for solar photocatalytic degradation experiments

3.3.1 Solar photocatalytic degradation of 4-Chlorophenol

In order to investigate the effect of initial concentration, different 4-CP concentrations (25, 50, 75 and 100 mg/L) were used. The suspensions were magnetically stirred in the dark for 30 min to attain adsorption–desorption equilibrium between 4-CP and 0.5 g/L TiO_2. Then, the suspensions were exposed to solar light for 180 min. At specific time intervals (30 min), 5 mL was withdrawn and filtered by PTFE 0.45-μm membrane filters to separate the catalyst particles for HPLC analysis.

3.3.2 Solar photocatalytic degradation of combined chlorophenols mixture

Different concentrations of 4-CP and 2,4-DCP (individually and combined) were investigated under solar light using 0.5g/L of TiO_2 as photocatalyst. First, different 4-CP and 2,4-DCP concentrations (25, 50, 75, 100 mg/L) were individually investigated at the same conditions (0.5g/L TiO_2 and 1000 mW/cm^2). For combined mixtures degradation, an equal amount (50 mg/L each) of 4-CP and 2,4-DCP was

dissolved in distilled water and transferred to the photoreactor before adding TiO_2. All suspensions were magnetically stirred in the dark for 30 min to attain adsorption-desorption equilibrium between chemical components and TiO_2. At specific time intervals (30 min), 5 mL and 15mL were withdrawn and filtered by PTFE 0.45 µm membrane filters to separate the catalyst particles for HPLC and TOC analysis. To determine the adsorption constants *K* for 4-CP, 2,4-DCP and their intermediates, different concentrations of each component were used. After adding 0.5g of TiO_2, the reacting solution was left running in the dark for 60 min in order to reach adsorption equilibrium. Then a sample was taken for measuring the equilibrium concentration (C_e) which will be used to calculate the adsorption capacity (Q_e).

3.3.3 Solar photocatalytic degradation of combined chlorophenols mixture using iron ions and hydrogen peroxide

Combined chlorophenols mixture (50 mg/L each of 4-CP and 2,4-DCP) was degraded under solar light using TiO_2, $FeCl_3 \cdot 6H_2O$, $FeSO_4 . 7H_2O$, and H_2O_2. A Pyrex glass beaker of 15.5 cm height and 11 cm diameter was employed as a reactor, equipped with a magnetic stirrer, and the volume of suspension used was 1 L. The experiments were conducted using Solar Simulator (Sun 2000 210 × 210 mm, Abet Technologies Model 11044) to irradiate the reactor. The light intensity of the Solar Simulator was 1000 mW/cm^2. The pH values of the solutions were monitored using a pH meter (SP-701LI 120). The combined mixture was dissolved in distilled water and transferred to the photoreactor before adding TiO_2. After that, the photocatalyst 0.5 g/L TiO_2 and the desired amounts of ferric ions ($FeCl_3 \cdot 6H_2O$) and/or H_2O_2 were suspended in 200 mL and then added to the mixture. All suspensions, which contain TiO_2, were magnetically stirred in the dark for 30 min to attain adsorption−desorption equilibrium between chemical components and TiO_2. Then, the lamp was turned on, and the timer was set to zero to start measuring the reaction time. All experiments were carried out at room temperature (26 ± 1°C). At specific time intervals of 30 min, 5 mL was withdrawn and filtered by PTFE 0.45 µm membrane filters to separate the catalyst particles from the liquid phase, and then the composition of the liquid phase was analysed by HPLC. The same procedures were conducted using ferrous ions ($FeSO_4 . 7H_2O$) instead of ferric ($FeCl_3 \cdot 6H_2O$). The photocatalytic degradation efficiency of each compound at different irradiation times was calculated using Equation 3.1

$$\eta(\%) = \frac{C_0 - C_t}{C_0} \times 100 \quad (3.1)$$

Where η is the degradation efficiency, C_0 is the initial concentration, and C_t is the concentration of the compound at any irradiation time.

3.3.4 Solar-photocatalytic degradation of real petroleum refinery effluent

Petroleum refinery effluent samples (Fig. 3.2) were collected from British Petroleum (BP) Kwinana Refinery located in Western Australia (32.2295° S, 115.7649° E) (Fig. 3.2). The samples were taken from the outlet of the Dissolved Air Flotation (DAF) system and before sending it to the Biological Treatment Unit (BTU). Upon arrival, all samples were stored at 5 ^{0}C. The samples were characterised before the experiments to obtain their chemical and physical properties. The characterisation of the petroleum refinery effluent samples is shown in Table 3.2.

Table 3.2 Chemical characteristics of Kwinana Refinery wastewater

Parameter	Value
Colour	Brown
pH	9.1
Turbidity (NTU)	7.4
COD (mg/L)	840
TOC (mg/L)	120
TDS (mg/L)	1750

The colour of the samples was slightly dark brown due to the some traces of oil. The pH samples of effluent samples used in the experimental studies was 9.1. The COD and TOC concentrations of the samples were 840 and 120 mg/L respectively. The solar-photocatalytic degradation of these samples was carried out using different concentrations of TiO_2, Fe^{2+}, and Fe^{3+} as well as various pH. All experiments were conducted using a 250 mL Pyrex glass beaker as a reactor, equipped with a magnetic stirrer. COD was the indicator for measuring the degradation efficiency of the samples.

Figure 3.2 Petroleum refinery effluent samples

3.4 HPLC Analysis

4-CP, 2,4-DCP and their intermediates were identified and quantified by High Performance Liquid Chromatograph (HPLC) analysis (Fig. 3.3). Detection of 4-CP and 2,4-DCP was done at 265nm and 275 respectively, using a Varian Prostar 210 chromatograph with UV-vis detector and a C18 reverse phase column (25cm x 4.6mm x 5µm). The mobile phase was a mixture of 30 % acetonitrile and 70 % water with a flow rate of 1 mL/min. The temperature of the column was kept at 25^{o} C throughout all the analysis. Injection volume for all samples was 5 µL. The identification of the intermediates by HPLC was performed by the comparison of the retention time of the peak in the discharged sample with that in the standard sample (see Appendix B). The concentrations of compounds were calculated using the equations derived from the calibration measurements for authentic samples.

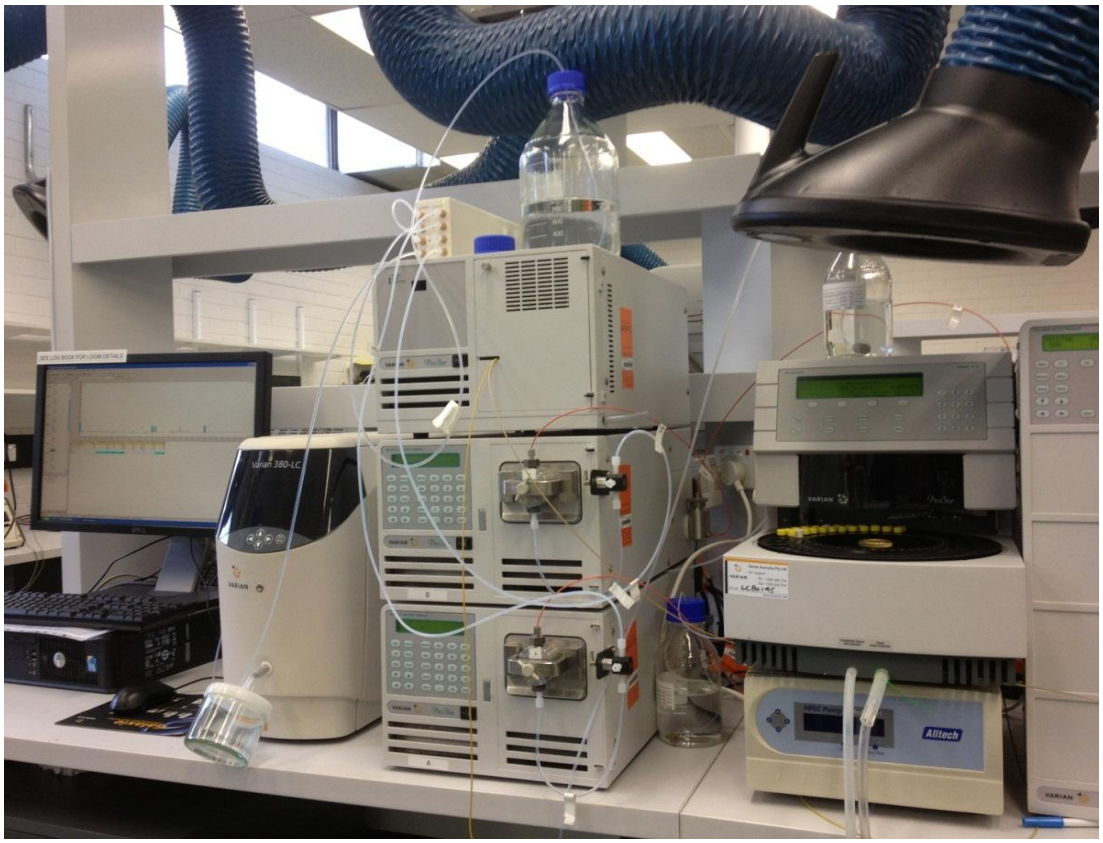

Figure 3.3 High Performance Liquid Chromatograph (HPLC)

3.5 TOC Analysis

To measure the Total Organic Carbon (TOC) in each sample, Total Organic Carbon Analyser (Shimadzu TOC-VCPH) was used (Fig. 3.4). Prior to sample injection into the TOC, the samples (15mL each) were filtered by PTFE 0.45 µm membrane filters to separate the catalyst particles.

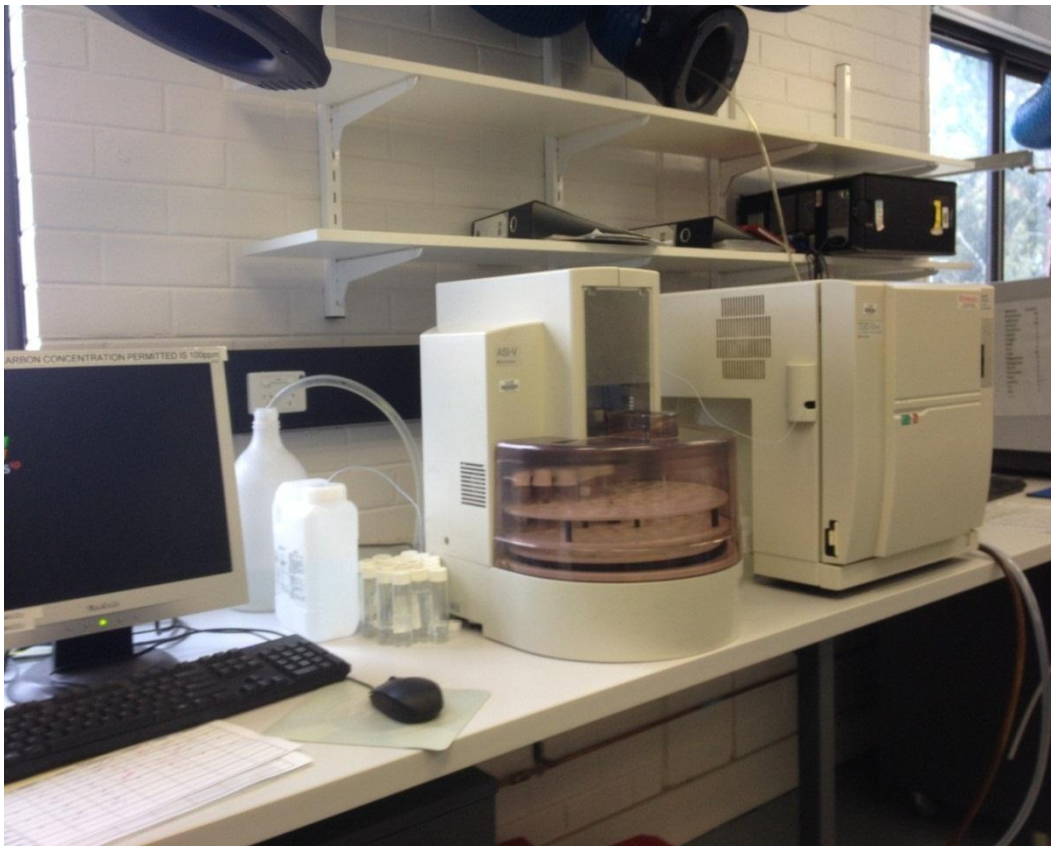

Figure 3.4 Total Organic Carbon (TOC) Analyser

3.6 COD and Fe Analysis

A DR/2400 HACH spectrophotometer was used to measure COD which follows the standard procedure of sample digestion (Fig. 3.5). The mg/L results are defined as the mg of O_2 consumed per litre of sample under conditions of this procedure. In this case, the sample is heated for two hours with a strong oxidising agent, potassium dichromate leading to reduce the dichromate ion ($Cr_2O_7^{2-}$) to green chromic ion (Cr^{3+}). Then, the amount of Cr^{3+} produced is determined. The COD reagent also contains silver and mercury ions. Silver is a catalyst, and mercury is used to complex the chloride interference. This equipment was also used to determine the concentration of Ferric and Ferrous (Phenanthroline method) in the solution at

different irradiation times. The 1,10-phenanthroline indicator in Ferrous Iron Reagent reacts with ferrous iron (Fe^{2+}) in the sample to form an orange colour in proportion to the iron concentration, however; ferric iron does not react. The ferric iron (Fe^{3+}) concentration can be determined by subtracting the ferrous iron concentration from the results of a total iron test.

Figure 3.5 A DR/2400 HACH spectrophotometer

CHAPTER 4

SOLAR PHOTOCATALYTIC DEGRADATION OF 4-CHLOROPHENOL: MECHANISM AND KINETIC MODEL

4.1 Introduction

This chapter deals with the solar photocatalytic degradation of 4-chlorophenol (4-CP) and reports a mechanism and kinetic model of this pollutant and its intermediates using 0.5 g/L TiO_2 as a photocatalyst. Furthermore, to obtain more details about the photocatalytic reaction pathway and the kinetic model, a set of experiments was carried out using the major intermediates (HQ and 4cCat) as model reactants. The adsorption constants of 4-CP and its intermediates were obtained experimentally to minimise the number of variables and give more accuracy to the kinetic model. The reaction mechanism for the photocatalytic degradation of 4-CP is proposed. The first section of this chapter reports the degradation profiles for 4-CP and its intermediates at different initial 4-CP concentrations as well as the proposed reaction pathways of 4-CP photocatalytic degradation. The second section includes the adsorption isotherms of 4-CP and its intermediates using TiO_2 as the photocatalyst. The final section in this chapter establishes a valuable approach for kinetic modelling to predict the degradation profiles of 4-CP and its intermediates under solar irradiation.

4.2 Experimental procedure

As mentioned in Chapter 3 (Section 3.3.1) the experiments were carried out in a slurry batch reactor. A 1 L Pyrex glass beaker was employed as a reactor to hold 1 L suspension solution, equipped with a magnetic stirrer. About 0.5 g/L of TiO_2 was used for all oxidation experiments. In order to investigate the effect of initial concentration, different 4-CP concentrations (25, 50, 75 and 100 mg/L) were used. The suspensions were magnetically stirred in the dark for 30 min to attain adsorption–desorption equilibrium between 4-CP and TiO_2. Then, the suspensions were exposed to solar light for 180 min. At specific time intervals (30 min), 5 mL was withdrawn and filtered through PTFE 0.45-μm membrane filters to separate the catalyst particles for HPLC analysis.

4.3 Solar photocatalytic degradation of 4-CP

The set of experiments were conducted to investigate the solar photocatalytic degradation of 4-CP and its intermediates using different initial concentrations and TiO_2. Figure 4.1 shows typical experimental results for the solar photocatalytic

degradation of 4-CP and the major detected intermediates at different initial 4-CP concentrations (50, 75, 100 mg/L) using 0.5g/L TiO_2. All of these intermediates have been previously identified (Elghniji et al. 2012, Bian et al. 2011). It should be mentioned that both HQ and 4cCat were the two main aromatic intermediates detected during 4-CP photocatalytic degradation on TiO_2. During 180 min solar degradation of 4-CP, increased HQ concentration may be due to the production of HQ from Ph and 4-CP degradation at the same time. In this case, dechlorination might occur on 4-CP to form Ph and then an OH radical adds onto the Ph ring at para-position, leading to the producing of HQ (Duan et al. 2012). Yang et al., (2009) pointed out that the HQ concentration starts decreasing after 180 min when using UV/TiO_2 to degrade 4-CP compound. Ph was also detected but at significantly lower concentration (Appendix A). Therefore, the Ph compound was not included as an intermediate in the proposed kinetic model. The degradation efficiencies at different 4-CP initial concentrations were also determined. Figure 4.2 shows the degradation efficiency of 4-CP at 50, 75 and 100 mg/L. It is clear that the degradation efficiency decreases with increasing the initial 4-CP concentration. This result can be clarified by the fact that, at high initial 4-CP concentration, the amount of 4-CP adsorbed onto the TiO_2 surface increases leading to decrease in the active sites and •OH radical formation (Romero et al. 1999).

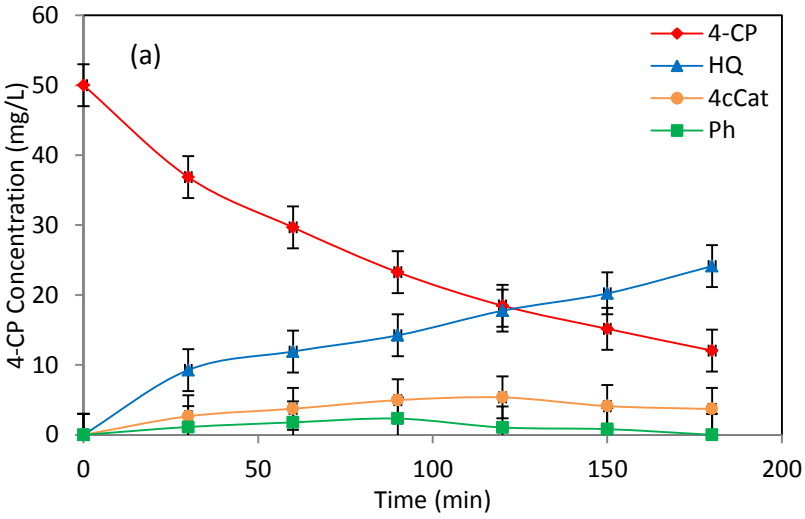

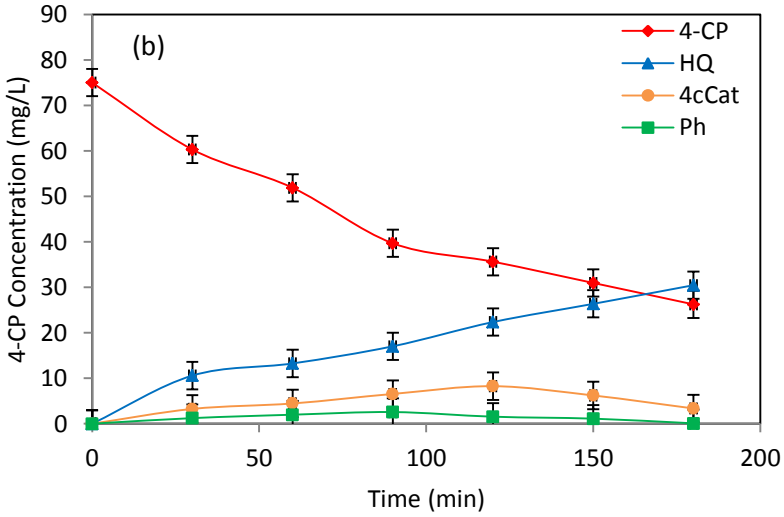

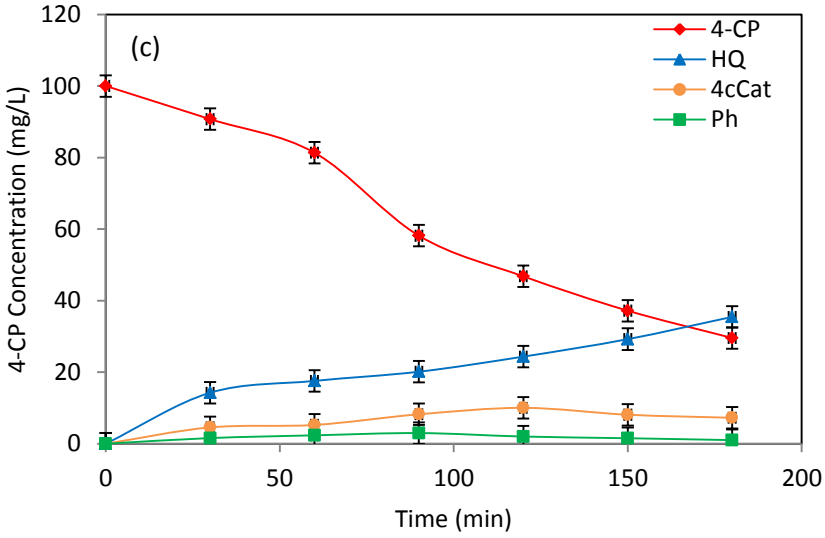

Figure 4.1 Concentration profiles of 4-CP and its intermediates at several initial concentrations (a) 50, (b) 75, and (c) 100 mg/L on 0.5 g/L TiO_2

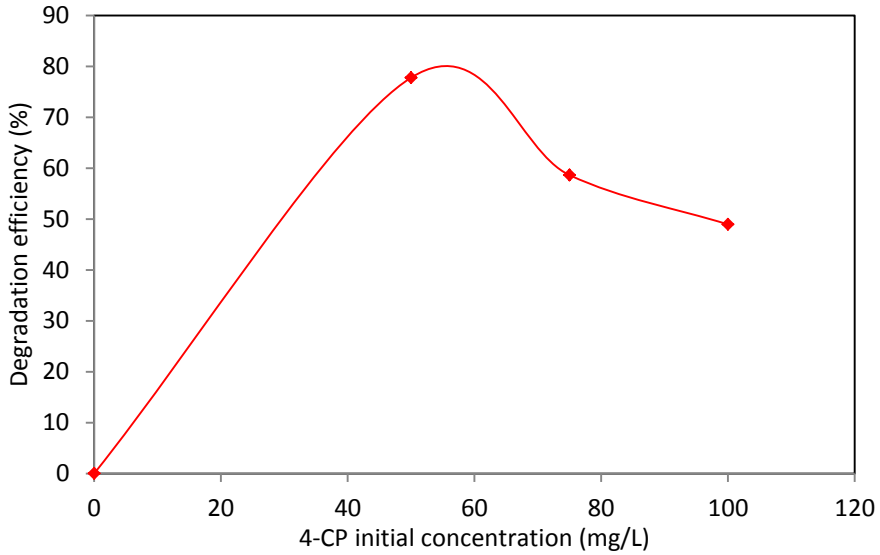

Figure 4.2 Effect of the 4-CP initial concentration on the degradation efficiency (0.5g/L TiO_2, 1000mW/cm^2).

4.4 Solar photocatalytic degradation of the intermediates

Solar photocatalytic oxidation experiments were carried out using the major intermediates observed during the solar photocatalytic degradation of 4-CP as the model reactants. These experiments conducted to get more details about the chemical behaviour of these intermediates and measure their adsorption constants experimentally. During 180 min photocatalytic degradation of HQ, a small amount of benzoquinone (BQ) was observed at the first 60 min then it rapidly degraded Fig. (4.3).

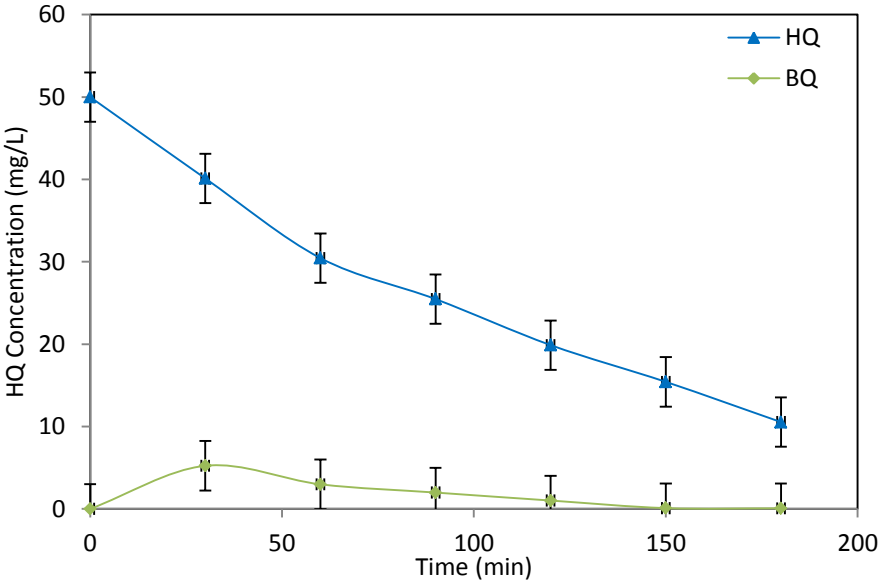

Figure 4.3 Concentration profiles of HQ photo degradation and its intermediate (0.5g/L TiO_2, 1000mW/cm^2).

However, for 4cCat no intermediates were detected Fig. (4.4). Some researchers have concluded that the 4cCat as an intermediate might convert to hydroxyhydroquinone (HHQ) (Lindner et al. 1997). Dhir et al. (2012) used 4cCat as a model pollutant without intermediate investigations, therefore; yet no clear investigations for solar photocatalytic degradation of 4cCat.

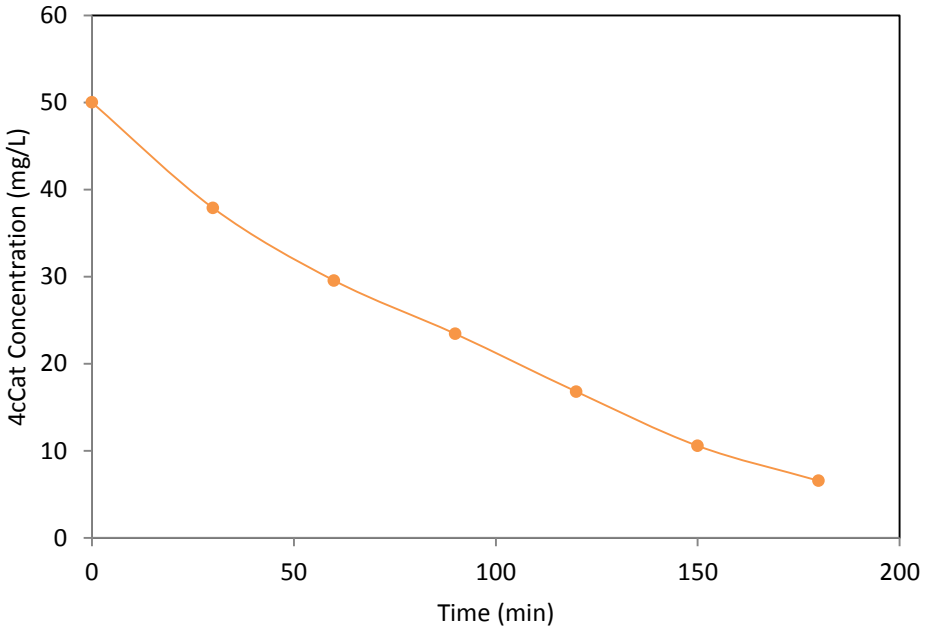

Figure 4.4 Concentration profile of 4cCat photo degradation on 0.5g/L TiO_2, 1000 mW/cm^2

4.5 Adsorption isotherms of 4-CP and the main intermediates on TiO_2

Several experiments for measuring the adsorption constants of 4-CP, HQ and 4cCat in the present of TiO_2 were carried out. After measuring C_e for all cases, Q_e can be determined using Equation 4.1 (Bekkouche et al. 2004):

$$Q_e = \frac{(C_0 - C_e)V}{M_{cat}} \qquad (4.1)$$

Where, C_0 and C_e are the initial and equilibrium concentrations of the adsorbate, respectively (mg/L). V is the total volume of the solution (L), and M_{cat} is the mass of the TiO_2 catalyst (mg). The Langmuir isotherm model, Eq. (4.2), can be used to

calculate the adsorption constants for 4-CP and its intermediates (Salaices et al. 2004).

$$Q_e = \frac{Q_{\max} K_i C_0}{(1 + K_i C_0)} \tag{4.2}$$

Where Q_e (mg/g_{cat}) and C_0 (mg/L) are the amount of compound adsorbed per unit weight and the concentration in the liquid phase at equilibrium, respectively. Q_{max} (mg/g_{cat}) is the maximum organic compound adsorbed and K_i ($mg^{-1}L$) is the adsorption constant of component *i*. To calculate K_i, Eq. (4.2) has to be rearranged to linear form as in the following equation:

$$\frac{1}{Q_e} = \frac{1}{Q_{\max}} + \frac{1}{Q_{\max} K_i} \frac{1}{C_e} \tag{4.3}$$

From the slope and the intercept of Eq. (4.3), the adsorption constant for each component can be obtained when experimental data of C_0 and Q_e are available. Figures 4.5-7 show the linear regressions of Langmuir isotherm (Eq. 4.3) for 4-CP, HQ and 4cCat, respectively.

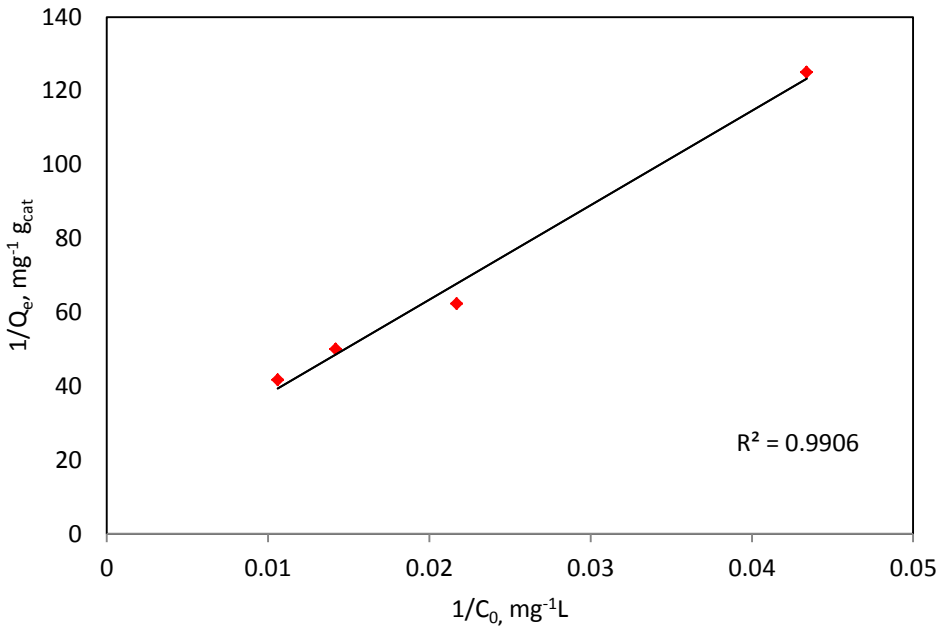

Figure 4.5 Linear regression for Langmuir isotherm: adsorption of 4-CP on 0.5g/L TiO_2, 1000 mW/cm^2

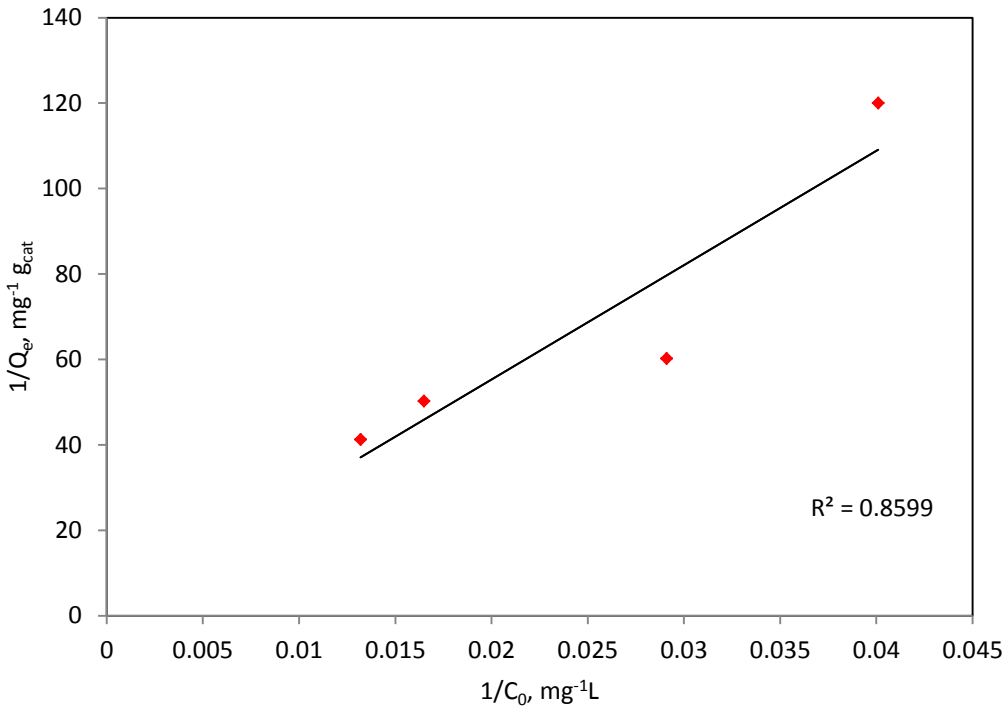

Figure 4.6 Linear regression for Langmuir isotherm: adsorption of HQ on 0.5g/L TiO_2, 1000 mW/cm^2

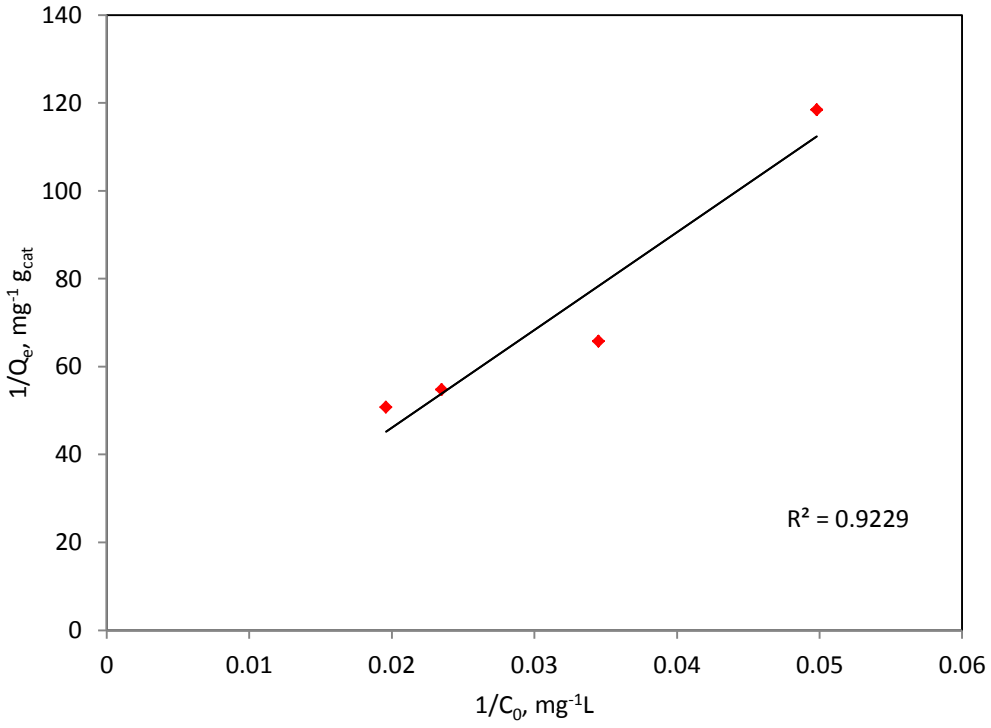

Figure 4.7 Linear regression for Langmuir isotherm: adsorption of 4cCat on 0.5g/L TiO_2, 1000 mW/cm^2

The adsorption constants (K_i) and the maximum organic adsorption (Q_{max}) for the investigated components are summarised in Table 4.1. It is clear that the adsorption constant of 4-CP is much higher than that of HQ and 4cCat which could be due to the high amount of 4-CP adsorbed onto the TiO_2 powder to form a monolayer (Huang et al. 2013).

Table 4.1 Adsorption constants for different compounds on TiO_2

Component	Maximum organic compound adsorbed, Q_{max} (mg/g_{cat})	Adsorption Constant, K_i (L/mg)	R^2
4-CP	0.0819	0.00476	0.9906
HQ	0.5671	0.000688	0.8599
4cCat	0.6329	0.00071	0.9229

4.6 The Reaction Mechanism

The suggested reaction mechanism was developed to involve all chemical components observed during the solar photocatalytic degradation of 4-CP. Three intermediate compounds (HQ, 4cCat, Ph) were identified during the solar 4-CP photocatalytic degradation. However, the Ph concentration was found to be very low and might be quickly converted to HQ. Therefore, it was neglected in the kinetic model of this study. During the course of solar irradiation (180 min), the 4-CP concentration significantly decreased with increasing HQ concentration which might be attributed to the direct attack of $^{\bullet}OH$ radical on Cl^- atom. Further solar irradiation degrades HQ to either CO_2 and H_2O or BQ which consequently converted to final products. However, hydroxyl radical might react with 4-CP and produce 4cCat (Fig. 4.8). These findings are in agreement with several studies (Vinu and Madras 2011b, Venkatachalam et al. 2007, Bian et al. 2011, Elghniji et al. 2012). Support for the reaction mechanism is based on the experimental observations. To derive the kinetic modelling of photocatalytic degradation of 4-CP, several assumptions have to be taken into account as follows: (a) The photocatalytic reactions occur on the catalyst surface; therefore, the rates of formation and disappearance of all components can be modelled using a Langmuir-Hinshelwood (L-H) equation; (b) All observed chemical species adsorb on the photocatalyst surface;

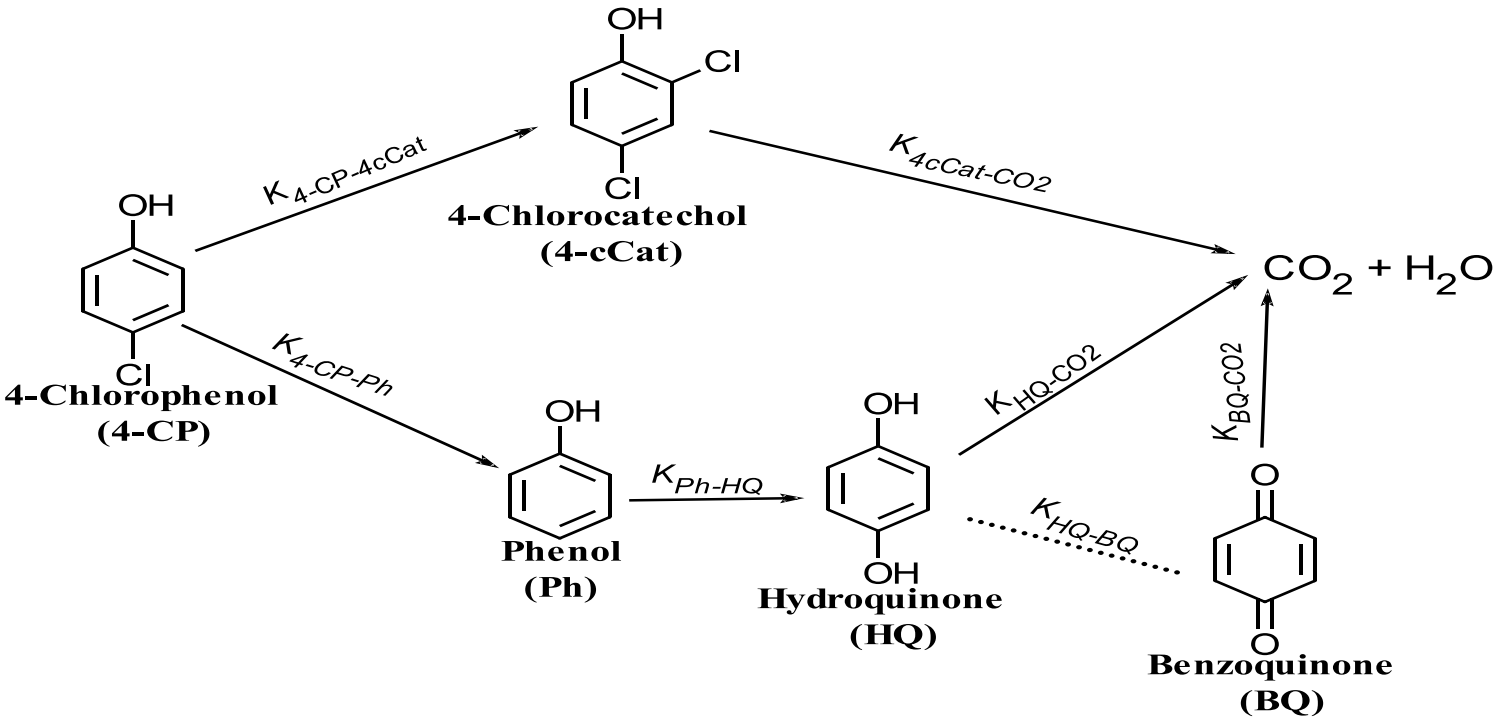

Figure 4.8 Proposed pathways of 4-CP photocatalytic degradation

(c) Carbon dioxide does not adsorb on the photocatalyst surface; and (d) There is no different behaviour for all chemical species when they are modelled either as a model pollutant or as an intermediate (Salaices et al. 2004, Ortiz-Gomez et al. 2008, Daneshvar et al. 2004). Additionally, in this work, the reaction rate constants forming HQ ($k_{4\text{-}CP\text{-}HQ}$) and 4cCat ($k_{4\text{-}CP\text{-}4cCat}$) as intermediates from the oxidation of 4-CP were assumed to be equal. However, their reaction rate constants ($k_{HQ\text{-}CO2}$) and ($k_{4cCat\text{-}CO2}$) are different (Fig. 4.8).

4.7 Kinetic modelling

Most of studies dealing with kinetic reactions of chlorophenols on TiO_2 photocatalyst were for a single compound. However, it has been well known that during photocatalytic degradation of organic compounds, some intermediate compounds are usually formed (Fujishima et al. 2000, Ortiz-Gomez et al. 2008). Therefore, there is a need to develop a model that considers all chemical species which might be formed during photocatalytic degradation of phenolic compounds. In this respect, a kinetic model for the oxidation of 4-CP and its main intermediates (HQ and 4cCat) has been developed considering all these chemical species formed during the oxidation. In photocatalytic degradation processes, there is an interaction between chemical species and the photocatalyst surface leading to absorb these species on the surface of TiO_2 (Mehrvar et al. 2000). Thus, it is well accepted that the rates of formation and disappearance of all components can be modelled using a L-H equation (Eq. 4.4) which considers the adsorption of the chemicals on the catalyst surface and the kinetic reaction constants. The general form of this equation for the system is represented by (Turchi and Ollis 1990).

$$r_i = \frac{dC_i}{dt} = \frac{k_i C_i}{1 + \sum_{j=1}^{n} K_j C_j} \qquad (4.4)$$

Where r_i is the reaction rate of component i in (mol g_{cat}^{-1} min^{-1}), k_i is the kinetic reaction constant for component i in (mol g_{cat}^{-1} min^{-1}), K_i is the adsorption constant

for each of the species participating in the reaction (mol^{-1} L), *n* denotes the number of participant in the reaction, and *C* is the species concentration (mol/L).

Applying Eq. (4.4) for all observed components (4-CP, HQ and 4cCat) results in three differential equations describing the photocatalytic degradation of 4-CP and its intermediates.

For 4-CP,

$$\frac{dC_{4-CP}}{dt} = \frac{-\left(k_{4-CP-HQ} + k_{4-CP-4cCat}\right)C_{4-CP}}{1 + K_{4-CP}C_{4-CP} + K_{HQ}C_{HQ} + K_{4cCat}C_{4cCat}} \tag{4.5}$$

Assuming: $k_{4\text{-}CP} = k_{4\text{-}CP\text{-}HQ} = k_{4\text{-}CP\text{-}4cCat}$

$$\frac{dC_{4-CP}}{dt} = \frac{-2k_{4-CP}C_{4-CP}}{1 + K_{4-CP}C_{4-CP} + K_{HQ}C_{HQ} + K_{4cCat}C_{4cCat}} \tag{4.6}$$

Similar equations can be written for each intermediate. For HQ and 4cCat as follows

$$\frac{dC_{HQ}}{dt} = \frac{\left(k_{4-CP-HQ}C_{4-CP} - k_{HQ-CO2}C_{HQ}\right)}{1 + K_{HQ}C_{HQ} + K_{4-CP}C_{4-CP} + K_{4cCat}C_{4cCat}} \tag{4.7}$$

Or

$$\frac{dC_{HQ}}{dt} = \frac{\left(k_{4-CP}C_{4-CP} - k_{HQ-CO2}C_{HQ}\right)}{1 + K_{HQ}C_{HQ} + K_{4-CP}C_{4-CP} + K_{4cCat}C_{4cCat}} \tag{4.8}$$

And for 4cCat;

$$\frac{dC_{4cCat}}{dt} = \frac{\left(k_{4-CP-4cCat}C_{4-CP} - k_{4cCat-CO2}C_{4cCat}\right)}{1 + K_{4cCat}C_{4cCat} + K_{4-CP}C_{4-CP} + K_{HQ}C_{HQ}} \tag{4.9}$$

Or

$$\frac{dC_{4cCat}}{dt} = \frac{\left(k_{4-CP}C_{4-CP} - k_{4cCat-CO2}C_{4cCat}\right)}{1 + K_{4cCat}C_{4cCat} + K_{4-CP}C_{4-CP} + K_{HQ}C_{HQ}} \tag{4.10}$$

Equations (4.6,8,10) represent the contribution of various steps of the model and involve the unknown reaction rate constants for each component that can be estimated by fitting the model to the experimental data. After estimating the best parameters, the mathematical model can be applied to predict the behaviour of the photocatalytic oxidation of 4-CP. The above equations cannot be solved analytically, therefore, for estimating the reaction rate constants; two built-in MATLAB subroutines were used: Least Square Curve Fit (lsqcurvefit) for the minimisation of the objective function and Ordinary Differential Equations Solver (ode45) for the numerical integration of the differential equations.

4.8 Model fitting to the experimental data

Kinetic reaction modell of 4-CP solar photocatalytic degradation involving two main intermediates (HQ and 4cCat) was developed. This kinetic model was based on the proposed degradation mechanism Fig. (4.8). However, the step of forming Ph in this scheme was dropped because of its low concentration and its fast degradation. Additionally, some assumptions have been applied in order to use the L-H equation (Eq. 4.4) and minimise the unknown variables. Furthermore, the adsorption constants of 4-CP, HQ and 4cCat were experimentally determined in order to provide the kinetic model more accuracy. Three ordinary differential equations Eqs. (4.6,8,10) describing the proposed degradation mechanism were developed for 4-CP, HQ and 4cCat, respectively. MATLAB software was used to solve these equations and estimate the reaction rate constants for all components involved in the developed model. Table 4.2 summarises the estimated reaction rate constants and measured adsorption constants for 4-CP, HQ and 4cCat, respectively.

Table 4.2 Estimated adsorption and reaction rate constants for the photocatalytic oxidation of 4-CP, HQ and 4cCat

Component	Measured adsorption constant K_j (mol. L^{-1})	Estimated reaction rate constant k_i (mol g_{cat}^{-1} min^{-1})
4-CP	0.00476	0.0055
HQ	0.000688	0.00034
4cCat	0.00071	0.03251

Figure 4.9 shows the experimental concentration profiles of 4-CP and its intermediates and the estimated profiles for different initial concentrations. The optimisation was performed at different initial concentrations of 4-CP (50, 75, and 100 mg/L). It can be seen that the kinetic model predicts very well the experimental data for wide range of initial concentrations.

Summary

Based on the results presented in this chapter, it can be concluded that the solar photocatalytic degradation method using TiO_2 photocatalyst can effectively mineralise 4-CP and its intermediates into CO_2 and H_2O within 180 min solar irradiation. The major organic intermediates formed during the degradation of 4-CP were HQ, 4cCat and Ph. Among these intermediates, HQ is the highest concentration and Ph the lowest. The reaction pathway for the solar photocatalytic oxidation of 4-CP is reported involving all detected chemical components. This proposed mechanism based on the experimental results obtained for the oxidation of 4-CP and its intermediates individually. However, Ph compound was detected in small amounts, therefore; it was neglected from the proposed kinetic model. All the adsorption constants of 4-CP and its major intermediates were determined experimentally. The reaction kinetic model was developed to predict the rate of reaction of 4-CP and its main aromatic intermediates. The proposed model provides very good fit to the experimental data and works very well for a wide range of 4-CP initial concentrations (50-100 mg/L).

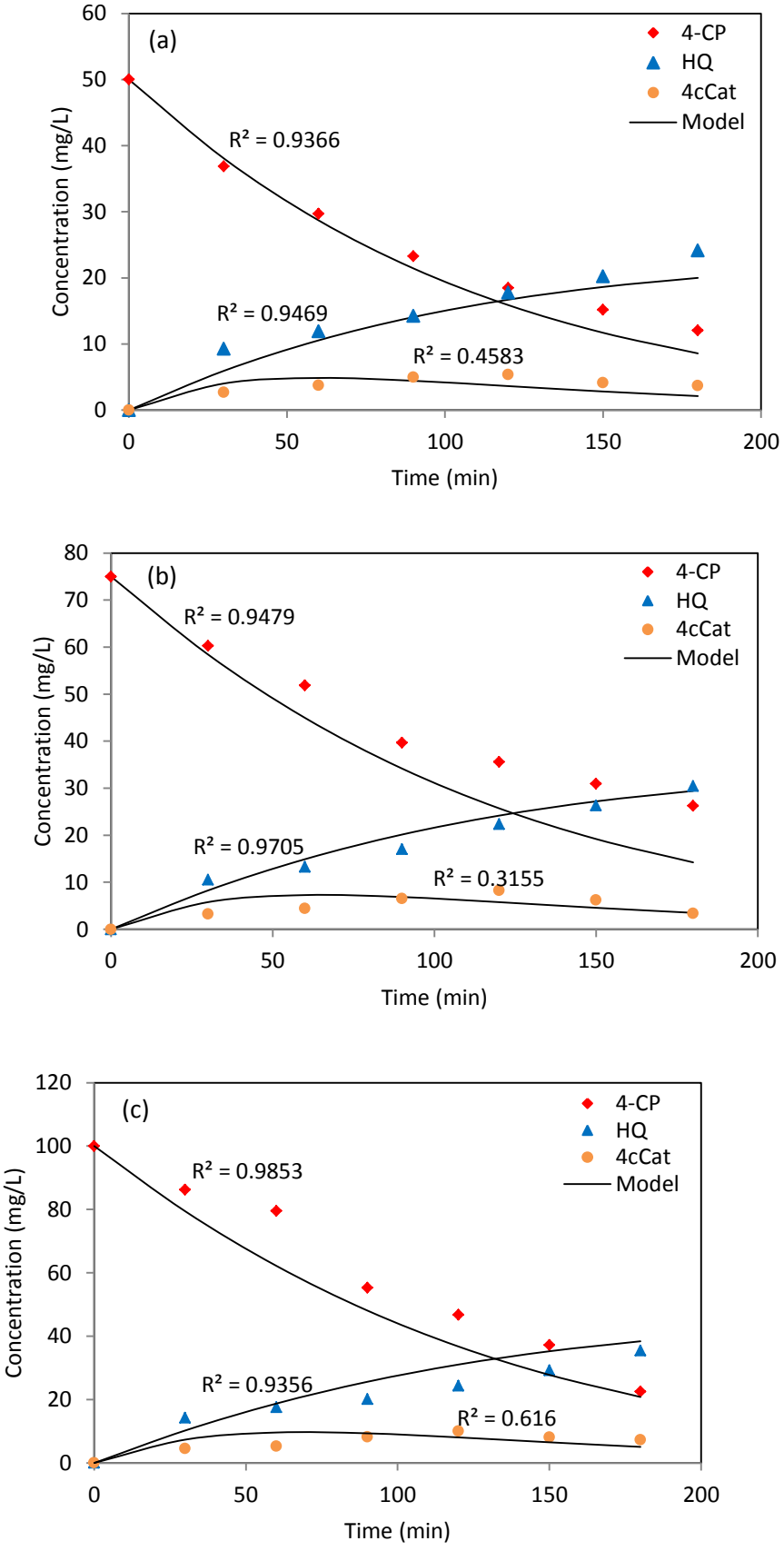

Figure 4.9 Experimental and estimated concentration profiles for photocatalytic degradation of 4-CP on 0.5g/L TiO_2 catalyst (a) 50, (b) 75 and (c) 100 mg/L 4-CP initial concentration

CHAPTER 5

KINETICS AND MECHANISMS OF SOLAR PHOTOCATALYTIC DEGRADATION FOR CHLOROPHENOLS MIXTURES

5.1 Introduction

In chapter 4, the solar photocatalytic degradation of 4-CP as model pollutant was studied including the mechanisms and kinetic modelling. Although photocatalytic degradations of chlorophenols using various photocatalysts and light sources have been widely studied, little attention has been paid to applications for the solar photocatalytic degradation of mixtures containing more than one organic pollutant. Therefore, this chapter focuses on the solar photocatalytic degradation of the chlorophenols mixture containing 4-CP and 2,4-DCP. These organic compounds were chosen as model pollutants as they are present in petroleum refinery effluent. Many researchers have investigated the photocatalytic degradation mechanisms and kinetic modelling of these pollutants (Ksibi et al. 2003a, Kusvuran et al. 2005, Chiou et al. 2008a, Lathasree et al. 2004, Chen and Ray 1999). However, most of these studies were for only one compound, meaning they cannot be applied to industrial effluents which contain many organic pollutants dissolved together. Only a few studies have investigated the photocatalytic degradation of pollutant mixtures containing multi phenolic compounds (Salaices et al. 2004, Chiou et al. 2008a, Lathasree et al. 2004, Krijgsheld and van der Gen 1986, Ksibi et al. 2003a, Pandiyan et al. 2002, Ortiz-Gomez et al. 2007b). Most of these studies have used the L-H kinetic model without considering the intermediates formed during photocatalytic degradation of these contaminants. For instance, Priya and Madras (2005) investigated the degradation of chlorophenols, nitrophenols, and their mixtures using TiO_2, they used a modified L-H kinetic model to determine the reaction rate constants of their pollutants. However, these kinetic models did not include the concentration of the intermediates that might affect the predictions of the degradation profiles of the main pollutants. Although, as mentioned above, though the photocatalytic degradation of organic pollutants has been extensively studied, there is still a lack of information regarding the quantification of intermediates and the kinetic modelling of binary mixtures, which need more attention and investigation. Therefore, the aim of this work is to investigate the solar photocatalytic degradation of single and combined chlorophenols mixture containing 4-CP and 2,4-DCP using TiO_2, also; to develop a kinetic model to determine the degradation kinetics. The model will consider the concentration of the main

pollutants as well as all detected intermediates formed during the solar-photocatalytic degradation. This chapter also aims to provide a good understanding of the combined mixture reaction pathways and propose a reaction mechanism.

5.2 Experimental procedure

As mentioned in Chapter 3 (Section 3.3.2) different concentrations of 4-CP and 2,4-DCP (individually and combined) were investigated under solar light using 0.5g/L of TiO_2 as photocatalyst. First, different 4-CP and 2,4-DCP concentrations (25, 50, 75, 100 mg/L) were individually investigated under the same conditions (0.5g/L TiO_2 and 1000 mW/cm^2). For combined mixtures degradation, an equal amount (50 mg/L each) of 4-CP and 2,4-DCP was dissolved in distilled water and transferred to the photoreactor before adding TiO_2.

5.3 Solar photocatalytic degradation of 4-CP and 2,4-DCP individually

The typical experimental results for the solar photocatalytic degradation of 4-CP and its main detected intermediates are illustrated in Figure 5.1. All of these intermediates were identified in previous studies (Elghniji et al. 2012, Bian et al. 2011). In Chapter 4, it was mentioned that both HQ and 4cCat were the two major aromatic intermediates detected during 4-CP photocatalytic degradation on TiO_2. Also, from these results, it can be seen that the HQ can be formed by Cl^- cleavage and hydroxylation of 4-CP, whereas 4cCat can be produced by hydroxylation only. Furthermore, during 180 min solar degradation of 4-CP, HQ was slightly increasing which might be due to the production of HQ from Ph and 4-CP degradation at the same time. In this case, dechlorination might occur on 4-CP to form Ph and then $^{\bullet}OH$ radical adds onto the Ph ring at para-position, leading to the production of HQ (Duan et al. 2012). However, after 60 min time, HQ starts decreasing and disappearing at 240 min. Yang et al., (2009) supported such results. Ph was also detected but at significantly low concentration and rapidly degraded after 120 min irradiation.

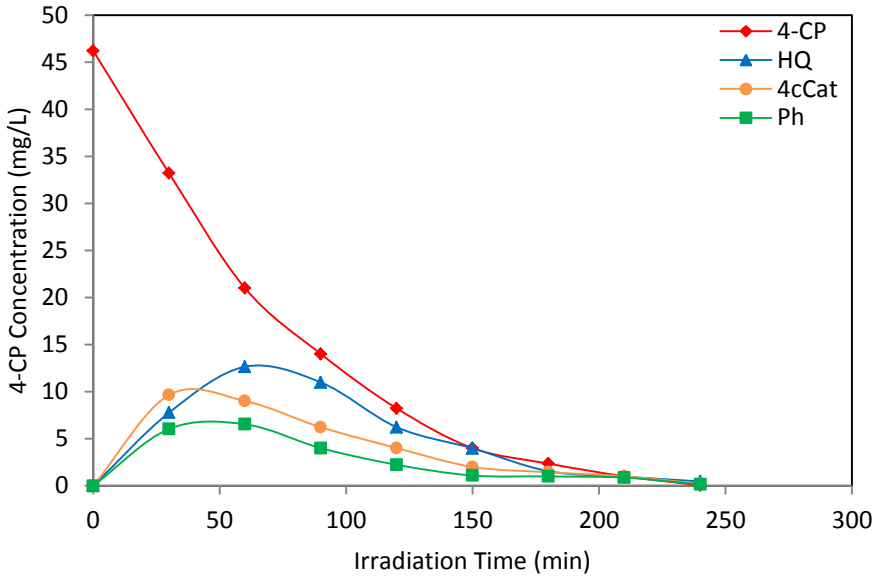

Figure 5.1 Solar photocatalytic degradation of 4-CP (0.5g/LTiO_2, pH=5 1000mW/cm^2)

The reaction rate of 4-CP degradation followed pseudo-first order reaction with 0.8142 min^{-1} reaction rate constant as shown in Figure 5.2.

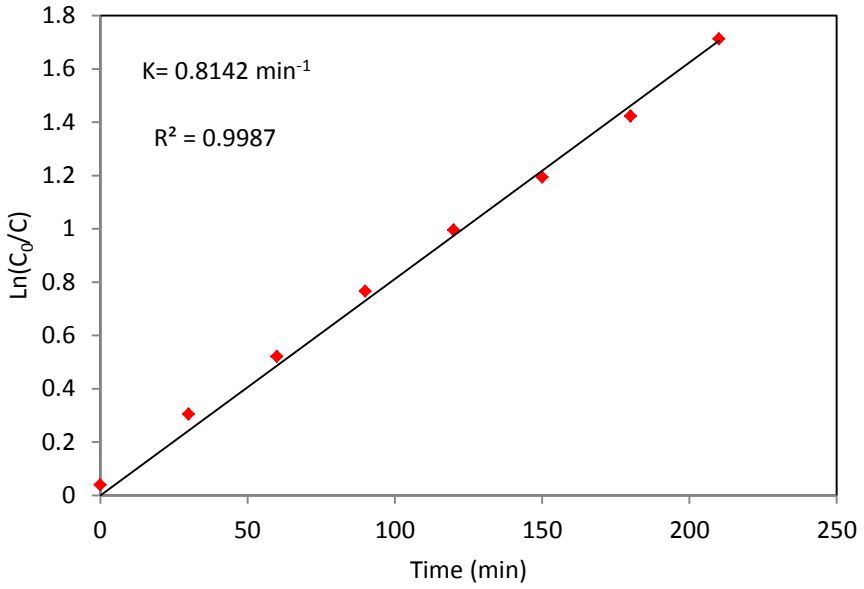

Figure 5.2 Reaction rate constant of 4-CP (C_0 = 50 mg/L)

Figure 5.3 shows the degradation profiles of 2,4-DCP and all detected intermediates. It can be seen that the photocatalytic degradation rate of 2,4-DCP was lower than that of 4-CP which might be due to the high chlorine atoms which consequently reduce the dechlorination process. In addition, Cl^- might be adsorbed onto the photocatalyst surface during the degradation process and reacting with electrons /

holes pairs leading to reduction of •OH radical (Temel and Sökmen 2011). It can be seen from this figure that the main 2,4-DCP intermediates are 4-CP and Ph. The 4-CP concentrations were higher than those of Ph. This result can be clarified by the fact that, the first step of 2,4-DCP photocatalytic degradation is dechlorination of *ortho*-position which might be much easier than *para*-position leading to form more 4-CP quantities than Ph. However, dechlorination might also occure for 4-CP and produce Ph. Figure 5.4 shows the degradation rate constant of 50 mg/L 2,4-DCP (0.5117 min^{-1}) which was lower than that of 4-CP.

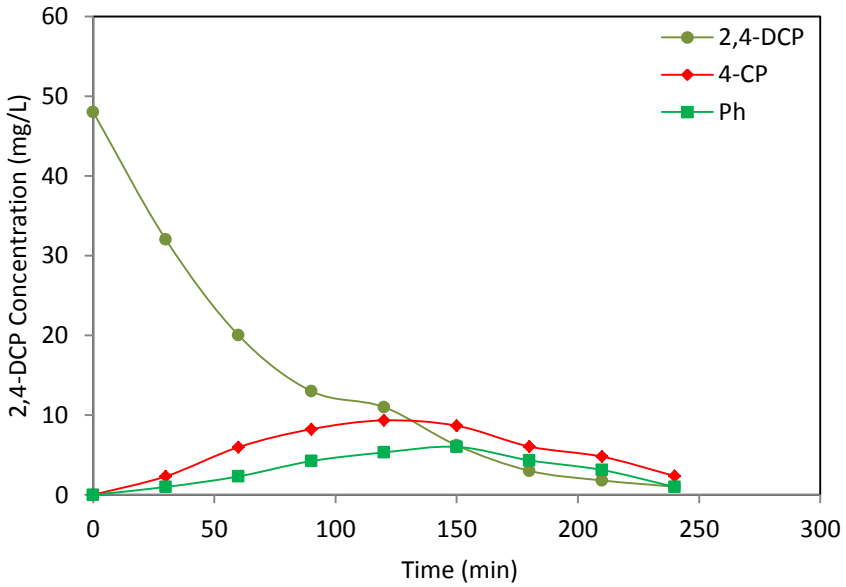

Figure 5.3 Solar photocatalytic degradation of 2,4-DCP (0.5g/LTiO_2, 1000mW/cm^2)

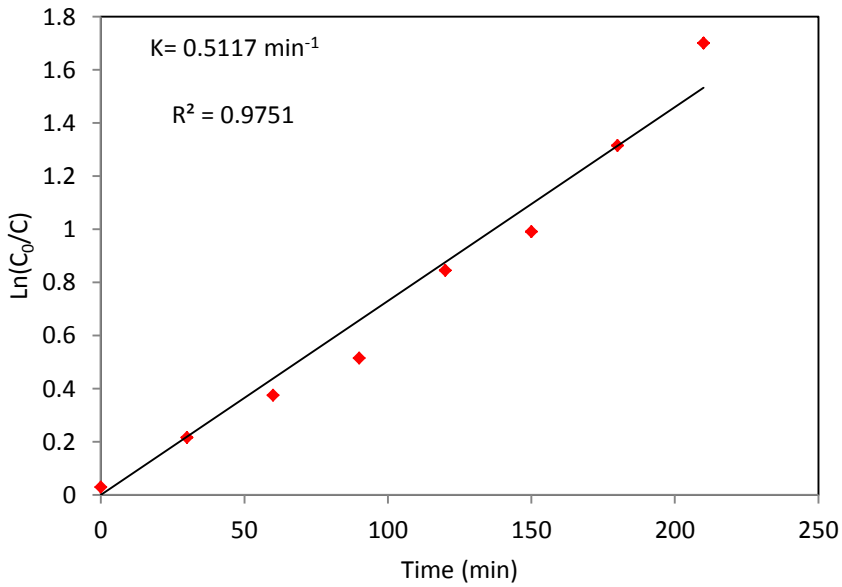

Figure 5.4 Reaction rate constant of 2,4-DCP (C_0 = 50 mg/L)

Figure 5.5 shows TOC experimental results of 4-CP and 2,4-DCP photocatalytic degradations. A significant reduction in the total organic carbon dissolved (TOC) of both compounds was observed. It can be concluded that the degradation rate of 4-CP is higher than that of 2,4-DCP. This result can be clarified by the fact that 2,4-DCP needs more steps than 4-CP to be mineralised because it has to convert into 4-CP, then form the intermediates and the final products.

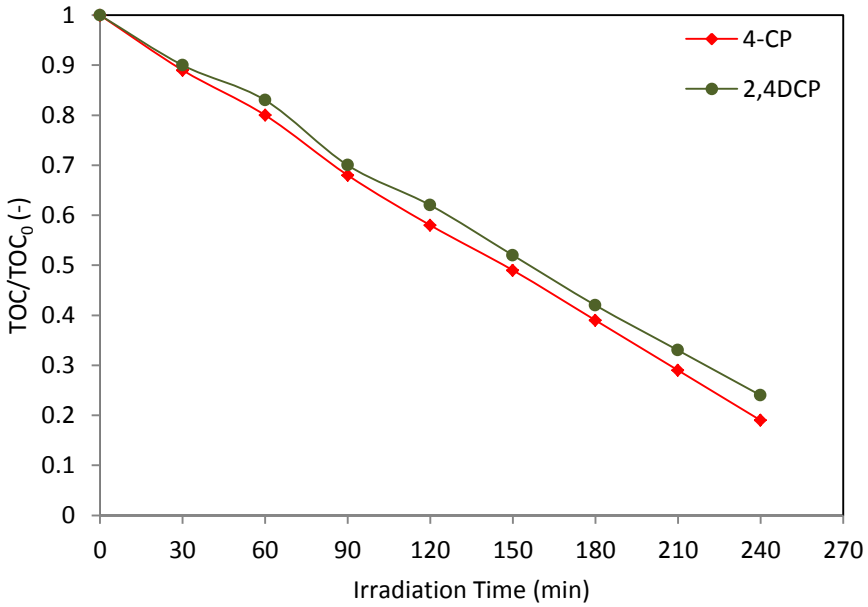

Figure 5.5 TOC degradations of 4-CP and 2,4-DCP (0.5g/LTiO_2, 1000mW/cm^2)

5.4 Solar photocatalytic degradation of the combined mixture

Figure 5.6 illustrates the solar photocatalytic degradation of combined mixtures containing equal concentrations (50 mg/L) of 4-CP and 2,4-DCP. The degradation rates of both compounds were significantly decreased compared to the individual degradation case (see Figs. 5.1,3). It is also worth mention that the 4-CP compound was the main intermediate of 2,4-DCP when it was degraded individually, therefore; reduced in mineralisation of 4-CP due to its generation as an intermediate from 2,4-DCP by the cleavage of *ortho*-Cl of 2,4-DCP ring during the solar photocatalytic degradation of the combined mixture. Moreover, both reductions of pollutants are due to competition for the catalyst active site and interaction between these compounds (Pera-Titus et al. 2004). This figure also shows the formation and destruction of three intermediates HQ, Ph and 4cCat together with the degradation of both models. It can be observed that the concentration of HQ was the highest one followed by Ph and then 4cCat. This result can be clarified by the fact that the $^{\bullet}OH$

radical rapidly attacks Ph and forms HQ meaning that the main oxidant in this degradation was the •OH radical. Pino and Encinas (2012) pointed out that the Ph has high activation with •OH radical to form HQ and hydroxyl products. It is clear to notice that the Ph and 4cCat intermediates increase at the first 100 min then begin to decrease until complete degradation at 240 min, whereas HQ starts to decrease at 180 min and then almost disappear at 240 min.

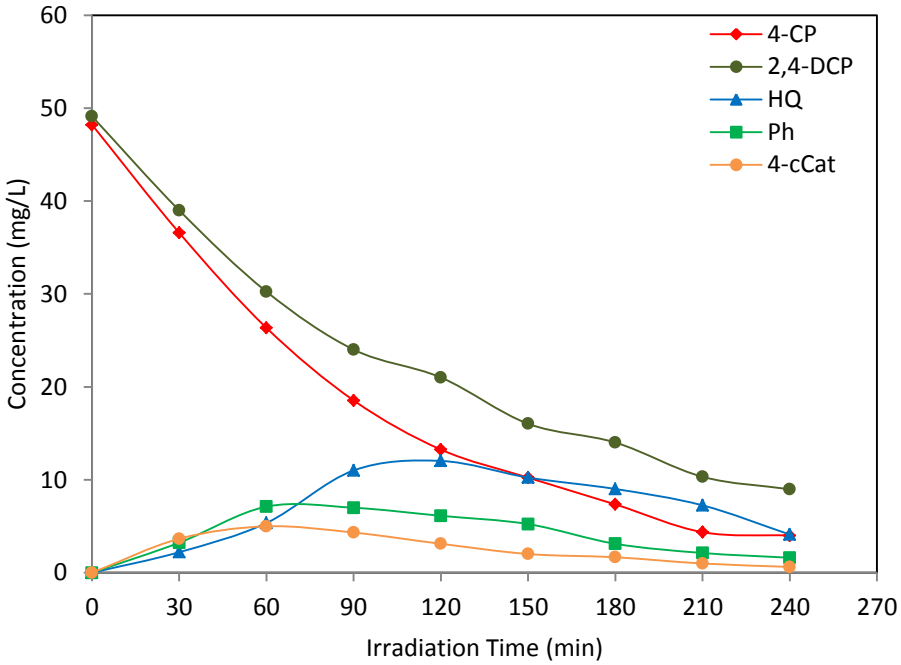

Figure 5.6 Solar photocatalytic degradation of the combined mixture with their intermediates (50 mg/L both 4-CP and 2,4-DCP) (0.5 g/LTiO_2, 1000 mW/cm^2)

The TOC degradation of the combined mixture (50 mg/L of both 4-CP and 2,4-DCP) was also investigated as shown in Figure 5.7. It was found that the TOC reduction of the combined mixture was lower than that of individual compound (4-CP or 2,4-DCP). The TOC reduction for the combined mixture was 60% while that of 4-CP and 2,4-DCP were 79% and 76% respectively. This is could be attributed to the increase of the initial concentrations of pollutants.

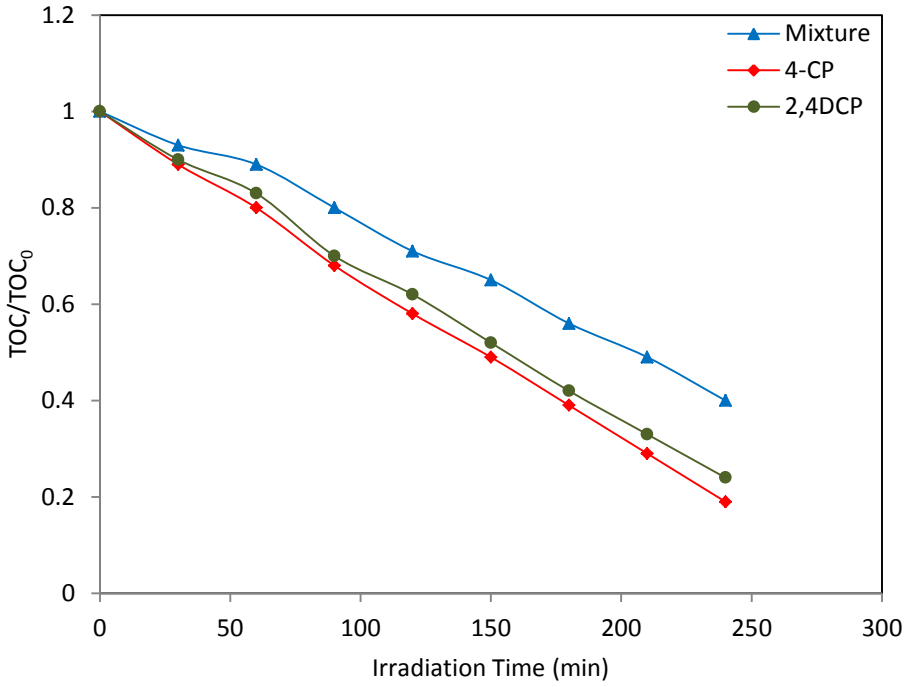

Figure 5.7 TOC degradation of the combined mixture (0.5 g/LTiO_2, 1000 mW/cm^2)

Several experiments were carried out using different 2,4-DCP initial concentration (25, 50, 75, 100 mg/L) with 50 mg/L 4-CP initial concentration in order to investigate the effect of second pollutant on the degradation rate constant and suggest a kinetic model for the solar-photocatalytic degradation of combined mixtures as shown in Figure 5.8. It is clear that the reaction rate constant of 4-CP decrease with increase of 2,4-DCP initial concentration due to the interaction between the pollutants and the intermediates. The results also show that the 4-CP initial rate of degradation decreased almost linearly with the increase in the 2,4-DCP initial concentration. Therefore, a mathematical relationship (Eq. 5.1) can be developed to estimate the reaction rate constant for each compound in this combined mixture as follows;

$$\left(k_{ii} - k_{ij}Cj\right) \qquad (5.1)$$

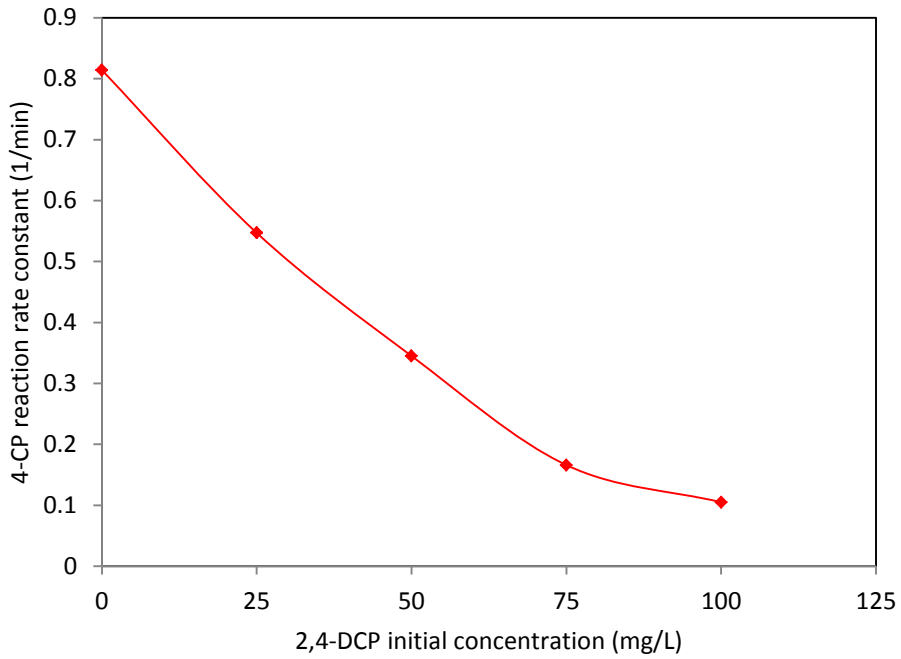

Figure 5.8 Effect of 2,4-DCP initial concentration on the 4-CP reaction rate constant (0.5g/L TiO_2, 1000 mW/cm^2)

5.5 Adsorption isotherms experiments

A set of experiments were carried out in order to measure the adsorption constants of 4-CP; 2,4-DCP and their intermediates (Ph, 4cCat and HQ) on TiO_2. After measuring C_e for all cases, Q_e can be determined as in Equation 5.1 (Bekkouche et al. 2004):

$$Q_e = \frac{(C_0 - C_e)V}{M_{cat}} \tag{5.2}$$

Where, C_0 and C_e are the initial and equilibrium concentrations of the adsorbate, respectively (mg/L). V is the total volume of the solution (L), and M_{cat} is the mass of the TiO_2 catalyst (g_{cat}). The Langmuir isotherm model (Eq. 5.2) can be used to calculate the adsorption constants for 4-CP and its intermediates (Salaices et al. 2004).

$$Q_e = \frac{Q_{\max} K_i C_e}{(1 + K_i C_e)} \tag{5.3}$$

Where, Q_e (mg/g_{cat}) and C_e (mg/L) are the amount of compound per unit weight and the concentration in the liquid phase at equilibrium, respectively. Q_{max} (mg/g_{cat}) is the maximum organic compound adsorbed and K_i (L/mg) is the adsorption constant of *i* component. To calculate K_i, Equation 5.2 can be rearranged in the linearized form as following:

$$\frac{1}{Q_e} = \frac{1}{Q_{\max}} + \frac{1}{Q_{\max} K_i} \frac{1}{C_e} \tag{5.4}$$

From the slope and the intercept of Equation 5.3, the adsorption constant for each component can be obtained when experimental data of C_e and Q_e are available. Figure 5.9 shows the linear regressions of Langmuir isotherm for 4-CP, 2,4-DCP, HQ, Ph and 4cCat.

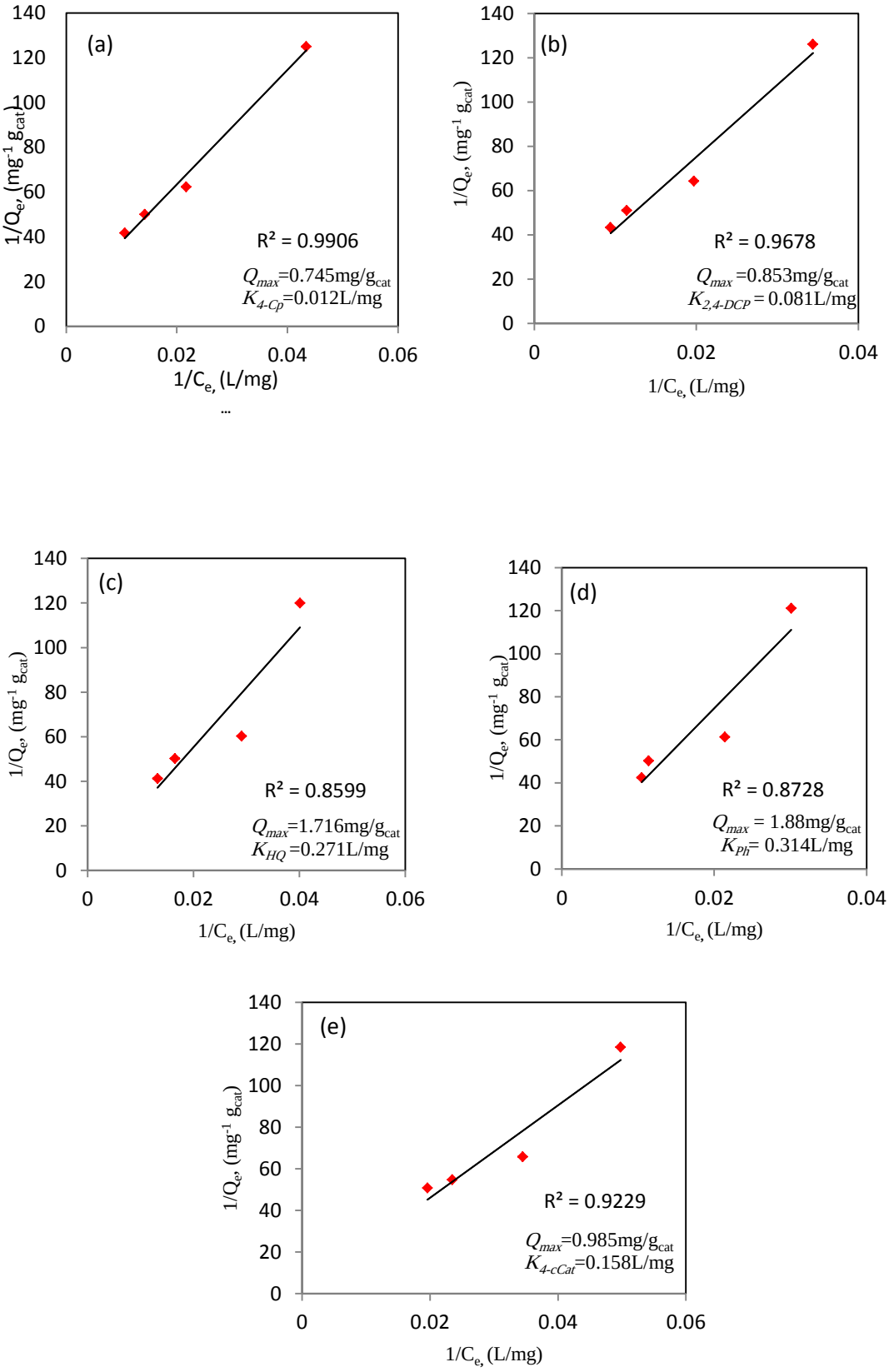

Figure 5.9 Linear regression for Langmuir isotherm: adsorption of (a) 4-CP (b) 2,4-DCP (c) HQ (d) Ph and (e) 4cCat on 0.5g/L TiO_2

5.6 Reaction pathway

Based on the present results, a series-parallel degradation pathway of combined chlorophenols mixture was proposed as shown in Figure 5.10. The suggested mechanism was developed to involve all intermediates detected during 240 min solar photocatalytic degradation of 4-CP and 2,4-DCP as a combined mixture. No main differences of intermediates were observed between individual and binary mixtures of these phenolic compounds. It can be noticed from this mechanism that the Ph compound can be formed from either 4-CP or 2,4-DCP degradation. In addition, due to the high activation of Ph to react with $^{\bullet}OH$ radical (Peng et al. 2012), Ph was rapidly converted to HQ, which resulted in making the HQ concentration the highest among all the intermediates. However, 4cCat was directly generated from hydroxylation of 4-CP by $^{\bullet}OH$ radical at significantly low concentration and rapidly degraded. Some traces of benzoquinone (BQ) were detected which might be formed from the oxidation of HQ by $O_2^{\bullet-}$ (Dhir et al. 2012, Lu et al. 2011, Turchi and Ollis 1990). Some researchers have suggested that the pathway of chlorophenols degradation can be adsorption, dechlorination, hydroxylation and cleavage the aromatic rings to form inorganic products (Liu et al. 2012a, Araña et al. 2007b). It can be concluded from Figure 5.10 that all intermediates are formed at low concentrations and CO_2 and H_2O were the main final products.

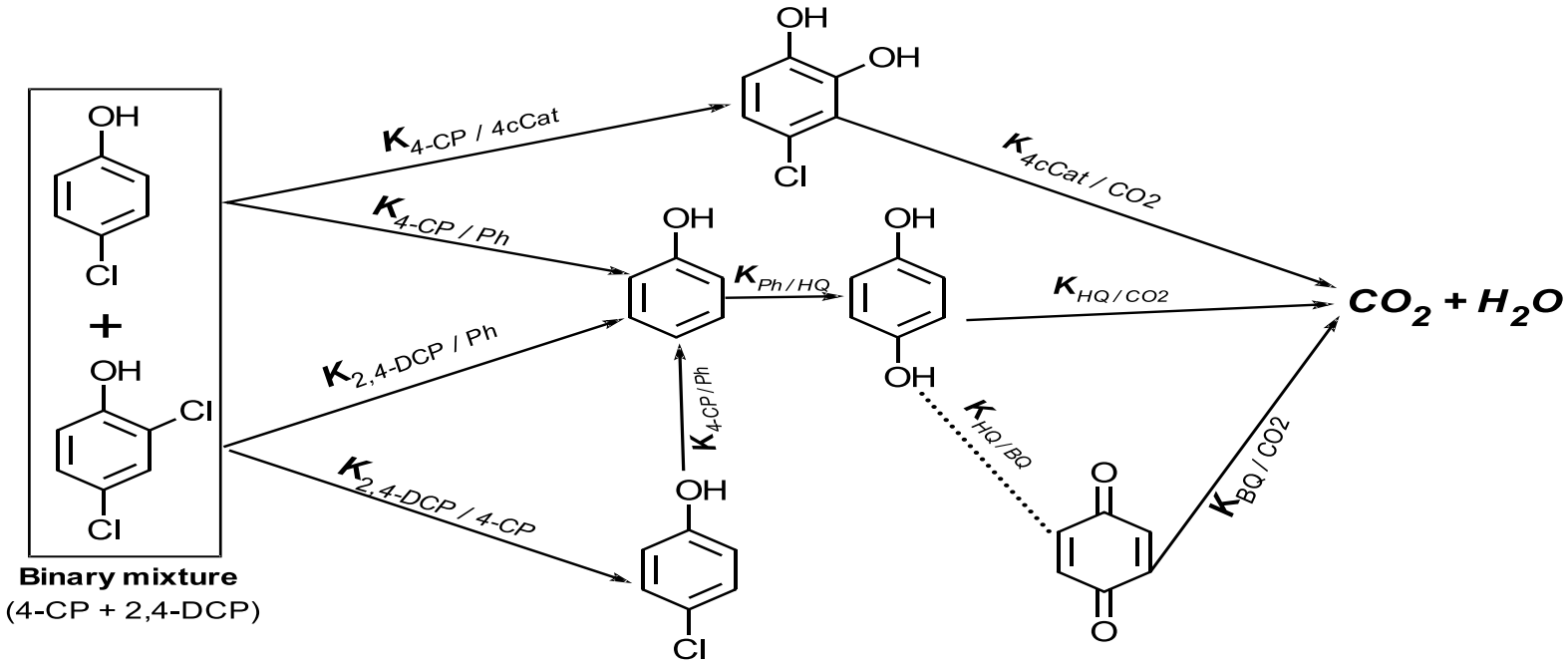

Figure 5.10 Proposed series-parallel solar-photocatalytic degradation pathways of 4-CP and 2,4-DCP mixture

5.7 Kinetic modelling

It is clear from the results that the degradation rate of 4-CP decreases with increase in the initial concentration of 2,4-DCP. Priya and Madras (2006a) had similar results for 4-CP and 4-nitrophenol (4-NP) and used the following expression to calculate the reaction rate constants and reaction rates for combined mixtures.

$$\left(k_{ii} - k_{ij}Cj\right) \tag{5.1}$$

Where, k_{ii} the kinetic constant influenced by the concentration of individual species, and k_{ij} the interaction parameter influenced by both species of combined mixture. With neglecting the influence and concentration of intermediates and applying expression 5.1 together with L-H equation for 4-CP and 2,4-DCP, the reaction rates of 4-CP and 2,4-DCP can be obtained from the following equations:

$$r_{4-CP} = \frac{\left(k_{4-CP} - k_{4-CPB}C_{2,4-DCP}\right)C_{4-CP}}{1 + K_{4-CP}C_{4-CP} + K_{2,4-DCP}C_{2,4-DCP}} \tag{5.5}$$

$$r_{2,4-DCP} = \frac{\left(k_{2,4-DCP} - k_{2,4-DCPB}C_{4-CP}\right)C_{2,4-DCP}}{1 + K_{4-CP}C_{4-CP} + K_{2,4-DCP}C_{2,4-DCP}} \tag{5.6}$$

Where, $k_{4\text{-}CP}$ and $k_{2,4\text{-}DCP}$ are the kinetic reaction constants of individual phenolic compounds and $k_{4\text{-}CPB}$, $k_{2,4\text{-}DCPB}$ are the interaction parameters. However, this method might not be effective to describe the photocatalytic degradation of combined phenolic mixtures due to neglecting influence of the intermediates formed during the mineralisation process which play a significant role by interacting between and with these intermediates. For instance, Bayarri et al., (2005) degraded 2,4-DCP using TiO_2/UV and concluded that the intermediates should consider in the kinetic model to be accurate for long degradation times. Priya and Madras (2006a) also used the initial rate method which means neglecting the concentration and influence of intermediates. Therefore, in this work the effect of second pollutant and the concentration of all observed intermediates formed during the solar-photocatalytic degradation of combined mixture (4-CP and 2,4-DCP) have been considered. Furthermore, four differential equations to estimate the concentration changes for the

modules and their intermediates have been derived. L-H equation describes the general case of multi compounds reaction as follows:

$$r_i = \frac{dC_i}{dt} = \frac{k_i C_i}{1 + \sum_{j=1}^{n} K_j C_j} \tag{5.7}$$

Where r_i is the reaction rate of component *i* in mg/(L min), k_i is the kinetic reaction constant for component *i* in min^{-1}, K_i is the adsorption constant for each of the species participating in the reaction L/mg, *n* denotes the number of participant in the reaction, and *C* is the species concentration mg/L. According to the suggested mechanism (Fig. 5.10), Equation 5.7 can be applied on each of the observed components (4-CP, 2,4-DCP, Ph, 4cCat and HQ) resulting in five differential equations (Eqs. 5.8-12), describing the solar-photocatalytic degradation of 4-CP and 2,4-DCP mixture and their intermediates.

For (4-CP)

$$\frac{dC_{4-CP}}{dt} = \frac{-\left(k_{4-CP} - k_{4-CPB}C_{DCP}\right)\left(C_{Ph} + C_{4cCat}\right) + \left(k_{2,4-DCP} - k_{2,4-DCPB}C_{4-CP}\right)C_{2,4-DCP}}{1 + K_{4-CP}C_{4-CP} + K_{2,4-DCP}C_{2,4-DCP} + K_{Ph}C_{Ph} + K_{4cCat}C_{4cCat} + K_{HQ}C_{HQ}} \tag{5.8}$$

For (2,4-DCP)

$$\frac{dC_{2,4-DCP}}{dt} = \frac{-\left(k_{2,4-DCP} - k_{2,4-DCPB}C_{4-CP}\right)\left(C_{Ph} + C_{4-CP}\right)}{1 + K_{4-CP}C_{4-CP} + K_{2,4-DCP}C_{2,4-DCP} + K_{Ph}C_{Ph} + K_{4-cCat}C_{4cCat} + K_{HQ}C_{HQ}} \tag{5.9}$$

For the intermediates:

(Ph)

$$\frac{dC_{Ph}}{dt} = \frac{2\left(k_{4-CP} - k_{4-CPB}C_{2,4-DCP}\right)C_{4-CP} + \left(k_{2,4-DCP} - k_{2,4-DCPB}C_{4-CP}\right)C_{2,4-DCP} - k_{Ph-HQ}C_{Ph}}{1 + K_{4-CP}C_{4-CP} + K_{2,4-DCP}C_{2,4-DCP} + K_{Ph}C_{Ph} + K_{4cCat}C_{4cCat} + K_{HQ}C_{HQ}} \quad (5.10)$$

(4cCat)

$$\frac{dC_{4cCat}}{dt} = \frac{\left(k_{4-CP} - k_{4-CPB}C_{2,4-DCP}\right)C_{4-CP} - k_{4cCat-CO_2}C_{4cCat}}{1 + K_{4-CP}C_{4-CP} + K_{2,4-DCP}C_{2,4-DCP} + K_{Ph}C_{Ph} + K_{4cCat}C_{4cCat} + K_{HQ}C_{HQ}} \quad (5.11)$$

(HQ)

$$\frac{dC_{HQ}}{dt} = \frac{k_{Ph-HQ}C_{Ph} - k_{HQ-CO_2}C_{HQ}}{1 + K_{4-CP}C_{4-CP} + K_{2,4-DCP}C_{2,4-DCP} + K_{Ph}C_{Ph} + K_{4cCat}C_{4cCat} + K_{HQ}C_{HQ}} \quad (5.12)$$

Assumptions made for the above equations are: (i) all detected components adsorb on the catalyst surface; (ii) the CO_2 species do not adsorb on the catalyst particle; (iii) the reaction rate constants of 4-CP and 2,4-DCP are the same whatever the formed product. Furthermore, all the adsorption constants were experimentally estimated to minimise unknown parameters in the present model.

5.8 Model fitting to the experimental data

A kinetic model of combined mixture (4-CP and 2,4-DCP) and their intermediates (Ph, 4cCat and HQ) was developed. This kinetic model was based on the proposed degradation mechanism (Fig. 5.10). Some assumptions have been applied in order to use the L-H equation (Eq. 5.7) and minimise the unknown variables. Furthermore, the adsorption constants of all components were experimentally determined in order to improve the kinetic model accuracy. Five ordinary differential equations (Eqs. 5.8-12) were developed to describe the proposed degradation mechanism for 4-CP, 2,4-DCP, Ph, 4cCat and HQ, respectively. These ordinary differential equations

cannot be solved analytically, therefore, MATLAB (Version 7.11.0.584; R2010b) was used to solve these equations and estimate the reaction rate constants for all components involved in the developed model. Table 5.1 summarises the estimated reaction rate constants for 4-CP; 2,4-DCP; Ph; HQ and 4cCat. It is clear that the reaction rate constant of 4-CP is higher than that of 2,4-DCP indicating that the mineralisation of 4-CP is faster than that of 2,4-DCP.

Table 5.1 Estimated reaction rate constants for the solar photocatalytic oxidation of 4-CP and 2,4-DCP mixture and their intermediates

Reaction rate constant	**Value (min^{-1})**
k_{4-CP}	0.051
$k_{2,4-DCP}$	0.034
k_{4-CPB}*	0.0047
$k_{2,4-DCPB}$*	0.0841
k_{Ph-HQ}	0.241
k_{HQ-CO_2}	0.145
$k_{4cCat-CO_2}$	0.078

***** The reaction rate constants in the mixtures of 4-CP and 2,4-DCP respectively.

Figure 5.11 presents the experimental concentration profiles (represented by dots) of 50 mg/L 4-CP at different 2,4-DCP (50, 75, 100 mg/L) initial concentrations and their intermediates as well as the estimated profiles for these different initial concentrations. It can be seen that the kinetic model predicts very well the experimental data over a wide range of initial concentrations. Also these figures show that the increase of second pollutant concentrations leads to decrease of the degradation efficiency of the other pollutant as well as the intermediates mineralisation.

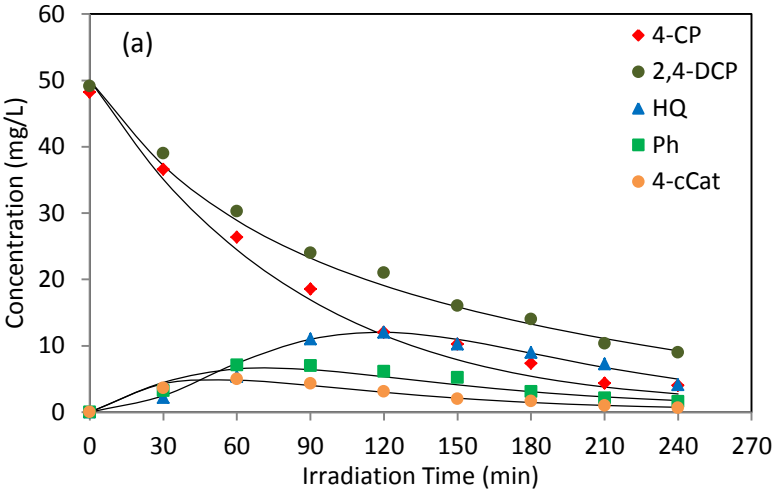

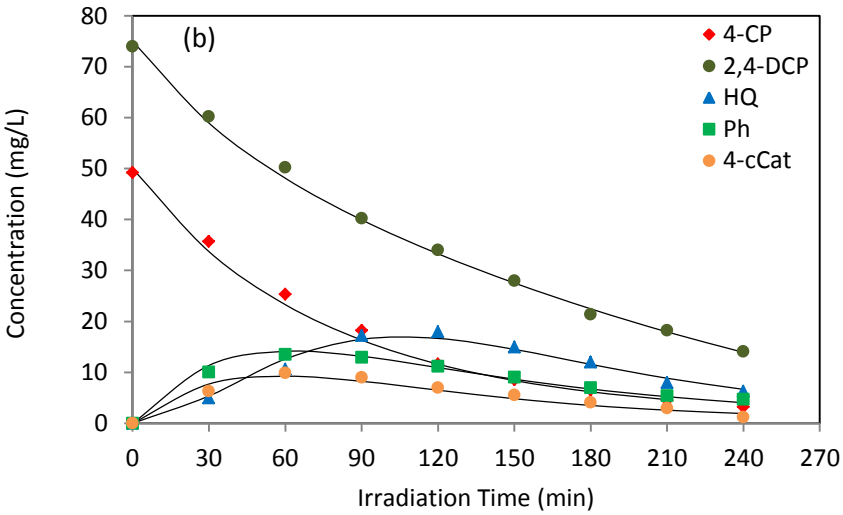

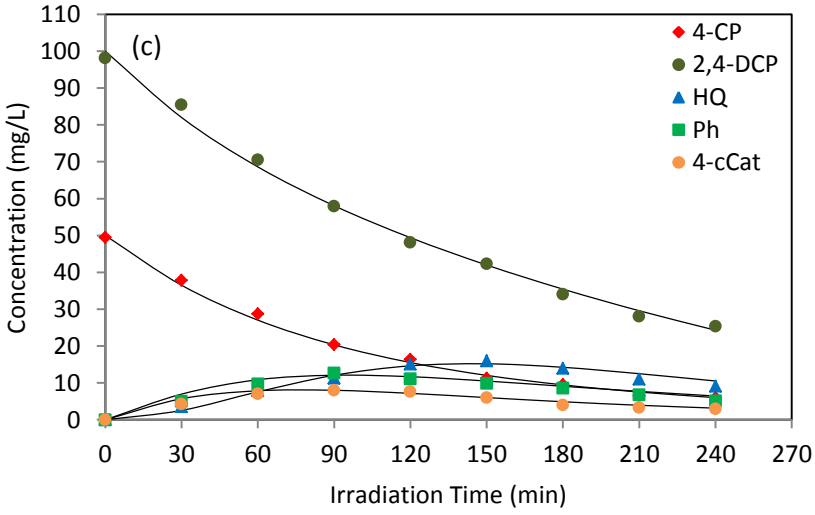

Figure 5.11 Experimental and estimated concentration profiles for photocatalytic degradation of 50 mg/L 4-CP on 0.5 g/L TiO_2 and 1000 mW/cm^2 at different 2,4-DCP initial concentrations (a) 50mg/L (b) 75mg/L (c) 100mg/L, (-) represents model results.

Summary

The solar photocatalytic degradation of single and combined mixtures of chlorophenols compounds was investigated at different initial concentrations. The degradation of 2,4-DCP was slower than that of 4-CP, indicating that high chlorine atoms could retard the dechlorination process. Three major intermediates named HQ, Ph, and 4cCat were observed during 240 min solar-photocatalytic degradation of 4-CP, whereas; only two main intermediates 4-CP and Ph were detected during the degradation of 2,4-DCP under the same conditions. The solar photocatalytic degradation of a mixture containing 4-CP and 2,4-DCP led to decrease in the degradation efficiency of both compounds compared to their individual degradations. This decrease of the efficiency was due to formation of 4-CP as intermediate from the degradation of 2,4-DCP and the competition for the catalyst active site and interaction between these compounds in the mixture. Based on the presented results, a kinetic reaction pathway for the combined mixture degradation was proposed. The mechanism involved all possible intermediates observed during the degradation. According to the suggested pathway, a modified L-H kinetic model including the interaction between the main pollutants and all detected intermediates was developed. Five ordinary differential equations representing the 4-CP; 2,4-DCP; HQ; Ph and 4cCat degradation profiles were numerically solved using MATLAB. The model was able to predict the concentration profiles for a wide range of 2,4-DCP initial concentrations (50-100 mg/L). A good agreement between estimated and experimental results was achieved.

CHAPTER 6

ENHANCED SOLAR PHOTOCATALYTIC DEGRADATION OF CHLOROPHENOLS MIXTURES USING IRON IONS AND HYDROGEN PEROXIDE

6.1 Introduction

The photocatalytic degradation process is an appropriate technique to destroy and mineralise refractory organic pollutants (Adán et al. 2009b). The efficiency of this method usually comes by using a suitable photocatalyst such as titanium dioxide (TiO_2) and UV/solar source. However, the main drawback of photocatalytic processes is the recombination of charges between e^- and h^+ leading to reduced degradation efficiency (Salaices et al. 2004). To overcome this issue, many techniques have been used in order to enhance the photocatalytic degradation efficiency such as the structural modification and doping of photocatalysts with metals or dyes (Biyoghe et al. 2014, Znad and Kawase 2009, Selvam et al. 2007). However, these methods might not be economically feasible for large-scale applications due to the expensive chemicals used and the high calcination temperatures applied (Arana et al. 2001). Therefore, the use of metals like iron ions (Fe^{2+}/Fe^{3+}) as additives in the photocatalytic process could reduce the operating cost as well as the experimental procedures. For example, Ortiz-Gomez et al., (2008) used ferric ions (Fe^{3+}) as an additive in the photocatalytic degradation process of phenol and other hydroxylated compounds. They concluded that the use of small amount of Fe^{3+} can effectively enhance the mineralisation of phenol and its intermediates. In fact iron ions used in photocatalytic degradation processes can be either ferrous (Fe^{2+}) or ferric (Fe^{3+}). Despite the use of ferrous ion in AOPs as reagent in Fenton-like or in photo-Fenton processes, a few studies have used it as additives for the photocatalytic degradation of organic pollutants and their intermediates (Sclafani et al. 1991; Selvam et al. 2005). The role of Fe^{2+}/Fe^{3+} ions in solar photocatalytic degradation processes strongly depend on several key parameters such as oxidation state, pH, and type of metallic salt used as a source of iron ion as well as the presence of other oxidants like H_2O_2 and O_2 (Kavitha and Palanivelu 2004). For instance, Nogueira et al. (2005) investigated the influence of two different iron sources, $Fe(NO_3)_3$ and complexed ferrioxalate (FeO_x) on the solar photocatalytic degradation of organic compounds. They found that the efficiency of $Fe(NO_3)_3$ is less than that of FeO_x due to the presence of nitrogen leading to low quantum yield of Fe^{2+} generation. Generally, the presence of iron ions (Fe^{2+} or Fe^{3+}) can effectively enhance the photocatalytic degradation efficiency of organic compounds. However, there is a need to determine the residual iron at the end of

degradation processes because the excess concentrations might negatively affect aquatic life. Thus, minimum amounts of iron should be used in this kind of degradation or alternatively the residual amounts might be recovered and used again in the treatment system. Muthuvel and Swaminathan (2007) stated that there are no negative impacts on the catalytic activity when using recovered iron in the degradation processes. There has been strong debate about the role of iron ions in photocatalytic degradation processes and which form gives better degradation efficiency. As a result there is a need for further investigations and clarifications to confirm if there is a significant difference between Fe^{2+} and Fe^{3+} in the oxidation processes. Another effective solution for reducing the e^-/h^+ recombination and enhancing the photocatalytic degradation efficiency is the use of strong inorganic oxidants such as $S_2O_8^{2-}$ and H_2O_2. The addition of H_2O_2 to the photocatalytic process helps to accelerate the rate of phenol decomposition by effectively generating hydroxyl radicals that can mineralise organic pollutants (Cornish et al. 2000). For instance, Aceituno et al., (2002) investigated the degradation of metol using $TiO_2/H_2O_2/UV$ and concluded that the H_2O_2 oxidant can increase the activity of TiO_2 leading to enhance the photocatalytic degradation efficiency. Also Nogueira et al., (2004) showed by applying the factorial analysis that the roles of both iron and H_2O_2 in the solar photo degradation of 4-CP are more important than that of TiO_2. Poulopoulos and Philippopoulos (2004) proved that addition of Fe^{3+} could enhance the photocatalytic oxidation of 4-CP markedly only in the presence of H_2O_2. Most of research studies have used either iron metals or inorganic oxidants in the photocatalytic process. Additionally, all of them have been implemented to degrade one compound (Selvam et al. 2005, Tryba et al. 2006, Quici et al. 2007). However, in real effluent many toxic organic contaminants can exist and there is a need to develop efficient and economic treatment methods. Therefore, the aim of this study is to investigate the solar photocatalytic degradation of combined chlorophenols mixture containing 4-CP and 2,4-DCP using a new method which is a hybrid photo-Fenton/photocatalytic (Photocatalytic-Fenton) degradation process. The role of $^{\bullet}OH$ radicals in the degradation and a comparison with other existing methods will be discussed in detail. Also, the degradation pathways and the reaction mechanism of the chlorophenols mixture are studied. Also, this work will investigate the influence of ferrous and ferric ions on the solar photocatalytic degradation of chlorophenols mixture consisting of 4-CP and 2,4-DCP and their intermediates. Finally, the role

and mechanism of Fe^{2+} and Fe^{3+} ions during the solar degradation was also discussed.

6.2 Experimental procedure

As mentioned in Chapter 3 (Section 3.3.3) a combined chlorophenols mixture (50 mg/L of both 4-CP and 2,4-DCP) was degraded under solar light using TiO_2, $FeCl_3 \cdot 6H_2O$, $FeSO_4. 7H_2O$ and H_2O_2. The combined mixture was dissolved in distilled water and transferred to the photoreactor before adding TiO_2. After that, the photocatalyst 0.5 g/L TiO_2 and the desired amounts of Fe^{3+} ($FeCl_3 \cdot 6H_2O$) and/or H_2O_2 were suspended in 200 mL and then added to the mixture. The total volume of the solution was 1 L. All suspensions, which contain TiO_2, were magnetically stirred in the dark for 30 min to attain adsorption−desorption equilibrium between chemical components and TiO_2. Then, the lamp was turned on, and the timer was set to zero to start measuring the reaction time. The same procedures were conducted using Fe^{2+} ($FeSO_4. 7H_2O$) instead of Fe^{3+}.

6.3 Solar/TiO_2/Fe^{3+}/H_2O_2 hybrid process

In order to enhance the efficiency of the Solar/TiO_2/Fe^{3+} process, different concentrations of H_2O_2 were used. To determine the optimum value of H_2O_2, all operating conditions (light intensity, TiO_2, Fe^{3+} and pH) were kept constant. It is evident from Figure 6.1 that the maximum degradation of 4-CP and 2,4-DCP in the combined mixture was achieved at 3.41 mM H_2O_2. Aceituno et al., (2002) investigated the effect of H_2O_2 on the photocatalytic degradation of metol under UV irradiation and the complete degradation was achieved at 0.4 M of H_2O_2 within about 2 h UV irradiation. The low concentration (3.41 mM) of H_2O_2 applied in our study played a significant role by generating more $^{\bullet}OH$ radicals which are powerful oxidants for aromatic compounds and enhancing the degradation efficiency. In addition, H_2O_2 can be effectively converted to $^{\bullet}OH$ radicals by photocatalytic reaction (Wei et al. 1990). However, increasing the amount of H_2O_2 further highly reduced the degradation efficiency due to the consumption of $^{\bullet}OH$ radicals by H_2O_2, Equation 6.1 (Malato et al. 1998).

$$H_2O_2 + {}^{\bullet}OH \rightarrow H_2O + HO_2{}^{\bullet} \qquad (6.1)$$

Where $HO_2^{\bullet}$ is a free radical but it is less reactive than $OH^{\bullet}$ radicals

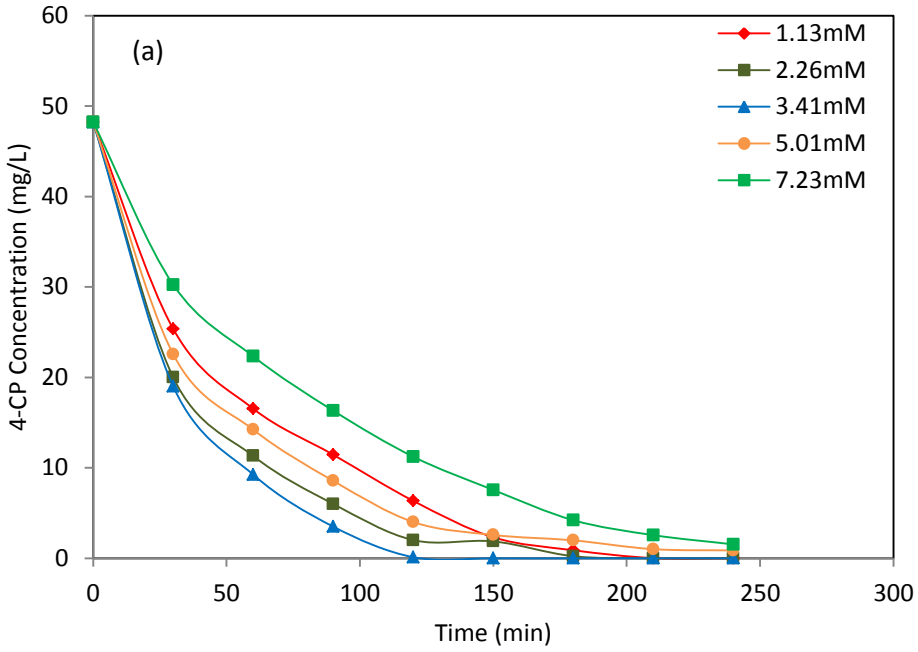

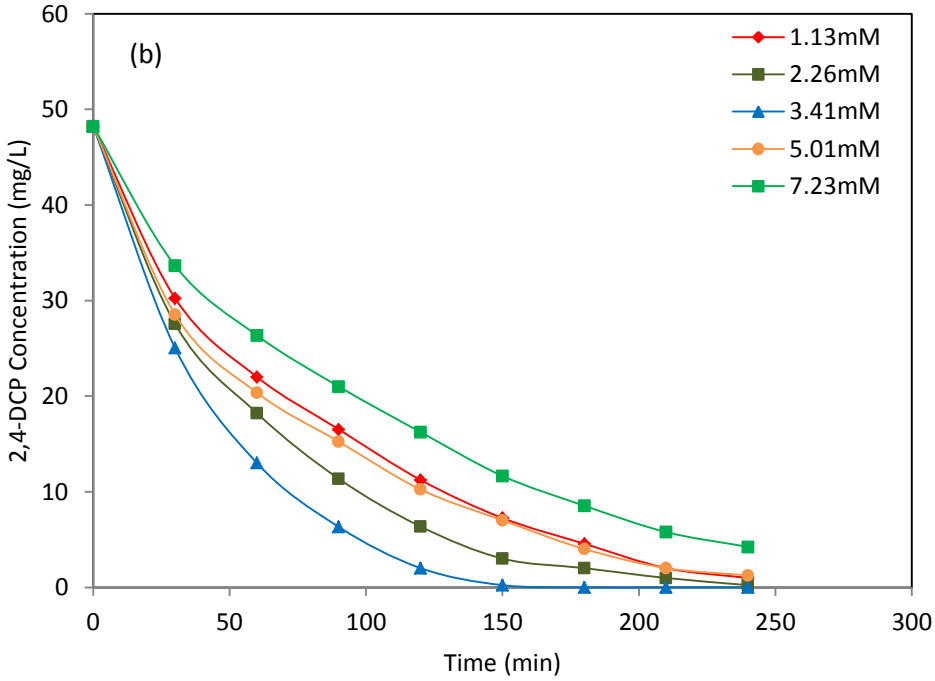

Figure 6.1 The effect of hydrogen peroxide on the photocatalytic degradation of: (a) 4-CP (b) 2,4-DCP (10 mg/L $FeCl_3$. $6H_2O$, 0.5 g/L TiO_2, 1000 mW/cm^2 light intensity)

The mechanism of generating the $^{\bullet}OH$ radicals with added H_2O_2 in the photocatalytic reaction system have been suggested in several studies (Malato et al. 1998, Wei et al. 1990, Matthews 1986).

$$H_2O_2 + h\nu \rightarrow 2^{\bullet}OH \quad (6.2)$$

$$H_2O_2 + O_2^{\bullet -} \rightarrow {}^{\bullet}OH + O_2 + OH^- \quad (6.3)$$

$$H_2O_2 + Fe^{3+} + h\nu \rightarrow Fe^{2+} + HO_2^{\bullet} + H^+ \quad (6.4)$$

$$H_2O_2 + Fe^{2+} \rightarrow Fe^{3+} + {}^{\bullet}OH + OH^- \quad (6.5)$$

$$H_2O_2 + TiO_2\,(e^-) \rightarrow TiO_2 + {}^{\bullet}OH + OH^- \quad (6.6)$$

Equations 6.2-6 obviously explain that H_2O_2 may react by four different ways in the suspension solution all of which lead to generation of $^{\bullet}OH$ radicals. Firstly, direct photolysis to H_2O_2 by UV light could be the first possibility in this mechanism (Eq. 6.2), however; the UV absorption of H_2O_2 at 365 nm is extremely low consequently the generation of the hydroxyl radical by photolysis of H_2O_2 is highly insignificant (Chu and Wong 2004). Secondly, the H_2O_2 oxidant might react with superoxide radicals ($O_2^{\bullet -}$) formed by dissolved oxygen during the solar irradiation time and produced $^{\bullet}OH$ radicals (Eq. 6.3). However, the amount of O_2 in the mixture is very low because the experiments were carried out at the ambient conditions without sparging the solution with air or pure O_2. Therefore, the amount of $^{\bullet}OH$ radicals generated via $O_2^{\bullet -}$ has to be very low and insignificant. Another chemical reaction route, which can occur in this kind of heterogeneous photo-Fenton degradation process, is the reaction between H_2O_2 and Fe^{3+}. This reaction can be considered as one of the main steps to produce $^{\bullet}OH$ radicals due to the influence of solar and UV light (290 - 400 nm) on Fe^{3+} leading to form ferrous ions (Fe^{2+}) and hydroxyl radicals (Eqs. 6.4,5) (Kavitha and Palanivelu 2004). Finally, the most effective degradation reaction in this hybrid degradation process is the reaction of hydrogen peroxide and ferric ions in the presence of TiO_2 photocatalyst (Poulopoulos and

Philippopoulos 2004). The presence of H_2O_2 together with TiO_2 can effectively enhance the photocatalytic degradation due to its ability to accept photogenerated electrons from the conduction band leading to enhance the charge separation (Eq. 6.6) (Toor et al. 2006). To give this kind of photocatalytic degradation process more enhancements, Fe^{3+} ions were added. These ions had a beneficial effect on the photocatalytic activity particularly at low levels due to their acts as h^+/e^- traps and reduce the recombination rate (Eqs. 6.7-10) (Zhao et al. 2010).

$$Fe^{3+} + e^- \rightarrow Fe^{2+} \quad (6.7)$$

$$Fe^{2+} + O_{2(ads)} \rightarrow Fe^{3+} + O^{\bullet-}_2 \quad (6.8)$$

$$Fe^{3+} + h^+_{vb} \rightarrow Fe^{4+} \quad (6.9)$$

$$Fe^{4+} + OH^- \rightarrow Fe^{3+} + {}^{\bullet}OH \quad (6.10)$$

However, recombination centres of h^+/e^- pairs might be formed by iron ions at high Fe^{3+} concentrations leading to decrease the photocatalytic activity (Eq. 6.11,12) (Kim et al. 2005).

$$Fe^{3+} + e^- \rightarrow Fe^{2+} \quad (6.11)$$

$$Fe^{2+} + h^+_{vb} \rightarrow Fe^{3+} \quad (6.12)$$

Figure 6.2 shows the effect of hydrogen peroxide on the degradation efficiency of 4-CP and 2,4-DCP at the optimum conditions (10 mg/L $FeCl_3$. $6H_2O$, 0.5 g/LTiO_2, 1000 mW/cm_2). The maximum degradation efficiencies (using Eq. 3.1 at C_t=150 min) of 4-CP and 2,4-DCP were 97% and 91% respectively.

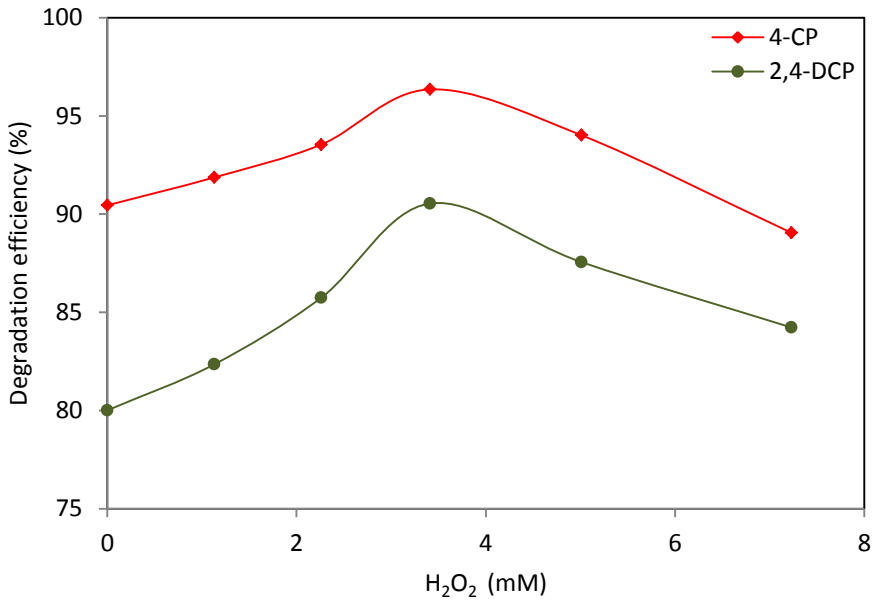

Figure 6.2 Effect of hydrogen peroxide on the degradation efficiency of 4-CP and 2,4-DCP (10 mg/L $FeCl_3$. $6H_2O$, 0.5 g/LTiO_2, C_t=150 min, 1000 mW/cm^2)

Figure 6.3 presents the typical concentration profiles of the combined mixture and their intermediates at optimal conditions of TiO_2, Fe^{3+} and H_2O_2. An extremely important finding from this figure is that one of the main intermediates (4cCat) has disappeared. In addition, the degradation time was considerably reduced from 150 min for Solar/TiO_2/Fe^{3+} system to less than 120 min for the system with H_2O_2.

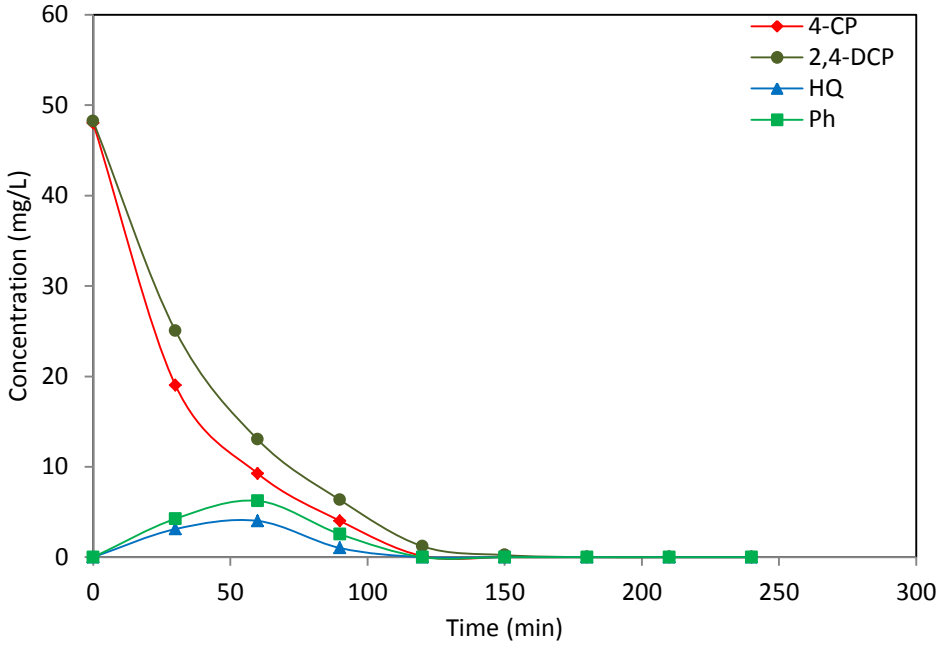

Figure 6.3 Concentration profiles of the combined mixture 50 mg/L of both 4-CP and 2,4-DCP with 10 mg/L $FeCl_3$. $6H_2O$ and 3.41 mM H_2O_2 optimum values. (0.5 g/LTiO_2, 1000 mW/cm^2)

6.4 Solar/H_2O_2/ Fe^{3+} photo-Fenton

In order to compare the degradation profile of the photo-Fenton process and Solar/TiO_2/Fe^{3+}/H_2O_2 Photocatalysis, set of photo-Fenton experiments using 3.41 mM and 10 mg/L of H_2O_2 and Fe^{3+} respectively were carried out. The aim of these experiments is to explain the effect of TiO_2 in the Solar/TiO_2/Fe^{3+}/H_2O_2 hybrid degradation process. Figure 6.4 shows the concentration profiles of the combined mixture and their intermediates. It is clear that the photo-Fenton degradation efficiencies of the main pollutants and their intermediates were lower than that of Solar/TiO_2/Fe^{3+}/H_2O_2 (see Fig. 6.3). The combined mixture and the intermediates formed were fully degraded at about 200 min (Fig. 6.4) using the photo-Fenton process, while full degradation needs about 150 min when the Solar/TiO_2/Fe^{3+} process applied (Fig. 6.3). Additionally, the organic intermediates found here were HQ, Ph and 4cCat whereas only HQ and Ph were observed in Solar/TiO_2/Fe^{3+}/H_2O_2. In order to quantify the enhancement of the combined mixture degradation, the half – life times ($t_{1/2}$) were calculated and summarized in Table 6.1.

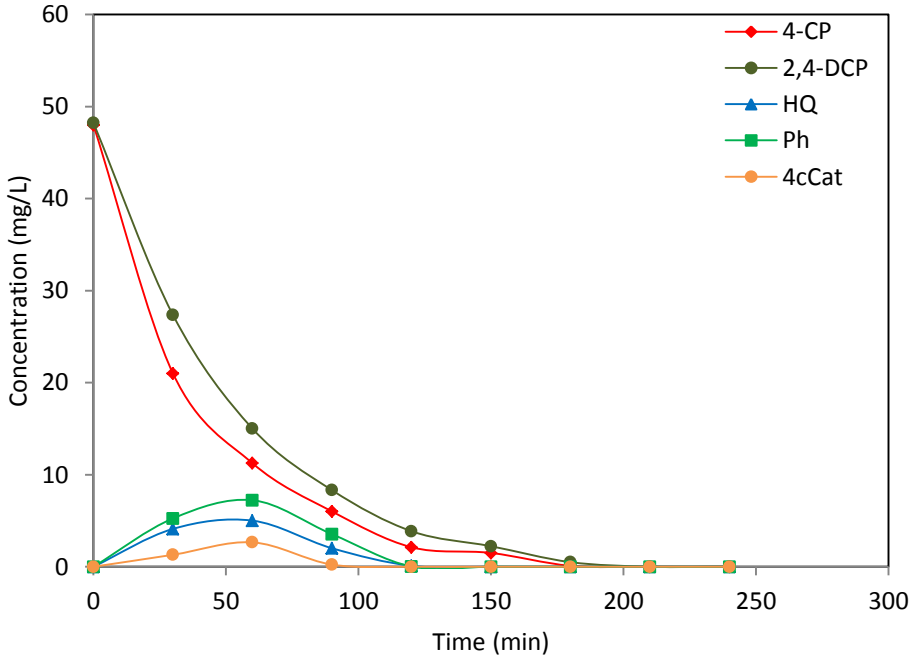

Figure 6.4 Concentration profiles of the combined mixture 50 mg/L of both 4-CP and 2,4-DCP with 10 mg/L $FeCl_3$. $6H_2O$ and 3.41 mM H_2O_2 optimum values. (pH=3, 1000 mW/cm^2)

Table 6.1: Half-life time for the combined mixture (4-CP and 2,4-DCP) photodegradation using different processes.

Process	4-CP Half-life time (min)	2,4-DCP Half-life time (min)
Solar/TiO_2/Fe^{3+}	37	43
Solar/Fe^{3+}/H_2O_2	26	32
Solar/TiO_2/Fe^{3+}/H_2O_2	14	22

6.5 Effect of ferrous and ferric ions

It is well known that the photocatalytic degradation of chlorophenols is more efficient in the acidic medium than in the basic medium (Selvam et al. 2007, Dhir et al. 2012).Thus, all experiments were conducted at pH 3. The initial concentration of both 4-CP and 2,4-DCP used in all solar photocatalytic degradation experiments was 50 mg/L with 0.5 g/L of TiO_2. To investigate the optimum value of ferrous ions, different concentrations of Fe^{2+} were used. Figure 6.5 illustrates the effect of Fe^{2+} on the solar photocatalytic degradations of 4-CP and 2,4-DCP. It is clear that the maximum degradation occurred at a Fe^{2+} concentration of 7 mg/L, for both the contaminants. However, at high ferrous concentrations the degradation efficiency decreases. This result can be clarified by the fact that the recombination of the e^-/h^+ pairs increases at high metal ions doses leading to reduced $^{\bullet}OH$ radicals.(Arslan et al. 2000)

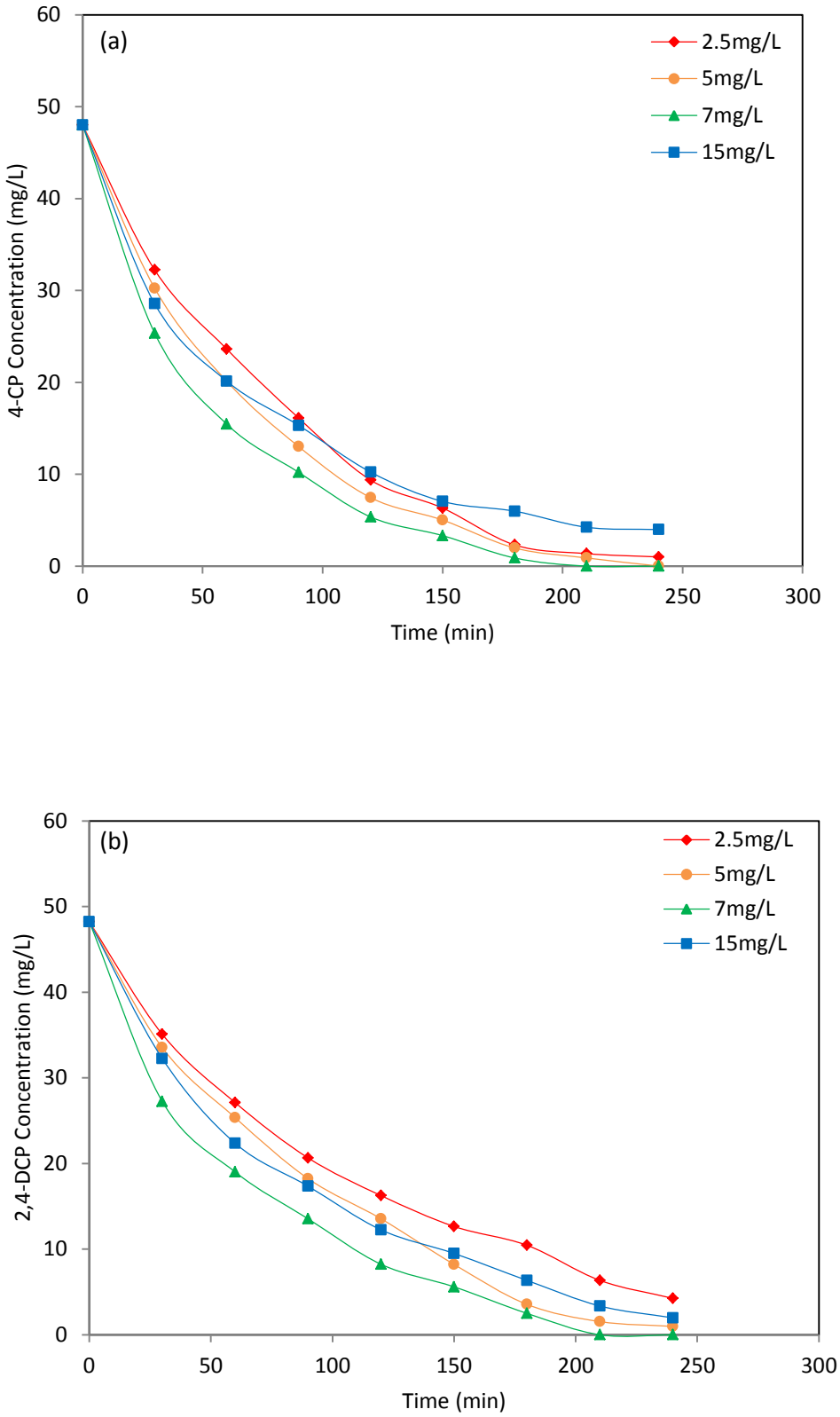

Figure 6.5 Effect of ferrous ions (Fe^{2+}) on the solar-photocatalytic degradation of (a) 4-CP and (b) 2,4-DCP (0.5 g/L TiO_2, 1000 mW/cm^2).

The influence of Fe^{3+} on the photocatalytic degradation of the same pollutants was also investigated under the same conditions (0.5 g/L TiO_2, 1000 mW/cm^2 light intensity). The results in Figure 6.6 showed that the optimum value of Fe^{3+} was 10 mg/L. Kim et al. (2005) investigated the effect of ferric ion on the photocatalytic degradation of alachlor in the presence of TiO_2 and UV radiation and found that the reaction rate constant was enhanced by 80% when 7.5 mg/L of Fe^{3+} was applied.

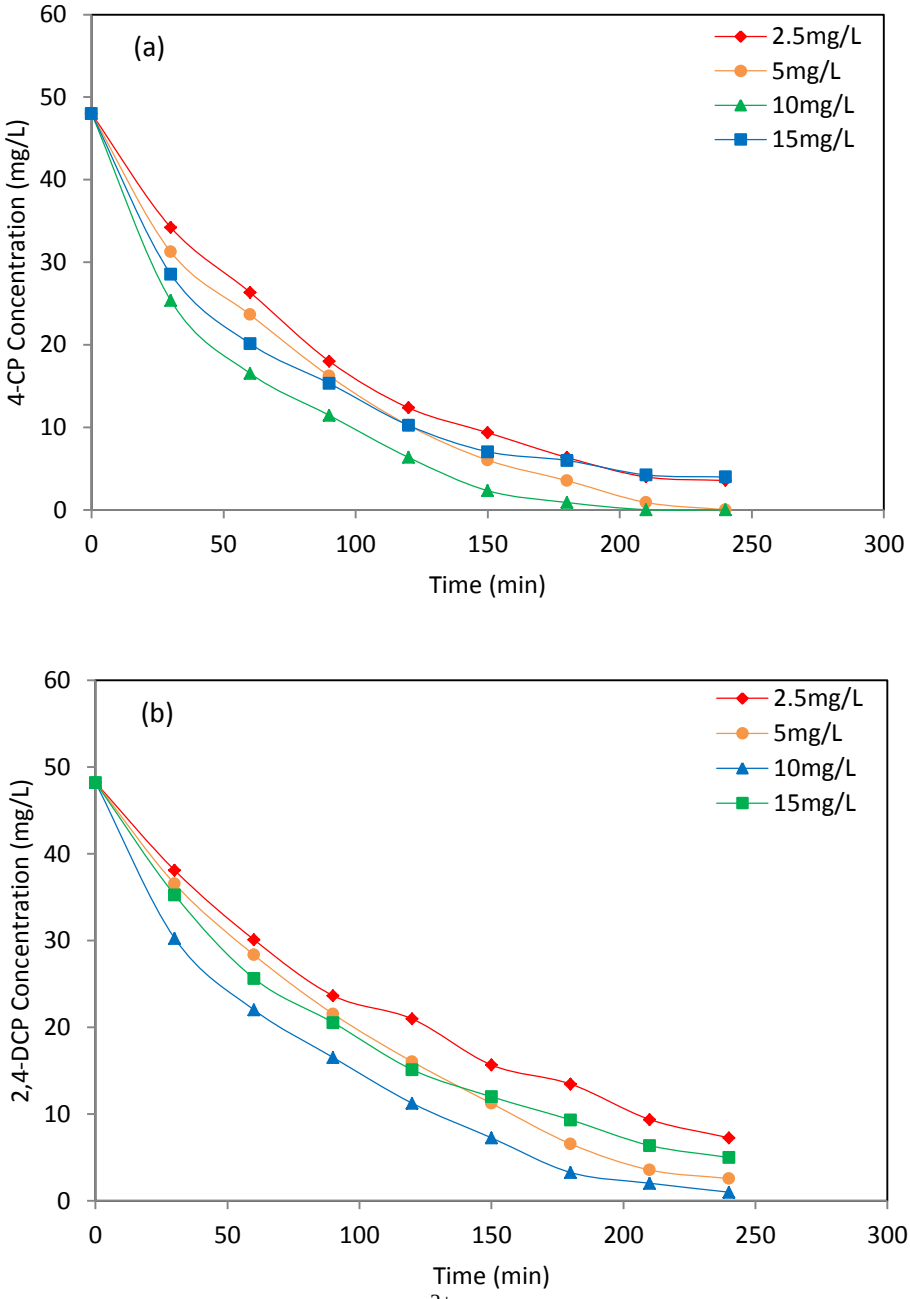

Figure 6.6 Effect of ferric ions (Fe^{3+}) on the solar-photocatalytic degradation of (a) 4-CP and (b) 2,4-DCP (0.5 g/L TiO_2, 1000 mW/cm^2 light intensity).

The degradation efficiencies of 4-CP and 2,4-DCP at different Fe^{2+} or Fe^{3+} doses were determined. Figure 6.7a shows the influence of ferrous ions on the degradation efficiency of both compounds. It can be seen that the maximum degradation efficiencies of 4-CP and 2,4-DCP were 93% and 87% respectively, achieved at 7 mg/L Fe^{2+} when the irradiation time reached 150 min where most of the intermediates formed had been degraded. The difference in the removal efficiency of 4-CP and 2,4-DCP can be attributed to the high Cl atoms in 2,4-DCP which need more irradiation time to be degraded. Ankova et al. (2005) investigated the effect of ferrous ions on the photocatalytic degradation of Monuron (3-(4-chlorophenyl)-1,1-dimethylurea) and found that the positive effect of ferrous was in the range 2 to 15.19 mg/L. Figure 6.7b shows the effect of ferric ions on the degradation efficiency of 4-CP and 2,4-DCP. The maximum degradation efficiencies of 4-CP and 2,4-DCP were 91% and 81% respectively. It can be seen that there is a difference between the efficiencies of the compounds which is very close to that achieved when using ferrous ions (Fig. 6.7a)

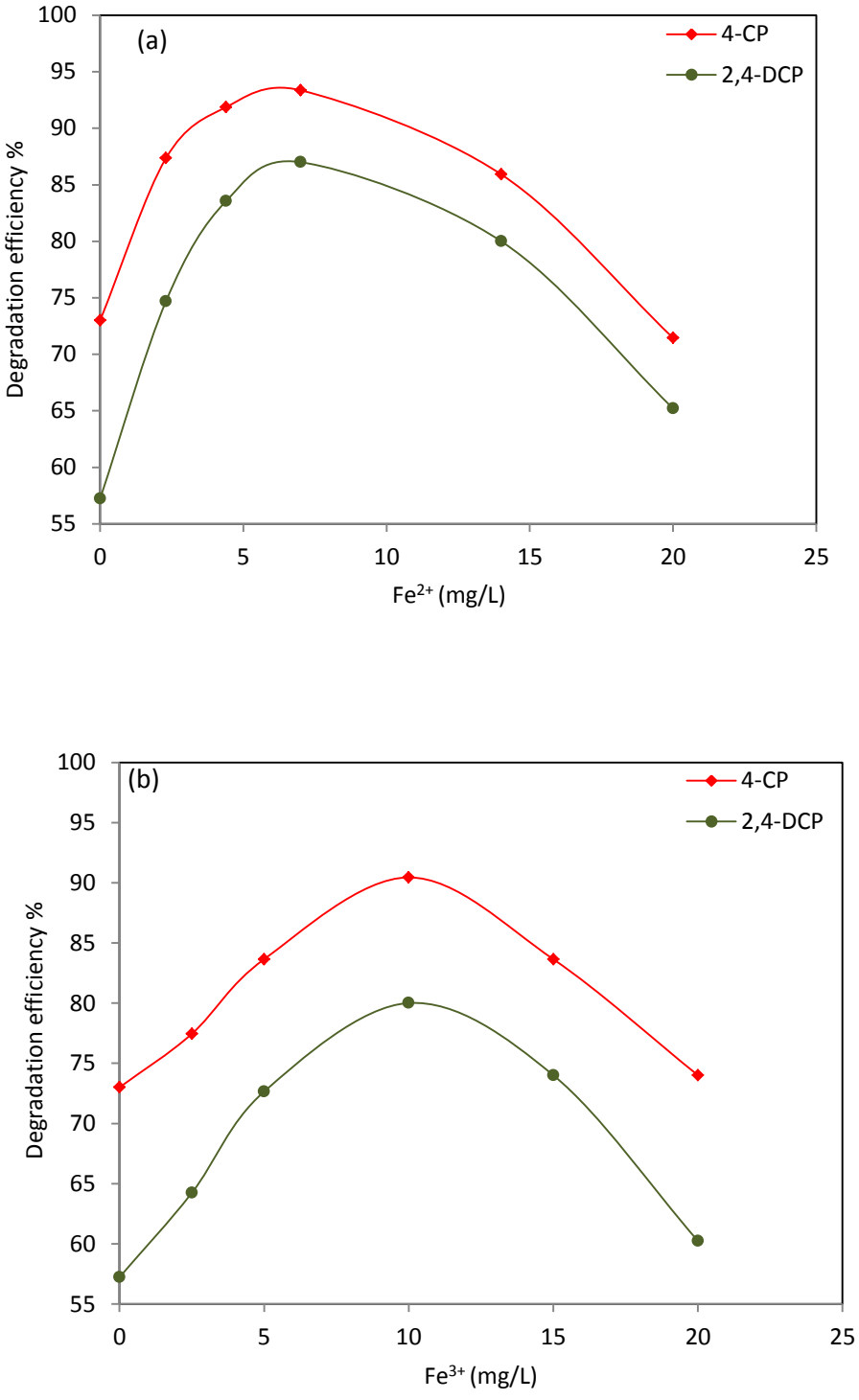

Figure 6.7 Effect of iron ions on the degradation efficiency of 4-CP and 2,4-DCP (0.5 g/L TiO_2, 1000 mW/cm^2, 150 min) (a) Fe^{2+} (b) Fe^{3+}

6.6 Solar photocatalytic degradation of the combined mixture using Fe^{2+} and Fe^{3+}

In the presence of the optimal concentrations of Fe^{2+} (7 mg/L) or Fe^{3+} (10 mg/L), the solar photocatalytic degradation of the chlorophenols mixture generated three main intermediates namely HQ, Ph, and 4cCat as shown in Figure 6.8. It can be seen from Figure 6.8a that all the formed intermediates have the maximum concentrations at around 60 min before they degraded at 120 min solar irradiation time. These results indicate that there is a significant enhancement of the degradation time compared with the results discussed in Chapter 5 where no iron ions were used and the complete degradation was obtained at 240 min. Figure 6.8b shows similar results for the influence of Fe^{3+} ions. It is clear that there is no considerable difference in terms of the types of intermediates formed compared to Fe^{2+}. However, the complete degradation time was reduced from 150 min to 120 min. This difference in the degradation time may indicate that ferrous is more active with TiO_2 than ferric ions. This activity might be achieved by at least two ways including (i) efficiently trapping the photogenerated electron e^- by Fe^{2+} leading to reduction in the e^-/h^+ recombination rate (ii) the reaction of Fe^{2+} with hydrogen peroxide generated from TiO_2 during solar irradiation time according to Equations 6.13-17 (Arslan et al. 2000):

$$TiO_2 + h_v \rightarrow h^+ + e^- \quad (6.13)$$

$$h^+ + OH^- \rightarrow {}^{\bullet}OH \quad (6.14)$$

$$O_2 + e^- \rightarrow O^{-\bullet}_2 \quad (6.15)$$

$$2O^{-\bullet}_2 + H_2O \rightarrow H_2O_2 + 2O_2 \quad (6.16)$$

$$Fe^{2+} + H_2O_2 \rightarrow Fe^{3+} + {}^{\bullet}OH + OH^- \quad (6.17)$$

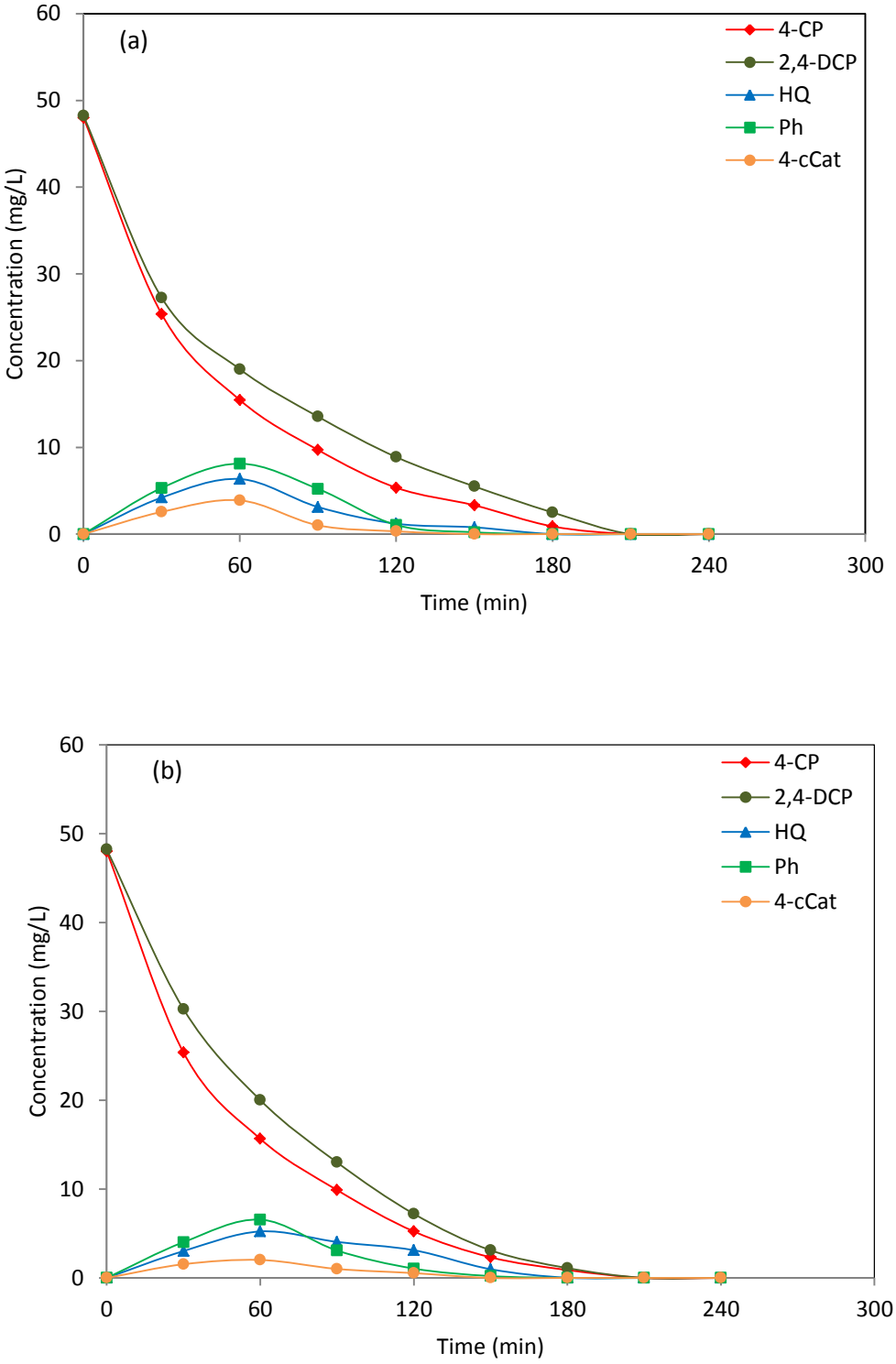

Figure 6.8 Concentration profiles of the combined mixture 50 mg/L of both 4-CP and 2,4-DCP (0.5 g/LTiO_2, 1000 mW/cm^2) with optimal values of (a) Fe^{2+}=7 mg/L (b) Fe^{3+}=10 mg/L

To monitor the total removal efficiency of the combined mixture, COD was continuously measured during the course of the reaction. Figure 6.9 illustrates the COD reduction of the mixture at the optimal conditions of Fe^{2+}=7 mg/L, and Fe^{3+}=10 mg/L. It can be seen from Figure 6.9a, which used Fe^{2+}, that significant reduction of COD started after 60 min. The low reduction rate during the first 60 min of the solar irradiation might be attributed to the formed intermediates (HQ, Ph, 4cCat) that make the solution rich of organic compounds Figure 6.8.

However, when using Fe^{3+} instead of Fe^{2+} under the same conditions the COD of the combined mixture decreased gradually as shown in Figure 6.9b. The maximum COD reduction achieved at 240 min was 79%. These results might indicate that there are still other intermediates (undetected) that were not degraded as the main pollutants completely degraded at this irradiation time.

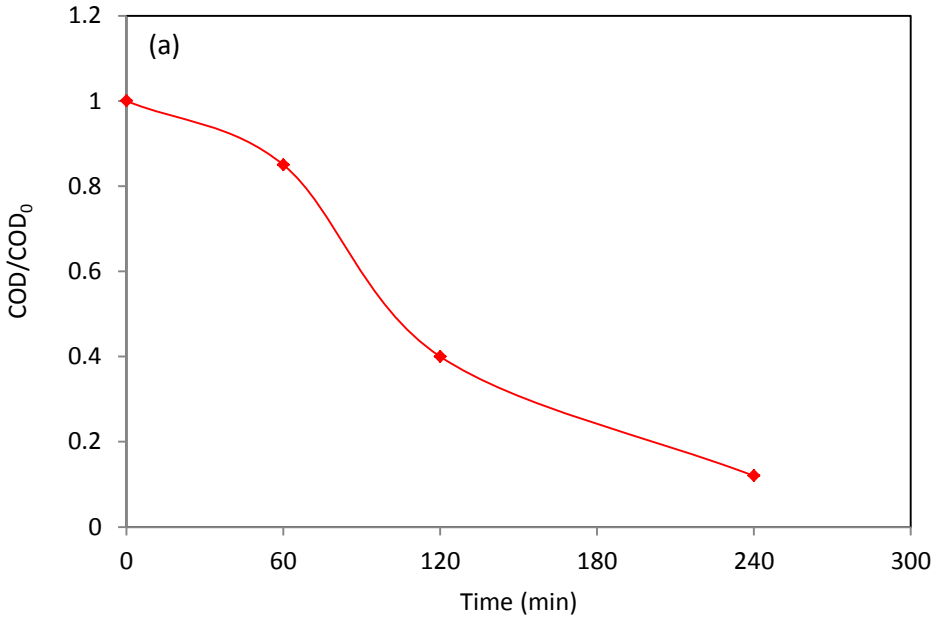

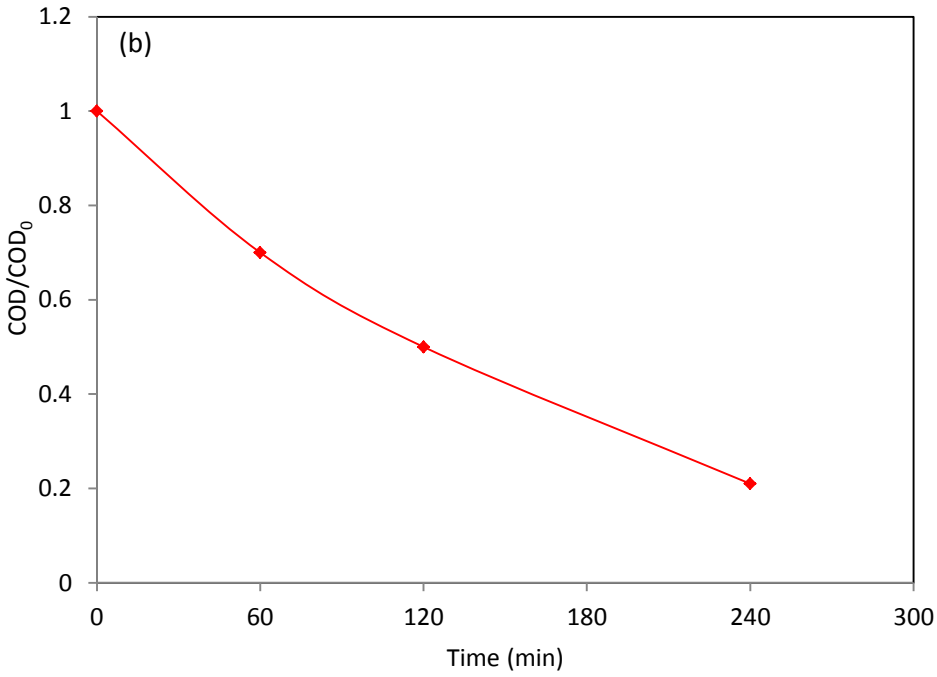

Figure 6.9 COD reduction of the combined mixture 50 mg/L of both 4-CP and 2,4-DCP (7 mg/L) (0.5 g/LTiO_2, 1000 mW/cm^2) with the optimum values of (a) Fe^{2+} =7 mg/L (b) Fe^{3+}=10 mg/L

6.7 Intermediates and mechanism

Based on the present results, two reaction pathways for Solar/TiO_2/Fe^{3+}, Solar/H_2O_2/ Fe^{3+} and Solar/TiO_2/Fe^{3+}/H_2O_2 were proposed (see Figs. 6.10,11). Regardless of the difference in the concentrations of the intermediates Figure 6.10 shows that in the presence of Fe^{3+} or H_2O_2 together with TiO_2 and solar light, three main intermediates named HQ, Ph and 4cCat were detected. It can be noticed from this mechanism that the Ph compound can be formed from either 4-CP or 2,4-DCP degradations. However, due to the high activation of Ph to react with $^{\bullet}OH$ radical it might be rapidly converted to HQ (Peng et al. 2012). In addition, 4cCat might be directly generated from hydroxylation of 4-CP by $^{\bullet}OH$ radical at significantly low concentration and rapidly degraded. Furthermore, some traces of benzoquinone (BQ) were detected which might be formed from the oxidation of HQ by $O_2^{\bullet-}$ degradation (Dhir et al. 2012). Generating these intermediates from the organic mixture mainly depends on the addition of hydroxyl radicals by three possible pathways including (a) hydroxylation of the aromatic rings, (b) substitution of Cl atom by $^{\bullet}OH$, and (c) oxidation of hydroxylated HQ to BQ (Li et al. 2012, Yang et al. 2009). Figure 6.11 shows the suggested reaction pathway of the combined mixture when using the Solar/TiO_2/Fe^{3+}/H_2O_2 Hybrid Process. It can be seen from this figure that only two major intermediates were observed namely HQ and Ph. This result could be due to the large number of •OH radical which can rapidly hydroxylase the main pollutants and their by-products and convert them into the final products. In addition, most of catechol and polar compounds have strong ability to adsorb onto TiO_2 particles leading to fast degradation (Ahmed et al. 2011). Generally, in the degradation of chlorophenols four steps can occur including adsorption, dechlorination, hydroxylation and cleavage the aromatic rings to form inorganic products (Araña et al. 2007a). It is clear from Figures 6.10,11 that all formed intermediates (HQ, Ph, and 4cCat) are completely degraded.

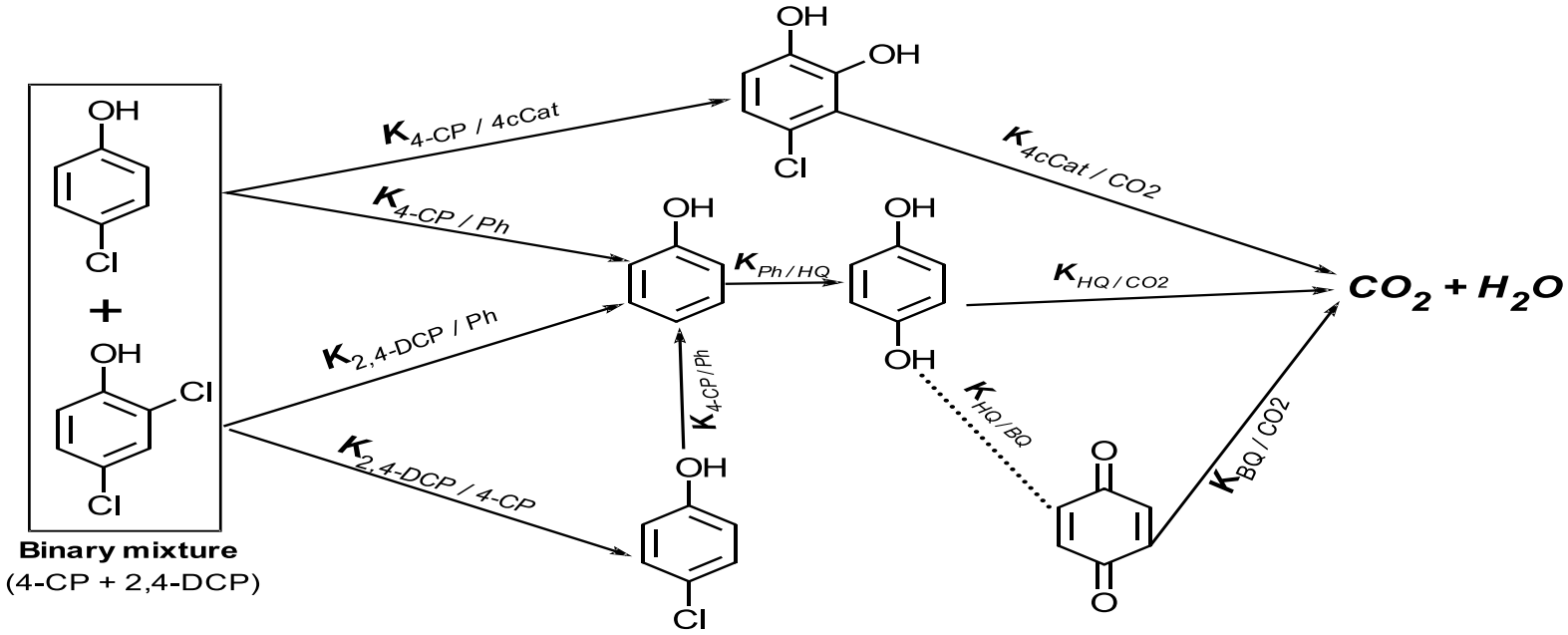

Figure 6.10 Proposed series-parallel solar photocatalytic degradation pathways of 4-CP and 2,4-DCP combined mixture (10 mg/L $FeCl_3$. $6H_2O$ Or 3.41 mM H_2O_2, 0.5 g/L TiO_2, 1000 mW/cm^2)

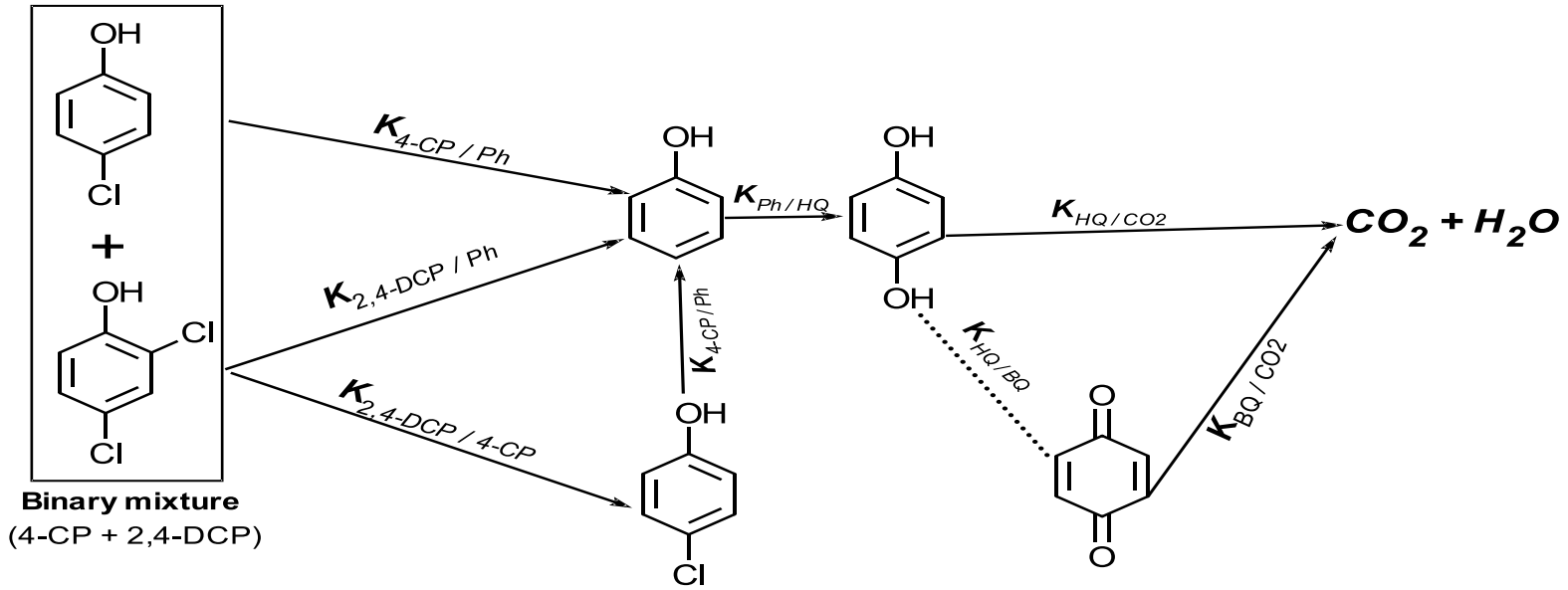

Figure 6.11 Proposed series-parallel solar photocatalytic degradation pathways of 4-CP and 2,4-DCP combined mixture (10 mg/L $FeCl_3$. $6H_2O$, 3.41 mM H_2O_2, 0.5 g/L TiO_2, 1000 mW/cm^2)

6.8 Iron concentration analysis

It is very important to follow the iron concentrations (Fe^{2+} and Fe^{3+}) during the solar irradiation time. This can effectively help to understand the reaction mechanism of iron and the residual amount at the end of the degradation. Therefore, an accurate evaluation for the Fe^{2+} and Fe^{3+} concentrations during the solar photocatalytic degradation of the combined mixture was conducted as shown in Figure 6.12.

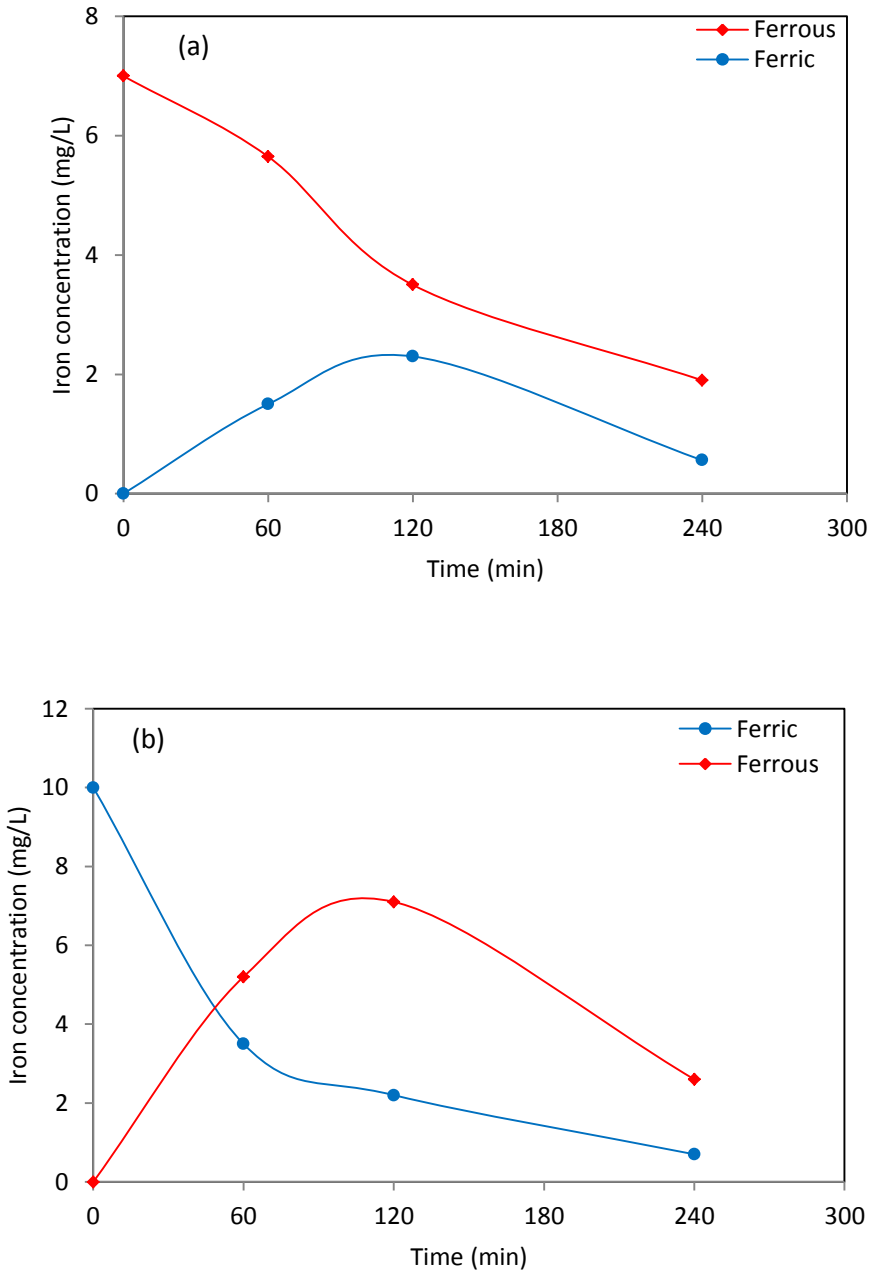

Figure 6.12 Evaluation of iron concentrations during solar photocatalytic degradation of the combined mixture 50 mg/L of both 4-CP and 2,4-DCP (0.5 g/LTiO_2, 1000 mW/cm^2) (a) Fe^{2+} (Fe_0^{2+}= 7 mg/L) (b) Fe^{3+} (Fe_0^{3+}=10 mg/L)

It is obvious from Figure 6.12a that ferrous ions decrease gradually from 7 mg/L initial value to 1.9 mg/L at 240 min to generate $^{\bullet}OH$ radicals (Eq. 6.17), furthermore; during the solar irradiation time some ferric ions were observed which might be due to the reaction between Fe^{2+} and H_2O_2 (Eq. 6.17) or the scavenging of $^{\bullet}OH$ radicals by Fe^{2+} Equation 6.18 (Hasan et al. 2012).

$$Fe^{2+} + {}^{\bullet}OH \rightarrow Fe^{3+} + OH^{-} \quad (6.18)$$

However, it is clear from Figure 6.12b that most of Fe^{3+} ions rapidly converted to Fe^{2+} due to photo reduction of Fe^{3+} during the solar irradiation as shown in Equations 6.19,20 (Selvam et al. 2005).

$$Fe^{3+} + e^{-} \rightarrow Fe^{2+} \quad (6.19)$$

$$Fe^{3+} + H_2O + h_v \rightarrow {}^{\bullet}OH + Fe^{2+} + H^{+} \quad (6.20)$$

These results indicate that Fe^{2+} ions play a significant role in both solar photocatalytic degradation processes, as Fe^{3+} is quickly reduced to Fe^{2+}. However, in terms of the reaction rate there is not much difference when using Fe^{2+} or Fe^{3+} because both lead to same results. Similar findings have been reported in some studies that used Fe^{2+} and Fe^{3+} ions as photocatalytic degradation enhancer (Ortiz-Gomez et al. 2008, Martinez et al. 2007). The mass balance of Fe^{2+} and Fe^{3+} in Figure 6.12 shows that there is iron missing which might be due to the precipitation and adsorption on the TiO_2 surface.

Summary

The results obtained in this study show that the solar photocatalytic degradation of the chlorophenols combined mixture (4-CP and 2,4-DCP) can be effectively enhanced by adding ferrous, ferric ions and hydrogen peroxide. Four different advanced oxidation processes were conducted including Solar/TiO_2/Fe^{2+}, Solar/TiO_2/Fe^{3+}, Solar/Fe^{3+}/H_2O_2 and Solar/TiO_2/Fe^{3+}/H_2O_2. Among these degradation methods Solar/TiO_2/Fe^{3+}/H_2O_2 has shown the highest degradation efficiency for the main pollutants and their intermediates. In addition, two main intermediates HQ and Ph were observed instead of three HQ, Ph and 4cCat in the other methods. The relative efficiencies of these processes are in the following order: Solar/TiO_2/Fe^{3+} < Solar/TiO_2/Fe^{2+} < Solar/Fe^{3+}/H_2O_2 < Solar/TiO_2/Fe^{3+}/H_2O_2. The results of the present study indicated that there is no significant difference between using ferrous (Fe^{2+}) and ferric (Fe^{3+}) ions as oxidants in the solar photocatalytic degradation of chlorophenols mixture. However, the results obtained from this work showed that the Fe^{2+} degradation efficiency was slightly higher than that of Fe^{3+}. In both cases, three intermediates namely HQ, Ph, and 4cCat were detected during 240 min solar irradiation time and all of them completely degraded before the main compounds. COD measurements implemented in this study showed that there was no complete COD removal which might be due to other undetected intermediates formed during the degradation. Iron concentration analysis clearly indicated that most of ferric ions rapidly converted to ferrous as soon as the irradiation time started. This result shows that Fe^{2+} plays an important role in both cases. In addition, small amounts of residual iron were detected which could be recovered and reused. According to the presented results, two kinetic reaction pathways for this combined mixture were proposed. This reaction mechanism involved all possible intermediates detected during the degradation.

CHAPTER 7

SOLAR PHOTOCATALYTIC DEGRADATION OF PETROLEUM REFINERY EFFLUENT

7.1 Introduction

British Petroleum (BP) Kwinana Refinery was built in 1955 on the eastern shore of Cockburn Sound, approximately 30 km south of Perth/Australia (32.2295° S, 115.7649° E). Neighbouring industries include a variety of mineral and chemical processing companies. Crude oil is delivered by ships to Kwinana Refinery, where it is refined into a wide range of products for distribution throughout Western Australia. These products include LPG, petrol and diesel for motor vehicles, aviation gasoline and jet fuel. The local wastewater treatment plant in BP Kwinana Refinery (Fig. 7.1) has been in operation since 1994. In the first stage of the treatment process the free oil is separated from the wastewater and sent back to the refinery for reprocessing. The separated wastewater is pumped to an equalisation tank where it is held and pH adjusted to the required conditions of the treatment plant. The second stage involves the removal of small suspended oil particles in the Dissolved Air Flotation (DAF) unit by binding the small particles into larger ones so that they can float and be skimmed off. Up to this stage the treatment process is covered to prevent volatile organic compound (VOC) emissions. The final stage involves the removal of dissolved contaminants and nutrients in the Activated Sludge Units (ASUs), where biological breakdown occurs. The partially treated effluent then enters the clarifiers, where microorganisms are settled before returning to the ASUs. The wastewater is then directed to the polishing ponds, which are another special feature of the treatment plant. Aerators aid the breakdown of any remaining organic compounds. Treated effluent is discharged to Cockburn Sound area under carefully controlled conditions and to strict regulatory requirements. Average daily discharges would place BP Kwinana Refinery as one of the best refineries in the world for wastewater quality. To reduce the phenolics concentration in the refinery wastewater, Minalk (Minimum Alkalinity) Unit was built in 1992. This unit can effectively treat catalytically cracked spirit using a weak caustic solution instead of 10% caustic solution which significantly reduce the phenolic compounds in the treated effluent discharged to Cockburn Sound.

Figure 7.1 Wastewater Treatment Plant of BP Refinery (Kwinana). On the left are two Salt Cooling Water Circulars, on the right the two Activated Sludge Units and clarifiers are visible [www.bp.com/content/dam/bp/pdf/.../Kwinana refinery]

The raw effluent characterisation and their suggested limtiations standards that should be followed by petroleum refineries such as Chemical Oxygen Demand (COD) and Phenols are shown in Table 7.1 (Al Zarooni and Elshorbagy 2006, Coelho et al. 2006).

Table 7.1 Typical Characteristic of raw petroleum refinery effluent and their limitations (Al Zarooni and Elshorbagy 2006, Coelho et al. 2006) .

Parameter	Symbol	Raw effluent(mg/L)	Suggested limit(mg/L)
Chemical oxygen demand	COD	850-1020	100-200
Biochemical oxygen demand	BOD_5	570-600	50-100
Total petroleum hydrocarbon	TPH	50-100	15-30
Phenols	Ph	98-120	0.1-5.0
pH	pH	8.0-9.3	7.0-8.0

7.2 Effluent sources of Kwinana Refinery

Effluent in the Kwinana refinery can be generated by the following ways:

- Crude oil which contains significant amounts of water coming from drilling processes. This water has to be extracted before the crude oil can be fed to the refining units.
- Washing the holds of the ships that deliver crude oil to the refinery.
- Refining processes that use massive amounts of water to produce the final products.
- The sealed surfaces that collect storm water during rainfall seasons which have potential to be contaminated.

7.3 Preliminary investigations

The collected samples from the refinery were physically and chemically checked in order to measure some key parameters such as pH, TOC, COD and turbidity. The values of these variables can highly affect selection of the proper chemical treatment for petroleum refinery effluent. The pH value of the samples was between 9 to 9.2 which is slightly high due to the high concentration of amino and alkaline organic compounds in the effluent. However, the solar photocatalytic degradation of organic contaminants present in wastewater is less effective in the base medium. Therefore, to overcome this issue all samples were adjusted to pH 5 before each experiment using HCl. Another significant key parameter that was measured before starting the degradation is Total Organic Carbon (TOC) which includes all organic compounds that completely dissolved in the effluent particularly phenolic compounds. The average value of TOC in all effluent samples was found around 120 mg/L which is quite high. To investigate the total measurement of all chemicals (organics and inorganics) in the refinery effluent samples, Chemical Oxygen Demand (COD) was

measured and found to be very high about 840 mg/L. This factor can provide a significant indication for the degree of photocatalytic degradation of petroleum refinery effluent, therefore; the COD removal efficiency was used as an indicator to monitor all degradation profiles of the real effluent samples. Turbidity in the effluent is caused by suspended matter, such as clay, silt, finely divided organic and inorganic matter, and other microscopic organisms. The colour of the Kwinana refinery samples were dark brown which gave the effluent high turbidity about 7.4 NTU.

7.4 Solar photocatalytic degradation experiments

As mentioned in Chapter 3 (section 3.3.4) all samples were collected from Kwinana refinery and kept at 5^0C, the regular experiments were carried out under different conditions. To minimise and save the amount of raw refinery effluent consumed in the experiments, 250 mL Pyrex glass beaker as a reactor equipped with a magnetic stirrer was used. Some key parameters that mainly affect the photocatalytic degradation of organic pollutants were investigated including TiO_2 doses, pH, ferrous ion (Fe^{2+}), and ferric ion (Fe^{3+}). The optimum values of these parameters to achieving the maximum degradation efficiency were obtained.

7.4.1 Effect of TiO_2 loading

It is necessary to choose the optimum dose of TiO_2 according to the type and concentration of pollutants. The influence of addition of TiO_2 (0.3 -0.9 g/L) on the solar photocatalytic degradation of the refinery effluent samples at raw pH (9.1) is shown in Figure 7.2. All experiments were conducted in the dark for 30 min to make sure that the steady state of adsorption is reached and the degradation initiates at the equilibrium of adsorption. The addition of TiO_2 from 0.3 g/L to 0.7 g/L increases the degradation from 42% to 72% within 240 min solar irradiation. This is an expected result as the increase of the active sites for adsorption of the pollutants on the photocatalyst surface as well as the enhanced generation of free hydroxyl radicals ($^{\bullet}OH$). However, when the TiO_2 concentration is higher than 0.7 g/L the degradation rate decreases due to the higher turbidity of the suspension which leads to absorb most of the incident photons by the slurry (Dhir et al. 2012). Thus, 0.7 g/L TiO_2 concentration was selected as an optimum dose for further photocatalytic degradation experiments.

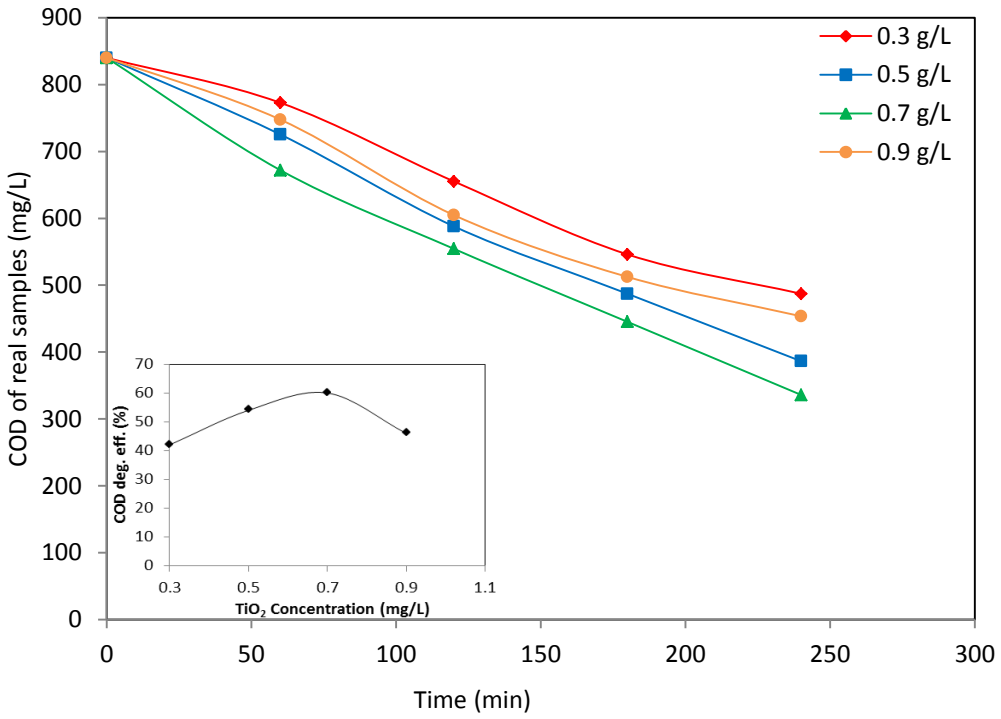

Figure 7.2 Influence of TiO_2 doses on solar photocatalytic degradation of Kwinana refinery effluent (pH=9.1, 1000 mW/cm^2)

7.4.2 Effect of pH

It is well known that pH can affect the mechanism and routes of photocatalytic degradation. The TiO_2 point of zero charge (pzc) is between pH 5.6 and 6.4 (Ho and Bolton 1998). Thus, based on the pH, the photocatalyst surface will be either charged positively (for pH < pzc) or negatively (for pH > pzc), or neutral (for pH ≈ pzc). This pH mechanism significantly affects the adsorption and desorption of pollutants on the TiO_2 surface. As petroleum refinery effluent contains different organic contaminants such as hydrocarbons and chlorophenols which are discharged at various pH values, thus; it is essential to investigate the role of pH on the solar photocatalytic degradation of the refinery effluent. To study the influence of pH on the photocatalytic degradation, set of experiments were carried out at various pH values, ranging from 3 to 9 using the optimum concentration TiO_2 (0.7 g/L) as shown in Figure 7.3. It can be observed that the maximum rate of degradation was achieved at pH 5. Some literature (Mills et al. 1993, Mills et al. 1993, Stafford et al. 1994) stated that TiO_2 surface has the net positive charge at low pH value, while the organic compounds such as chlorophenols are mainly negatively charged. Consequently, at low pH values the adsorption of pollutants on TiO_2 active sites can

be significantly enhanced leading to increase in degradation rates. Therefore, all samples were adjusted to pH 5 prior to each experiment to ensure that the maximum degradation efficiency can be achieved.

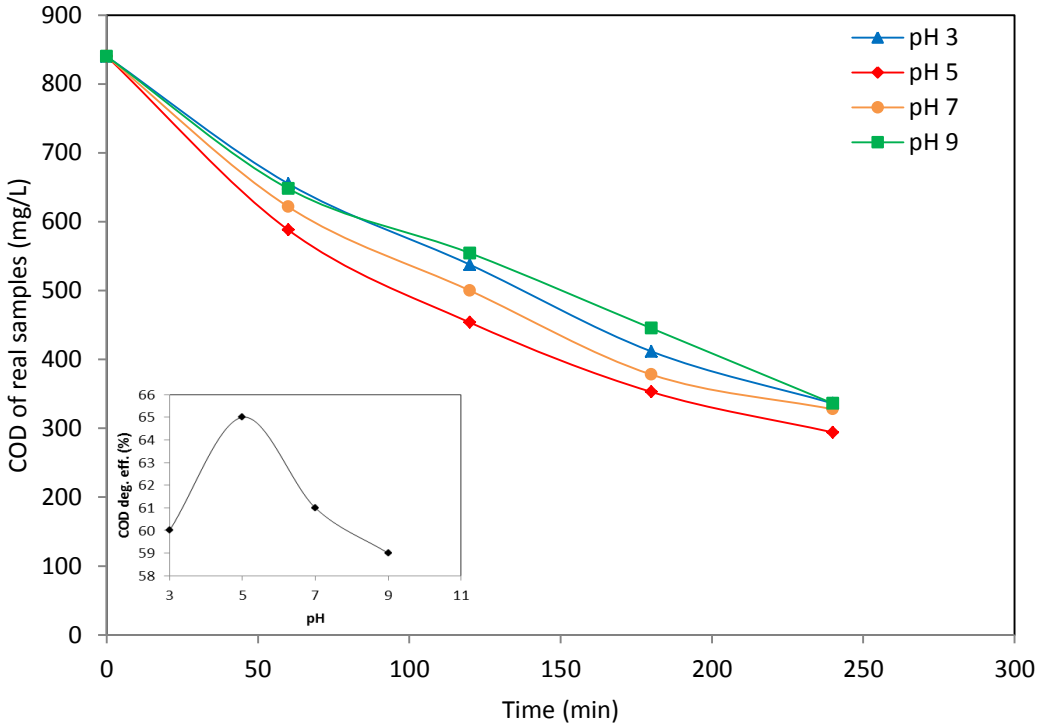

Figure 7.3 Influence of pH on the on solar photocatalytic degradation of petroleum refinery effluent (0.7 mg/L TiO_2, 1000 mW/cm^2)

7.4.3 Effect of ferrous ions (Fe^{2+})

The use of metal ions like ferrous/ferric ions in the solar photocatalytic degradation can effectively increase the degradation rate of organic pollutants. Therefore, to enhance the efficiency of solar photocatalytic degradation of the petroleum refinery effluent, different ferrous ions (Fe^{2+}) concentrations were used as additives (Fig. 7.4). It can be noticed from Figure 7.4 that the maximum COD removal was at 15 mg/L Fe^{2+}. However, at high ferrous concentrations the degradation efficiency decreases. This result can be clarified by the fact that the recombination of the e^-/h^+ pairs increases at high metal ions doses leading to reduce $^{\bullet}OH$ radicals.(Arslan et al. 2000).

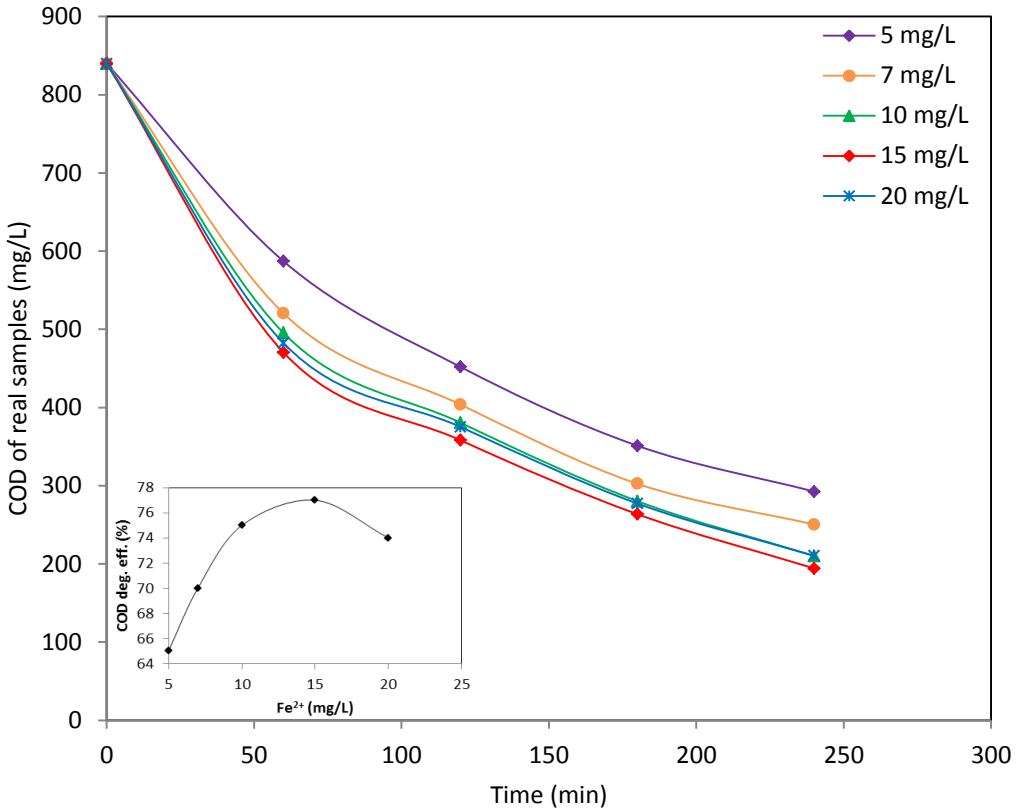

Figure 7.4 Influence of ferrous (Fe^{2+}) ions the on solar photocatalytic degradation of petroleum refinery effluent (0.7 mg/L, pH=5, 1000 mW/cm^2)

7.4.4 Effect of Ferric Ions (Fe^{3+})

Another metal ion which is ferric ion (Fe^{3+}) was also used in the solar photocatalytic degradation of the petroleum refinery effluent. Influence of various Fe^{3+} doses (7 – 25 mg/L) on the photocatalytic degradation was investigated (Fig. 7.5). It can be observed that the COD degradation rate increases with the increase of Fe^{3+} concentration up to 20 mg/L and then decreases. As mentioned before that all metal ions (Fe^{2+} and Fe^{3+}) at certain concentrations could significantly enhance the degradation rate due to their ability to reduce the e^-/h^+ recombination by trapping the electrons. To compare the effectiveness of ferric ions with ferrous ions, it is clear that the efficiency of ferrous is slightly higher than that of ferric. However, both of them can be considered as effective enhancers for solar photocatalytic degradation of petroleum refinery effluent.

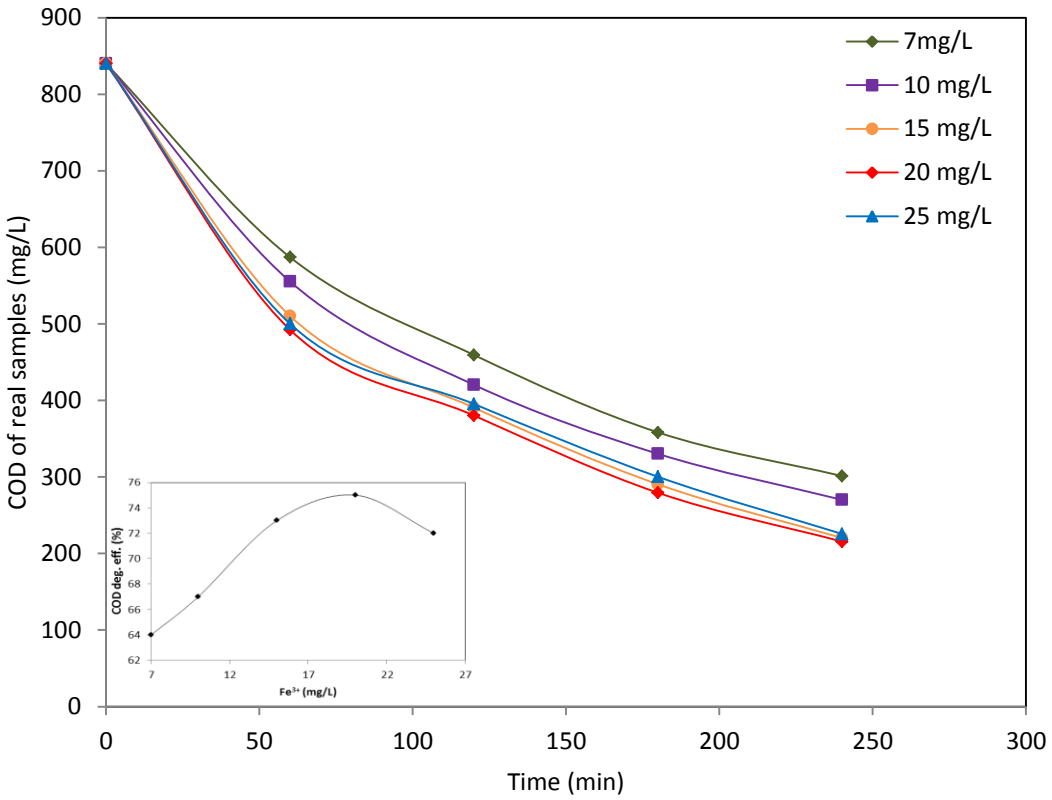

Figure 7.5 Influence of ferric (Fe^{3+}) ions on solar photocatalytic degradation of petroleum refinery effluent

7.5 Comparison between synthetic and real samples

As mentioned in Chapters 4, 5, and 6, all samples used in the solar photocatalytic degradation were synthetically made which include 4-chlorophenol (4-CP) and 2,4-dichlorophenol (2,4-DCP). In order to investigate the potential of solar photocatalytic degradation for treating petroleum refinery effluent, a comparison between synthetic and real samples involving the key parameters was performed in this chapter. This study can significantly give a good approach for using solar photocatalytic oxidation as an effective large-scale method. Table 7.2 summarises the maximum degradation efficiency at optimum concentrations of TiO_2 used in different cases: 4-CP; 4-CP & 2,4-DCP mixture; and real petroleum refinery effluent. It is clear that there is no difference between one and two compounds mixture and the optimum concentration was 0.5 g/L TiO_2. This is due to the low concentrations of organic compounds used and no other pollutants present in the suspension.

Table 7.2 Maximum degradation efficiencies at optimum values of TiO_2 used in different cases

Model pollutant	Initial concentration (mg/L)	pH	Light intensity (mW/cm^2)	Solar irradiation time (min)	Optimum TiO_2 loading (g/L)	Maximum degradation efficiency (%)
4-CP	50	3	1000	180	0.5	76
4-CP & 2,4-DCP	50 (for each)	3	1000	240	0.5	92(4-CP) 82(2,4-DCP)
Petroleum refinery effluent	840 (COD)	5	1000	240	0.7	65 (COD)

It should be noted that the lower degradation efficiency of 4-CP is due to a lower irradiation time of 180 min instead of 240 min as used in the combined mixture. However, the maximum degradation of the petroleum refinery samples (Kwinana refinery) was achieved at 0.7 g/L. This indicates that the more polluted water needs more active sites requiring high photocatalyst doses. On the contrary, due to the higher turbidity of petroleum refinery samples with higher doses of TiO_2 (above 0.7 g/L), the light inside the suspension solution can be scattered leading to lower the degradation efficiency.

The iron ions including ferrous (Fe^{2+}) and ferric (Fe^{3+}) ions were used to enhance the solar photocatalytic degradation efficiency of synthetic chlorophenols mixtures as mentioned in Chapter 6. These chemical enhancers were also used in the solar photocatalytic degradation of the petroleum refinery effluent. Table 7.3 illustrates the optimum values of Fe^{2+} and Fe^{3+} achieved in the solar photocatalytic degradation of two compounds (4-CP and 2,4-DCP) and the petroleum refinery effluent. The maximum COD degradation efficiencies of chlorophenols mixture (4-CP and 2,4-DCP) using Fe^{2+} and Fe^{3+} were achieved at 7 and 10 mg/L respectively. However, the highest COD removals of the petroleum refinery effluent using Fe^{2+} and Fe^{3+} were 15 and 20 mg/L respectively. It is clear that the highly polluted water needs more iron ions to achieve the best results.

Table 7.3 Maximum degradation efficiencies at the optimum values of ferrous and ferric ions used in two cases

Model pollutant	COD Initial concentration (mg/L)	pH	Light intensity (mW/cm^2)	Solar irradiation time (min)	Optimum TiO_2 loading (mg/L)	Iron ions concentration (mg/L)	Maximum degradation efficiency (%)
4-CP & 2,4-DCP	120	3	1000	240	0.5	Fe^{2+} = 7	88
						Fe^{3+} = 10	79
Petroleum refinery effluent	840	5	1000	240	0.7	Fe^{2+} = 15	77
						Fe^{3+} = 20	75

However; these chemicals can significantly increase the operation cost of the solar photocatalytic degradation process, therefore; it is essential to search for natural iron sources to make this method cost-effective.

Although, the overall COD removal efficiency of the solar photocatalytic degradation decreases with the increase of pollutant concentration, this method significantly shows a good potential to degrade most of organic pollutants. The solar photocatalytic degradation of one compound (4-CP) and two compounds (4-CP and 2,4-DCP) have been mentioned in chapters 4 and 6 respectively. Figure 7.6 shows COD concentrations before and after the treatment for different cases at their optimum conditions. It can be noticed that the initial COD concentration increases with the increase of organic pollutants. The initial COD concentration (before treatment) of 4-CP, a mixture of 4-CP and 2,4-DCP and real petroleum refinery samples were 70, 120, and 840 mg/L respectively. The final COD concentration (after treatment) of 4-CP, 4-CP&2,4-DCP, and real sample were 20, 50, and 195 mg/L respectively. It is very important to mention that the real samples contain various inorganic and organic pollutants which can highly reduce the degradation efficiency.

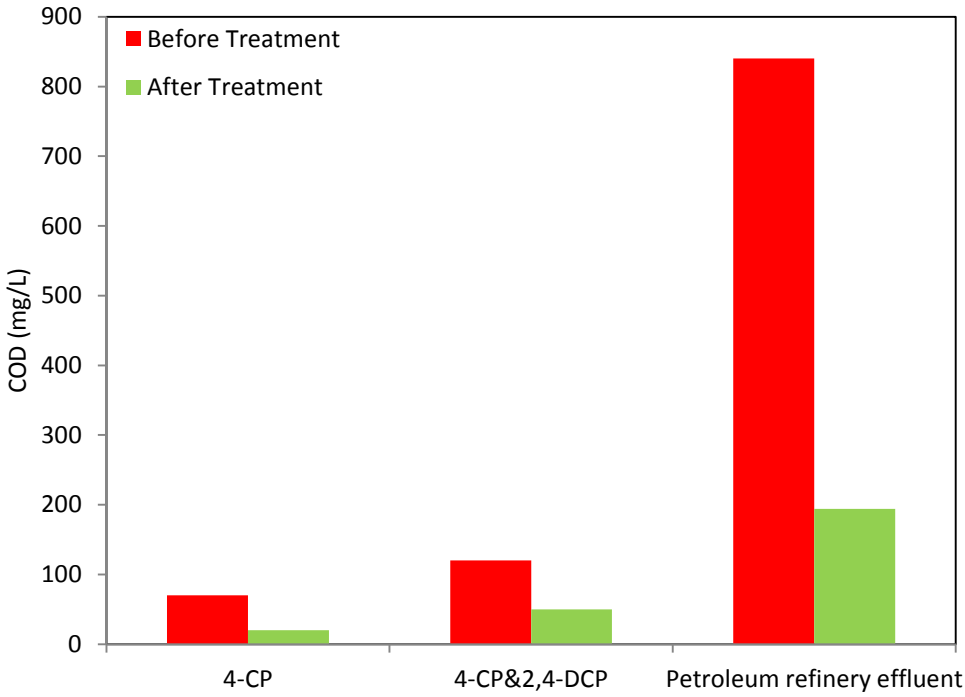

Figure 7.6 COD concentrations before and after the treatment of different cases at the optimum conditions

However, the COD removal efficiency of the petroleum refinery effluent (77%) obtained in this study clearly shows that the solar photocatalytic degradation process can effectively degrade highly polluted effluent.

7.6 Reaction pathway of petroleum refinery effluent

A raw petroleum refinery effluent consists of oil, grease, chlorides, ammonia, sulphides, phenols, chlorophenols and many other various organic compounds. In fact, COD degradation measurement gives only a general picture about the quality of treatment. Therefore, it is hard to know the reaction pathway of each pollutant present in the effluent and the final compounds produced. However, the degradation mechanism of organic pollutants in the petroleum refinery effluent can be described based on the $^{\bullet}OH$ radical attack theory. This reaction occurs between $^{\bullet}OH$ radical and the benzene ring of each organic compound to produce less biodegradable compounds. For instance, benzene react with $^{\bullet}OH$ radicals generating phenol and then converts to dihydroxybenzenes which has two hydroxyl groups substituted onto a benzene ring such as catechol, hydroquinone, and resorcinol (Aranda et al., 2010). For $^{\bullet}OH$ reaction with 4-chlorophenol (4-CP) in aqueous media, hydroquinone (HQ)

concentration significantly increases which is attributed to the direct attack of $^{\bullet}OH$ radical on Cl^- atom. Further solar irradiation degrades HQ to either CO_2 and H_2O or BQ which consequently converted to final products (Vinu and Mdras 2011; Bian et al., 2011). However, hydroxyl radical might react with 4-CP and produce 4cCat (Elghniji et al., 2012; Venkatachalam et al., 2007). Xylene which usually presents in petroleum refinery effluent can be oxidised to primary compounds such as methylbenzene and benzoquinone which convert to carboxylic acids such as oxalic and malonic acids (Gai, K., 2009).

7.7 Kinetic modelling

It is well accepted that the rates of formation and disappearance of all chemicals during the photocatalytic degradation time can be modelled using Langmuir-Hinshelwood L-H equation (Eq. 7.1) which considers the adsorption of the chemicals on the catalyst surface and the kinetic reaction constants. The general form of this equation for the system is represented by (Turchi and Ollis 1990).

$$r_i = \frac{dC_i}{dt} = \frac{k_i C_i}{1 + \sum_{j=1}^{n} K_j C_j} \tag{7.1}$$

Equation 7.1 can be used in terms of COD degradation as following:

$$r_{COD} = -\frac{dC_{COD}}{dt} = \frac{k_{COD} C_{COD}}{1 + K_{COD} C_{COD}} \tag{7.2}$$

Or

$$\frac{dC_{COD}}{dt} = -\frac{k_{COD} C_{COD}}{1 + K_{COD} C_{COD}} \tag{7.3}$$

Where, C_{COD} is the COD at any time (mg/L), k_{COD} is the reaction rate constant of COD (min^{-1}), and K_{COD} is the adsorption constant of COD (min^{-1})

After estimating the best parameters, the mathematical model can be applied to predict the behaviour of the photocatalytic degradation of COD in the petroleum

refinery effluent. Equation 7.3 cannot be solved analytically, therefore, for estimating the reaction and adsorption rate constants; two built-in MATLAB subroutines were used: Least Square Curve Fit (lsqcurvefit) for the minimisation of the objective function and Ordinary Differential Equations Solver (ode45) for the numerical integration of the differential equations. Equation 7.3 has been applied to estimate k_{COD} and K_{COD} in both cases of using ferrous and ferric ions. Table 7.4 summarises the reaction rate constants and the adsorption constants of the COD degradation in both cases.

Table 7.4 Reaction and adsorption rate constants of COD degradation in case of ferrous and ferric use

Parameter (min^{-1})	Ferrous (Fe^{2+}) ion	Ferric (Fe^{3+}) ion
k_{COD}	0.04	0.03
K_{COD}	0.01	0.0065

It can be clearly seen from Table 7.4 that the reaction rate constant of COD (k_{COD}) of ferrous is slightly higher than that of ferric. This indicates that the photocatalytic degradation activity of ferrous is better than that of ferric. Figure 7.7 shows the experimental and estimated concentration profiles for the solar photocatalytic degradation of petroleum refinery effluent at 0.7g/L TiO_2, 15 mg/L Fe^{2+}. It can be seen that the kinetic model predicts very well the experimental data of COD solar photocatalytic degradation.

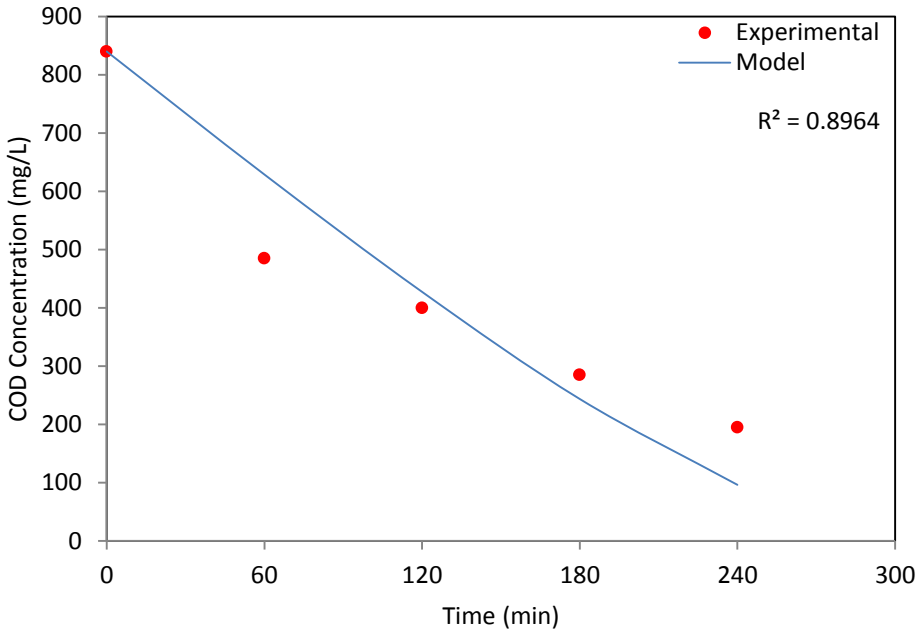

Figure 7.7 Experimental and estimated concentration profiles for photocatalytic degradation of petroleum refinery effluent (0.7g/L TiO_2, 15 mg/L Fe^{2+}).

Figure 7.8 also represents the experimental and estimated concentration profiles for photocatalytic degradation of petroleum refinery effluent at 0.7g/L TiO_2, 20 mg/L Fe^{3+}. It is clear that there is no much difference between using ferrous and ferric and the kinetic model can effectively fit the experimental data.

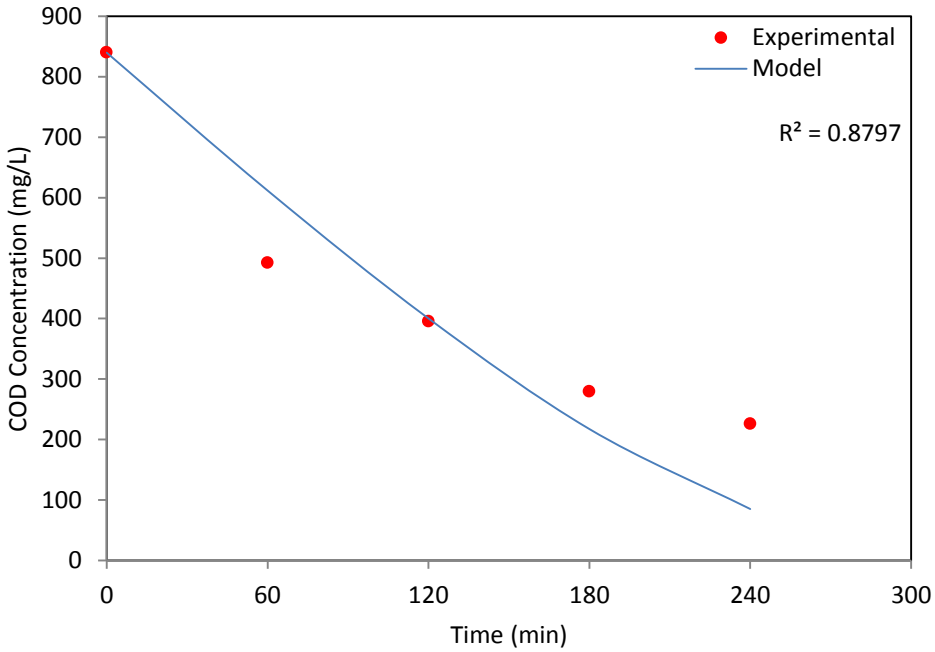

Figure 7.8 Experimental and estimated concentration profiles for photocatalytic degradation of petroleum refinery effluent (0.7g/L TiO_2, 20 mg/L Fe^{3+}).

Summary

Petroleum refinery effluent samples were collected from BP Kwinana Refinery. Primary investigations for these samples were conducted including pH, TOC, COD and turbidity. The effectiveness of solar photocatalytic degradation to remove organic pollutants from the refinery effluent was discussed in this chapter in terms of COD reduction. Several parameters such as TiO_2 loading, pH, ferrous ions (Fe^{2+}) and ferric ions (Fe^{3+}) were studied in order to optimise the performance of the solar photocatalytic degradation to remove the organic pollutants. Results of the effect of TiO_2 loading indicated that COD removal efficiency increased with increasing TiO_2 doses due to the higher total available surface area of the adsorbent. The highest COD removal was found at 0.7 mg/L TiO_2. The photocatalytic degradation rate in the acidic medium was higher than that of the base medium. The maximum degradation efficiency of COD was found at pH 5. The influence of iron ions on the solar photocatalytic degradation of the refinery effluent was investigated in this chapter. The addition of ferrous ions (Fe^{2+}) to the suspension solution significantly increased the degradation efficiency. The optimum value of ferrous ions (Fe^{2+}) was found at 15 mg/L. The COD reduction of petroleum refinery effluent was also enhanced when Fe^{3+} added to the suspension solution. The optimum value of Fe^{3+} concentration was found at 20 mg/L. However, the solar photocatalytic degradation efficiency of using ferrous ions (Fe^{2+}) was slightly higher than that of ferric ions (Fe^{3+}). Compared with the solar photocatalytic degradation of the synthetic samples (4-CP and 2,4-DCP), the degradation efficiency of the petroleum refinery effluent is less than that of synthetic samples. This is attributed to the high COD concentration in the real samples which requires more chemicals and irradiation time. However, the maximum COD degradation efficiency (77%) achieved significantly shows the ability of the solar photocatalytic degradation process to effectively treat highly polluted water.

CHAPTER 8

CONCLUSIONS AND RECOMMENDATIONS

8.1 Introduction

This chapter summarises the overall results and presents some recommendations for further research. Solar photocatalytic degradation shows an effective ability to degrade organic pollutants present in petroleum refinery effluents. Most of the key parameters such as photocatalyst loading, pH, and metal irons (Fe^{2+} and Fe^{3+}) that affected this technique were investigated. Additionally, intermediates formed during the photocatalytic degradation of the organic pollutants were identified and considered in the modelling and kinetic studies. Based on the results obtained, recommendations for further work involve some obstacles associated with the solar photocatalytic process were reported.

8.2 Conclusions

This thesis shows the findings of the study on the feasibility and enhancement of using a solar photocatalytic degradation process as an effective method to remove organic pollutants from synthetic effluent and petroleum refinery effluent. The following conclusions were obtained from the experimental and kinetic modelling investigations of organic pollutants (4-CP and 2,4-DCP) present in petroleum refinery effluent.

- An extensive review of using photocatalytic degradation processes to treat biorefractory pollutants in petroleum refinery effluent was reported in Chapter 2. This review presents the advantages, limitations, and future work of this method.

- Solar photocatalytic degradation can be considered as an efficient method for wastewater treatment containing recalcitrant, inhibitory, and toxic pollutants with low biodegradability. It is also an efficient and cost-effective technique that is suitable for petroleum refinery effluent treatment at the advanced stage.

- Two organic pollutants (4-CP and 2,4-DCP) usually present in petroleum refinery effluent were chosen as models in the current study. The study proved that TiO_2 photocatalyst can effectively mineralise 4-CP and its intermediates (HQ, 4cCat and Ph) into CO_2 and H_2O within 180 min solar irradiation.

- A chlorophenols mixture containing two compounds (4-CP and 2,4-DCP) was successfully degraded with their formed intermediates into CO_2 and H_2O using solar light and TiO_2 photocatalyst. The maximum degradation efficiencies of 4-CP and 2,4-DCP in the chlorophenols mixture were 92% and 82% respectively at optimum conditions (pH= 3.0, TiO_2 = 0.5 g/L, light intensity = 1000 mW/cm^2, and solar irradiation time = 240 min). Two kinetic reaction models involving the solar photocatalytic degradation of a single compound (4-CP) and chlorophenols mixture (4- CP and 2,4-DCP) as well as their intermediates were successfully developed. These models were able to predict the concentration profiles for a wide range of initial concentrations. A good agreement between estimated and experimental results was achieved.

- The solar photocatalytic degradation of organic pollutants was enhanced using several chemical additivities. Ferrous (Fe^{2+}) and ferric (Fe^{3+}) ions associated with TiO_2 and solar light significantly increased the degradation efficiencies of the organic pollutants and their intermediates. The presented results showed that the degradation efficiency of Fe^{2+} was slightly higher than that of Fe^{3+}. The maximum removal efficiencies of 4-CP and 2,4-DCP were 93% and 87% respectively at optimum conditions (pH = 3.0, TiO_2 = 0.5 g/L, Fe^{2+} = 7 mg/L, 1000 mW/cm^2, and solar irradiation time = 240 min)

- The chemical enhancers of the solar photocatalytic degradation used in this study showed promising results with respect to the complete mineralisation of biorefractory organic pollutants found in petroleum refinery effluent.

- The enhanced solar photocatalytic degradation was successfully applied on raw petroleum refinery effluent. The maximum COD removal efficiency of (77%) was achieved at the optimum conditions (TiO_2 = 0.7 g/L, pH = 5.0, Fe^{2+} = 15 mg/L, 1000 mW/cm^2, and solar irradiation time = 240 min). the degradation efficiency of the raw petroleum refinery samples was less than that of synthetic samples (4-CP and 2,4-DCP) due to the higher COD concentration which requires more chemicals and irradiation time.

- In terms of kinetic modelling, three models of one-compound, two-compound and COD degradation of raw refinery samples were performed. A Langmuir-Hinshelwood (L-H) model was developed to involve kinetic and adsorption constants. These models were able to effectively predict the degradation rate of the main pollutants and their intermediates during the solar irradiation time. A good agreement between estimated and experimental results was achieved.

8.3 Recommendations for future research

The ability of solar photocatalytic degradation for removal of organic pollutants from petroleum refinery effluent was extensively studied. The results showed the effectiveness of this technique to completely mineralise biorefractory pollutants. However, some issues need to be investigated to complement and enhance this work before applying to industrial applications. Based on the findings of the current study the following future research is recommended:

- Further research can focus on the enhancement of photocatalytic degradation to increase utilisation of solar light. This can be achieved either by modifying TiO_2 or looking for a new effective photocatalyst. Thus, the design of new and novel photocatalytic materials with higher efficiency is an interesting subject in the field of photocatalysis.

- Some crucial key parameters of photocatalytic degradation processes such as light distribution and photoreactor geometry need further investigations. Hence, it is recommended to perform experiments at different solar radiation intensities and develop photoreactor configurations.

- Alternative inexpensive iron sources such as soil and organic materials should be investigated to minimise the operation cost and save the environment.

- The physical separation of oil and suspended solids present in petroleum refinery effluent is essential. Thus, some pretreatments such as Dissolved Air Flotation (DAF) and API - Oil Water Separator need to be done before using a solar photocatalytic degradation method.

- Characterising petroleum refinery effluent is very essential in order to identify the kinds of pollutants for suitable treatment. Therefore, more research work should be performed in this direction.

- Integration of treatment processes such as a photocatalytic-biological process can be beneficial to minimise the drawback of each method and enhance the degradation efficiency as well as reducing the operation cost.

- Future research in wastewater treatment should focus on the photocatalytic degradation of real effluents which are polluted with a number of inorganic/organic compounds, heavy metals and microorganisms.

- The potential of using solar photocatalytic degradation on a large scale need to be evaluated. The cost for operation of the large scale slurry photoreactor is too expensive due to the cost of photocatalyst separation. Thus, it is recommended to investigate the possibility of using solar light and immobilised photocatalyst which could significantly reduce the operational cost of a large scale process.

REFERENCE

Abdelwahab, O, NK Amin, and ES El-Ashtoukhy. 2009. "Electrochemical removal of phenol from oil refinery wastewater." *Journal of Hazardous Materials* no. 163 (2):711-716.

Abdullah, Mohammad, Gary KC Low, and Ralph W Matthews. 1990. "Effects of common inorganic anions on rates of photocatalytic oxidation of organic carbon over illuminated titanium dioxide." *Journal of Physical Chemistry* no. 94 (17):6820-6825.

Aceituno, Mónica, Constantine D Stalikas, Loreto Lunar, Soledad Rubio, and Dolores Pérez-Bendito. 2002. "H_2O_2/TiO_2 photocatalytic oxidation of metol. Identification of intermediates and reaction pathways." *Water research* no. 36 (14):3582-3592.

Adán, C, J Carbajo, A Bahamonde, and A Martínez-Arias. 2009a. "Phenol photodegradation with oxygen and hydrogen peroxide over TiO_2 and Fe-doped TiO_2." *Catalysis Today* no. 143 (3):247-252.

Adán, C., J. Carbajo, A. Bahamonde, and A. Martínez-Arias. 2009b. "Phenol photodegradation with oxygen and hydrogen peroxide over TiO_2 and Fe-doped TiO_2." *Catalysis Today* no. 143 (3-4):247-252.

Adishkumar, S, and S Kanmani. 2010. "Treatment of phenolic wastewaters in single baffle reactor by Solar/TiO_2/H_2O_2 process." *Desalination and Water Treatment* no. 24 (1-3):67-73.

Ahmed, Saber, MG Rasul, R Brown, and MA Hashib. 2011. "Influence of parameters on the heterogeneous photocatalytic degradation of pesticides and phenolic contaminants in wastewater: a short review." *Journal of Environmental Management* no. 92 (3):311-330.

Ahmed, Saber, MG Rasul, Wayde N Martens, R Brown, and MA Hashib. 2010. "Heterogeneous photocatalytic degradation of phenols in wastewater: a review on current status and developments." *Desalination* no. 261 (1):3-18.

Akbal, Feryal, and A Nur Onar. 2003. "Photocatalytic degradation of phenol." *Environmental monitoring and assessment* no. 83 (3):295-302.

Al Zarooni, Mohamed, and Walid Elshorbagy. 2006. "Characterization and assessment of Al Ruwais refinery wastewater." *Journal of hazardous materials* no. 136 (3):398-405.

Alhakimi, Gamil, Saleh Gebril, and Lisa H Studnicki. 2003. "Comparative photocatalytic degradation using natural and artificial UV-light of 4-chlorophenol as a representative compound in refinery wastewater." *Journal of Photochemistry and Photobiology A: Chemistry* no. 157 (1):103-109.

Alimoradzadeh, Roya, Ali Assadi, Simin Nasseri, and Mohammad Reza Mehrasbi. 2012. "Photocatalytic degradation of 4-chlorophenol by UV/H_2O_2/NiO process in aqueous solution." *Iranian journal of environmental health science & engineering* no. 9 (1):1-8.

Alva-Argáez, Alberto, Antonis C Kokossis, and Robin Smith. 2007. "The design of water-using systems in petroleum refining using a water-pinch decomposition." *Chemical Engineering Journal* no. 128 (1):33-46.

Arana, J, O González Díaz, M Miranda Saracho, JM Doña Rodríguez, JA Herrera Melián, and J Pérez Peña. 2001. "Photocatalytic degradation of formic acid using Fe/TiO_2 catalysts: the role of Fe^{3+}/Fe^{2+} ions in the degradation mechanism." *Applied Catalysis B: Environmental* no. 32 (1-2):49-61.

Araña, J, VM Rodríguez López, E Pulido Melián, MI Suárez Reyes, JM Doña Rodríguez, and O González Díaz. 2007a. "Comparative study of phenolic compounds mixtures." *Catalysis Today* no. 129 (1):177-184.

Araña, J., V. M. Rodríguez López, E. Pulido Melián, M. I. Suárez Reyes, J. M. Doña Rodríguez, and O. González Díaz. 2007b. "Comparative study of phenolic compounds mixtures." *Catalysis Today* no. 129 (1–2):177-184.

Aranda, E., Marco-Urrea, E. Caminal, G. Arias, M. García-Romera, I. Guillén, F. 2010. "Advanced oxidation of benzene, toluene, ethylbenzene and xylene isomers (BTEX) by Trametes versicolor." Journal of hazardous materials no. 181 (1):181-186.

Arslan, Idil, Işil Akmehmet Balcioğlu, and Detlef W Bahnemann. 2000. "Advanced chemical oxidation of reactive dyes in simulated dyehouse effluents by ferrioxalate-Fenton/UV-A and TiO_2/UV-A processes." *Dyes and pigments* no. 47 (3):207-218.

Aruldoss, John Antony, and T Viraraghavan. 1998. "Toxicity testing of refinery wastewater using Microtox." *Bulletin of environmental contamination and toxicology* no. 60 (3):456-463.

Attiogbe, FK, Mary Glover-Amengor, and KT Nyadziehe. 2007. "Correlating biochemical and chemical oxygen demand of effluents–A case study of selected industries in Kumasi, Ghana." *West African Journal of Applied Ecology* no. 11 (1).

Augugliaro, Vincenzo, Elisa Garcia-Lopez, Vittorio Loddo, Sixto Malato-Rodriguez, Ignacio Maldonado, Giuseppe Marcì, Raffaele Molinari, and Leonardo Palmisano. 2005. "Degradation of lincomycin in aqueous medium: coupling of solar photocatalysis and membrane separation." *Solar Energy* no. 79 (4):402-408.

Ba-Abbad, Muneer M, Abdul Amir H Kadhum, Abu Bakar Mohamad, Mohd S Takriff, and Kamaruzzaman Sopian. 2013. "Photocatalytic degradation of chlorophenols under direct solar radiation in the presence of ZnO catalyst." *Research on Chemical Intermediates* no. 39 (5):1981-1996.

Ba-Abbad, Muneer M., Abdul Amir H. Kadhum, Abu Bakar Mohamad, Mohd S. Takriff, and Kamaruzzaman Sopian. 2012. "Photocatalytic degradation of chlorophenols under direct solar radiation in the presence of ZnO catalyst." *Research on Chemical Intermediates* no. 39 (5):1981-1996.

Bahnemann, W, M Muneer, and MM Haque. 2007. "Titanium dioxide-mediated photocatalysed degradation of few selected organic pollutants in aqueous suspensions." *Catalysis Today* no. 124 (3):133-148.

Bandala, Erick R, Camilo A Arancibia-Bulnes, Sayra L Orozco, and Claudio A Estrada. 2004. "Solar photoreactors comparison based on oxalic acid photocatalytic degradation." *Solar energy* no. 77 (5):503-512.

Bandara, J, JA Mielczarski, A Lopez, and J Kiwi. 2001a. "2. Sensitized degradation of chlorophenols on iron oxides induced by visible light: comparison with titanium oxide." *Applied Catalysis B: Environmental* no. 34 (4):321-333.

Bandara, J., J. A. Mielczarski, A. Lopez, and J. Kiwi. 2001b. "2. Sensitized degradation of chlorophenols on iron oxides induced by visible light: Comparison with titanium oxide." *Applied Catalysis B: Environmental* no. 34 (4):321-333.

Barakat, MA, H Schaeffer, G Hayes, and S Ismat-Shah. 2005. "Photocatalytic degradation of 2-chlorophenol by Co-doped TiO_2 nanoparticles." *Applied Catalysis B: Environmental* no. 57 (1):23-30.

Bayarri, B, J Giménez, MI Maldonado, S Malato, and S Esplugas. 2013. "2, 4-Dichlorophenol degradation by means of heterogeneous photocatalysis. Comparison between laboratory and pilot plant performance." *Chemical Engineering Journal* no. 232:405-417.

Bayarri, B, MI Maldonado, J Giménez, S Esplugas, and O González. 2007. "Comparative study of 2, 4-dichlorophenol degradation with different

advanced oxidation processes." *Journal of Solar Energy Engineering* no. 129 (1):60-67.

Bayarri, B., J. Giménez, D. Curcó, and S. Esplugas. 2005. "Photocatalytic degradation of 2,4-dichlorophenol by TiO_2/UV: Kinetics, actinometries and models." *Catalysis Today* no. 101 (3–4):227-236.

Bekkouche, S., M. Bouhelassa, N. Hadj Salah, and F. Z. Meghlaoui. 2004. "Study of adsorption of phenol on titanium oxide (TiO_2)." *Desalination* no. 166 (0):355-362.

Bhatkhande, Dhananjay S, Vishwas G Pangarkar, and Anthony A Beenackers. 2002. "Photocatalytic degradation for environmental applications–a review." *Journal of Chemical Technology and Biotechnology* no. 77 (1):102-116.

Bian, Wenjuan, Xuehong Song, Deqi Liu, Jiao Zhang, and Xihua Chen. 2011. "The intermediate products in the degradation of 4-chlorophenol by pulsed high voltage discharge in water." *Journal of Hazardous Materials* no. 192 (3):1330-1339.

Biyoghe Bi Ndong, Landry, Murielle Primaelle Ibondou, Xiaogang Gu, Shuguang Lu, Zhaofu Qiu, Qian Sui, and Serge Maurice Mbadinga. 2014. "Enhanced Photo-catalytic Activity of TiO_2 Nano-sheets by Doping with Cu for Chlorinated Solvent Pollutants Degradation." *Industrial & Engineering Chemistry Research*.

Burns, Robert A, John C Crittenden, David W Hand, Volker H Selzer, Lawrence L Sutter, and Salman R Salman. 1999. "Effect of inorganic ions in heterogeneous photocatalysis of TCE." *Journal of Environmental Engineering* no. 125 (1):77-85.

Cao, Chun-Yan, Li-Kai Meng, and Yong-Hua Zhao. 2013. "Fe-pillared bentonite, a stable Fenton catalyst for treatment of petroleum refinery wastewater." *Toxicological & Environmental Chemistry* no. 95 (5):747-756.

Chan, H. 2011. "Biodegradation of petroleum oil achieved by bacteria and nematodes in contaminated water." *Separation and Purification Technology* no. 80 (3):459-466.

Chavadej, Sumaeth, Penny Ratanarojanatam, Wisakha Phoochinda, Ummarawadee Yanatatsaneejit, and John F Scamehorn. 2004. "Clean-up of oily wastewater by froth flotation: effect of microemulsion formation II: use of anionic/nonionic surfactant mixtures." *Separation science and technology* no. 39 (13):3079-3096.

Chen, Dingwang, and Ajay K. Ray. 1999. "Photocatalytic kinetics of phenol and its derivatives over UV irradiated TiO_2." *Applied Catalysis B: Environmental* no. 23 (2–3):143-157.

Chiou, Chwei-Huann, and Ruey-Shin Juang. 2007. "Photocatalytic degradation of phenol in aqueous solutions by Pr-doped TiO_2 nanoparticles." *Journal of hazardous materials* no. 149 (1):1-7.

Chiou, Chwei-Huann, Cheng-Ying Wu, and Ruey-Shin Juang. 2008a. "Photocatalytic degradation of phenol and m-nitrophenol using irradiated TiO_2 in aqueous solutions." *Separation and Purification Technology* no. 62 (3):559-564.

Chiou, Chwei-Huann, Cheng-Ying Wu, and Ruey-Shin Juang. 2008b. "Photocatalytic degradation of phenol and m-nitrophenol using irradiated TiO_2 in aqueous solutions." *Separation and Purification Technology* no. 62 (3):559-564.

Chong, Meng Nan, Bo Jin, Christopher WK Chow, and Chris Saint. 2010. "Recent developments in photocatalytic water treatment technology: a review." *Water research* no. 44 (10):2997-3027.

Chowdhury, Pankaj, Jesus Moreira, Hassan Gomaa, and Ajay K Ray. 2012. "Visible-solar-light-driven photocatalytic degradation of phenol with dye-sensitized TiO_2: parametric and kinetic study." *Industrial & Engineering Chemistry Research* no. 51 (12):4523-4532.

Chu, W, and CC Wong. 2004. "The photocatalytic degradation of dicamba in TiO_2 suspensions with the help of hydrogen peroxide by different near UV irradiations." *Water research* no. 38 (4):1037-1043.

Coelho, Alessandra, Antonio V Castro, and Márcia Dezotti. 2006. "Treatment of petroleum refinery sourwater by advanced oxidation processes." *Journal of hazardous materials* no. 137 (1):178-184.

Cornish, Benjamin JPA, Linda A Lawton, and Peter KJ Robertson. 2000. "Hydrogen peroxide enhanced photocatalytic oxidation of microcystin-LR using titanium dioxide." *Applied Catalysis B: Environmental* no. 25 (1):59-67.

Czaplicka, M. 2006a. "Photo-degradation of chlorophenols in the aqueous solution." *Journal of hazardous materials* no. 134 (1-3):45-59.

Czaplicka, Marianna. 2006b. "Photo-degradation of chlorophenols in the aqueous solution." *Journal of hazardous materials* no. 134 (1):45-59.

da Rocha, Otidene Rossiter Sá, Renato F Dantas, Marta MM Bezerra Duarte, Márcia Maria Lima Duarte, and Valdinete Lins da Silva. 2013. "Solar photo-Fenton treatment of petroleum extraction wastewater." *Desalination and Water Treatment* no. 51 (28-30):5785-5791.

Daneshvar, N., D. Salari, and A. R. Khataee. 2004. "Photocatalytic degradation of azo dye acid red 14 in water on ZnO as an alternative catalyst to TiO_2." *Journal of Photochemistry and Photobiology A: Chemistry* no. 162 (2–3):317-322.

Dhir, Amit, Nagaraja Tejo Prakash, and Dhiraj Sud. 2012. "Comparative studies on TiO_2/ZnO photocatalyzed degradation of 4-chlorocatechol and bleach mill effluents." *Desalination and Water Treatment* no. 46 (1-3):196-204.

Di Paola, Agatino, Elisa García-López, Giuseppe Marcì, and Leonardo Palmisano. 2012. "A survey of photocatalytic materials for environmental remediation." *Journal of hazardous materials* no. 211:3-29.

Diebold, Ulrike. 2003. "The surface science of titanium dioxide." *Surface Science Reports* no. 48 (5–8):53-229.

Dillert, Ralf, Alberto E Cassano, Roland Goslich, and Detlef Bahnemann. 1999. "Large scale studies in solar catalytic wastewater treatment." *Catalysis today* no. 54 (2):267-282.

Dimoglo, A, HY Akbulut, F Cihan, and M Karpuzcu. 2004. "Petrochemical wastewater treatment by means of clean electrochemical technologies." *Clean Technologies and Environmental Policy* no. 6 (4):288-295.

Ding, Z, GQ Lu, and PF Greenfield. 2000. "Role of the crystallite phase of TiO_2 in heterogeneous photocatalysis for phenol oxidation in water." *The Journal of Physical Chemistry B* no. 104 (19):4815-4820.

Diya'uddeen, Basheer Hasan, Wan Mohd Ashri Wan Daud, and AR Abdul Aziz. 2011. "Treatment technologies for petroleum refinery effluents: a review." *Process Safety and Environmental Protection* no. 89 (2):95-105.

Doong, R, R Maithreepala, and S Chang. 2000. "Heterogeneous and homogeneous photocatalytic degradation of chlorophenolsin aqueous titanium dioxide and ferrous ion." *Water science & technology* no. 42 (7-8):253-260.

Duan, Xiaoyue, Fang Ma, Zhongxin Yuan, Limin Chang, and Xintong Jin. 2012. "Lauryl benzene sulfonic acid sodium-carbon nanotube-modified PbO_2

electrode for the degradation of 4-chlorophenol." *Electrochimica Acta* no. 76 (0):333-343.

El-Naas, Muftah H, Sulaiman Al-Zuhair, and Manal Abu Alhaija. 2010. "Reduction of COD in refinery wastewater through adsorption on date-pit activated carbon." *Journal of hazardous materials* no. 173 (1):750-757.

Elghniji, Kais, Olfa Hentati, Najwa Mlaik, Ayman Mahfoudh, and Mohamed Ksibi. 2012. "Photocatalytic degradation of 4-chlorophenol under P-modified TiO_2/UV system: Kinetics, intermediates, phytotoxicity and acute toxicity." *Journal of Environmental Sciences* no. 24 (3):479-487.

Fernandez-Ibañez, Pilar, Sixto Malato, and Octav Enea. 1999. "Photoelectrochemical reactors for the solar decontamination of water." *Catalysis Today* no. 54 (2):329-339.

Fratila-Apachitei, Lidy E, Maria D Kennedy, John D Linton, Ingo Blume, and Jan C Schippers. 2001. "Influence of membrane morphology on the flux decline during dead-end ultrafiltration of refinery and petrochemical waste water." *Journal of Membrane Science* no. 182 (1):151-159.

Fujishima, Akira, Tata N. Rao, and Donald A. Tryk. 2000. "Titanium dioxide photocatalysis." *Journal of Photochemistry and Photobiology C: Photochemistry Reviews* no. 1 (1):1-21.

Fujishima, Akira, Xintong Zhang, and Donald A. Tryk. 2008. "TiO_2 photocatalysis and related surface phenomena." *Surface Science Reports* no. 63 (12):515-582.

Gai, Ke. 2009. "Anodic oxidation with platinum electrodes for degradation of p-xylene in aqueous solution." Journal of Electrostatics no. 67 (4):554-557.

Gaya, Umar Ibrahim, and Abdul Halim Abdullah. 2008. "Heterogeneous photocatalytic degradation of organic contaminants over titanium dioxide: a

review of fundamentals, progress and problems." *Journal of Photochemistry and Photobiology C: Photochemistry Reviews* no. 9 (1):1-12.

Gaya, Umar Ibrahim, Abdul Halim Abdullah, Mohd Zobir Hussein, and Zulkarnain Zainal. 2010. "Photocatalytic removal of 2, 4, 6-trichlorophenol from water exploiting commercial ZnO powder." *Desalination* no. 263 (1):176-182.

Gaya, Umar Ibrahim, Abdul Halim Abdullah, Zulkarnain Zainal, and Mohd Zobir Hussein. 2009. "Photocatalytic treatment of 4-chlorophenol in aqueous ZnO suspensions: Intermediates, influence of dosage and inorganic anions." *Journal of hazardous materials* no. 168 (1):57-63.

Gaya, Umar Ibrahim, Abdul Halim Abdullah, Zulkarnain Zainal, and Mohd Zobir Hussein. 2010a. "Photocatalytic Degradation of 2, 4-dichlorophenol in Irradiated Aqueous ZnO Suspension." *International Journal of Chemistry* no. 2 (1).

Gaya, Umar Ibrahim, Abdul Halim Abdullah, Zulkarnain Zainal, and Mohd Zobir Hussein. 2010b. "Photocatalytic degradation of 2, 4-dichlorophenol in irradiated aqueous ZnO suspension." *International Journal of Chemistry* no. 2 (1):P180.

Gernjak, W., M. I. Maldonado, S. Malato, J. Cáceres, T. Krutzler, A. Glaser, and R. Bauer. 2004. "Pilot-plant treatment of olive mill wastewater (OMW) by solar TiO_2 photocatalysis and solar photo-Fenton." *Solar Energy* no. 77 (5):567-572. doi: 10.1016/j.solener.2004.03.030.

Gogate, Parag R, and Aniruddha B Pandit. 2004. "A review of imperative technologies for wastewater treatment I: oxidation technologies at ambient conditions." *Advances in Environmental Research* no. 8 (3):501-551.

Gomez, M., M. D. Murcia, J. L. Gomez, G. Matafonova, V. Batoev, and N. Christofi. 2010. "Testing a KrCl excilamp as new enhanced UV source for 4-chlorophenol degradation: Experimental results and kinetic model."

Chemical Engineering and Processing: Process Intensification no. 49 (1):113-119.

Gondal, MA, MN Sayeed, and A Alarfaj. 2007. "Activity comparison of Fe_2O_3, NiO, WO_3, TiO_2 semiconductor catalysts in phenol degradation by laser enhanced photo-catalytic process." *Chemical physics letters* no. 445 (4-6):325-330.

Gora, Alexander, Bea Toepfer, Valeria Puddu, and Gianluca Li Puma. 2006. "Photocatalytic oxidation of herbicides in single-component and multicomponent systems: Reaction kinetics analysis." *Applied Catalysis B: Environmental* no. 65 (1–2):1-10.

GUNES, Y. 2008. "Removal of COD from oil recovery industry wastewater by the advanced oxidation processes (AOP) based on H_2O_2."

Harbour, John R, John Tromp, and Michael L Hair. 1985. "Photogeneration of hydrogen peroxide in aqueous TiO_2 dispersions." *Canadian journal of chemistry* no. 63 (1):204-208.

Hasan, Diya'uddeen Basheer, AR Abdul Aziz, and Wan Mohd Ashri Wan Daud. 2012. "Oxidative mineralisation of petroleum refinery effluent using Fenton-like process." *Chemical Engineering Research and Design* no. 90 (2):298-307.

Herney-Ramirez, J., Miguel A. Vicente, and Luis M. Madeira. 2010. "Heterogeneous photo-Fenton oxidation with pillared clay-based catalysts for wastewater treatment: A review." *Applied Catalysis B: Environmental* no. 98 (1–2):10-26.

Herrmann, J-M. 2005. "Heterogeneous photocatalysis: state of the art and present applications In honor of Pr. RL Burwell Jr.(1912–2003), Former Head of Ipatieff Laboratories, Northwestern University, Evanston (Ill)." *Topics in Catalysis* no. 34 (1-4):49-65.

Herrmann, Jean-Marie. 1999. "Heterogeneous photocatalysis: fundamentals and applications to the removal of various types of aqueous pollutants." *Catalysis today* no. 53 (1):115-129.

Ho, Te-Fu L, and James R Bolton. 1998. "Toxicity changes during the UV treatment of pentachlorophenol in dilute aqueous solution." *Water Research* no. 32 (2):489-497.

Hoffmann, Michael R, Scot T Martin, Wonyong Choi, and Detlef W Bahnemann. 1995. "Environmental applications of semiconductor photocatalysis." *Chemical reviews* no. 95 (1):69-96.

Hong, Seong-Soo, Chang-Sik Ju, Chang-Gyu Lim, Byung-Hyun Ahn, Kwon-Taek Lim, and Gun-Dae Lee. 2001. "A photocatalytic degradation of phenol over TiO_2 prepared by sol-gel method." *Journal of Industrial and Engineering Chemistry* no. 7 (2):99-104.

Huang, Jianhan, Xiaofei Wu, Hongwei Zha, Bin Yuan, and Shuguang Deng. 2013. "A hypercrosslinked poly(styrene-co-divinylbenzene) PS resin as a specific polymeric adsorbent for adsorption of 2-naphthol from aqueous solutions." *Chemical Engineering Journal* no. 218 (0):267-275.

Ireland, John C, Brunilda Davila, Hector Moreno, Shannon K Fink, and Stephanie Tassos. 1995. "Heterogeneous photocatalytic decomposition of polyaromatic hydrocarbons over titanium dioxide." *Chemosphere* no. 30 (5):965-984.

Ishak, Syukriyah, Amirhossein Malakahmad, and MH Isa. 2012. "Refinery wastewater biological treatment: A short review." *Journal of Scientific & Industrial Research* no. 71:251-256.

Janin, Thomas, Vincent Goetz, Stephan Brosillon, and Gaël Plantard. 2013. "Solar photocatalytic mineralization of 2, 4-dichlorophenol and mixtures of pesticides: Kinetic model of mineralization." *Solar Energy* no. 87:127-135.

Jia, Jingbo, Songping Zhang, Ping Wang, and Huajun Wang. 2012. "Degradation of high concentration 2,4-dichlorophenol by simultaneous photocatalytic–enzymatic process using TiO_2/UV and laccase." *Journal of Hazardous Materials* no. 205–206 (0):150-155.

Jou, Chih-Ju G, and Guo-Chiang Huang. 2003. "A pilot study for oil refinery wastewater treatment using a fixed-film bioreactor." *Advances in Environmental Research* no. 7 (2):463-469.

Jr., Amilcar Machulek, Silvio C. Oliveira, Marly E. Osugi, Valdir S. Ferreira, Frank H. Quina, Renato F. Dantas, Samuel L. Oliveira, Gleison A. Casagrande, Fauze J. Anaissi, Volnir O. Silva, Rodrigo P. Cavalcante, Fabio Gozzi, Dayana D. Ramos, Ana P.P. da Rosa, Ana P.F. Santos, Douclasse C. de Castro, and Jéssica A. Nogueira. 2013. *Application of Different Advanced Oxidation Processes for the Degradation of Organic Pollutants, Organic Pollutants - Monitoring, Risk and Treatment*.

Juang, Lain-Chuen, Dyi-Hwa Tseng, and Shyh-Chaur Yang. 1997. "Treatment of petrochemical wastewater by UV/H_2O_2 photodecomposed system." *Water science and technology* no. 36 (12):357-365.

Kamble, Sanjay P, Sudhir P Deosarkar, Sudhir B Sawant, Jacob A Moulijn, and Vishwas G Pangarkar. 2004. "Photocatalytic degradation of 2, 4-dichlorophenoxyacetic acid using concentrated solar radiation: batch and continuous operation." *Industrial & engineering chemistry research* no. 43 (26):8178-8187.

Kansal, Sushil Kumar, and Mani Chopra. 2012. "Photocatalytic Degradation of 2, 6-Dichlorophenol in Aqueous Phase Using Titania as a Photocatalyst." *Engineering* no. 4 (8).

Karthik, Manikavasagam, Nishant Dafale, Pradyumna Pathe, and Tapas Nandy. 2008. "Biodegradability enhancement of purified terephthalic acid

wastewater by coagulation–flocculation process as pretreatment." *Journal of hazardous materials* no. 154 (1):721-730.

Karunakaran, C, and R Dhanalakshmi. 2008. "Semiconductor-catalyzed degradation of phenols with sunlight." *Solar Energy Materials and Solar Cells* no. 92 (11):1315-1321.

Kashif, Naeem, and Feng OUYANG. 2009. "Parameters effect on heterogeneous photocatalysed degradation of phenol in aqueous dispersion of TiO_2." *Journal of Environmental Sciences* no. 21 (4):527-533.

Kavitha, V, and K Palanivelu. 2004. "The role of ferrous ion in Fenton and photo-Fenton processes for the degradation of phenol." *Chemosphere* no. 55 (9):1235-1243.

Kim, Moon-Sun, Chun Soo Ryu, and Byung-Woo Kim. 2005. "Effect of ferric ion added on photodegradation of alachlor in the presence of TiO_2 and UV radiation." *Water research* no. 39 (4):525-532.

Konstantinou, Ioannis K, and Triantafyllos A Albanis. 2003. "Photocatalytic transformation of pesticides in aqueous titanium dioxide suspensions using artificial and solar light: intermediates and degradation pathways." *Applied Catalysis B: Environmental* no. 42 (4):319-335.

Kositzi, M, I Poulios, S Malato, J Caceres, and A Campos. 2004. "Solar photocatalytic treatment of synthetic municipal wastewater." *Water research* no. 38 (5):1147-1154.

Krijgsheld, K. R., and A. van der Gen. 1986. "Assessment of the impact of the emission of certain organochlorine compounds on the aquatic environment: Part I: Monochlorophenols and 2,4-dichlorophenol." *Chemosphere* no. 15 (7):825-860.

Ksibi, Mohamed, Asma Zemzemi, and Rachid Boukchina. 2003a. "Photocatalytic degradability of substituted phenols over UV irradiated TiO_2." *Journal of Photochemistry and Photobiology A: Chemistry* no. 159 (1):61-70.

Ksibi, Mohamed, Asma Zemzemi, and Rachid Boukchina. 2003b. "Photocatalytic degradability of substituted phenols over UV irradiated TiO_2." *Journal of Photochemistry and Photobiology A: Chemistry* no. 159 (1):61-70.

Kusvuran, Erdal, and Oktay Erbatur. 2004. "Degradation of aldrin in adsorbed system using advanced oxidation processes: comparison of the treatment methods." *Journal of Hazardous Materials* no. 106 (2–3):115-125.

Kusvuran, Erdal, Ali Samil, Osman Malik Atanur, and Oktay Erbatur. 2005. "Photocatalytic degradation kinetics of di- and tri-substituted phenolic compounds in aqueous solution by TiO_2/UV." *Applied Catalysis B: Environmental* no. 58 (3–4):211-216.

Lapertot, Milena, Pierre Pichat, Sandra Parra, Chantal Guillard, and Cesar Pulgarin. 2006. "Photocatalytic degradation of p-halophenols in TiO_2 aqueous suspensions: halogen effect on removal rate, aromatic intermediates and toxicity variations." *Journal of Environmental Science and Health Part A* no. 41 (6):1009-1025.

Lathasree, S., A. Nageswara Rao, B. SivaSankar, V. Sadasivam, and K. Rengaraj. 2004. "Heterogeneous photocatalytic mineralisation of phenols in aqueous solutions." *Journal of Molecular Catalysis A: Chemical* no. 223 (1–2):101-105.

Lazar, Manoj A, Shaji Varghese, and Santhosh S Nair. 2012. "Photocatalytic water treatment by titanium dioxide: recent updates." *Catalysts* no. 2 (4):572-601.

Li, Guiying, Taicheng An, Jiaxin Chen, Guoying Sheng, Jiamo Fu, Fanzhong Chen, Shanqing Zhang, and Huijun Zhao. 2006. "Photoelectrocatalytic decontamination of oilfield produced wastewater containing refractory

organic pollutants in the presence of high concentration of chloride ions." *Journal of hazardous materials* no. 138 (2):392-400.

Li Puma, Gianluca, Bea Toepfer, and Alexander Gora. 2007. "Photocatalytic oxidation of multicomponent systems of herbicides: Scale-up of laboratory kinetics rate data to plant scale." *Catalysis Today* no. 124 (3–4):124-132.

Li, Xiaojing, Jerry W Cubbage, and William S Jenks. 1999. "Photocatalytic degradation of 4-chlorophenol. 2. The 4-chlorocatechol pathway." *The Journal of Organic Chemistry* no. 64 (23):8525-8536.

Li, Xiaojing, Jerry W Cubbage, Troy A Tetzlaff, and William S Jenks. 1999. "Photocatalytic degradation of 4-chlorophenol. 1. The hydroquinone pathway." *The Journal of Organic Chemistry* no. 64 (23):8509-8524.

Li, Yue, Bo Wen, Wanhong Ma, Chuncheng Chen, and Jincai Zhao. 2012. "Photocatalytic degradation of aromatic pollutants: a pivotal role of conduction band electron in distribution of hydroxylated intermediates." *Environmental science & technology* no. 46 (9):5093-5099.

Lindner, Martin, Jörn Theurich, and Detlef W. Bahnemann. 1997. "Photocatalytic degradation of organic compounds: accelerating the process efficiency." *Water Science and Technology* no. 35 (4):79-86.

Lipczynska-Kochany, Ewa, and James R Bolton. 1991. "Flash photolysis/HPLC method for studying the sequence of photochemical reactions: applications to 4-chlorophenol in aerated aqueous solution." *Journal of Photochemistry and Photobiology A: Chemistry* no. 58 (3):315-322.

Liu, Lifen, Fang Chen, Fenglin Yang, Yongsheng Chen, and John Crittenden. 2012a. "Photocatalytic degradation of 2,4-dichlorophenol using nanoscale Fe/TiO_2." *Chemical Engineering Journal* no. 181–182 (0):189-195.

Liu, Lifen, Fang Chen, Fenglin Yang, Yongsheng Chen, and John Crittenden. 2012b. "Photocatalytic degradation of 2, 4-dichlorophenol using nanoscale Fe/TiO_2." *Chemical Engineering Journal* no. 181:189-195.

Lu, Sheng-yong, Di Wu, Qiu-lin Wang, Jianhua Yan, Alfons G. Buekens, and Ke-fa Cen. 2011. "Photocatalytic decomposition on nano-TiO_2: Destruction of chloroaromatic compounds." *Chemosphere* no. 82 (9):1215-1224.

Ma, Fang, Jing-bo Guo, Li-jun Zhao, Chein-chi Chang, and Di Cui. 2009. "Application of bioaugmentation to improve the activated sludge system into the contact oxidation system treating petrochemical wastewater." *Bioresource technology* no. 100 (2):597-602.

Ma, Yunfei, Jinlong Zhang, Baozhu Tian, Feng Chen, and Lingzhi Wang. 2010. "Synthesis and characterization of thermally stable Sm, N co-doped TiO_2 with highly visible light activity." *Journal of Hazardous Materials* no. 182 (1):386-393.

Mahamuni, Naresh N, and Yusuf G Adewuyi. 2010. "Advanced oxidation processes (AOPs) involving ultrasound for waste water treatment: a review with emphasis on cost estimation." *Ultrasonics Sonochemistry* no. 17 (6):990-1003.

Malato, S, J Blanco, C Richter, B Braun, and MI Maldonado. 1998. "Enhancement of the rate of solar photocatalytic mineralization of organic pollutants by inorganic oxidizing species." *Applied Catalysis B: Environmental* no. 17 (4):347-356.

Malato, S, J Blanco, C Richter, D Curco, and J Gimenez. 1997. "Low-concentrating CPC collectors for photocatalytic water detoxification: comparison with a medium concentrating solar collector." *Water Science and Technology* no. 35 (4):157-164.

Malato, Sixto, Julián Blanco, Alfonso Vidal, and Christoph Richter. 2002. "Photocatalysis with solar energy at a pilot-plant scale: an overview." *Applied Catalysis B: Environmental* no. 37 (1):1-15.

Malato, Sixto, P Fernández-Ibáñez, MI Maldonado, J Blanco, and W Gernjak. 2009. "Decontamination and disinfection of water by solar photocatalysis: recent overview and trends." *Catalysis Today* no. 147 (1):1-59.

Marci, Giuseppe, Vincenzo Augugliaro, Maria J Lopez-Munoz, Cristina Martin, Leonardo Palmisano, Vicente Rives, Mario Schiavello, Richard JD Tilley, and Anna Maria Venezia. 2001. "Preparation characterization and photocatalytic activity of polycrystalline ZnO/TiO_2 systems. 2. Surface, bulk characterization, and 4-nitrophenol photodegradation in liquid-solid regime." *The Journal of Physical Chemistry B* no. 105 (5):1033-1040.

Martinez, F, G Calleja, JA Melero, and R Molina. 2007. "Iron species incorporated over different silica supports for the heterogeneous photo-Fenton oxidation of phenol." *Applied Catalysis B: Environmental* no. 70 (1):452-460.

Matos, J, J Laine, and J-M Herrmann. 2001. "Effect of the type of activated carbons on the photocatalytic degradation of aqueous organic pollutants by UV-irradiated titania." *Journal of Catalysis* no. 200 (1):10-20.

Matos, J, J Laine, J-M Herrmann, D Uzcategui, and JL Brito. 2007. "Influence of activated carbon upon titania on aqueous photocatalytic consecutive runs of phenol photodegradation." *Applied Catalysis B: Environmental* no. 70 (1):461-469.

Matos, Juan, Jorge Laine, and Jean-Marie Herrmann. 1998. "Synergy effect in the photocatalytic degradation of phenol on a suspended mixture of titania and activated carbon." *Applied Catalysis B: Environmental* no. 18 (3):281-291.

Matthews, Ralph W. 1986. "Photo-oxidation of organic material in aqueous suspensions of titanium dioxide." *Water Research* no. 20 (5):569-578.

Mehrvar, Mehrab, William A. Anderson, Murray Moo-Young, and Park M. Reilly. 2000. "Non-linear parameter estimation for a dynamic model in photocatalytic reaction engineering." *Chemical Engineering Science* no. 55 (21):4885-4891.

Melián, E. Pulido, O. González Díaz, J. M. Doña Rodríguez, J. Araña, and J. Pérez Peña. 2013. "Adsorption and photocatalytic degradation of 2,4-dichlorophenol in TiO_2 suspensions. Effect of hydrogen peroxide, sodium peroxodisulphate and ozone." *Applied Catalysis A: General* no. 455 (0):227-233.

Měšťánková, Hana, Gilles Mailhot, Jaromír Jirkovský, Josef Krýsa, and Michèle Bolte. 2005. "Mechanistic approach of the combined (iron–TiO_2) photocatalytic system for the degradation of pollutants in aqueous solution: an attempt of rationalisation." *Applied Catalysis B: Environmental* no. 57 (4):257-265.

Mills, Andrew, Richard H Davies, and David Worsley. 1993. "Water purification by semiconductor photocatalysis." *Chem. Soc. Rev.* no. 22 (6):417-425.

Mills, Andrew, and Stephen Le Hunte. 1997. "An overview of semiconductor photocatalysis." *Journal of photochemistry and photobiology A: Chemistry* no. 108 (1):1-35.

Mills, Andrew, and Siân Morris. 1993. "Photomineralization of 4-chlorophenol sensitized by titanium dioxide: a study of the initial kinetics of carbon dioxide photogeneration." *Journal of Photochemistry and Photobiology A: Chemistry* no. 71 (1):75-83.

Mills, Andrew, Sian Morris, and Richard Davies. 1993. "Photomineralisation of 4-chlorophenol sensitised by titanium dioxide: a study of the intermediates." *Journal of Photochemistry and Photobiology A: Chemistry* no. 70 (2):183-191.

Modirshahla, Nasser, Aydin Hassani, Mohammad A Behnajady, and Rajab Rahbarfam. 2011. "Effect of operational parameters on decolorization of Acid Yellow 23 from wastewater by UV irradiation using ZnO and ZnO/SnO_2 photocatalysts." *Desalination* no. 271 (1):187-192.

Moreira, Jesus, Benito Serrano, Aaron Ortiz, and Hugo de Lasa. 2012. "A unified kinetic model for phenol photocatalytic degradation over TiO_2 photocatalysts." *Chemical Engineering Science* no. 78 (0):186-203.

Mota, ALN, LF Albuquerque, LT C Beltrame, O Chiavone-Filho, A Machulek Jr, and CAO Nascimento. 2009. "Advanced oxidation processes and their application in the petroleum industry: a review." *Brazilian Journal of Petroleum and Gas* no. 2 (3).

Muthuvel, Inbasekaran, and Meenakshisundaram Swaminathan. 2007. "Photoassisted Fenton mineralisation of Acid Violet 7 by heterogeneous Fe (III)–Al_2O_3 catalyst." *Catalysis Communications* no. 8 (7):981-986.

Naeem, Kashif, Pan Weiqian, and Feng Ouyang. 2010. "Thermodynamic parameters of activation for photodegradation of phenolics." *Chemical Engineering Journal* no. 156 (2):505-509.

Nogueira, R, A Trov, and W Paterlini. 2004. "Evaluation of the combined solar TiO_2/photo-Fenton process using multivariate analysis." *Water Science & Technology* no. 49 (4):195-200.

Nogueira, Raquel Fernandes Pupo, Milady Renata Apolinário da Silva, and AG Trovó. 2005. "Influence of the iron source on the solar photo-Fenton degradation of different classes of organic compounds." *Solar Energy* no. 79 (4):384-392.

Oller, I, S Malato, and JA Sánchez-Pérez. 2011. "Combination of advanced oxidation processes and biological treatments for wastewater

decontamination—a review." *Science of the total environment* no. 409 (20):4141-4166.

Ortiz-Gomez, Aaron, Benito Serrano-Rosales, and Hugo de Lasa. 2008. "Enhanced mineralization of phenol and other hydroxylated compounds in a photocatalytic process assisted with ferric ions." *Chemical Engineering Science* no. 63 (2):520-557.

Ortiz-Gomez, Aaron, Benito Serrano-Rosales, Miguel Salaices, and Hugo de Lasa. 2007a. "Photocatalytic oxidation of phenol: reaction network, kinetic modeling, and parameter estimation." *Industrial & Engineering Chemistry Research* no. 46 (23):7394-7409.

Ortiz-Gomez, Aaron, Benito Serrano-Rosales, Miguel Salaices, and Hugo de Lasa. 2007b. "Photocatalytic Oxidation of Phenol: Reaction Network, Kinetic Modeling, and Parameter Estimation." *Industrial & Engineering Chemistry Research* no. 46 (23):7394-7409.

Pandiyan, T., O. Martínez Rivas, J. Orozco Martínez, G. Burillo Amezcua, and M. A. Martínez-Carrillo. 2002. "Comparison of methods for the photochemical degradation of chlorophenols." *Journal of Photochemistry and Photobiology A: Chemistry* no. 146 (3):149-155.

Pardeshi, SK, and AB Patil. 2008. "A simple route for photocatalytic degradation of phenol in aqueous zinc oxide suspension using solar energy." *Solar Energy* no. 82 (8):700-705.

Pariente, MI, JA Melero, F Martinez, JA Botas, and AI Gallego. 2010. "Catalytic wet hydrogen peroxide oxidation of a petrochemical wastewater." *Water Science & Technology* no. 61 (7).

Parilti, Neval BAYCAN. 2010. "Treatment of a petrochemical industry wastewater by a solar oxidation process using the box-wilson experimental design method." *Ekoloji* no. 19 (77):9-15.

Parra, S, J Olivero, L Pacheco, and C Pulgarin. 2003. "Structural properties and photoreactivity relationships of substituted phenols in TiO_2 suspensions." *Applied Catalysis B: Environmental* no. 43 (3):293-301.

Pelizzetti, E, and C Minero. 1993. "Mechanism of the photo-oxidative degradation of organic pollutants over TiO_2 particles." *Electrochimica acta* no. 38 (1):47-55.

Peng, Yunxia, Shijun He, Jianlong Wang, and Wenqi Gong. 2012. "Comparison of different chlorophenols degradation in aqueous solutions by gamma irradiation under reducing conditions." *Radiation Physics and Chemistry* no. 81 (10):1629-1633.

Pera-Titus, Marc, Verónica García-Molina, Miguel A. Baños, Jaime Giménez, and Santiago Esplugas. 2004. "Degradation of chlorophenols by means of advanced oxidation processes: a general review." *Applied Catalysis B: Environmental* no. 47 (4):219-256.

Pineda Arellano, Carlos Antonio, A Jiménez González, Susana Silva Martínez, Iván Salgado-Tránsito, and Cesar Pérez Franco. 2013. "Enhanced mineralization of atrazine by means of photodegradation processes using solar energy at pilot plant scale." *Journal of Photochemistry and Photobiology A: Chemistry* no. 272:21-27.

Pino, Eduardo, and Maria Victoria Encinas. 2012. "Photocatalytic degradation of chlorophenols on TiO_2-325mesh and TiO_2-P25. An extended kinetic study of photodegradation under competitive conditions." *Journal of Photochemistry and Photobiology A: Chemistry* no. 242:20-27.

Poulopoulos, SG, and CJ Philippopoulos. 2004. "Photo-assisted oxidation of chlorophenols in aqueous solutions using hydrogen peroxide and titanium dioxide." *Journal of Environmental Science and Health, Part A* no. 39 (6):1385-1397.

Priya, M. H., and Giridhar Madras. 2005. "Kinetics of Photocatalytic Degradation of Chlorophenol, Nitrophenol, and Their Mixtures." *Industrial & Engineering Chemistry Research* no. 45 (2):482-486.

Priya, MH, and Giridhar Madras. 2006a. "Kinetics of photocatalytic degradation of chlorophenol, nitrophenol, and their mixtures." *Industrial & engineering chemistry research* no. 45 (2):482-486.

Priya, MH, and Giridhar Madras. 2006b. "Kinetics of photocatalytic degradation of phenols with multiple substituent groups." *Journal of Photochemistry and Photobiology A: Chemistry* no. 179 (3):256-262.

Quici, Natalia, María E Morgada, Raquel T Gettar, Michele Bolte, and Marta I Litter. 2007. "Photocatalytic degradation of citric acid under different conditions: TiO_2 heterogeneous photocatalysis against homogeneous photolytic processes promoted by Fe (III) and H_2O_2." *Applied Catalysis B: Environmental* no. 71 (3):117-124.

Rayne, Sierra, Kaya Forest, and Ken J. Friesen. 2009. "Mechanistic aspects regarding the direct aqueous environmental photochemistry of phenol and its simple halogenated derivatives. A review." *Environment International* no. 35 (2):425-437.

Rincon, AG, and C Pulgarin. 2003. "Photocatalytical inactivation of E. coli: effect of (continuous–intermittent) light intensity and of (suspended–fixed) TiO_2 concentration." *Applied Catalysis B: Environmental* no. 44 (3):263-284.

Rodriguez, E. M., G. Fernandez, P. M. Alvarez, and F. J. Beltran. 2012. "TiO_2 and Fe (III) photocatalytic ozonation processes of a mixture of emergent contaminants of water." *Water Res* no. 46 (1):152-66.

Rodríguez, Eva, Guadalupe Fernández, Beatriz Ledesma, Pedro Álvarez, and Fernando J Beltrán. 2009. "Photocatalytic degradation of organics in water in

the presence of iron oxides: Influence of carboxylic acids." *Applied Catalysis B: Environmental* no. 92 (3):240-249.

Rodríguez, Eva M, Guadalupe Fernández, Pedro M Álvarez, Rebeca Hernández, and Fernando J Beltrán. 2011. "Photocatalytic degradation of organics in water in the presence of iron oxides: effects of pH and light source." *Applied Catalysis B: Environmental* no. 102 (3):572-583.

Rodríguez, Eva M, Guadalupe Fernández, Nikolaus Klamerth, M Ignacio Maldonado, Pedro M Álvarez, and Sixto Malato. 2010. "Efficiency of different solar advanced oxidation processes on the oxidation of bisphenol A in water." *Applied Catalysis B: Environmental* no. 95 (3):228-237.

Romero, Manuel, Julián Blanco, Benigno Sánchez, Alfonso Vidal, Malato Sixto, Ana I. Cardona, and Elisa Garcia. 1999. "SOLAR PHOTOCATALYTIC DEGRADATION OF WATER AND AIR POLLUTANTS: CHALLENGES AND PERSPECTIVES." *Solar Energy* no. 66 (2):169-182.

Saggioro, Enrico Mendes, Anabela Sousa Oliveira, Thelma Pavesi, Margarita Jiménez Tototzintle, Manuel Ignacio Maldonado, Fábio Verissimo Correia, and Josino Costa Moreira. 2014. "Solar CPC pilot plant photocatalytic degradation of bisphenol A in waters and wastewaters using suspended and supported-TiO_2. Influence of photogenerated species." *Environmental Science and Pollution Research*:1-10.

Saien, J, and H Nejati. 2007. "Enhanced photocatalytic degradation of pollutants in petroleum refinery wastewater under mild conditions." *Journal of hazardous materials* no. 148 (1):491-495.

Saien, Javad, and Fatemeh Shahrezaei. 2012. "Organic Pollutants Removal from Petroleum Refinery Wastewater with Nanotitania Photocatalyst and UV Light Emission." *International Journal of Photoenergy* no. 2012.

Salaices, M., B. Serrano, and H. I. de Lasa. 2004. "Photocatalytic conversion of phenolic compounds in slurry reactors." *Chemical Engineering Science* no. 59 (1):3-15.

Santo, Carlos E, Vítor JP Vilar, Amit Bhatnagar, Eva Kumar, Cidália MS Botelho, and Rui AR Boaventura. 2012. "Sulphide removal from petroleum refinery wastewaters by catalytic oxidation." *Desalination and Water Treatment* no. 46 (1-3):256-263.

Santo, Carlos E, Vítor JP Vilar, Cidalia Botelho, Amit Bhatnagar, Eva Kumar, and Rui AR Boaventura. 2012. "Optimization of coagulation–flocculation and flotation parameters for the treatment of a petroleum refinery effluent from a Portuguese plant." *Chemical Engineering Journal* no. 183:117-123.

Santos, FV, EB Azevedo, and M Dezotti. 2006. "Photocatalysis as a tertiary treatment for petroleum refinery wastewaters." *Brazilian Journal of Chemical Engineering* no. 23 (4):451-460.

Sayama, Kazuhiro, Hiroki Hayashi, Takeo Arai, Masatoshi Yanagida, Takahiro Gunji, and Hideki Sugihara. 2010. "Highly active WO_3 semiconductor photocatalyst prepared from amorphous peroxo-tungstic acid for the degradation of various organic compounds." *Applied Catalysis B: Environmental* no. 94 (1):150-157.

Sclafani, A, L Palmisano, G Marcı, and AM Venezia. 1998. "Influence of platinum on catalytic activity of polycrystalline WO_3 employed for phenol photodegradation in aqueous suspension." *Solar energy materials and solar cells* no. 51 (2):203-219.

Sclafani, Antonino, Leonardo Palmisano, and Eugenio Davi. 1991. "Photocatalytic degradation of phenol in aqueous polycrystalline TiO_2 dispersions: the influence of Fe^{3+}, Fe^{2+} and Ag^{+} on the reaction rate." *Journal of photochemistry and photobiology. A, Chemistry* no. 56 (1):113-123.

Selvam, K, M Muruganandham, I Muthuvel, and M Swaminathan. 2007. "The influence of inorganic oxidants and metal ions on semiconductor sensitized photodegradation of 4-fluorophenol." *Chemical Engineering Journal* no. 128 (1):51-57.

Selvam, K, M Muruganandham, and M Swaminathan. 2005. "Enhanced heterogeneous ferrioxalate photo-fenton degradation of reactive orange 4 by solar light." *Solar energy materials and solar cells* no. 89 (1):61-74.

Shahrezaei, F, Yadollah Mansouri, Ali Akbar Lorestani Zinatizadeh, and Aazam Akhbari. 2012. "Process modeling and kinetic evaluation of petroleum refinery wastewater treatment in a photocatalytic reactor using TiO_2 nanoparticles." *Powder technology* no. 221:203-212.

Shinde, SS, PS Shinde, CH Bhosale, and KY Rajpure. 2011. "Zinc oxide mediated heterogeneous photocatalytic degradation of organic species under solar radiation." *Journal of Photochemistry and Photobiology B: Biology* no. 104 (3):425-433.

Singh, Jyoti, and S Uma. 2009. "Efficient photocatalytic degradation of organic compounds by ilmenite $AgSbO_3$ under visible and UV light irradiation." *The Journal of Physical Chemistry C* no. 113 (28):12483-12488.

Sivalingam, G, MH Priya, and Giridhar Madras. 2004. "Kinetics of the photodegradation of substituted phenols by solution combustion synthesized TiO_2." *Applied Catalysis B: Environmental* no. 51 (1):67-76.

Snider, EH, and FS Manning. 1982. "A survey of pollutant emission levels in wastewaters and residuals from the petroleum refining industry." *Environment International* no. 7 (4):237-258.

Souza, Bianca M, Ana C Cerqueira, Geraldo L Sant'Anna Jr, and Marcia Dezotti. 2011. "Oil-Refinery Wastewater Treatment Aiming Reuse by Advanced

Oxidation Processes (AOPs) Combined with Biological Activated Carbon (BAC)." *Ozone: Science & Engineering* no. 33 (5):403-409.

Stafford, Ulick, Kimberly A Gray, and Prashant V Kamat. 1994. "Radiolytic and TiO_2-assisted photocatalytic degradation of 4-chlorophenol. A comparative study." *The Journal of Physical Chemistry* no. 98 (25):6343-6351.

Stepnowski, P, EM Siedlecka, P Behrend, and B Jastorff. 2002. "Enhanced photo-degradation of contaminants in petroleum refinery wastewater." *Water research* no. 36 (9):2167-2172.

Sun, Yong, Yaobin Zhang, and Xie Quan. 2008. "Treatment of petroleum refinery wastewater by microwave-assisted catalytic wet air oxidation under low temperature and low pressure." *Separation and Purification Technology* no. 62 (3):565-570.

Svetlichnyi, VA, ON Chaikovskaya, RT Kuznetsova, IV Sokolova, TN Kopylova, and Yu P Meshalkin. 2001. "Photolysis of phenol and para-chlorophenol by UV laser excitation." *High Energy Chemistry* no. 35 (4):258-264.

Tansel, Berrin, and Jayadev Regula. 2000. "Coagulation enhanced centrifugation for treatment of petroleum hydrocarbon contaminated waters." *Journal of Environmental Science & Health Part A* no. 35 (9):1557-1575.

Tatem, HE, BA Cox, and JW Anderson. 1978. "The toxicity of oils and petroleum hydrocarbons to estuarine crustaceans." *Estuarine and Coastal Marine Science* no. 6 (4):365-373.

Temel, Nuket Kartal, and Münevver Sökmen. 2011. "New catalyst systems for the degradation of chlorophenols." *Desalination* no. 281 (0):209-214.

Theurich, J, M Lindner, and DW Bahnemann. 1996. "Photocatalytic degradation of 4-chlorophenol in aerated aqueous titanium dioxide suspensions: a kinetic and mechanistic study." *Langmuir* no. 12 (26):6368-6376.

Thu, Hoai Bui, Maithaa Karkmaz, Eric Puzenat, Chantal Guillard, and Jean-Marie Herrmann. 2005. "From the fundamentals of photocatalysis to its applications in environment protection and in solar purification of water in arid countries." *Research on chemical intermediates* no. 31 (4-6):449-461.

Tony, Maha A, Patrick J Purcell, and Yaqian Zhao. 2012. "Oil refinery wastewater treatment using physicochemical, Fenton and Photo-Fenton oxidation processes." *Journal of Environmental Science and Health, Part A* no. 47 (3):435-440.

Tony, Maha A, Patrick J Purcell, YQ Zhao, Aghareed M Tayeb, and MF El-Sherbiny. 2009. "Photo-catalytic degradation of an oil-water emulsion using the photo-Fenton treatment process: effects and statistical optimization." *Journal of Environmental Science and Health Part A* no. 44 (2):179-187.

Tony, Maha A, YQ Zhao, Patrick J Purcell, and MF El-Sherbiny. 2009. "Evaluating the photo-catalytic application of Fenton's reagent augmented with TiO_2 and ZnO for the mineralization of an oil-water emulsion." *Journal of Environmental Science and Health Part A* no. 44 (5):488-493.

Toor, Amrit Pal, Anoop Verma, C. K. Jotshi, P. K. Bajpai, and Vasundhara Singh. 2006. "Photocatalytic degradation of Direct Yellow 12 dye using UV/TiO_2 in a shallow pond slurry reactor." *Dyes and Pigments* no. 68 (1):53-60.

Tryba, Beata, Antoni W Morawski, Michio Inagaki, and Masahiro Toyoda. 2006. "The kinetics of phenol decomposition under UV irradiation with and without H_2O_2 on TiO_2, Fe-TiO_2 and Fe-C-TiO_2 photocatalysts." *Applied catalysis. B, Environmental* no. 63 (3-4):215-221.

Turchi, Craig S., and David F. Ollis. 1990. "Photocatalytic degradation of organic water contaminants: Mechanisms involving hydroxyl radical attack." *Journal of Catalysis* no. 122 (1):178-192.

Vargas, Ronald, and Oswaldo Núñez. 2010. "Photocatalytic degradation of oil industry hydrocarbons models at laboratory and at pilot-plant scale." *Solar Energy* no. 84 (2):345-351.

Venkatachalam, N, M Palanichamy, and V Murugesan. 2007. "Sol–gel preparation and characterization of alkaline earth metal doped nano TiO_2: Efficient photocatalytic degradation of 4-chlorophenol." *Journal of Molecular Catalysis A: Chemical* no. 273 (1):177-185.

Venkatachalam, N., M. Palanichamy, Banumathi Arabindoo, and V. Murugesan. 2007. "Enhanced photocatalytic degradation of 4-chlorophenol by Zr^{4+} doped nano TiO_2." *Journal of Molecular Catalysis A: Chemical* no. 266 (1–2):158-165.

Vineetha, MN, Manickam Matheswaran, and KN Sheeba. 2013. "Photocatalytic colour and COD removal in the distillery effluent by solar radiation." *Solar Energy* no. 91:368-373.

Vinu, R, and Giridhar Madras. 2011a. "Photocatalytic Degradation of water pollutants using nano-TiO_2." In *Energy Efficiency and Renewable Energy Through Nanotechnology*, 625-677. Springer.

Vinu, R, and Giridhar Madras. 2012. "Environmental remediation by photocatalysis." *Journal of the Indian Institute of Science* no. 90 (2):189-230.

Vinu, R., and Giridhar Madras. 2011b. "Photocatalytic Degradation of Water Pollutants Using Nano-TiO_2."625-677.

Wake, Helen. 2005. "Oil refineries: a review of their ecological impacts on the aquatic environment." *Estuarine, Coastal and Shelf Science* no. 62 (1):131-140.

Wang, Kuo-Hua, Yung-Hsu Hsieh, Ming-Yeuan Chou, and Chen-Yu Chang. 1999. "Photocatalytic degradation of 2-chloro and 2-nitrophenol by titanium

dioxide suspensions in aqueous solution." *Applied Catalysis B: Environmental* no. 21 (1):1-8.

Wang, Zhengpeng, Weimin Cai, Xiaoting Hong, Xiaolian Zhao, Fang Xu, and Chuenguang Cai. 2005. "Photocatalytic degradation of phenol in aqueous nitrogen-doped TiO_2 suspensions with various light sources." *Applied Catalysis B: Environmental* no. 57 (3):223-231.

Wei, Tsong-Yang, Yung-Yun Wang, and Chi-Chao Wan. 1990. "Photocatalytic oxidation of phenol in the presence of hydrogen peroxide and titanium dioxide powders." *Journal of Photochemistry and Photobiology A: Chemistry* no. 55 (1):115-126.

Wong, Joseph M, and Yung-Tse Hung. 2004. "Treatment of oilfield and refinery wastes." *Handbook of industrial and hazardous wastes treatment*:131.

Yan, Long, Hongzhu Ma, Bo Wang, Wei Mao, and Yashao Chen. 2010. "Advanced purification of petroleum refinery wastewater by catalytic vacuum distillation." *Journal of hazardous materials* no. 178 (1):1120-1124.

Yan, Long, Yufei Wang, Jian Li, Hongzhu Ma, Huijin Liu, Te Li, and Yujia Zhang. 2014. "Comparative study of different electrochemical methods for petroleum refinery wastewater treatment." *Desalination* no. 341:87-93.

Yang, Juan, Jun Dai, Chuncheng Chen, and Jincai Zhao. 2009. "Effects of hydroxyl radicals and oxygen species on the 4-chlorophenol degradation by photoelectrocatalytic reactions with TiO2-film electrodes." *Journal of Photochemistry and Photobiology A: Chemistry* no. 208 (1):66-77.

Yavuz, Yusuf, A Savaş Koparal, and Ülker Bakır Öğütveren. 2010. "Treatment of petroleum refinery wastewater by electrochemical methods." *Desalination* no. 258 (1):201-205.

Zhang, Qingxuan, and Guohua Yang. 2011. The removal of COD from refinery wastewater by Fenton reagent. Paper read at Remote Sensing, Environment and Transportation Engineering (RSETE), 2011 International Conference on.

Zhang, Zizhong, Xuxu Wang, Jinlin Long, Quan Gu, Zhengxin Ding, and Xianzhi Fu. 2010. "Nitrogen-doped titanium dioxide visible light photocatalyst: Spectroscopic identification of photoactive centers." *Journal of catalysis* no. 276 (2):201-214.

Zhao, Binxia, Giuseppe Mele, Iolanda Pio, Jun Li, Leonardo Palmisano, and Giuseppe Vasapollo. 2010. "Degradation of 4-nitrophenol (4-NP) using Fe–TiO_2 as a heterogeneous photo-Fenton catalyst." *Journal of hazardous materials* no. 176 (1):569-574.

Zhong, Jing, Feng Chen, and Jinlong Zhang. 2009. "Carbon-deposited TiO_2: synthesis, characterization, and visible photocatalytic performance." *The Journal of Physical Chemistry C* no. 114 (2):933-939.

Znad, H, and Y Kawase. 2009. "Synthesis and characterization of S-doped Degussa P25 with application in decolorization of Orange II dye as a model substrate." *Journal of Molecular Catalysis A: Chemical* no. 314 (1):55-62.

APPENDIX A

Raw data for solar photocatalytic degradation

A-1 Concentration profiles of 4-CP and its intermediates at several initial concentrations (a) 50, (b) 75, and (c) 100 mg/L on 0.5 g/L TiO_2

(a)

t (min)	4-CP(mg/L)	HQ(mg/L)	4cCat(mg/L)	Ph(mg/L)
0	50	0	0	0
30	36.86	9.27	2.65	1.12
60	29.67	11.92	3.73	1.78
90	23.26	14.23	4.96	2.32
120	18.47	17.75	5.35	1.05
150	15.16	20.23	4.11	0.81
180	12.05	24.13	3.69	0.001

(b)

t(min)	4-CP(mg/L)	HQ(mg/L)	4cCat(mg/L)	Ph(mg/L)
0	75	0	0	0
30	60.29	10.58	3.25	1.23
60	51.87	13.25	4.45	1.98
90	39.67	17.02	6.54	2.56
120	35.62	22.35	8.25	1.54
150	30.95	26.35	6.21	1.11
180	26.24	30.45	3.35	0.08

(c)

t(min)	4-CP(mg/L)	HQ(mg/L)	4cCat(mg/L)	Ph(mg/L)
0	100	0	0	0
30	90.72	14.25	4.56	1.58
60	81.34	17.56	5.25	2.35
90	58.14	20.13	8.23	2.98
120	46.79	24.35	10.03	2.01
150	37.19	29.23	8.11	1.54
180	29.56	35.45	7.25	1.01

A-2 Effect of the 4-CP initial concentration on the degradation efficiency (0.5 g/L, 1000mW/cm^2)

C (mg/L)	η %
0	0
50	77.77
75	58.63
100	48.94

A-3 Concentration profiles of HQ photocatalytic degradation and its intermediate (0.5g/L TiO_2, 1000mW/cm^2).

T (min)	HQ (mg/L)	BQ (mg/L)
0	50	0
30	40.12	5.23
60	30.45	2.98
90	25.47	1.98
120	19.88	1.01
150	15.42	0.09
180	10.54	0.01

A-4 Concentration profile of 4cCat photocatalytic degradation on 0.5g/L TiO_2, 1000 mW/cm^2

t (min)	4cCat (mg/L)
0	50
30	37.87
60	29.54
90	23.42
120	16.78
150	10.56
180	6.54

A-5 Experimental and estimated concentration profiles for photocatalytic degradation of 4-CP on 0.5g/L TiO_2 catalyst: (a) 50, (b) 75 and (c) 100 mg/L 4-CP initial concentration

(a)

t (min)	4-CP(theo)	HQ(theo)	4cCat(theo)	4-CP(exp)	HQ(exp)	4cCat(exp)
0	50	0	0	50	0	0
30	38.08388	5.931934	4.019579	36.86	9.27	2.65
60	28.70281	10.54944	4.860094	29.67	11.92	3.73
90	21.4356	14.07114	4.434829	23.26	14.23	4.96
120	15.88713	16.70226	3.630631	18.47	17.75	5.35
150	11.70305	18.62689	2.817511	15.16	20.23	4.11
180	8.579651	20.00285	2.123895	12.05	24.13	3.69

(b)

t(min)	$4CP_{(theo)}$	$HQ_{(theo)}$	$4cCat_{(theo)}$	$4\text{-}CP_{(exp)}$	$HQ_{(exp)}$	$4cCat_{(exp)}$
0	75	0	0	75	0	0
30	58.42433	8.254603	5.772081	60.29	10.58	3.25
60	44.93879	14.90222	7.270076	51.87	13.25	4.45
90	34.16801	20.13816	6.858697	39.67	17.02	6.54
120	25.71684	24.16827	5.764749	35.62	22.35	8.25
150	19.19148	27.19787	4.565735	30.95	26.35	6.21
180	14.22246	29.41961	3.495772	26.24	30.45	3.35

(c)

t	$4\text{-}CP_{(theo)}$	$HQ_{(theo)}$	$4cCat_{(theo)}$	$4\text{-}CP_{(exp)}$	$HQ_{(exp)}$	$4cCat_{(exp)}$
0	100	0	0	100	0	0
30	79.41589	10.25408	7.367153	86.23	14.25	4.56
60	62.21353	18.74449	9.61903	79.56	17.56	5.25
90	48.10702	25.62021	9.359678	55.32	20.13	8.23
120	36.75913	31.0574	8.071151	46.79	24.35	10.03
150	27.79606	35.25159	6.525949	37.19	29.23	8.11
180	20.83314	38.40406	5.078985	22.56	35.45	7.25

A-6 Concentration profiles of 4-CP (0.5g/LTiO_2, 1000mW/cm^2)

t (min)	4-CP(mg/L)	HQ(mg/L)	4cCat(mg/L)	Ph(mg/L)
0	46.21	0	0	0
30	33.21	7.77	9.65	6.04
60	21.01	12.65	9.01	6.54
90	14.01	10.99	6.23	4.01
120	8.23	6.23	4.02	2.24
150	4.01	3.98	2.01	1.1
180	2.36	1.56	1.45	1
210	1.023	0.98	1.01	0.87
240	0.056	0.47	0.235	0.158

A-7 Concentration profiles of 2,4-DCP (0.5g/LTiO_2, 1000mW/cm^2)

t (min)	2,4-DCP(mg/L)	4-CP(mg/L)	Ph(mg/L)
0	23.99	0	0
30	16.23	2.32	0.98
60	10	5.98	2.31
90	6.75	8.23	4.23
120	5.23	9.33	5.31
150	3.01	8.66	6.01
180	1.56	6.05	4.32
210	0.91	4.78	3.11
240	0.501	2.35	0.98

A-8 TOC degradations of 4-CP and 2,4-DCP (0.5g/LTiO_2, 1000mW/cm^2)

t (min)	4-CP(TOC/TOC_0)	2,4DCP(TOC/TOC_0)
0	1	1
30	0.89	0.9
60	0.8	0.83
90	0.68	0.7
120	0.58	0.62
150	0.49	0.52
180	0.39	0.42
210	0.29	0.33
240	0.19	0.24

A-9 Concentration profiles of the combined mixture (50 mg/L both 4-CP and 2,4-DCP) (0.5 g/LTiO_2, 1000 mW/cm^2)

t (min)	4-CP(mg/L)	2,4-DCP(mg/L)	HQ(mg/L)	Ph(mg/L)	4cCat(mg/L)
0	48.21	49.12	0	0	0
30	36.58	39	2.21	3.23	3.65
60	26.35	30.25	5.35	7.11	4.99
90	18.54	24.01	11.01	6.99	4.32
120	13.25	21.01	12.03	6.12	3.11
150	10.23	16.03	10.24	5.23	2.012
180	7.35	14.01	9.01	3.11	1.66
210	4.36	10.32	7.25	2.12	0.99
240	4	8.98	4.11	1.61	0.62

A-10 TOC degradation of the combined mixture (0.5 g/LTiO_2, 1000 mW/cm^2)

t (min)	TOC/TOC0
0	1
30	0.93
60	0.89
90	0.8
120	0.71
150	0.65
180	0.56
210	0.49
240	0.4

A-11 Experimental and estimated concentration profiles for photocatalytic degradation of 50 mg/L 4-CP on 0.5 g/L TiO_2 and 1000mW/cm^2

t (min)	4-CP	2,4-DCP	HQ	Ph	4-cCat	4-CP	2,4-DCP	HQ	Ph	4cCat
0	50	25	0	0	0	46.21	23.99	0	0	0
30	32.21	14.98	9.498	10.45	6.670	33.21	16.23	7.77	9.65	6.04
60	20.36	9.816	12.93	8.919	5.741	21.01	10	12.65	9.01	6.54
90	12.27	6.501	10.13	5.923	3.730	14.01	6.75	10.99	6.23	4.01
120	6.606	4.227	6.053	3.391	2.56	8.23	5.23	6.23	4.02	3.24
150	3.255	2.656	3.086	1.98	1.57	4.01	3.01	3.98	2.01	2.54
180	1.554	1.606	1.483	1.012	0.89	2.36	1.56	1.56	1.45	1.56
210	0.763	0.938	0.726	0.89	0.547	1.023	0.91	0.98	1.01	0.87
240	0.392	0.535	0.372	0.227	0.115	0.056	0.501	0.47	0.235	0.158

A-12 Effect of hydrogen peroxide on the photocatalytic degradation of: (a) 4-CP (b) 2,4-DCP (10 mg/L $FeCl_3$. $6H_2O$, 0.5 g/L TiO_2, 1000 mW/cm^2 light intensity)

(a)

t (min)	1.13mM	2.26mM	3.41mM	5.01mM	7.23mM
	4-CP (mg/L)	4-CP (mg/L)	4-CP (mg/L)	4-CP (mg/L)	4-CP (mg/L)
0	48.23	48.23	48.23	48.23	48.23
30	25.36	20	19.01	22.56	30.25
60	16.54	11.32	9.25	14.23	22.33
90	11.45	6.01	3.5	8.56	16.32
120	6.35	2.01	0.12	4.01	11.23
150	2.32	1.87	0	2.58	7.56
180	0.89	0.23	0	1.98	4.21
210	0.02	0.001	0	1.01	2.56
240	0.001	0	0	0.87	1.54

(b)

t (min)	1.13mM	2.26mM	3.41mM	5.01mM	7.23mM
	2,4-DCP (mg/L)	2,4-DCP (mg/L)	2,4-DCP (mg/L)	2,4-DCP (mg/L)	2,4-DCP (mg/L)
0	48.23	48.23	48.23	48.23	48.23
30	30.25	27.56	25.04	28.54	33.65
60	22.01	18.23	13.01	20.36	26.35
90	16.52	11.36	6.32	15.24	21
120	11.23	6.36	2.01	10.23	16.23
150	7.25	3.01	0.23	7.01	11.65
180	4.56	2.01	0	4.01	8.54
210	2.01	0.98	0	2.01	5.78
240	0.98	0.23	0	1.25	4.23

A-13 Concentration profiles of the combined mixture 50 mg/L of both 4-CP and 2,4-DCP with 10 mg/L $FeCl_3$. $6H_2O$ and 3.41 mM H_2O_2 optimum values. (0.5 g/LTiO_2, 1000 mW/cm^2)

t (min)	4-CP (mg/L)	2,4DCP (mg/L)	HQ (mg/L)	Ph (mg/L)	4cCat (mg/L)
0	48	48.23	0	0	0
30	25.36	30.25	3.02	4.02	1.54
60	15.65	20.01	5.23	6.56	2.02
90	9.89	13	4.05	3.08	1.01
120	5.23	7.21	3.12	1.05	0.54
150	2.32	3.11	0.98	0.21	0.001
180	0.89	1.11	0.02	0.01	0
210	0	0	0	0	0
240	0	0	0	0	0

A-14 Effect of ferrous ions (Fe^{2+}) on the solar photocatalytic degradation of (a) 4-CP and (b) 2,4-DCP (0.5 g/L TiO_2, 1000 mW/cm^2 light intensity).

(a)

t (min)	2.5mg/L/Fe^{2+}	5mg/L/Fe^{2+}	7mg/L/Fe^{2+}	15mg/L/Fe^{2+}
	4-CP(mg/L)	4-CP(mg/L)	4-CP(mg/L)	4-CP(mg/L)
0	48	48	48	48
30	32.24	30.25	25.36	28.56
60	23.63	20.13	15.46	20.14
90	16.12	13.01	10.21	15.32
120	9.36	7.45	5.35	10.23
150	6.32	5.01	3.32	7.04
180	2.31	1.98	0.89	5.98
210	1.36	0.89	0	4.23
240	1	0.01	0	3.98

(b)

t (min)	2.5mg/L/Fe^{2+}	5mg/L/Fe^{2+}	7mg/L/Fe^{2+}	15mg/L/Fe^{2+}
	2,4-DCP(mg/L)	2,4-DCP(mg/L)	2,4-DCP(mg/L)	2,4-DCP(mg/L)
0	48.23	48.23	48.23	48.23
30	35.1	33.54	27.25	32.26
60	27.11	25.35	19.01	22.36
90	20.65	18.23	13.54	17.35
120	16.25	13.54	8.23	12.25
150	12.65	8.22	5.6	9.5
180	10.45	3.55	2.5	6.35
210	6.35	1.54	0	3.36
240	4.25	0.98	0	1.98

A-15 Effect of ferric ions (Fe^{3+}) on the solar photocatalytic degradation of (a) 4-CP and (b) 2,4-DCP (0.5 g/L TiO_2, 1000 mW/cm^2 light intensity).

(a)

t (min)	2.5mg/L/Fe^{3+}	5mg/L/Fe^{3+}	7mg/L/Fe^{3+}	15mg/L/Fe^{3+}
	4-CP(mg/L)	4-CP(mg/L)	4-CP(mg/L)	4-CP(mg/L)
0	48	48	48	48
30	32.24	30.25	25.36	28.56
60	23.63	20.13	15.46	20.14
90	16.12	13.01	10.21	15.32
120	9.36	7.45	5.35	10.23
150	6.32	5.01	3.32	7.04
180	2.31	1.98	0.89	5.98
210	1.36	0.89	0	4.23
240	1	0.01	0	3.98

(b)

t (min)	2.5mg/L/Fe^{3+}	5mg/L/Fe^{3+}	7mg/L/Fe^{3+}	15mg/L/Fe^{3+}
	2,4-DCP(mg/L)	2,4-DCP(mg/L)	2,4-DCP(mg/L)	2,4-DCP(mg/L)
0	48.23	48.23	48.23	48.23
30	35.1	33.54	27.25	32.26
60	27.11	25.35	19.01	22.36
90	20.65	18.23	13.54	17.35
120	16.25	13.54	8.23	12.25
150	12.65	8.22	5.6	9.5
180	10.45	3.55	2.5	6.35
210	6.35	1.54	0	3.36
240	4.25	0.98	0	1.98

A-16 Concentration profiles of the combined mixture 50 mg/L of both 4-CP and 2,4-DCP (0.5 g/LTiO_2, 1000 mW/cm^2) with optimal values of Fe^{2+}=7 mg/L

t (min)	4CP(mg/L)	2,4-DCP(mg/L)	HQ(mg/L)	Ph(mg/L)	4cCat(mg/L)
0	48	48.23	0	0	0
30	25.36	27.25	4.21	5.32	2.56
60	15.46	19.01	6.35	8.12	3.89
90	9.7	13.54	3.12	5.21	1.01
120	5.35	8.88	1.2	1.05	0.32
150	3.32	5.5	0.78	0.21	0
180	0.89	2.5	0	0	0
210	0	0	0	0	0
240	0	0	0	0	0

A-17 Influence of TiO_2 doses on the solar photocatalytic degradation of Kwinana refinery effluent

t (min)	0.3 g/L/TiO_2	0.5 g/L/TiO_2	0.7 g/L/TiO_2	0.9 g/L/TiO_2
	COD(mg/L)	COD(mg/L)	COD(mg/L)	COD(mg/L)
0	840	840	840	840
60	772.8	725.4	672	747.6
120	655.2	588	554.4	604.8
180	546	487.2	445.2	512.4
240	487.2	386.4	336	453.6

A-18 Influence of pH on the on the solar photocatalytic degradation of petroleum refinery effluent

t (min)	pH 3	pH 5	pH 7	pH 9
	COD(mg/L)	COD(mg/L)	COD(mg/L)	COD(mg/L)
0	840	840	840	840
60	655.2	588	621.6	648
120	537.6	453.6	500	554.4
180	411.6	352.8	378	445.2
240	336	294	327.6	336

A-19 Influence of ferrous (Fe^{2+}) ions the on the solar photocatalytic degradation of petroleum refinery effluent

t (min)	5 mg/L	7 mg/L	10 mg/L	15 mg/L	20 mg/L
	COD(mg/L)	COD(mg/L)	COD(mg/L)	COD(mg/L)	COD(mg/L)
0	840	840	840	840	840
60	587	520.3	495.3	470.3	482.3
120	452	403.8	380.6	358.2	375.2
180	351.1	302.5	280.3	263.6	277.2
240	292.5	250.3	210.2	194.2	210.3

A-20 Influence of ferric (Fe^{3+}) ions the on solar photocatalytic degradation of petroleum refinery effluent

t (min)	7mg/L	10 mg/L	15 mg/L	20 mg/L	25 mg/L
	COD(mg/L)	COD(mg/L)	COD(mg/L)	COD(mg/L)	COD(mg/L)
0	840	840	840	840	840
60	587	555.3	510.3	492.3	500.1
120	459.3	420.3	390.5	380.2	395.3
180	358.2	330.2	290.4	279.3	300.2
240	301.2	270.1	220.3	215.6	225.6

APPENDIX B

Detection of Organic Compounds

HPLC Detections

As explained in the experimental section (Chapter 3). Detection of the main pollutants and their intermediates identified and quantified by High Performance Liquid Chromatograph (HPLC) analysis. Detection of 4-CP and 2,4-DCP was done at 265nm and 275 respectively, using a Varian Prostar 210 chromatograph with UV-vis detector and a C18 reverse phase column (25cm x 4.6mm x 5µm). The mobile phase was a mixture of 30 % acetonitrile and 70 % water with a flow rate of 1 mL/min. The temperature of the column was kept at 25^{o} C throughout all the analysis. Injection volume for all samples was 5 µL. The identification of the intermediates by HPLC was performed by the comparison of the retention time of the peak in the discharged sample with that in the standard sample. The concentrations of compounds were calculated using the equations derived from the calibration measurements for authentic samples. Figure B-1 shows the typical HPLC chromatograms results of the retention time for all organic compounds used in this research. It is worth to mention that each compound has different peak due to different absorption rates even their concentrations are equal.

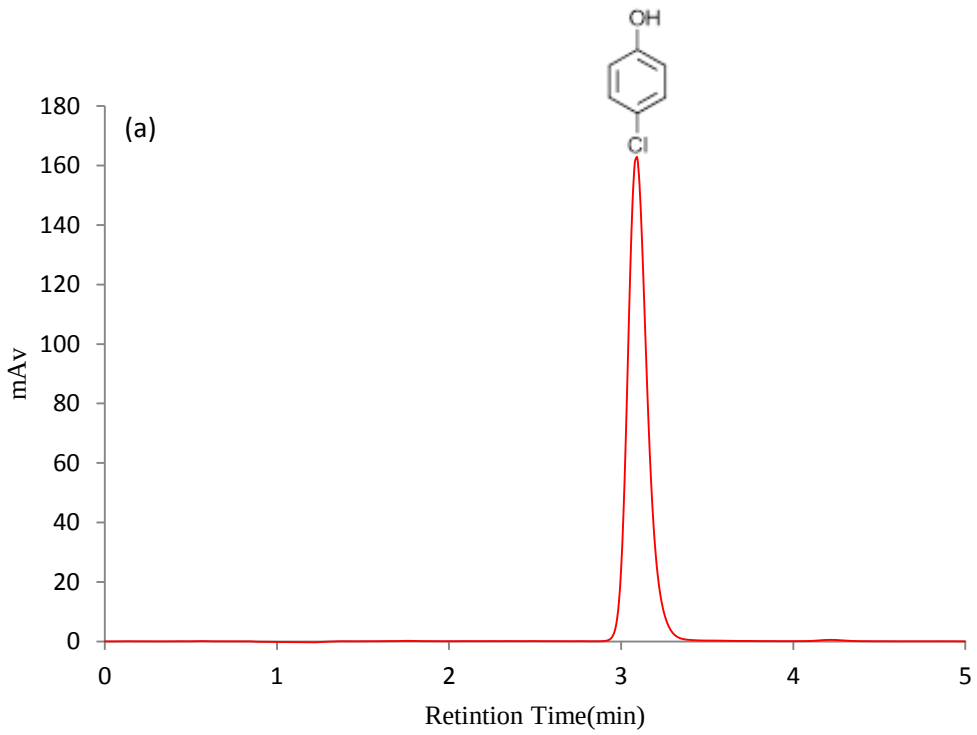

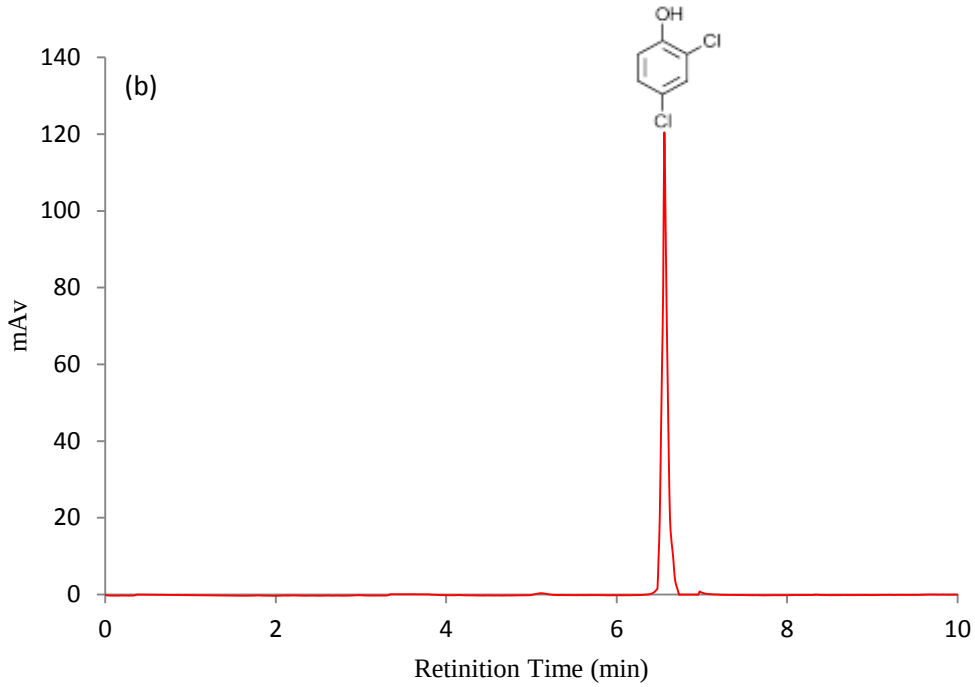
(b)
OH
Cl
Cl
140
120
100
80
60
40
20
0
mAv
0
2
4
6
8
10
Retinition Time (min)

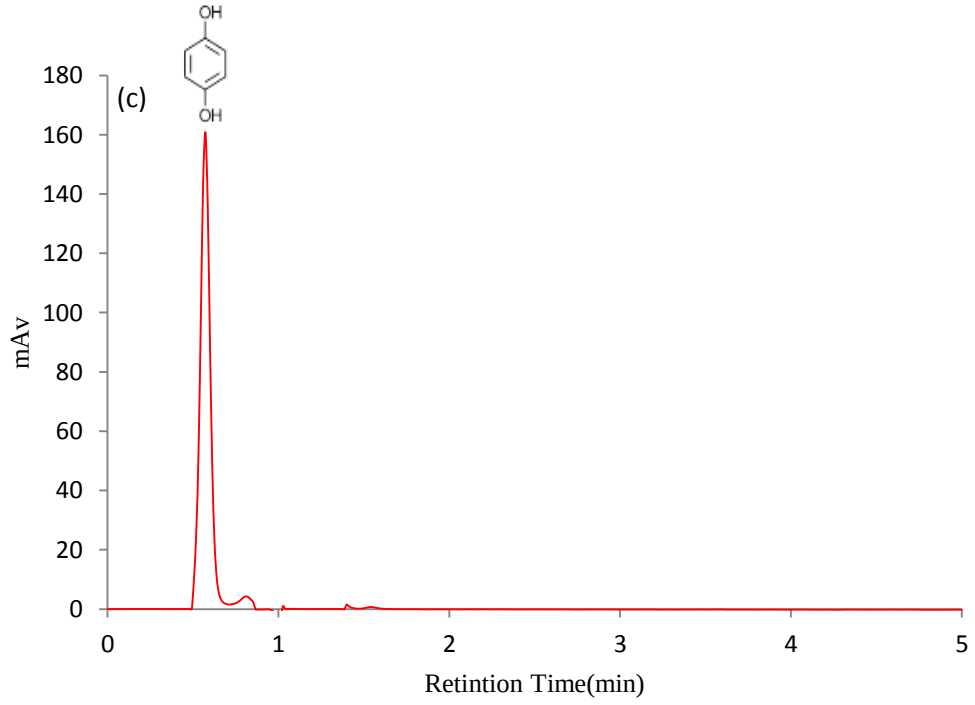
(c)
OH
OH
180
160
140
120
100
80
60
40
20
0
mAv
0
1
2
3
4
5
Retintion Time(min)

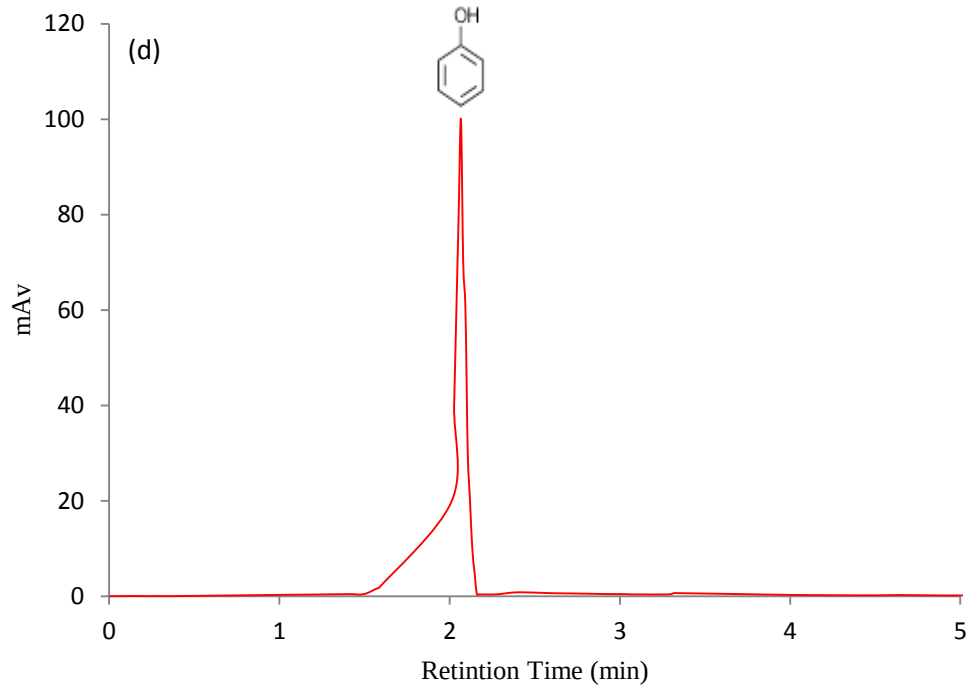
(d)
OH
120
100
80
60
40
20
0
mAv
0
1
2
3
4
5
Retintion Time (min)

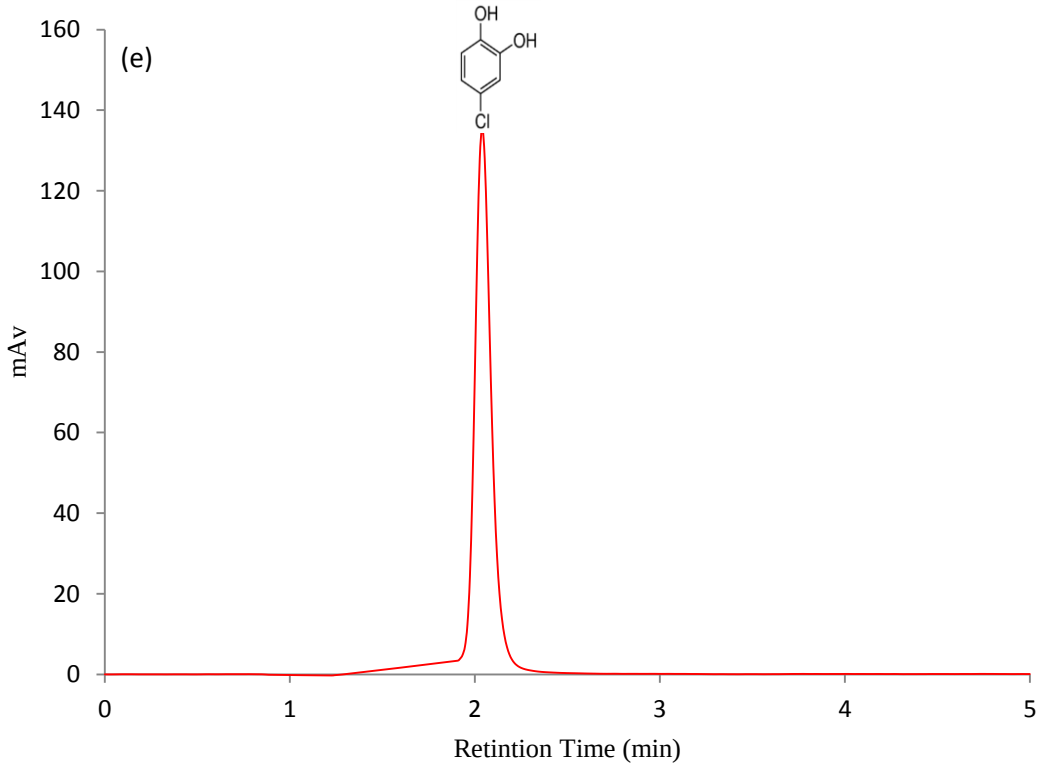
(e)
OH
OH
Cl
160
140
120
100
80
60
40
20
0
mAv
0
1
2
3
4
5
Retintion Time (min)

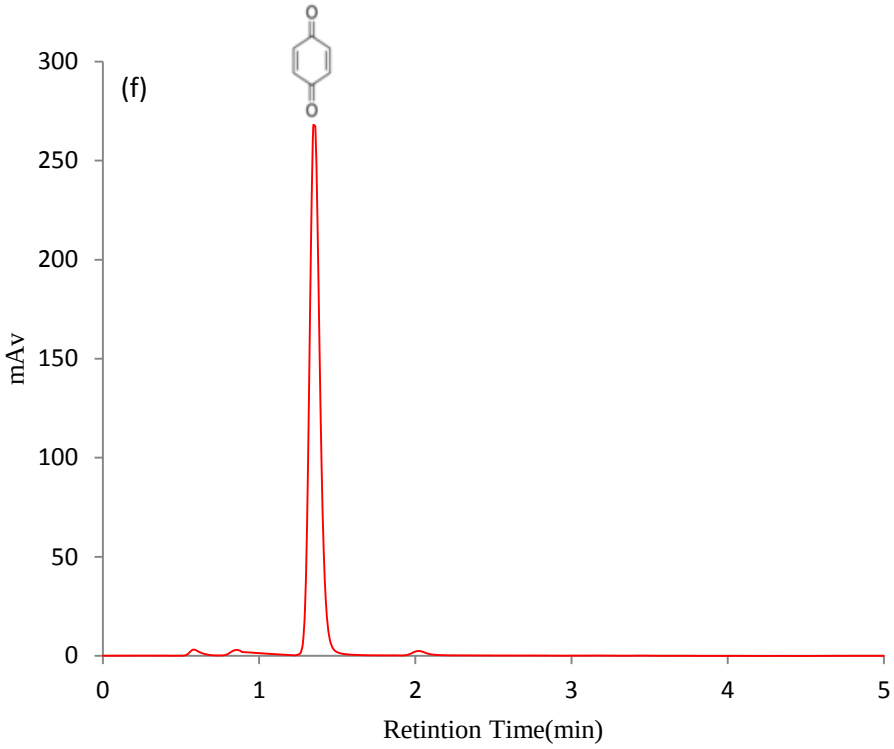

Figure B-1 typical HPLC chromatograms results of the retention time for all organic compounds used in this research: (a) 4-CP (b) 2,4-DCP (c) HQ (d) Ph (e) 4cCat (f) BQ.

Information about the retention time of all pollutants and their intermediates are given in Table B-1.

Table B-1 Identification of the organic pollutants and their intermediates in the solar photocatalytic degradation

Component	Retention time (min)
4-chlorophenol (4-CP)	3.08
2,4-dichlorophenol (2,4-DCP)	6.56
Hydroquinone (HQ)	0.57
Phenol (Ph)	2.06
4-chlorocatechol (4cCat)	1.91
Benzoquinone (BQ)	1.34